UNIVERSIDADE FEDERAL DE SÃO CARLOS
CENTRO DE CIÊNCIAS BIOLÓGICAS E DA SAÚDE
DEPARTAMENTO DE GENÉTICA E EVOLUÇÃO
PROGRAMA DE PÓS-GRADUAÇÃO EM GENÉTICA EVOLUTIVA E BIOLOGIA MOLECULAR

JULIANA AFONSO

EXPRESSÃO GÊNICA ASSOCIADA AO CONTEÚDO DE MINERAIS NO MÚSCULO *LONGISSIMUS THORACIS* E SEUS PROCESSOS REGULATÓRIOS EM BOVINOS NELORE (*BOS INDICUS*)

SÃO CARLOS -SP
2019

JULIANA AFONSO

EXPRESSÃO GÊNICA ASSOCIADA AO CONTEÚDO DE MINERAIS NO MÚSCULO *LONGISSIMUS THORACIS* E SEUS PROCESSOS REGULATÓRIOS EM BOVINOS NELORE (*BOS INDICUS*)

Tese apresentada ao programa de Pós-graduação em Genética Evolutiva e Biologia Molecular do Centro de Ciências Biológicas e da Saúde da Universidade Federal de São Carlos – UFSCar, como parte dos requisitos para obtenção do título de Doutor em Ciências (Ciências Biológicas), área de concentração: Genética e Evolução.

Orientadora: Profa. Dra. Luciana Correia de Almeida Regitano

Coorientadora: Profa. Dra. Marina Rufino Salinas Fortes

SÃO CARLOS -SP

2019

UNIVERSIDADE FEDERAL DE SÃO CARLOS

Centro de Ciências Biológicas e da Saúde
Programa de Pós-Graduação em Genética Evolutiva e Biologia Molecular

Folha de Aprovação

Assinaturas dos membros da comissão examinadora que avaliou e aprovou a Defesa de Tese de Doutorado da candidata Juliana Afonso, realizada em 06/09/2019:

Profa. Dra. Luciana Correia de Almeida Regitano
EMBRAPA

Prof. Dr. Anderson Ferreira da Cunha
UFSCar

Profa. Dra. Simone Cristina Méo Niciura
EMBRAPA

Prof. Dr. Luiz Lehmann Coutinho
USP

Prof. Dr. Laércio Ribeiro Porto Neto
CSIRO

I dedicate this thesis to my parents who have heard me say for 6 years:

"I am going to do research in Australia".

ACKNOWLEDGEMENTS

I would like to first thank my parents, Edson and Inês, for all the help, love, support, patience and for all the times when they got as excited as me about my achievements. Without their love I would not be who I am today. Also, my grandfather Humberto and my grandmother Isolina, who were always there for me.

A special thanks to my boyfriend, Gustavo, for the irrevocable partnership and love during these two last years, for encouraging my dreams and for living them with me.

I would also want to thank:

- My supervisor, Dr. Luciana Regitano, for believing in me, for the dream project that we build together, for the help with my dream to do research in Australia, for improving my sometimes crazy scientific ideas and for all the opportunities that I had during these four years, regarding partnerships and friendships.
- My co-supervisor, Dra. Marina Fortes, for all the help in this work, all the scientific discussions and for personally making my stay in Australia perfect.
- Dr. Toni Reverter, Dr. Gerson Mourão and Dr. Juliana Petrini, for the help with the statistical part of this thesis and, above all, for the statistical free lessons during our discussing sections, filled with jokes and ideas.
- Dr. Aline Cesar and Dr. Polyana Tizioto, for the help with the initial files necessary for the realization of this thesis and for all the help with the R and Unix scripts in the beginning.
- Dr. Ana Rita Nogueira and Dr. Caio Gromboni, for the mineral concentration data that originates this work.
- Dr. Mikael Bodén, for letting me participate in interesting and helpful bioinformatic lab meetings, and his PhD student Woo, for helping me learning a new methodology that sparks the idea for a future project.
- My friends from the Animal Biotechnology group, Wellison, Andressa, Marina, Carlos, Edy, Jennifer, Karina, Marcela, Jessica, Priscila, Tainã, Bruno, Juliana (Ruth), Laura, Janssen and Otávio, for the contribution for this work and my professional growth, and mainly for their friendship. The times that we passed together talking and having fun will be the things that will make me smile 30 years for now, when remembering this phase.
- Dr. Flavia Bressani, for the help with this thesis and for the friendship during these four years.

- My friends, in special Alzira, Mayara, Cuca, Diego, Vanessa, Tati, Angela, Mara, Nathália, Ana and Flaviane, for being there in all the moments that we passed together that reminded me that there is life outside of a PhD.
- All the employees and trainess from Embrapa Pecuaria Sudeste that I have interact during these four years, for the funny lunches and coffee breaks.
- The professors of the Program of Evolutionary Genetics and Molecular Biology of the Federal University of São Carlos, for all the help and guidance during my doctoral studies.
- Ivanildes, the program "angel" secretary, for all the answers and tutoring about the non-ending bureaucracy, always with a smile on her face.
- My aunts, uncles and cousins, for the patience when I was trying to explain what I do and for the moral support during all these years.
- The people that I met during my stay in Australia, specially Eunice, Sajid, Kurt, Steph and Silja for the good conversations and laughs in our common room; Sonia and Letícia for the best beginning in a new city and Nathália, Alanny, Bárbara, Camila, Daniel, Natália, Mariana, Bruna and Eli for the lunches, vacations and heartful conversations.
- My therapist, Ana, for helping me understand that we need to solve one problem at a time.
- CAPES for my two scholarships.
- CNPq and FAPESP for the financial support for the project.

"It does not do to dwell on dreams and forget to live, remember that"

Dumbledore in Harry Potter and the Sorcerer's Stone, J. K. Rowling

RESUMO

Expressão gênica associada ao conteúdo de minerais no músculo *Longissimus thoracis* e seus processos regulatórios em bovinos Nelore (*Bos indicus*): A concentração mineral do músculo bovino não depende somente do equilíbrio entre a ingestão e a excreção de minerais, mas também do ambiente, da raça, do estado fisológico e de fatores genéticos. Além disso, o conteúdo mineral pode afetar processos biológicos relacionados à qualidade da carne, atuando em reações químicas relacionadas à maciez no *post mortem* e, na manutenção das células musculares, através de sua ação no metabolismo, como co-fatores enzimáticos e na regulação da replicação e diferenciação celular. Visto que detectar elementos genéticos envolvidos com a homeostase mineral é de interesse da indústria de produção da carne, apresentamos análises executadas para este fim. Testes de expressão gênica diferencial foram realizados em músculo *Longissimus thoracis* de grupos de novilhos Nelore contrastantes separadamente para a concentração dos minerais cálcio, cobre, potássio, magnésio, sódio, fósforo, enxofre, selênio e zinco. O mineral ferro não foi incluído nessas análises pois os genes diferencialmente expressos relacionados à concentração de ferro na mesma população em estudo já foram previamente publicados por nosso grupo de pesquisa. Um enriquecimento funcional dos genes diferencialmente expressos foi feito, verificando também interações proteína-proteína conhecidas entre eles, em busca de processos biológicos relacionados a cada mineral. Em seguida, incluindo-se também dados de concentração de ferro, desenvolveram-se duas novas abordagens de utilização dos algoritmos PCIT *(Partial Correlation Coefficient with Information Theory*) e RIF (*Regulatory Impact Factor*). Essas abordagens permitiram a identificação direta de elementos genéticos correlacionados à concentração de minerais, de forma contínua, em nossa população e a quantificação do impacto regulatório dos genes e miRNAs correlacionados a um mineral sobre a concentração deste mineral. A regulação das vias relacionadas à adipogênese foi significativa e genes apontados aqui podem explicar o efeito antagônico conhecido entre Cu e Zn na biossíntese de ácidos graxos. Com as novas abordagens de utilização dos algoritmos PCIT e RIF, foram identificados genes sabidamente ligados à homeostase mineral, com alto impacto regulatório e previamente apontados como regulatórios em nossa população por serem fatores de transcrição, eQTLs ou miRNAs. O gene *PLCB2* é correlacionado com Fe e S, sendo esse gene a provável conexão entre Fe e os demais minerais. O gene *NOX1* possuiu impacto regulatório significativo sobre a concentração de Se e Zn. Em humanos, a concentração de zinco regula *NOX1*. Concluímos que o cerne da regulação genética da concentração tecidual para todos os minerais estudados

parece estar nas interações entre os componentes da matriz extracelular. Podemos inferir que a integração das técnicas realizadas em nosso trabalho pode incluir um novo nível de informação acerca dos elementos regulatórios envolvidos na homeostase mineral.

Palavras-chave: músculo bovino, RNA-seq, Nelore, minerais, genes, miRNAs, PCIT, RIF, ECM.

ABSTRACT

Gene expression associated with mineral content in the *Longissimus thoracis* muscle and its regulatory processes in Nelore cattle (*Bos indicus*): The mineral concentration of the bovine muscle does not only depend on the balance between the ingestion and excretion of minerals, but also the environment, breed and genetic factors. In addition, mineral content can affect biological processes related to meat quality, acting in chemical reactions related to tenderness in *postmortem* as well as in the maintanance of muscular cells throught its action in methabolism, as enzimatic co-factors and in the regulation of cell replication and differentiation. Since detecting genetic elements involved with mineral homeostasis is of interest to the meat industry, we present analyzes performed for this purpose. Differential gene expression tests were performed in muscle *Longissiumus thoracis* of groups of Nelore steers contrasting separately to the concentration of the minerals calcium, copper, potassium, magnesium, sodium, phosphorus, sulfur, selenium and zinc. The iron mineral was not included in these analyses because the differentially expressed genes related to iron concentration in the same population in study were already published by our research group. A functional enrichment of the differentially expressed genes was made, also verifying protein-protein interactions known among them, in search of biological processes related to each mineral. Then, also including iron concentration data, two new approaches were developed to use the PCIT *(Partial Correlation Coefficient with Information Theory*) and RIF algorithms (*Regulatory Impact Factor*). The new applications for using these algorithms allowed the direct identification of genetic elements correlated to the mineral concentration continuously in our population and the quantification of the regulatory impact of the genes and miRNAs correlated to a mineral on the concentration of this mineral. The regulation of the pathways related to adipogenesis was significant and the genes indicated here may explain the antagonistic effect known between Cu and Zn in the biosynthesis of fatty acids. With the new applications to use the PCIT and RIF algorithms, genes known to be linked to mineral homeostasis with high regulatory impact were identified and previously indicated as regulatory in our population for being transcription factors, eQTLs or miRNAs. The *PLCB2* gene is correlated with Fe and S, the latter correlates to the other minerals. The *NOX1 gene* possessed significant RIF and is correlated to Se. In humans, the concentration of zinc regulates *NOX1*. We conclude that the core of genetic regulation for all minerals studied seems to be in the interactions between the components of the extracellular matrix. We can infer that the integration of the proposed techniques in our work may include a new level of

information about the regulatory elements involved in mineral homeostasis.

Keywords: bovine muscle, RNA-seq, Nelore, minerals, genes, miRNAs, PCIT, RIF, ECM.

TABLE OF FIGURES

TABLE LIST

TABLE OF CONTENT

CHAPTER 1: A BRIEF OVERVIEW OF THE PROBLEM

1.1. INTRODUCTION

1.1.1. Beef cattle industry in Brazil

In the year 2018, Brazil exported a total of 1,643,000 tons of beef to more than 100 countries, with an income of 6,572,30 million US dollars (ABIEC, 2019). Brazil is considered the world's largest exporter of beef in volume and monetary value and is the second-largest producer in the world, with 15.3% of the production, standing behind the United States of America, which produces around 17.2% of the globally consumed meat. To maintain this prominent position, a quality increase of the final product, without an increment of production costs and damages to the environment, is demanded.

The production of beef in Brazil is favored by characteristics such as the broad expanse of pastures, abundant water, food, low-cost labor (HÉLYETTE, 1991), and a herd of cattle composed mostly of Nelore animals, a zebu breed highly adapted to Brazilian tropical climate.

1.1.2. Main differences regarding adaptation to environment between *Bos indicus* and *Bos taurus*

Nelore animals (FIGURE 1.1), as other zebu breeds (*Bos indicus*), have increased tolerance to the tropical climate and to parasites as the main differences when compared with *Bos taurus*. CHAN, NAGARAJ and REVERTER (2010) found that *Bos indicus* individuals present 14 regions containing known SNPs with significantly different allele frequencies in comparison to *Bos taurus*. These SNPs are harbored in regions of genes related to keratins, heat-shock proteins, and heat resistance; attributes likely to be related to tropical conditions. Nelore breed also has significant structural variations in the genome, as copy number variation (CNVs) affecting genes with functions in vasodilation regulation, immune system response and hair follicle morphogenesis, putatively related to environmental adaptation (ANTUNES DE LEMOS et al., 2018).

Regarding to the high parasite tolerance, in a genome-wide association study (GWAS) (PORTO NETO et al., 2014), aiming to detect regions related to ten traits of tropical cattle production, using animals with indicine ancestor varying from 0% to 100%, the authors identified a genetic region affecting parasite resistance, yearling weight, body

condition score, coat color and penile sheath score.

Additionally, genetic variation for fertility has been described in a study comparing protein markers between groups of bulls (RONCOLETTA et al., 2006). The authors identified 27 spots prevalent in the higher fertility group and one in the lower fertility group. From these markers, two spots can be proteins that putatively predict bull fertility, BSP-A3 and aSFP. In a GWAS study with males and females (IRANO et al., 2016), the authors identified genomic windows explaining 7.91% of early pregnancy variation and 6.78% of scrotal circumference variation.

FIGURE 1.1 Nelore animals.

Source: Karina Santos

1.1.3. Minerals in biological processes

Minerals have an impact on biological processes responsible for mammals' biology, including bovines. They are associated with metabolism, homeostasis maintenance, growth, cellular structural components, enzyme cofactors, regulation of cell replication, and differentiation (SUTTLE, 2010). In this thesis we discussed the genetic elements related to the macrominerals calcium (Ca), phosphorus (P), sodium (Na), potassium (K), magnesium (Mg) and sulfur (S), and to the microminerals copper (Cu), iron (Fe), selenium (Se) and zinc (Zn).

1.1.3.1. Macrominerals

Calcium is mainly essential to the mammals because it is the principal constituent of

the bones, in which its concentration can change due to differences in extracellular Ca availability, dysfunctions of the parathyroid hormone or vitamin D deficiency (HOWARD, 1957). This mineral acts in muscle contraction, mediating the actin-myosin-tropomyosin interaction (EBASHI and ENDO, 1968). Calcium can be a second messenger regulating cell shape, *e.g.*, in endothelial cells, where Ca concentration disrupts cell-matrix and cell-cell adhesion, changing the endothelial format and providing a paracellular transport pathway (CIOFFI et al., 2011). It can also influence enzyme secretion (CASE and CLAUSEN, 1973), modulate mitochondria oxidative phosphorylation in skeletal muscle cells (GLANCY et al., 2013), act in the cell death process and chromatin remodeling (BANO, JEWELL and NICOTERA, 2017).

In the presence of oxygen, P forms phosphate, the second most common constituent of the bones, and a central constituent of all metabolic pathways (WAMELINK, STRUYS and JAKOBS, 2008), for being part of the DNA, phospholipids, phosphoproteins and energy molecules, like ATP. This mineral is part of the pentose phosphate pathway, a fundamental process of cellular metabolism (STINCONE et al., 2015).

Among the other macrominerals, S takes part in methionine, cysteine, homocysteine and taurine amino acids (BROSNAN and BROSNAN, 2006), proteins, enzymes, vitamins and other biomolecules (KOMARNISKY, CHRISTOPHERSON and BASU, 2003). Sodium channels are responsible for the transmission of nerve impulses and play a key role in pain sensation (DEVOR, 2006). Sodium and potassium influx regulates the extracellular fluids and maintains osmotic pressure (KUMAR and BERL, 1998) as well as acid-base equilibrium. Magnesium is a co-factor of enzymatic reactions, affecting, for example, the rate of enzymatic synthesis of ATP (BUCHACHENKO et al., 2008) and is important to nerve conduction (FLEMING, LENMAN and STEWART, 1972) .

1.1.3.2. Microminerals

The mineral copper is part of enzymes, like the copper amine oxidases, dopamine β-monooxygenase, and galactose oxidase, involved in oxidation processes (KLINMAN et al., 1991). Iron is most known for its role in the oxygen transport by hemoglobin and myoglobin, but this mineral is also a co-factor for enzymes such as the ones in the respiratory chain (CAMMACK, WRIGGLESWORTH and BAUM, 1990). Selenium is part of enzymes, such as peroxidases (FLOHE, 1997) and acts in the thyroid hormone metabolism (ARTHUR et al., 1992). Zinc is also part of enzymes (MCCALL, HUANG and FIERKE, 2000) and is a

component of the thymulin, a hormone produced by thymic epithelial cells (BACH and DARDENNE, 1989).

1.1.4. Mineral concentration influence on meat quality and production

Because of the involvment of minerals in biological processes that impact on meat quality and production traits, it is important to understand all the factors influencing mineral concentration in bovine muscle.

Among the factors that influence beef quality traits, we can cite the concentration of muscular minerals (TIZIOTO et al., 2015). Minerals participate in muscle cell maintenance and contribute to meat quality sensory, nutritional and toxicological aspects. The sensory aspect is exemplified by the effect of Ca and K in the meat tenderization process. Ca-dependent proteolytic enzymes act in the post-mortem improving tenderness (GEESINK and KOOHMARAIE, 1999), and higher levels of K are related to lower meat tenderness since this mineral positively affects the Warner-Bratzler shear force (WBSF) (TIZIOTO et al., 2014).

A minimum amount of minerals is required for a healthy human die (GHARIBZAHEDI and JAFARI, 2017), exemplifying the nutritious aspect. The toxicological aspect is due to the potential of the meat to accumulate toxic minerals, representing a source of heavy metals for humans (BADIS, 2014). Ca, P, Mg and Na partake in enzymatic reactions and in keeping cell membrane potentials (CAMPBELL, 2017) hence contributing to a healthy muscle tissue.

Mineral concentration can also impact on reproduction, health and growth performance in bovines. Zinc, Cu and Mn supplementation improve pregnancy rate, mineral concentration, and kilograms in calf weaned per cow (AHOLA et al., 2004). An adequate trace mineral nutrition improves marbling development during growth and finishing phases. Trace mineral injections can improve rib eye area despite trace mineral initial concentration and can improve growth in mildly trace mineral deficient steers (GENTHER and HENSEN, 2014).

1.1.5. Aspects influencing muscle mineral concentration

Mineral concentration in the muscle is partially genetically determined (TIZIOTO et al., 2013; MATEESCU et al., 2013a; MATEESCU et al., 2013b), with heritability values

between 0.29 and 0.33 (TIZIOTO et al., 2015; MATEESCU et al., 2013a) depending on the mineral, being suitable to genetic improvement. It is also affected by diet, breed (HOLLÓ et al., 2007), physiological status, environment and muscle type (SOMOGYI et al., 2015). The concentration of a specific mineral can also affect the concentration of another. Among the known mineral interactions, we can highlight the positive interaction between Cu and Fe and the negative between Zn and Cu, Zn and Fe, P and Fe, Mn and Fe, P and Zn, Fe and Zn, Cu and Se, S and Se, Na and K, Ca and Mg and P and Mg (DELL, 1989).

While most studies in cattle mainly investigated the function of minerals in biological events within the organism and its relationship with meat quality traits (TIZIOTO et al, 2015; MATEESCU et al., 2013b; DINIZ et al., 2016) there are still few studies regarding the genetic factors acting in the maintenance of the mineral concentrations, or regarding the regulatory mechanisms associated with these genetic variations.

Thus, studies aiming the identification of genes involved in mineral homeostasis, their functions, metabolic pathways and possible relationships with mineral concentration maintenance in the bovine muscle, may provide subsidies for breeding and management programs. This information can also benefit the establishment of proper mineral supplementation strategies, since there are interactions that affect mineral absorption and bioavailability (SANDSTRÖM, 2001).

1.1.6. Searching for the genetic aspects of mineral homeostasis

There are several possible approaches to be used in the search of genetic elements linked to a trait of interest, *e.g.*, differential expression, co-expression networks, genome-wide association studies (GWAS), in addition to *in silico* prediction of regulatory elements, such as transcription factor (TF), miRNA binding sites and CpG islands, by sequence similarity. These approaches already identified some of the genetic aspects linked to different mineral concentration, but there is a lack of comparisons involving several minerals and their relationship.

With animals from the same Nelore population and the same muscle tissue as in our study, our research group described genetic regions involved in mineral concentration. Under a candidate gene approach, a significant effect of an SNP on the *CAPN1* gene on Ca concentration was found (Tizioto et al., 20014), with the rare genotype associated with less Ca content. A GWAS study detected genes in quantitative trait loci (QTL) involved with signaling pathways, membrane proteins, transcription regulation and metal ion binding,

concluding that mineral concentrations seem to be affected by several QTLs with small effects (TIZIOTO et al., 2015). In a differential expression analysis between contrasting groups regarding Fe concentration, the authors identified genes linked to lipid transport and metabolism and to cell growth. They also take part on interferon signaling, thyroid receptor activation, and complement system pathways (DINIZ et al., 2016). Lastly, a co-expression analysis detected seven gene modules associated with at least two traits considering 13 minerals concentrations and three meat quality-related traits (intramuscular fat, meat pH and tenderness), being part of over-represented pathways related to energy and protein metabolism (DINIZ et al., 2019).

1.1.7. Searching for the genetic regulation of mineral homeostasis

More than identifying genes and regions related to mineral concentration, it is important to understand the role of these elements in the phenotype. Our group also identified regulatory elements involved in the regulation of the general expression in the muscle of the same population. The association of these elements with phenotypes can be tested, and regulation relationships can be inferred. Analysis based on annotated bovine genes DNA-binding domains comparisons with known human transcription factors (TFs), identified 865 sequence-specific DNA-binding bovines TFs and putative transcription cofactors in several tissues (DE SOUZA et al., 2018). An integrative analysis of high throughput DNA genotyping and mRNA-Sequencing data identified quantitative trait loci (eQTL) controlling muscle gene expression, being 1,268 cis-eQTL and 10,334 trans-eQTL affecting the expression of 119 genes (CESAR et al., 2018).

Other research groups have been studying genetic elements related to mineral concentration in bovine muscle. In a GWAS study with Angus cattle, the authors detected seven regions in six chromosomes having a major effect on Fe content, as well as other QTLs with small effect over the concentration of Mg, Mn, P, K, Na, and Zn (MATEESCU et al., 2013). Another QTL study identified a total of 15 regions related to the concentration of several minerals in the liver, muscle and kidney of crossbred calves with Jersey and Limousin ancestry (MORRIS et al., 2013).

Given the above mentioned, herein we identified genes and miRNA related to mineral concentration, their regulatory impact and the over-represented pathways in which they take part. The relationships between pathways and minerals, as well as the possible influence of minerals in the expression of genes in over-represented pathways are the core discussion of

this thesis.

1.2. HYPOTHESIS

Differences in gene expression may reveal mechanisms related to bovine muscle mineral concentration.

1.3. AIMS

1.3.1. General aim

To identify genes and miRNAs related to mineral homeostasis in a Nelore steer population, using mRNA-Seq and miRNA-Seq data from *Longissimus thoracis* samples and data on Ca, Cu, K, Mg, Na, P, S, Se, Zn and Fe concentration.

1.3.2. Specific aims

i) To identify differentially expressed genes (DEGs), using the RNA-Seq approach, in Nelore contrasting *Longissimus thoracis* samples for the individual concentration of Ca, Cu, K, Mg, Na, P, S, Se, and Zn;

ii) To identify genes and miRNAs correlated to the *Longissimus thoracis* concentration of Ca, Cu, K, Mg, Na, P, S, Se, Zn and Fe regarding the entire Nelore population;

iii) To identify genes and miRNAs with regulatory impact on mineral concentration;

iv) To identify metabolic pathways in which the DEGs and the correlated genes partake and their putative role in regulating muscle mineral homeostasis;

1.4. REFERENCES

ABIEC. Perfil da pecuária no Brasil. **Associação Brasileira das indústrias de Exportação de Carnes Bovina**, v. 4, 2019.

ANTUNES DE LEMOS, M. V. et al. Copy number variation regions in Nellore cattle: Evidences of environment adaptation. **Livestock Science**, v. 207, p. 51–58, 2018.

ARTHUR, J. R. et al. The role of selenium in thyroid hormone metabolism and effects of selenium deficiency on thyroid hormone and iodine metabolism. **Biological Trace Element Research**, v. 34, 1992.

BACH, J. F. & DARDENNE, M. Thymulin, a zinc-dependent hormone. **Medical Oncology and Tumor Pharmacotherapy**, v. 6, p. 25–29, 1989.

BADIS, B. Levels of Selected Heavy Metals in Fresh Meat from Cattle, Sheep, Chicken and Camel Produced in Algeria. **Annual Research and Review in Biology**, v. 4, p. 1260–1267, 2014.

BANO, D., JEWELL, S. A. & NICOTERA, P. Calcium signaling then and now, via Stockholm. **Biochemical and Biophysical Research Communications**, v. 482, p. 384–387, 2017.

BROSNAN, J. & BROSNAN, M. The sulfur-containing amino acids: An overview. In 5th Amino Acid Assessment Workshop. **American Society for Nutrition**, v.136, p. 16365–16405, 2006.

BUCHACHENKO, A. L. et al. Magnesium isotope effects in enzymatic phosphorylation. **The Journal of physical chemistry B**, v. 112, p. 2548–2556, 2008.

CAMMACK, R., WRIGGLESWORTH, J. M. & BAUM, H. Chapter 2: Iron-dependent enzymes in mammalian systems. **In Iron: transport and storage**, p. 17–39,1990.

CAMPBELL, I. Macronutrients, minerals, vitamins and energy. **Anaesthesia and Intensive Care Medicine**, v. 18, p. 141–146, 2017.

CASE, B. R. M. & CLAUSEN, T. The relationship between calcium exchange and enzyme secretion in the isolated rat pancreas. **Journal of Physiology**, v. 235, p. 75–102, 1973.

CESAR, A. S. M. et al. Identification of putative regulatory regions and transcription factors associated with intramuscular fat content traits. **BMC Genomics**, v. 19, p. 1–20, 2018.

CHAN, E. K. F.; NAGARAJ, S. H. & REVERTER, A. The evolution of tropical adaptation: Comparing taurine and zebu cattle. **Animal Genetics**, v. 41, p. 467–477, 2010.

CIOFFI, D. L., BARRY, C. J. & STEVENS, T. Role of Calcium as a Second Messenger in Signaling: A Focus on Endothelium. **Textbook of Pulmonary Vascular Disease**, p. 261–

272, 2011.

DE SOUZA, M. M. et al. A comprehensive manually-curated compendium of bovine transcription factors. **Scientific Reports**, v. 8, p. 1–12, 2018.

DELL, B. L. O. Mineral Interactions Relevant to Nutrient Requirements. **The Journal of Nutrition**, v. 119, p. 1832-1838, 1989.

DEVOR, M. Sodium channels and mechanisms of neuropathic pain**. Journal of Pain**, v. 7, p. S3, 2006.

DINIZ, W. J. et al. Iron content affects lipogenic gene expression in the muscle of Nelore beef cattle. **PLoS One**, v.11, p. 1–19, 2016.

DINIZ, W. J. S. et al. Detection of Co-expressed Pathway Modules Associated With Mineral Concentration and Meat Quality in Nelore Cattle. **Frontiers in Genetics**, v. 10, p. 1–12, 2019.

EBASHI, S. & ENDO, M. Calcium and muscle contraction. **Progress in Biophysics and Molecular Biology**, v. 18, p. 123–183, 1968.

FLEMING, L. W.; LENMAN, J. A.; STEWART, W. K. Effect of magnesium on nerve conduction velocity during regular dialysis treatment. **Journal of neurology, neurosurgery and psychiatry**, v. 35, p. 342–355, 1972.

FLOHE, L. Selen im Peroxidstoffwechsel. **Medizinische Klinik**, v. 92, p. 5–7, 1997.

GEESINK, G. H. & KOOHMARAIE, M. Effect of calpastatin on degradation of myofibrillar proteins by μ-calpain under postmortem conditions. **Journal of Animal Science**, v. 77, p. 2685–2692, 1999.

GENTHER, O. N. & HANSEN, S. L. Effect of dietary trace mineral supplementation and a multi-element trace mineral injection on shipping response and growth performance of beef cattle. **Journal of Animal Science**, v. 92, p. 2522–30, 2014.

GHARIBZAHEDI, S. M. T. & JAFARI, S. M. The importance of minerals in human nutrition: Bioavailability, food fortification, processing effects and nanoencapsulation. **Trends in Food Science and Technology**, v. 62, p. 119–132, 2017.

GLANCY, B. et al. Effect of Calcium on the Oxidative Phosphorylation Cascade in Skeletal Muscle Mitochondria, **Biochemistry**, v. 52, p. 2793–2809, 2013.

HÉLYETTE GEMAN, P. V. E. Live Cattle as a New Frontier in Commodity Markets. **Journal of Agriculture and Sustainability**, v. 12, p. 461–474, 1991.

HOLLÓ, G. et al. Effect of feeding on the composition of l*ongissimus* muscle of Hungarian Grey and Holstein Friesian bulls. **Arch. Tierzucht**, v. 50, p. 575–586, 2007.

HOWARD, J. E. Calcium metabolism, bones and calcium homeostasis; a review of certain current concepts. **The Journal of Clinical Endocrinology and Metabolism**, v. 17, p. 1105–1123, 1957.

IRANO, N. et al. Genome-wide association study for indicator traits of sexual precocity in Nellore cattle. **PLoS One**, v. 11, p. 1–14, 2016.

AHOLA, J. K. et al. Effect of copper, zinc, and manganese supplementation and source on reproduction, mineral status, and performance in grazing beef cattle over a two-year period. **Journal of Animal Science**, v. 95, p. 47–47, 2004.

KLINMAN, J. P. et al. Status of the cofactor identity in copper oxidative enzymes. **FEBS Letters**, v. 282, p. 1–4, 1991.

KOMARNISKY, L. A., CHRISTOPHERSON, R. J. & BASU, T. K. Sulfur: Its clinical and toxicologic aspects. **Nutrition**, v. 19, p. 54–61, 2003.

KUMAR, S. & BERL, T. Electrolyte quintet: Sodium. **The Lancet**, v. 352, p. 220–8, 1998.

MATEESCU, R. G. et al. Genetic parameters for concentrations of minerals in *longissimus* muscle and their associations with palatability traits in angus cattle. **Journal of Animal Science**, v. 91, p. 1067–1075, 2013a.

MATEESCU, R. G. et al. Genome-wide association study of concentrations of iron and other minerals in *longissimus* muscle of Angus cattle. **Journal of Animal Science**, v. 91, p. 3593–3600, 2013b.

MCCALL, K. A., HUANG, C.-C. & FIERKE, C. A. Zinc and Health: Current Status and Future Directions. Function and Mechanism of Zinc Metalloenzymes. **American Society for Nutritional Sciences**, v. 130, p. 1437–1446, 2000.

MORRIS, C. A. et al. Effects of quantitative trait loci and the myostatin locus on trace and macro elements (minerals) in bovine liver, muscle and kidney. **Animal Genetics**, v. 44, p. 361–368, 2013.

PORTO-NETO, L. R. et al. The genetic architecture of climatic adaptation of tropical cattle. **PLoS One**, v. 9, p. 1–22, 2014.

RONCOLETTA, M et al. Fertility-associated proteins in Nelore bull sperm membranes. **Animal Reproduction Science**, v. 91, p. 77–87, 2006.

SANDSTRÖM, B. Micronutrient interactions: effects on absorption and bioavailability. **The British Journal of Nutrition**, v. 85, p. S181, 2001.

SOMOGYI, T. et al. Mineral Content of Three Several Muscles from Six Cattle Genotypes. **Acta Alimentaria**, v. 44, p. 51–59, 2015.

STINCONE, A. et al. The return of metabolism: Biochemistry and physiology of the pentose phosphate pathway. **Biological Reviews of the Cambridge Philosophical Society**, v. 90, p. 927–963, 2015.

SUTTLE, N. **Mineral nutrition of livestock**, **chapter 13: Iron**, 2010. doi:10.1079/9781845934729.0000

TIZIOTO, P. C. et al. Calcium and potassium content in beef: Influences on tenderness and associations with molecular markers in Nellore cattle. **Meat Science**, v. 96, p. 436–440, 2014.

TIZIOTO, P. C. et al. Detection of quantitative trait loci for mineral content of Nelore *longissimus dorsi* muscle. **Genetics Selection Evolution**, v. 47, p. 1–9, 2015.

TIZIOTO, P. C. et al. Genome scan for meat quality traits in Nelore beef cattle. **Physiological Genomics**, v. 45, p. 1012–1020, 2013.

WAMELINK, M. M. C., STRUYS, E. A. & JAKOBS, C. The biochemistry, metabolism and inherited defects of the pentose phosphate pathway: A review. Journal of Inherited Metabolic Disease, v. 31, p. 703–717, 2008.

CHAPTER 2: MUSCLE TRANSCRIPTOME ANALYSIS REVEALS GENES AND METABOLIC PATHWAYS RELATED TO MINERAL CONCENTRATION IN *BOS INDICUS*

2.1. ABSTRACT

Mineral content affects the biological processes underlying beef quality. Muscle mineral concentration depends not only on intake-outtake balance and muscle type, but also on age, environment, breed, and genetic factors. To unveil the genetic factors involved in muscle mineral concentration, we applied a pairwise differential gene expression analysis in groups of Nelore steers genetically divergent for nine different mineral concentrations. Here, based on significant expression differences between contrasting groups, we presented candidate genes for the genetic regulation of mineral concentration in muscle. Functional enrichment and protein-protein interaction network analyses were carried out to search for gene regulatory processes concerning each mineral. The core genetic regulation for all minerals studied, except Zn, seems to rest on interactions between components of the extracellular matrix. Regulation of adipogenesis-related pathways was also significant in our results. Antagonistic patterns of gene expression for fatty acid metabolism-related genes may explain the Cu and Zn antagonistic effect on fatty acid accumulation. Our results shed light on the role of these minerals on cell function. This chapter was already published in the Scientific Reports journal in September, 2019 with the same title and with Juliana Afonso, Luiz Lehmann Coutinho, Polyana Cristine Tizioto, Wellison Jarles da Silva Diniz, Andressa Oliveira de Lima, Marina Ibelli Pereira Rocha, Carlos Eduardo Buss, Bruno Gabriel Nascimento Andrade, Otávio Piaya, Juliana Virginio da Silva, Laura Albuquerque Lins, Caio Fernando Gromboni, Ana Rita Araújo Nogueira, Marina Rufino Salinas Fortes, Gerson Barreto Mourao and Luciana Correia de Almeida Regitano as authors (doi: 10.1038/s41598-019-49089-x).

Keywords: RNA-seq, beef cattle, Zinc, Copper, Calcium

2.2. INTRODUCTION

The role of minerals in meat quality traits is perceived in the nutritional value of beef. For example, high iron content is a major player in the claims regarding nutritional value (DUAN et al., 2011). The second meat quality trait affected by minerals is beef tenderness since calcium related-proteases take part in the *post-mortem* degradation of myofibrillar proteins (GEESINK et al., 1999). As minerals are essential for a variety of biological processes such as metabolism, homeostasis maintenance, growth, influencing cellular structural components, enzyme cofactors, regulation of cell replication, and differentiation (SUTTLE, 2010), they may affect other economically important traits in livestock production.

Mineral concentration in mammalian muscles depends on animal intake-outtake imbalance (MORRIS et al., 2013), muscle type (SOMOGYI et al., 2015), age, environment (TIZIOTO et al., 2014), breed (HOLLÓ et al., 2007), and other genetic factor (MATEESCU et al., 2013). Minerals can only perform their biological function in muscle cells if they are available in the right amount (SUTTLE, 2010). Their concentration is under strict control for homeostasis maintenance. The genetic control of mineral homeostasis is not fully understood, although there is evidence regarding specific genes and certain gene functions linked to mineral concentration in many species. Calcium concentration in humans depends upon a complex network of hormones (BONNY and BOCHUD, 2014). The same authors showed that both serum and urinary calcium were deemed continuous heritable traits, in a study with twins. Genes related to sodium and potassium homeostasis in humans were reviewed elsewere (UDENSI and TCHOUNWOU, 2017). Magnesium absorption in bovine is breed dependent (MARTENS et al., 2018). Zinc homeostasis is poorly understood, but in *C. elegans* there is a conserved motif called low zinc activation element in promoters that seems to be involved in the process (DIETRICH, SCHNEIDER and KORNFELD, 2017) Genes associated to copper transport in higher eukaryotes (hCTR1/2, Atox1 and Atp7A/B) were detected in a yeast functional screen that aimed to find genes linked to copper-dependent respiratory growth, which could be candidate markers to human mitochondrial diseases (SCHLECHT et al., 2014). Genes related to iron concentration participate in lipid metabolism in Nelore cattle (DINIZ et al., 2016). Still, information about genes associated with mineral composition in beef is scarce.

Scientific evidence about genetic mechanisms associated with bovine mineral deposition regulation in muscle comes from a limited number of studies. Quantitative trait loci (QTLs) related to mineral concentration were described in Jersey x Limousin crosses

(MORRIS et al., 2013), Nelore (TIZIOTO et al., 2015), Holstein, and Jersey (BUITENHUIS et al., 2015) cattle. These studies reported some overlapping QTLs and enriched functional processes among different minerals, indicating shared genetic regulation.

Once minerals participate in a variety of biochemical processes that might affect production traits, understanding the genetic and physiological processes underlying muscle mineral concentration might provide the basis for modulating these processes to the benefit of cattle production. Selective breeding could incorporate gene polymorphisms that influence mineral composition to improve the nutritional value of beef (HILL, 2012). Understanding the genetics and gene regulation associated with muscle minerals in cattle may also provide some evidence for how conserved these are across species. Given biochemical similarities across mammals, it is possible that increased knowledge from cattle studies might be generalized to humans.

Herein, to characterize the biological pathways involved in muscle mineral deposition, we described a differential expression RNA-seq analysis from *Longissimus thoracis* muscle of contrasting mineral content Nelore steers, pinpointing genes, processes, and pathways related to mineral homeostasis. The minerals analyzed were Calcium (Ca), Copper (Cu), Potassium (K), Magnesium (Mg), Sodium (Na), Phosphorus (P), Sulfur (S), Selenium (Se), and Zinc (Zn).

2.3. METHODS

2.3.1. Animals

All animal and experimental procedures were carried out following the guidelines provided by the Institutional Animal Care and Use Committee Guidelines of Embrapa Pecuária Sudeste ethics committee (São Carlos, São Paulo, Brazil. Protocol CEUA 01/2013). The Ethical Committee of Embrapa Pecuária Sudeste (São Carlos, São Paulo, Brazil) approved all experimental and animal protocols (approval code CEUA 01/2013). A group of 133 Nelore steers composes our samples that previous projects already used to produce data for mineral concentration (TIZIOTO et al., 2015), and RNA-Seq (DINIZ et al., 2016). The entire sample group comes from a population of 373 Nelore steers fathered by 34 purebred Nelore sires in half-sibling families.

The animals used in our work result from artificial insemination, were born in two different breeding seasons, in two different farms. Approximately at 21 months of age, all

animals used in this research were transferred and maintained in a feedlot at Embrapa Pecuária Sudeste (São Carlos, São Paulo, Brazil). After a 28 days adaptation period, they received food, water, and had a similar nutritional and sanitary management until the slaughter. The animals had *ad libitum* feed access twice a day with 5% refusals, discarded daily. The diet contained 40% of dry matter constituted by corn silage, crude protein, ground corn, soybean meal, cottonseed, soybean hull, limestone, mineral mixture, urea and monensin (Rumensin®).

2.3.2. Mineral concentration genetic breeding value and contrasting groups

Mineral concentrations were measured as described elsewhere (TIZIOTO et al., 2014) from *Longissimus thoracis* muscle steaks sampled between 11th and 13th ribs. Briefly, the samples were lyophilized and digested with microwave assistance using a closed-vessel microwave digestion system (Ethos-1600, Milestone-MLS, Sorisole, Italy). The mineral quantification was obtained in the Vista Pro-CCD ICP-OES spectrometer with a radial view (Varian, Mulgrave, Australia). Among measured minerals we selected Calcium (Ca), Copper (Cu), Potassium (K), Magnesium (Mg), Sodium (Na), Phosphorus (P), Sulfur (S), Selenium (Se), and Zinc (Zn) for our analyses because they have distinguished extreme animal groups.

The genetic breeding values (GEBV) for all mineral's concentration were estimated elsewhere (TIZIOTO et al., 2015) for 373 animals encompassing our samples using a Bayesian model implemented in GenSel software (FERNANDO and GARRICK, 2008). The model considered contemporary groups formed by birthplace, feedlot location, and breeding season as fixed effects and age at slaughter as a covariate. The GEBVs were used to select 12 animals for each mineral with extreme phenotypes (six with high GEBV, called H, and six with low GEBV, called L).

2.3.3. RNA-Seq data

We used muscle samples from all animals in each contrasting group for RNA extraction and RNA-Seq analysis as described elsewhere (DINIZ et al., 2016). Total RNA was extracted using TRIzol® (Life Technologies, Carlsbad, CA). Its integrity was analyzed in a Bioanalyzer 2100® (Agilent, Santa Clara, CA, USA). Library preparation for RNA-Seq analysis was carried out using the TruSeq RNA Sample Preparation Kit (Illumina, San Diego,

CA). Sequencing was carried out in an Illumina HiSeq 2500®. All laboratory procedures were carried out in ESALQ Genomics Center (Piracicaba, SP, Brazil).

2.3.4. DEGs identification

RNA-Seq data obtained from muscle samples belonging to contrasting groups for a given mineral were used to determine DEGs for each mineral. The pipeline was as described in Diniz et al. (2016), with the insertion of StringTie v1.2.2 (PERTEA et al., 2015) instead of Cufflinks in Tuxedo Suite pipeline (TRAPNELL et al., 2011).

SeqClean software (http://sourceforge.net/projects/seqclean/files/) was used to trim low-quality sequences and adapters. TopHat software v2.0.11 (TRAPNELL et al., 2011) was used to align reads to the reference bovine genome (*Bos taurus* UMD 3.1, http://www.ensembl.org/Bos_taurus/Info/Index). After that, the StringTie v1.2.2 (PERTEA et al., 2015) was used to assemble the transcripts and to estimate their expression levels, normalized as FPKM (fragments per kilobases per million). Cuffdiff v2.2.1 (TRAPNELL et al., 2011) was then used to test for differential expression, calculating the average of each gene expression among the samples of the same contrasting group and calculating the FC. Only transcripts that passed the threshold of at least ten fragments aligned entered the differential expression test.

We performed a functional annotation analysis using Trinotate pipeline (http://trinotate.sourceforge.net/) to identify possible functions of non-annotated and predicted differentially expressed proteins for the minerals.

2.3.5. Relationship among minerals

We used a pairwise Pearson correlation analysis for the GEBVs of all minerals to quantify their dependency. Also, we performed a Pearson correlation analysis between GEBV and raw concentration measure for each mineral in order to convey the reliability of the GEBVs. A t-test was applied to verify if the mean GEBVs of the samples for all contrasting groups would also be statistically different for any other mineral.

2.3.6. Biological Processes and Pathways

We performed enrichment analysis using DAVID v6.8 software (HUANG, SHERMAN and LEMPICKI, 2009) to discover biological processes in which the DEGs are acting. To access known protein-protein interaction regarding DEGs and pathways in which they may participate, we used STRING v10.5 software (SZKLARCZYUK et al., 2017).

2.4. RESULTS

2.4.1. Animals and RNA-Seq analysis

Each contrasting group for a specific mineral was called Low (L) or High (H) and differentiated by the corresponding mineral symbol. Due to the overlapping of samples among groups, 44 samples comprised our 18 groups. The average GEBV (TIZIOTO et al., 2015) and mineral concentration for contrasting groups confirmed they were significantly different and comparable, as shown in Table 2.1. The average number of read pairs aligned was 13,333,842, and the average percentage of reads aligned to the reference Bovine Genome (UMD 3.1) was 91.82%. Our sequencing allowed the identification of a significant number of transcripts. The transcripts discovery saturation curves (discovered transcripts *versus* reads sequenced) from the samples assessed here are shown in Supplementary Figure S2.1.

We identified 29,312 transcripts but tested only 15,012 for differential expression due to their expression levels, since Cuffdiff v2.2.1 (TRAPNELL et al., 2011) parameters were set to do not take into account genes with less than ten reads aligned, in both differential expression analysis and multiple test correction.

TABLE 2.1. Statistics of the genetic estimated breeding values and RNA-Seq for each extreme group. All values presented are averages of the values inside each extreme group.

Group	GEBV	St. Error[a]	Concentration[b]	St. Error[c]	Read aligned pairs	Alignment (%)	T-test p-value[d]
Low-Ca	-0.1122	0.007	85.75	9.1261	10,103,844	93.98	
High-Ca	0.1366	0.0247	346.71	31.3709	16,664,657	91.48	8.55E-05
Low-Cu	-0.0607	0.0015	1.13	0.0396	10,280,771	92.9	
High-Cu	0.1228	0.0378	4.46	1.6121	12,204,273	92.15	4.70E-03
Low-K	-0.0447	0.0035	976.05	26.2935	14,682,381	91.22	
High-K	0.0872	0.0028	2152.36	65.5082	13,526,576	91.63	1.30E-10
Low-Mg	-0.0435	0.0026	668.6	14.788	14,682,381	91.22	
High-Mg	0.0773	0.0038	1401.05	32.1704	15,112,850	91.67	1.05E-09
Low-Na	-0.0478	0.0035	1544.6	57.8293	13,098,861	91.57	
High-Na	0.097	0.0047	3807.57	136.1052	15,112,850	91.67	1.05E-09
Low-P	-0.0459	0.002	6354.98	232.1688	13,827,066	91.68	
High-P	0.0843	0.0031	14128.47	523.2822	13,526,576	91.63	1.30E-10
Low-S	-0.061	0.0017	4650.32	260.7678	11,665,773	92.07	
High-S	0.0832	0.0041	11783.28	588.4472	14,037,706	91.23	1.63E-08
Low-Se	-0.1703	0.0087	0.0765	0.0052	12,902,391	91.97	
High-Se	0.1143	0.0066	0.32	0.0209	10,678,101	91.05	5.02E-10
Low-Zn	-0.071	0.0058	58.59	2.6137	13,370,593	91.98	
High-Zn	0.1115	0.0061	183.17	9.4696	14,531,511	91.63	1.04E-09

[a]standard error of the media for GEBV of each mineral, [b]average mineral concentration in mg/Kg for each extreme group, [c]standard error of the media for the mineral concentration of each mineral, [d]p-value of the test of significance (t-test) between the extreme group samples' GEBVs for each mineral.

2.4.2. Differentially expressed genes (DEGs)

We identified 327 annotated DEGs considering all minerals. The number and annotation status of the DEGs were variable among the evaluated groups (Table 2.2). All DEGs and their fold change (FC) values between contrasting groups for each mineral are in Supplementary Table S2.1. There were no common DEGs to all minerals. However, 27 genes were common to at least five minerals. From these, we can highlight *COL11A1*, *COMP* and *TNMD* genes, common to eight minerals (all, except Zn). The minerals with more DEGs overlapping were Mg, Na, K, and P, with 25. In all expression comparisons between contrasting groups, upregulation means higher expression in H-groups than in L-groups. Conversely, downregulation means lower expression in H-groups than in L-groups. Unlike Zn, which had 50% of the DEGs downregulated, the remaining minerals presented at least 66% of the DEGs as downregulated.

TABLE 2.2. Number and Annotation status of DEGs per mineral.

Mineral	**Ca**	**Cu**	**P**	**Mg**	**K**	**Se**	**Na**	**Zn**	**S**
Annotated genes[a]	170	125	43	53	51	25	55	27	15
Predicted proteins[b]	24	7	6	5	5	6	5	4	3
Non-annotated genes[c]	35	23	17	22	23	6	13	4	4
Upregulated[d]	34	13	8	10	9	9	13	15	6
Downregulated[e]	160	119	41	48	47	22	47	16	12
Total	229	155	66	80	79	37	73	35	22

[a] genes with known annotation based on the bovine reference genome (UMD 3.1), [b] transcripts with predicted annotation, [c] transcripts with unknown annotation, [d] annotated genes and predicted proteins more expressed in the high groups, [e] annotated genes and predicted proteins more expressed in the low groups.

DEGs with the highest estimated FC (>1.9) between each contrasting mineral group were *MT2A* for K, Mg, Na, and P; *RN5-8S1* for Se and S; *HSPA6* for Cu, Zn, P and Se; *PMP2* for Cu, and *GBP4* for Ca. DEGs with lowest FC (<1.9) between groups were *TNMD*, *COMP*, and *COL11A1* for eight minerals (except for Zn); *FBLN7* in seven of them (except for S and Zn), and *CILP2* in six (except for S, Zn, and Na). Among DEGs with the lowest FC (downregulated in the H-group) for at least two minerals, we found *PERP* for Cu, K, Mg, P, and Se; *TNC* and *THBS4* for Cu, K, Mg, and P; *COL22A1* for Cu, Na, P, and Se; *ADAM12* for Cu and Se; *ACTC1* for *K* and *P*; *CRABP2* and *CRTAC1* for K, Mg, and P; *KCNK2*, *MKX* and *MXRA5* for Ca and Cu.

Regarding individual minerals, we found *TF*, *HOXA9*, *MIR196B*, and *SYT4* genes as top downregulated in H-Ca group; *ELOVL6*, *PTGIR*, *COL12A1*, *GAS2*, *POSTN*, *WISP1*, *MLLT11*, and *THRSP* for Cu; *PI1S for* Na; *MYLK3* for S; and *RN5-8S1* for Zn. From Se and S analyses, *RN5851* gene was upregulated in higher mineral concentration group.

2.4.3. Functional enrichment analysis

We performed a functional annotation analysis applying the Trinotate pipeline (http://trinotate.sourceforge.net/) to identify possible biological functions of non-annotated DEGs. We retrieved possible functions for 31 transcripts. From these, 18 presented functions related to LINE-1 retrotransposable elements, retrovirus-related Pol polyprotein, and immune response related functions. We also recovered the function “similar to the protein SAMHD1”, a restriction nuclease that suppresses LINE-1 retrotransposition activity (HU et al., 2015) (Supplementary Table S2.2). Among the non-annotated transcripts from Cu DEGs, one is highly similar to a myoregulin (GO: 0016021), with high homology to a human *MRLN* gene (91.30% of similarity). Another one was annotated as the Sentrin-specific protease 3, having homology with a mouse *SENP3* gene (92.86% of similarity).

We clustered annotated functions obtained with DAVID software (HUANG, SHERMAN and LEMPICKI, 2009) for each predicted protein whose coding gene was a DEG for each mineral. The summarized significant analysis is presented in Table 2.3. We did not obtain substantial annotated function clusters for Zn and S. Common functions in at least four minerals were related to the extracellular matrix (enriched in seven minerals), extracellular matrix-receptor interaction (ECM-receptor interaction), collagen and secretion, the latest three enriched in six minerals. Also, for five minerals we identified disulfide bond, epidermal growth factor-like domain, focal adhesion and, for four minerals, protein digestion and absorption.

TABLE 2.3. DEGs summarized significative annotated function clusters. The results were obtained using DAVID software. There are no significative results for Zn e S. Results are displayed for each mineral and in alphabetic order.

Ca	Cu	P	Mg	K	Se	Na
Cell-cell interaction	Calcium ion binding	Cell adhesion	Carboxypeptidase	Collagen	Extracellular matrix	Carboxypeptidase
Collagen	Carboxypeptidase	Collagen	Collagen	Disulfide bond		Cell adhesion
ECM-receptor interaction	Cell adhesion	Disulfide bond	Disulfide bond	ECM-receptor interaction		Collagen
Extracellular matrix	Cell-cell interaction	ECM-receptor interaction	ECM-receptor interaction	Epidermal growth factor-like domain		Disulfide bond
Protein digestion and absorption	Collagen	Epidermal growth factor-like domain	Epidermal growth factor-like domain	Extracellular matrix		ECM-receptor interaction
Proteoglycans	Disulfide bond	Extracellular matrix	Extracellular matrix	Focal adhesion		Epidermal growth factor-like domain
Secretion	ECM-receptor interaction	Focal adhesion	Focal adhesion	Glycoprotein		Extracellular matrix
Signaling	Epidermal growth factor-like domain	PI3K-Akt signaling pathway	Glycoprotein	Immunoglobulin-like domain		Focal adhesion
	Extracellular matrix	Protein digestion and absorption	Secretion	Secretion		Glycoprotein
	Fatty acid metabolism	Secretion				Leucine-rich repeat
	Focal adhesion					Protein digestion and absorption
	PI3K-Akt signaling pathway					Secretion
	Protein digestion and absorption					
	Secretion					
	Signaling					

2.4.4. Relationship among minerals

The GEBVs for most mineral concentrations showed significant Pearson correlations in our population, ranging from -0.2 to 0.97 (Supplementary Table S2.3). Also, high significant correlations were observed between each GEBV and their correspondent raw mineral concentrations, varying from 0.77 to 0.86 (Supplementary Table S2.4). Results of t-tests to verify if the mean GEBVs of the samples used to represent the contrasting groups for one mineral would also be statistically different for any other mineral are shown in Supplementary Table S2.5.

2.4.5. Protein-protein interaction and pathways among DEGs

To identify biological processes involving the DEGs, we performed a protein-protein interaction (PPI) network analysis among DEGs for each mineral using STRING v.1.2.2 software (TRAPNELL et al., 2011), which retrieves pathways from KEGG database (KANEHISA et al., 2017). DEGs for each mineral partaking in known PPI, and its significant pathways, are shown in Figure 2.1. Sulfur did not present a significant pathway.

All DEGs presented in the same pathway for a given mineral had the same direction of expression, *i.e.*, they were either all upregulated or all downregulated (Supplementary Table S2.1). DEGs presented in each pathway across mineral analyses can be seen in Figure 2.2. Significant pathways for all minerals are shown in Table 2.4. ECM-receptor interaction pathway was common to seven minerals (except Zn and S), protein digestion and absorption pathway was common to six (except Zn, S, and K), and focal adhesion pathway and PI3K-Akt signaling pathway to five (except Ca, Se, Zn, and S). All DEGs presented in these pathways were downregulated.

Fatty acid metabolism pathway was common to Zn and Cu. This was the only pathway where DEGs had different regulation between both minerals. Of all DEGs in this pathway, three were common for both minerals (*ELOVL6*, *FASN*, and *SCD*) and two were exclusive to Cu concentration analysis (*ELOVL5* and *ACACA*) (Figure 2.2). From all minerals, Cu retrieved more enriched pathways (N = 10), whereas prion disease and phagosome pathways were identified only in Ca and K analyses, respectively.

After filtering out DEGs that did not interact in our PPI network, 96 remained for Ca, 64 for Cu, 17 for K, 18 for Mg, 19 for Na, 20 for P, two for S, 11 for Se, and 10 for Zn. In total, Ca and Cu had more than 50% of their DEGs taking part in an interaction (56.47% and

51.2%, respectively), P and Se had around 45% (46.5% and 44%, respectively), K, Na, Mg, and Zn had about 35% (33.3%, 34.5%, 33.96%, and 37%,) and S had the lowest rate of DEGs in interactions, 13.3%. From DEGs' products that did not take part in protein-protein interactions, only five were part of a pathway: *COL11A2* for K, Ca, Na, Mg and Cu; *COL11A1* for P; *CILP2* for K; *CD44* for Na; and *PTGIR* for Cu.

TABLE 2.4. DEGs significative KEGG Pathways enriched for each mineral. Sulfur do not present a significative KEGG pathway. P-values displayed for each pathway.

KEGG Pathways	Ca	Cu	P	Mg	K	Se	Na	Zn
ECM-receptor interaction	0,012	2.85e-08	1.45e-07	5.65e-07	4.27e-07	0.0229	9.57e-07	-
Protein digestion and absorption	0,012	0.0009	0.0028	0.0060	-	0.0229	0.0005	-
Focal adhesion	-	0.0006	0.0006	0.0019	0.0015	-	0.002	-
PI3K-Akt signaling pathway	-	0.0024	0.0053	0.0153	0.0165	-	0.023	-
Fatty acid metabolism	-	0.0009	-	-	-	-	-	0.0104
AMPK signaling pathway	-	0.0056	-	-	-	-	-	-
Biosynthesis of unsaturated fatty acids	-	0.0121	-	-	-	-	-	-
Fatty acid biosynthesis	-	0.0206	-	-	-	-	-	-
PPAR signaling pathway	-	0.0283	-	-	-	-	-	-
Platelet activation	-	0.0311	-	-	-	-	-	-
Phagosome	-	-	-	-	0.0421	-	-	-
Prion diseases	0,014	-	-	-	-	-	-	-

FIGURE 2.1. DEGs' products protein-protein interaction network for each mineral. Proteins not partaking in an interaction are not shown. The line thickness between two proteins indicates the strength of data support. The colors inside the circles represent DEGs participating in the same pathway. The yellow halos represent DEGs upregulated in the H groups in relation to the L groups. The DEGs without a yellow halo were downregulated in the H groups in relation to L groups. **A) S, B) K, C) P, D) Ca, E) Na, F) Mg, G) Se, H) Cu, and I) Zn.**

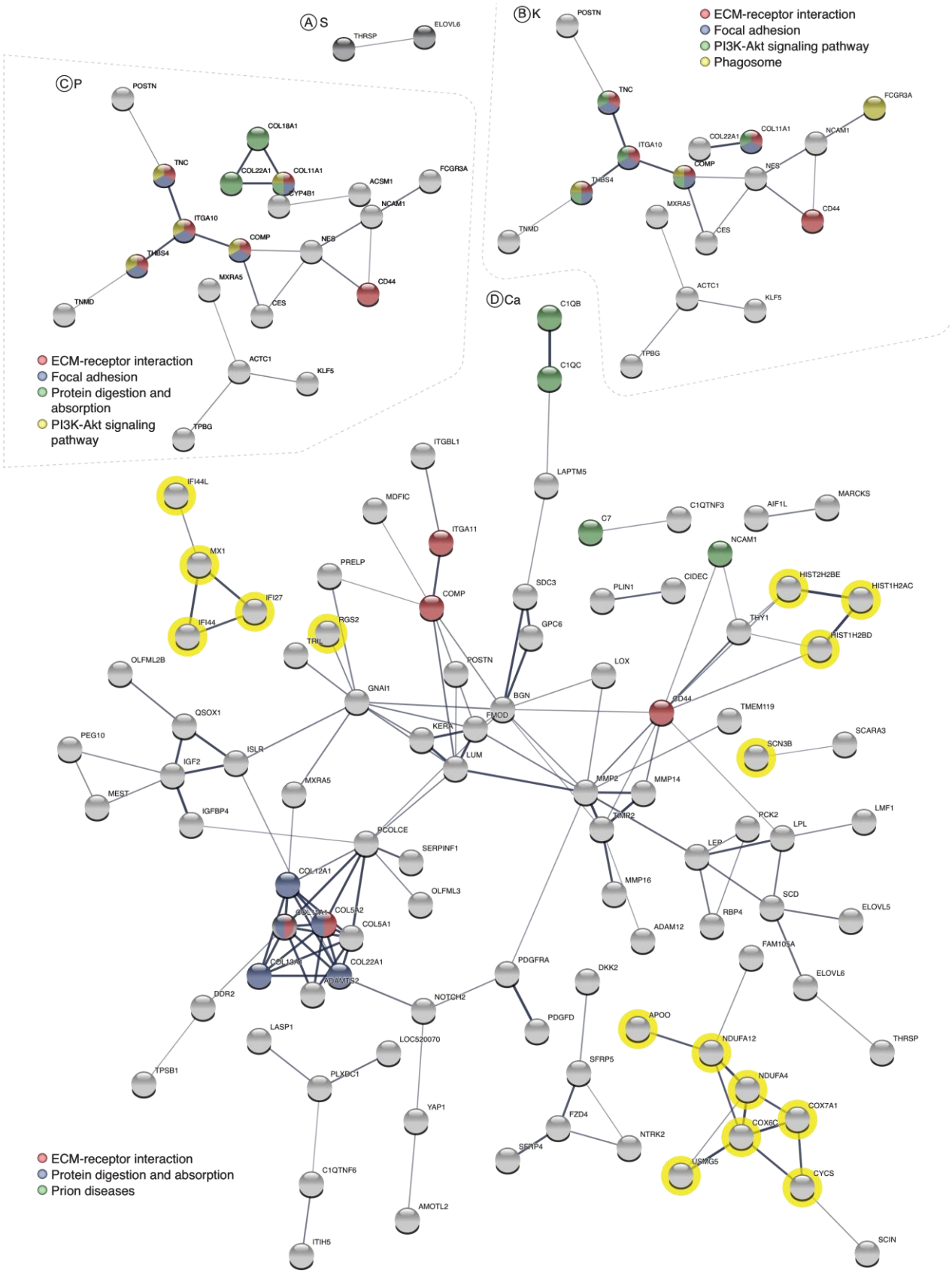

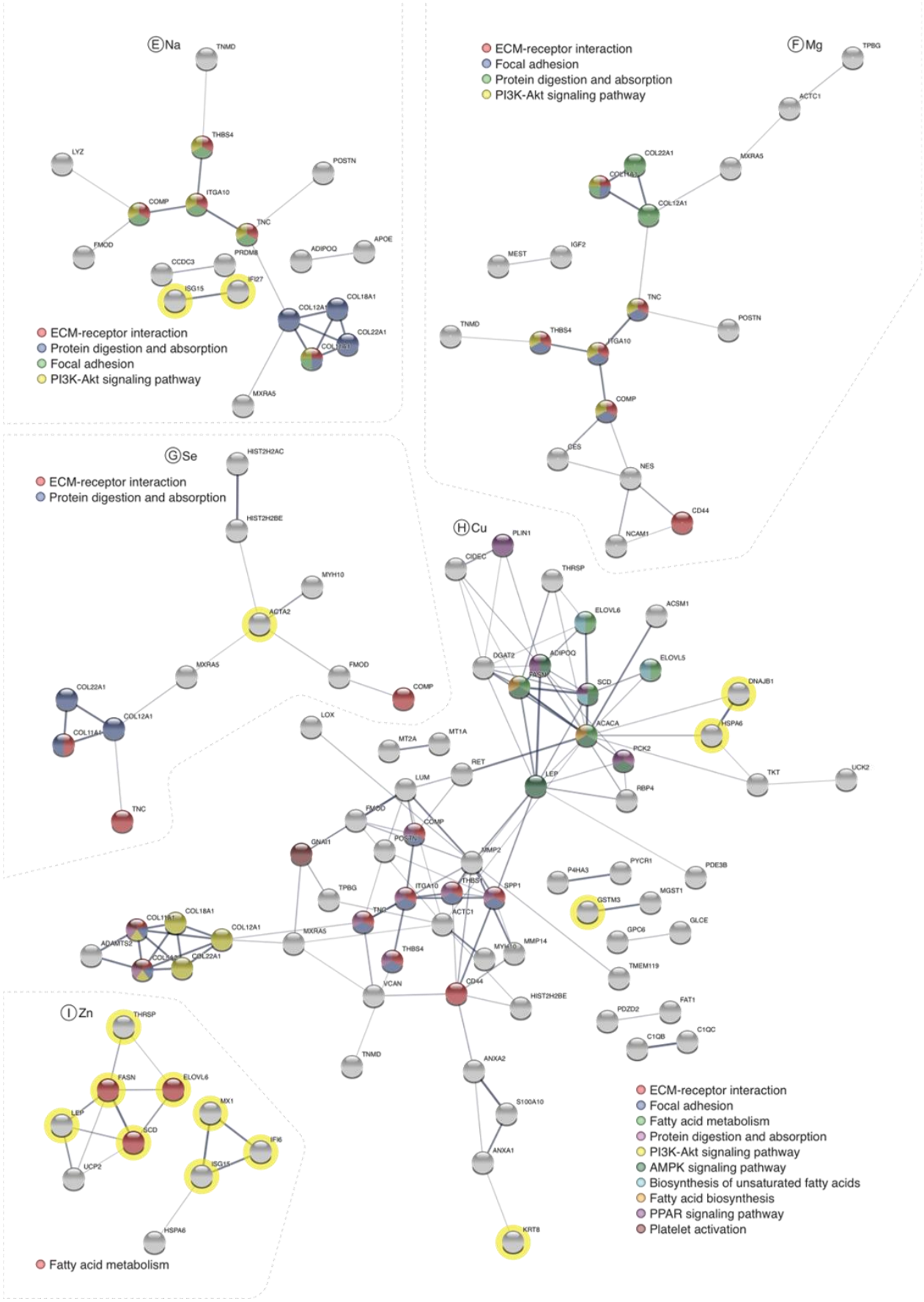
Ⓔ Na
ECM-receptor interaction
Protein digestion and absorption
Focal adhesion
PI3K-Akt signaling pathway
Ⓕ Mg
ECM-receptor interaction
Focal adhesion
Protein digestion and absorption
PI3K-Akt signaling pathway
Ⓖ Se
ECM-receptor interaction
Protein digestion and absorption
Ⓗ Cu
Ⓘ Zn
Fatty acid metabolism
ECM-receptor interaction
Focal adhesion
Fatty acid metabolism
Protein digestion and absorption
PI3K-Akt signaling pathway
AMPK signaling pathway
Biosynthesis of unsaturated fatty acids
Fatty acid biosynthesis
PPAR signaling pathway
Platelet activation

FIGURE 2.2. DEGs partaking in significant pathways. Rows: DEGs partaking in the significant pathways, columns: minerals presenting the significant pathways, colors: different significant pathways.

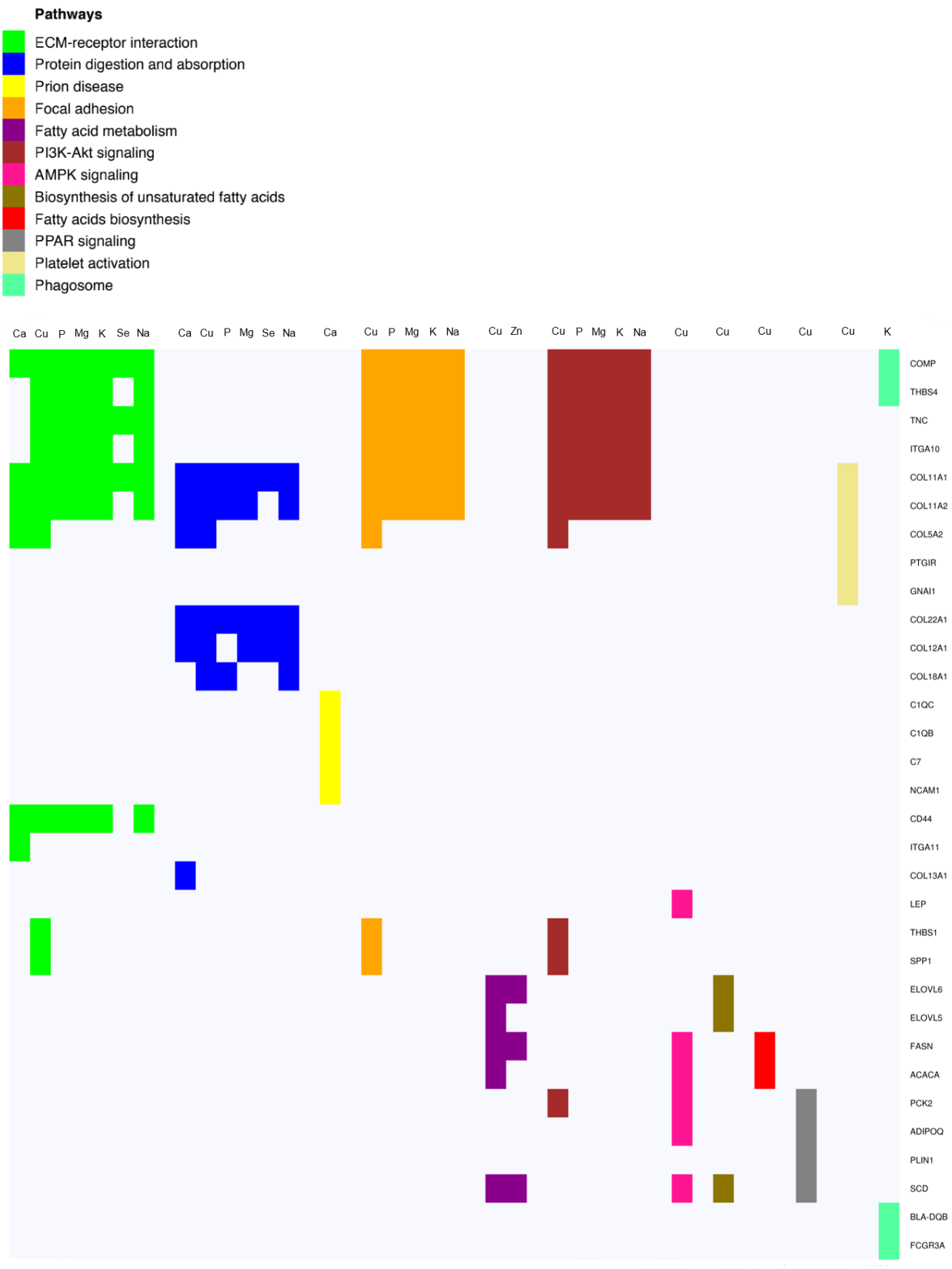

2.5. DISCUSSION

2.5.1. Heritability, GEBVs, and correlations for mineral concentration

Muscle mineral concentrations are moderately heritable traits. Estimates of heritability from our Nelore population ranged from 0.29 to 0.33 (TIZIOTO et al., 2015). Understanding the genetic component related to muscle mineral concentration might be useful to better comprehend mineral metabolism and metabolic diseases.

As expected from the correlations among GEBVs for the minerals and from the biological interconnection among them, most contrasting groups for each mineral also differed concerning other mineral's GEBVs, except for Cu and Se, even though they did not meet the criteria of representing both 5% extremes from the normal distribution. The most extreme example comes from the minerals Mg, Na, K, and P, presenting a correlation higher than 0.88 among their GEBVs. As a consequence, the same samples comprised the low-Mg and low-K, the high-Mg and high-Na and in the high-K and high-P groups. As the complementary contrasting group for each mineral had at least one different sample, the DEGs, functions, and pathways are not entirely the same among these minerals. Given this fact, one should consider that some correlated response regarding other than the mineral in discussion could exist within our results.

Mg and K, which in our analysis showed a correlation of 0.97 and 46 DEGs in common, presented the same QTLs in previous experiments with this population, thus reinforcing the common genetic control for these minerals. However, Mg and P showed the same pairwise correlation and presented 38 common DEGs, but did not showed QTLs in common (TIZIOTO et al., 2015). Similarly, despite the correlations, there were no common QTLs among Mg, K, Na, and P[15]. Thus, although not fully explained by pairwise correlation, to some extent, the common DEGs, functions, and pathways among these four minerals can result from the high correlation and sample overlapping among them.

2.5.2. Detected functions and previous works

All the enriched gene functions convey to one or more enriched pathways. The previous detection of similar functional gene clusters in a GWAS for 14 minerals (TIZIOTO et al., 2015), whose dataset included our samples, indicates conserved mechanisms affecting

mineral concentration. The involvement of common DEGs in shared pathways among minerals reinforces that various genes affect these phenotypes.

Differential expression and QTL analyses can produce similar functional annotation results, but different gene lists due to differences in the methodologies (GORLOV et al., 2009). Our DEGs were not harbored in/or near QTL regions already reported (TIZIOTO et al., 2015). However, the functional analyses of DEGs and QTLs pointed to similar gene functions. Due to this fact, we will focus our discussion on the genetic similarities among different mineral analyses.

2.5.3. DEGs with opposite FC among minerals

MT2A and *HSPA6* were the DEGs with the expression pattern presenting the highest FC contrariety and discrepancy among minerals. Both genes have a known relationship with heavy metals. The *MT2A* gene encodes a metallothionein protein that binds divalent heavy metals and participates in metal control and Zn homeostasis in the cell, affecting apoptotic and autophagy pathways (JAYAWARDENA et al., 2017) . *MT2A* was a DEG for almost all minerals in this study, except Ca and Se. It is downregulated in the H-Cu group and upregulated in the H-groups of Mg, P, Zn, Na, S, and K. From these, only Cu and Zn are divalent heavy metals. Different polymorphisms in *MT2A* or its promoter disturb Zn and Cd concentrations in human blood of healthy patients (KAYAALTI, ALIYEV and SOYLEMEZOGLU, 2011) and carotid artery stenosis patients (GIACCONI et al., 2007). Our results suggest that, apart from the already described in the literature, this gene could also be related to the concentration of other non-heavy metal minerals like Mg, K, Na, P, and S.

The *HSPA6* gene was upregulated in the H-Cu and H-S groups, while the opposite occurs for Zn and P. This gene product responds to stress, and its expression increases with the increase of heavy metal, like Cu, concentration (KOHLER et al., 1996). This protein takes part in the fatty acid metabolism pathway (FAM), where Zn and Cu are essential. The relationship between *HSPA6*, P, and S is still unknown.

2.5.4. Extracellular matrix interactions

Among the downregulated DEGs with the lowest FC accross minerals, lower than -1.9, we found *COMP*, *COL11A1*, *TNC*, *THBS4*, and *COL22A*. They were involved in common pathways for at least six minerals, which may indicate a potential common genetic

regulation of mineral concentration or a possible role of mineral concentration in the control of these genes' expression. They genes act in pathways such as ECM-receptor interaction, focal adhesion, PI3K-Akt signaling pathway, and protein digestion and absorption. The first three pathways are interconnected (http://www.genome.jp/kegg/pathway/hsa/hsa04510.html).

The DEGs *COMP* and *COL11A1*, common to eight minerals, are part of the ECM-receptor pathway. They encode cell membrane proteins that mediate the interaction between the cell and extracellular matrix (CHEN et al., 2005). Ligands such as *COL11A1* and *COMP* are essential for the initial steps of the ECM-receptor interaction pathway. Integrins continue the pathway processes, culminating in different cell functions such as growth and regeneration (IVASCA, 2012). Also, the same authors stated that focal adhesion and PI3K-Akt signaling pathways specifically need the involvement of integrins to start their metabolic processes.

The integrin gene *ITGA10* was predicted to interact with *COL11A1* and *COMP*. All analyses showing *COL11A1*, *COMP*, and *ITGA10* also showed the *TNMD* gene. This gene possibly interacts with *ITGA10* by the *THBS4* gene, which is also part of the three connected pathways. Moreover, *ITGA10* connects to *TNC*, involved in collagen formation. Thus, *COL11A1*, *COMP*, and *TNMD* take part in the three integrated pathways for K, P, Na, Mg, and Cu by its interaction with *ITGA10*. Their downregulation in H-groups suggests that a high concentration of these minerals suppresses these pathways.

The ECM-receptor interaction pathway plays an essential role in skeletal muscle development (THORSTEINSDÓTTIR ET AL., 2011), which explains this pathway being found in muscle transcriptome. Simple diffusion of minerals can occur through pores in the tight junctions if the electrochemical gradient exists to push the ions through the pores (GOFF, 2018). The *CD44* gene, a DEG for almost all minerals, has a possible role in tight junction regulation (KIRSCHNER et al., 2011). The relation of ECM-receptor interaction pathway to mineral concentration may be partially explained by the tight junctions' role in mineral absorption.

The protein digestion and absorption pathway was significant for six minerals (Ca, Cu, P, Mg, Na, and Se). The DEGs in this pathway encompass genes from the collagen family. Collagens are the most abundant protein in the ECM and take part in cell adhesion regulation, cell migration, and direct tissue development, the latest initiating after modifications in the ECM structure mediated by substrates (TIZIOTO et al., 2014). These results indicate that ECM-interactions are related to mineral concentration regulation for most of the minerals in this study.

2.5.5. Zn and Cu antagonism on fatty acid metabolism

Fatty acid metabolism pathway (FAM) was enriched in Zn and Cu analyses. Cu analysis identified five DEGs in this pathway, *ACACA*, *FASN*, *SCD*, *ELOVL6* and *ELOVL5*. From these, *FASN*, *SCD* and *ELOVL6* were the only genes for Zn content in the same pathway. They all showed interactions between their encoded proteins. All DEGs included in this pathway were downregulated in Cu and upregulated in Zn analyses.

Animals with clinical Cu deficiency tend to accumulate fat due to disturbances in FAM (ENGLE, 2011), and Zn has an antagonistic relationship in this phenomenon (MORRIS, AMYES and HICKEY, 2006). The five FAM related genes involved in Cu analysis take part in the cytoplasmic portion of the pathway, in which fatty acids biosynthesis occurs by the addition of one or more acetyl-CoA molecules, doubling the number of carbons in the fatty acid molecule produced in each cycle, as per KEGG data (https://www.genome.jp/kegg-bin/show_pathway?map01212).

Fatty acid biosynthesis can start with the co-enzyme Acetyl-CoA carboxylase, the product of *ACACA*, that catalyzes the carboxylation of acetyl-CoA to malonyl-CoA (FOSTER, 2012). Subsequently, the product of *FASN* is responsible for the elongation of the fatty acid chains to precursors with 16 carbons. The elongation to 18 carbons requires the product of *ELOVL6* (FOSTER, 2012). After that, the Stearoyl-CoA desaturase enzyme, which is the product of *SCD*, catalyzes the synthesis of Oleic acid (GOFF, 2018). Cu is a cofactor of this enzyme (CUNNANE, 1981) and, in the presence of this mineral, the FAM progresses just until the production of fatty acids with 20 carbons by the product of *ELOVL5 (*GOFF, 2018), because it inhibits the production of Linoleic acid by increasing the Oleic acid synthesis (CUNNANE, 1981). The downregulation of *ACACA*, *FASN*, *ELOVL6*, *SCD*, and *ELOVL5* in the H-Cu group can explain the inhibition of long-chain fatty acids and fat accumulation under low Cu.

A second hypothesis is that malonyl-CoA can also be the switch from fatty acids biosynthesis to fatty acids oxidation and energy production, which can lead to less fatty acid biosynthesis (FOSTER, 2012). In rabbits, copper supplementation in the diet decreased the intramuscular fat content by improving fatty acid uptake and fatty acid oxidation (LEI, XIAOYI and FUCHANG, 2017). This switch depends on the regulation of malonyl-CoA. For example, in ketosis, ketonic bodies accumulate in the tissue, and the activation of malonyl-CoA activates AMPK. This activation breaks malonyl-CoA, stopping the biosynthesis and

starting the oxidation of fatty acids (FOSTER, 2012). The AMPK signaling pathway was enriched for Cu.

The second hypothesis can be reinforced by the simultaneous presence among DEGs for Cu of the genes *FASN*, *ACACA* and *SCD*, belonging both to AMPK and FAM pathways, as well as *ADIPOQ, PCK2* and *LEP* genes, which are exclusive from the AMPK pathway. Thus, animals with less Cu can have higher fat accumulation by biosynthesis (FAM) (CUNNANE et al., 1982) or oxidation (AMPK signaling pathway) (LEI, XIAOYI and FUCHANG, 2017); probably by both processes.

Zn is a known Cu antagonist in FAM, due to its role in the stimulation of linoleic acid desaturation (CUNNANE et al., 1982). In the Zn analysis, we did not identify the *ACACA* gene as a DEG. Therefore, we hypothesized that, in this case, the product of *FASN* does the first step of fatty acid synthesis. As already discussed, the pathway continues to the precursor of oleic acid. However, in the presence of high Zn, the pathway does not stop on fatty acids with 20 carbons and Zn stimulates the linoleic acid desaturation and the production of long-chain fatty acids (IVASKA, 2012) .

In Japanese Black Cattle, there is a low negative correlation between Cu concentration and oleic acid (-0.15), between Cu and linoleic acid (-0,29), and between Zn and linoleic acid (-0.05) (KITAGAWA, FUNABA and MATSUI, 2018). This breed has more intramuscular fat than European cattle breeds. In our population, we did not identify a significant correlation between the GEBVs for oleic acid and the GEBVs for Zn and Cu concentration. We found a weak positive correlation ($r = 0.23$) between linoleic acid and Cu GEBVs (data not shown). The absence of higher correlations can be attributed to the little variation of these minerals (TIZIOTO et al., 2015) and fat deposition in our samples (CESAR et al., 2014). The samples used in the two contrasting groups for Cu and Zn analyses did not present significant ($p > 0.05$) difference for seven fatty acids concentrations obtained elsewhere (CESAR et al., 2016) (data not shown). Also, our animals did not exhibit a clinical deficiency of these minerals. Thus, we can assume that, even if the difference in expression did not lead to a significant increase in fat, animals with low Cu concentration present modifications in FAM.

PPAR signaling pathway, enriched in Cu analysis, was also identified and is related to FAM. PPAR is one of the significant adipogenesis activators (BRUN et al., 1996). Only *PLIN1* gene was in the other fatty acid associated pathways. This gene was found downregulated in Cu, like all the other FAM related genes, and its product is involved directly in lipid metabolism (TANSEY et al., 2004) and adipocyte differentiation (LYU et al., 2015). *LEP* gene is also related to Cu and Zn and has an alleged role in the PPAR pathway

regulation. It has a well-known relationship with obesity and stimulus for fatty acid oxidation (MINOKOSHI et al., 2012). As all the DEGs mentioned in FAM, *LEP* was upregulated in Zn and downregulated in Cu analyses and interacted with all DEG products in this pathway, when considering Cu, and with *FASN* and *SCD*, when considering Zn. FAM genes were already shown to be related to iron concentration in a differential expression analysis with samples from the same population used in this study (DINIZ et al., 2016).

We retrieved high similarity with known proteins for two non-annotated DEGs for Cu. One of them, downregulated for Cu, is similar to the mouse *SENP3* gene. This gene has high similarity to other SENP family protein gene, *SENP2 (*TATHAM et al., 2001). Both encode proteases that release SUMO3 and SUMO2 monomers, involved in several biological processes *(*TATHAM et al., 2001). Regarding fat deposition, overexpression of *SENP2* increases fatty acid oxidation by upregulating the expression of enzymes linked to this process (KOO et al., 2015). This non-annotated DEG can corroborate the hypothesis of the involvement of Cu concentration in fatty acid oxidation in cattle.

The *THRSP* gene, identified as upregulated for Cu and Zn, encodes a nuclear protein involved in fatty acid synthesis (DONNELLY, 2009) interacting with *FASN* and *ELOVL6. THRSP* upregulation activates *FASN* (YAO et al., 2016), being a candidate to the mechanism of FAM regulation by Zn.

Among the other four genes downregulated for Cu, *PCK2* is a candidate for obesity (BEALE, HARVEY and FOREST, 2007) and is part of AMPK and PPAR signaling pathways. This gene's product interacts with *ACACA*. It has an impact in FAM by receptor interaction and changes in *RBP4* gene, which plays a role in non-alcoholic fatty liver disease and can contribute to insulin resistance (ROMEO and VALENTI, 2016). All these genes and pathways linking Cu and Zn to lipid metabolism can explain the genetic mechanisms underlying Cu associations to FAM and Zn antagonism in these processes.

2.5.6. Pathways enriched for just one mineral

COMP, *FCGR3A*, *BLA-DQB*, and *THBS4* genes are involved in the phagosome pathway, all downregulated for K. *BLA-DQB* encodes an antigen, and the other genes encode glycoproteins with already known roles in phagocytosis. Potassium channels are known to modulate changes in the membrane during phagocytosis (DEMAUREX, 2012), which can explain the relationship between the expression of these genes and K concentration.

The genes *C1QB*, *C1QC*, *C7*, and *NCAM1* were downregulated for Ca and partake in the prion disease pathway. The first two genes showed an interaction, and they encode proteins that form the complement component 1, involved in the immune complement system. These genes are linked to the *LAPTM5* gene, which encodes a lysosomal transmembrane protein. *C7* gene encodes a serum protein involved in the immune system and is connected to *C1QTNF3*, a gene that encodes another protein involved in the immune complement system. *NCAM1* gene encodes a protein that is a cell adhesion linked to *CD44*, part of the ECM-receptor pathway, showing that all pathways detected in this study are linked.

2.6. CONCLUSION

By comparing the expression of genes in muscle samples with contrasting mineral concentrations, we hypothesized that the genetic regulation core for all minerals studied, except Zn, resides in events of extracellular matrix interaction. ECM-receptor interaction, focal adhesion, and PI3k-Akt signaling pathways seem to be related to K, P, Na, Mg, Cu, and Ca content profiles in skeletal muscle. We also pointed out genes that may explain Cu and Zn association to adipogenesis-related pathways, as well as their antagonism on fat accumulation. Future studies can target our raised hypotheses and validate our DEGs to elucidate these biological mechanisms, since our main goal was *in silico* prediction.

2.7. AUTHORS CONTRIBUTION

J.A., L.L.C., A.R.A.N., G.B.M. and L.C.A.R. designed the experiments and analysis. J.A., W.J.S.D., A.O.L., M.I.P.R., B.G.N.A., O.P., J.V.S., L.A.L. and C.F.G. performed the experiments and analysis. J.A., P.C.T., W.J.S.D., C.E.B., B.G.N.A., O.P. and M.R.S.F. interpreted the results. J.A. and L.C.A.R. drafed the manuscripts. All authors revised the manuscripts and read and approved the fnal manuscript.

2.8. REFERENCES

BEALE, E. G., HARVEY, B. J. & FOREST, C. PCK1 and PCK2 as candidate diabetes and obesity genes. **Cell Biochemistry and Biophysics**, v. 48, p. 89–95, 2007.

BONNY, O. & BOCHUD, M. Genetics of calcium homeostasis in humans: Continuum between monogenic diseases and continuous phenotypes. **Nephrology, dialysis and transplantation**, v. 29, p. iv55–iv62, 2014.

BRUN, R. P. et al. Differential activation of adipogenesis by multiple PPAR isoforms. **Genes Development**, v. 10, p. 974–984, 1996.

BUITENHUIS, B. et al. Estimation of genetic parameters and detection of quantitative trait loci for minerals in Danish Holstein and Danish Jersey milk. **BMC Genetics**, v. 16, p. 1–8, 2015.

CESAR, A. S. et al. Genome-wide association study for intramuscular fat deposition and composition in Nellore cattle. **BMC Genomics**, v. 15, p. 1-15, 2014.

CESAR, A. S. M. et al. Differences in the skeletal muscle transcriptome profile associated with extreme values of fatty acids content**. BMC Genomics**, v. 17, p. 1–16, 2016.

CHEN, F. H. et al. Cartilage Oligomeric Matrix Protein/Thrombospodin 5 Supports Chondrocyte Attachment through Interaction with Integrins. **The Journal of Biological Chemistry**, v. 292, p. 342–351, 2005.

CUNNANE, S. C. Differential regulation of essential fatty acid metabolism to the prostaglandins: possible basis for the interaction of zinc and copper in biological systems. **Progress in Lipid Research,** v. 21, p. 73-90, 1982.

CUNNANE, S. C. Zinc and copper interact antagonistically in the regulation of linoleic acid metabolism. **Progress in Lipid Research**, v. 20, p. 601-603, 1981.

DEMAUREX, N. Functions of proton channels in phagocytes. **Membrane Transport and Signaling**, v. 1, p. 3–15, 2012.

DIETRICH, N., SCHNEIDER, D. L. & KORNFELD, K. A pathway for low zinc homeostasis that is conserved in animals and acts in parallel to the pathway for high zinc homeostasis. **Nucleic Acids Research**, v. 45, p. 11658–11672, 2017.

DINIZ, W. J. et al. Iron content affects lipogenic gene expression in the muscle of Nelore beef cattle. **PLoS One**, v. 11, p. 1–19, 2016.

DUAN, Q. et al. Genetic polymorphisms in bovine transferrin receptor 2 (TFR2) and solute carrier family 40 (iron-regulated transporter), member 1 (SLC40A1) genes and their association with beef iron content. **Animal Genetics**, v. 43, p. 115–122, 2011.

ENGLE, T. E. Copper and lipid metabolism in beef cattle: A review. **Journal of Animal Science**, v. 89, p. 591–596, 2011.

FERNANDO, R. L. & GARRICK, D. J. GenSel-User manual for a portfolio of genomic selection related analyses. **Animal Breeding and Genetics**, p. 0–24, 2008.

FOSTER, D. W. Malonyl-CoA: The regulator of fatty acid synthesis and oxidation. **The Journal of Clinical Investigation**, v. 122, p. 1958–1959, 2012.

GEESINK, G. H. & KOOHMARAIE, M. Effect of Calpastatin on Degradation of Myofibrillar

GIACCONI, R. et al. The + 838 C/G MT2A Polymorphism, Metals, and the Inflammatory/Immune Response in Carotid Artery Stenosis in Elderly People. **Molecular Medicine**, v. 13, p. 388–395, 2007.

GOFF, J. P. Invited review: Mineral absorption mechanisms, mineral interactions that affect acid–base and antioxidant status, and diet considerations to improve mineral status. Journal of Dairy Science, v. 4, p. 1–51, 2018.

GORLOV, I. P. et al. GWAS meets microarray: Are the results of genome-wide association studies and gene-expression profiling consistent? Prostate cancer as an example. **PLoS One**, v. 4, 2009.

HILL, W. Quantitative Genetics in the Genomics Era. **Current Genomics**, v.13, p. 196–206, 2012.

HOLLÓ, G. et al. Effect of feeding on the composition of longissmus muscle of Hungarian Grey and Holstein Friesian bulls. **Arch. Tierzucht**, v. 50, p. 575–586, 2007.

HU, S. et al. SAMHD1 Inhibits LINE-1 Retrotransposition by Promoting Stress Granule Formation. **PLoS Genetics**, v. 11, p. 1–27, 2015.

HUANG, D. W., SHERMAN, B. T. & LEMPICKI, R. A. Systematic and integrative analysis of large gene lists using DAVID bioinformatics resources. **Nature Protocols**, v. 4, p. 44–57, 2009.

IVASKA, J. Unanchoring integrins in focal adhesions. **Nature Cell Biology**, v. 14, p. 981–983 2012.

JAYAWARDENA, D. P., HEINEMANN, I. U. & STILLMAN, M. J. Zinc binds non-cooperatively to human liver metallothionein 2a at physiological pH. **Biochemical and Biophysical Research Communications**, v. 493, p. 650–653, 2017.

KANEHISA, M. et al. KEGG: New perspectives on genomes, pathways, diseases and drugs. **Nucleic Acids Research**, v. 45, p. D353–D361, 2017.

KAYAALTI, Z., ALIYEV, V. & SÖYLEMEZOĞLU, T. The potential effect of metallothionein 2A -5 A/G single nucleotide polymorphism on blood cadmium, lead, zinc and copper levels. **Toxicology and Applied Pharmacology**, v. 256, p. 1–7, 2011.

KIRSCHNER, N. et al. CD44 regulates tight-junction assembly and barrier function. **The Journal of Investigative Dermatology**, v. 131, p. 932–943, 2011.

KITAGAWA, T., FUNABA, M. & MATSUI, T. Relationships between mineral concentrations and physicochemical characteristics in the Longissimus thoracis muscle of Japanese Black cattle. **Journal of Animal Science**, v. 89, p. 211–218, 2018.

KOHLER, H. R. et al. Expression of the stree-70 protein family (hsp70) due to heavy metal contamination in the slug, deroceras reticulatum: and approach to monitor sublethal stress conditions. **Chemosphere**, v. 33, p. 1327–1340, 1996.

KOO, Y. et al. SUMO-Specific Protease 2 (SENP2) is an important regulator of fatty acid metabolism in skeletal muscle. **Diabetes**, v. 64, p. 2420–2431, 2015.

LEI, L., XIAOYI, S. & FUCHANG, L. Effect of dietary copper addition on lipid metabolism in rabbits. Food and Nutrition Research, v. 61, p. 1348866, 2017.

LI, Y. et al. A fibrillar collagen gene, Col11a1, is essential for skeletal morphogenesis. **Cell**, v. 80, p. 423–430, 1995.

LYU, Y. et al. Defective differentiation of adipose precursor cells from lipodystrophic mice lacking perilipin 1. **PLoS One**, v. 10, p. 1–18, 2015.

MARTENS, H. et al. Magnesium homeostasis in cattle: absorption and excretion. **Nutrition Research Reviews**, v. 25, p. 1–17, 2018.

MATEESCU, R. G. et al. Genetic parameters for concentrations of minerals in longissimus muscle and their associations with palatability traits in angus cattle. **Journal of Animal Science**, v. 91, p. 1067–1075, 2013.

MINOKOSHI, Y., OKAMOTO, S. & TODA, C. Regulatory role of leptin in glucose and lipid metabolism in skeletal muscle. Indian Journal of Endocrinology and Metabolism, v. 16, p. 562, 2012.

MORRIS, C. A. et al. Effects of quantitative trait loci and the myostatin locus on trace and macro elements (minerals) in bovine liver, muscle and kidney. **Animal Genetics**, v. 44, p. 361–368, 2013.

MORRIS, C. A., AMYES, N. C. & HICKEY, S. M. Genetic variation in serum copper concentration in Angus cattle. **Animal Science**, v. 82, p. 798–803, 2006.

PERTEA, M. et al. StringTie enables improved reconstruction of a transcriptome from RNA-seq reads. **Nature Biotechnology**, v. 33, p. 290–295, 2015.

ROMEO, S. & VALENTI, L. Regulation of retinol-binding protein 4 and retinol metabolism in fatty liver disease. **Hepatology**, v. 64, p. 1414–1416, 2016.

SCHLECHT, U. et al. A functional screen for copper homeostasis genes identifies a pharmacologically tractable cellular system. **BMC Genomics**, v. 15, p. 1–14, 2014.

SOMOGYI, T. ET al. Mineral Content of Three Several Muscles From Six Cattle Genotypes. **Acta Alimentaria**, v. 44, p. 51–59, 2015.

SUTTLE, N. **13. Iron. Mineral nutrition of livestock**, 2010. doi:10.1079/9781845934729.0000

SZKLARCZYK, D. et al. The STRING database in 2017: Quality-controlled protein-protein association networks, made broadly accessible. **Nucleic Acids Research**, v. 45, p. D362–D368, 2017.

TANSEY, J. T. et al. The central role of perilipin A in lipid metabolism and adipocyte lipolysis. **IUBMB Life**, v. 56, p. 379–385, 2004.

TATHAM, M. H. et al. Polymeric Chains of SUMO-2 and SUMO-3 are Conjugated to Protein Substrates by SAE1/SAE2 and Ubc9. **The Journal of Biological Chemistry**, v. 276, p. 35368–35374, 2001.

THORSTEINSDÓTTIR, S., DERIES, M., SO, A. & BAJANCA, F. The extracellular matrix dimension of skeletal muscle development. **Developmental Biology**, v.354, p. 191–207,

2011.

TIZIOTO, P. C. et al. Calcium and potassium content in beef: Influences on tenderness and associations with molecular markers in Nellore cattle. **Meat Science**, v. 96, p. 436–440, 2014.

TIZIOTO, P. C. et al. Detection of quantitative trait loci for mineral content of Nelore longissimus dorsi muscle. **Genetics Selection Evolution**, v. 47, p. 1–9, 2015.

TRAPNELL, C. et al. Transcript assembly and abundance estimation from RNA-Seq reveals thousands of new transcripts and switching among isoforms. **Nature Biotechnology**, v. 28, p. 511–515, 2011.

UDENSI, U. K. & TCHOUNWOU, P. B. Potassium Homeostasis, Oxidative Stress, and Human Disease. **International Journal of Clinical and Experimental Physiology**, v. 4, p. 15–20, 2017.

YAO, D. W. et al. Thyroid hormone responsive (THRSP) promotes the synthesis of medium-chain fatty acids in goat mammary epithelial cells. **Journal of Dairy Science**, v. 99, p. 3124–3133, 2016.

CHAPTER 3: GENETIC REGULATORS OF MINERAL AMOUNT IN NELORE CATTLE MUSCLE PREDICTED BY A NEW CO-EXPRESSION AND REGULATORY IMPACT FACTOR APPROACH

3.1. ABSTRACT

Mineral amount in bovine muscle impacts meat quality, growth, health and reproductive traits in beef cattle. To better understand the genetic basis of this phenotype, we implemented new applications of use for two complementary algorithms: the partial correlation and information theory (PCIT) and the regulatory impact factor (RIF), by including GEBVs as part of the imput. We used PCIT to determine putative regulatory relationships based on significant associations between gene expression and mineral amount. Then, RIF was used to determine the regulatory impact of genes and miRNA over mineral amount. We also investigated over-represented pathways, as well as evidences from previous studies carried in the same population, to determine regulatory genes for mineral amount *e.g. NOX1*, whose expression was positively correlated to Zn and was described as regulated by this mineral in humans. With this methodology, we were able to identify genes, miRNAs and pathways not yet described as important for mineral amount. The results support the hypothesis that extracellular matrix interactions are the core regulator of mineral amount in muscle cells. Putative regulators described here add information to this hypothesis, expanding the molecular relationships between gene expression and minerals. This manuscript will be submitted to Genomics, Proteomics and Bioinformatics journal with the same title and with Juliana Afonso, Marina Rufino Salinas Fortes, Antonio Reverter, Wellison Jarles da Silva Diniz, Aline Silva Mello Cesar, Andressa Oliveira de Lima, Juliana Petrini, Marcela Maria de Souza, Luiz Lehmann Coutinho, Gerson Barreto Mourao, Adhemar Zerlotini, Caio Fernando Gromboni, Ana Rita Araujo Nogueira e Luciana Correia de Almeida Regitano as authors.

Keywords: Nelore, minerals, muscle, genes, miRNA, PCIT, RIF.

3.2. INTRODUCTION

Mineral amount affects meat quality (GEESINK and KOOHMARAIE, 1999; WILLIAMS, 2007; DOYLE and SPAULDING, 1978; CAMPBELL, 2016), reproduction (AHOLA et al., 2004), health and growth performance (GENTHER and HANSEN, 2014; ENJALBERT, LEBRETON and SALAT, 2006) in beef cattle. Mineral homeostasis is affected by genetic factors (MATEESCU et al., 2013). Understanding the genetic aspects linked to mineral concentration in bovine muscle can lead to a better modulation of this trait, allowing for future production of healthier, more productive animals, and better-quality meat.

A differential expression approach detects genes and pathways underlying mineral amount in Nelore cattle, by comparing extremes of the population used herein (AFONSO et al., 2019; DINIZ et al., 2016). However, as mineral mass fraction traits occur in a continuous distribution, to verify these relationships and infer regulatory modes of action, it is necessary to study the whole population. It is possible to go beyond contrasting extreme phenotypes, beyond differential expression (HUDSON, DALRYMPLE and REVERTER, 2012). Thus, by applying a co-expression network approach it is possible to identify genome-wide genes with similar expression patterns related to specific phenotypes or conditions. In this methodology, traits are usually integrated into the analysis in a condition-dependent network, by previous selection of genes or sample clusters related to the trait before the analysis (SERIN et al., 2016). Another way of including phenotypes to select gene groups putatively involved with them, already used for mineral concentration in our population (DINIZ et al., 2019), is to cluster all expressed genes by their co-expression profiles and then associate these clusters to the phenotypes using the Weighted correlation network analysis (WGCNA) in R package (LANGFELDER and HORVATH, 2008). In this case, groups of genes with similar functions are identified and associated with the phenotypes.

Among the challenges of these methods regarding phenotype inclusion is that no single approach is used to search genome-wide for specific genes linked to phenotypes without prior selection. Also, it is challenging to pinpoint the direction of interactions or the regulation, as co-expression networks do not provide this information a priori (SERIN et al., 2016). To overcome these limitations, we propose a new application of the partial correlation and information theory (PCIT) algorithm, originally used for deriving gene co-expression networks, by identifying significant associations between expression profiles (REVERTER and CHAN, 2008). Additionally, we propose a new application of the regulatory impact factor (RIF) algorithm (REVERTER et al., 2010) to identify significant genes and miRNAs whose

expression have regulatory impact over mineral amount in bovine muscle. To this end, we used the expression values of genes and miRNAs correlated to minerals instead of transcription factors (TFs), allowing the regulatory role to go beyond current functional annotation of the cattle genome. Mineral mass fraction genomic estimates of breeding values (GEBVs) were used instead of the expression data of selected genes to calculate the regulatory impact of genes and miRNA correlated to a mineral over the concentration of this mineral. Therefore, we were able to use GEBVs on the networks to identify regulatory elements. This new use of the PCIT-RIF algorithms identified genes and miRNAs having their expression related to the mass fraction of calcium (Ca), copper (Cu), potassium (K), magnesium (Mg), sodium (Na), phosphorus (P), sulfur (S), selenium (Se), zinc (Zn) and iron (Fe) in Nelore steers' *Longissimus thoracis* muscle. In short, we aimed to predict the regulatory impact of the expression of genes and miRNAs over mineral concentration in Nelore muscle.

3.3. METHODS

Figure 3.1 contains a flowchart of the steps of our methodology.

3.3.1. Samples

The Ethical Committee of Embrapa Pecuária Sudeste (São Carlos, São Paulo, Brazil) approved all experimental and animal protocols (CEUA 01/2013). We used the GEBVs from mineral mass fraction (TIZIOTO et al., 2015) and the mRNA-Seq (DINIZ et al., 2016), and miRNA-Seq (OLIVEIRA et al., 2018) expression data from 113 samples of *Longissimus thoracis* muscle from Nelore steers that are part of the population already described in previous differential expression analysis related to mineral amount (AFONSO et al., 2019; DINIZ et al., 2016).

The animals forming our samples came from a Nelore steer population described elsewhere (TIZIOTO et al., 2015; DE OLIVEIRA et al., 2014). In summary, all animals come from half-sibling families, generated by artificial insemination in two different farms, transferred to Embrapa Pecuária Sudeste (São Carlos, São Paulo, Brazil) and maintained in feedlot system with *ad libitum* feed and water access until slaughter, approximately 70 days after the start of the confinement, where the muscle sample collection was done.

3.3.2. Mineral mass fraction and genetic estimated breeding value (GEBV)

Calcium (Ca), copper (Cu), potassium (K), magnesium (Mg), sodium (Na), phosphorus (P), sulfur (S), selenium (Se), zinc (Zn) and iron (Fe) mass fractions were determined from lyophilized and microwave-assisted digested samples, such as described elsewhere (TIZIOTO et al., 2015). Calcium, Cu, K, Mg, Na, P, S, Zn, and Fe were determined by inductively coupled plasma optical spectrometry (ICP OES, Vista Pro-CCD with a radial view, Varian, Mulgrave, Australia). Selenium was determined by inductively coupled plasma mass spectrometry (ICP-MS 820-MS, Varian, Mulgrave, Australia).

The estimation of the genetic breeding value (GEBVs) for all the minerals' amount was previously made (TIZIOTO et al., 2015) through a Bayesian model that considered birthplace, feedlot location and breeding season in the contemporary groups as fixed effects and age at slaughter as a linear covariate.

3.3.3. mRNA-Seq and miRNA-Seq sequencing and quality control

The total RNA extraction, quality control, and sequencing were described elsewhere (OLIVEIRA et al., 2018). In summary, total RNA from all the 113 samples was extracted using Trizol® (Life Technologies, Carlsbad, CA) and its integrity was evaluated in a Bioanalyzer 2100® (Agilent, Santa Clara, CA, USA). Regarding the mRNA-Seq data, the library preparation was made with the TruSeq® sample preparation kit, and the paired-end sequencing (DINIZ et al., 2016) was made in an Illumina HiSeq 2500®. For the miRNA-Seq data, the library preparation was made with TruSeq® small RNA sample preparation kit, and the single-end sequencing (OLIVEIRA et al., 2018) was made in a MiSeq sequencer.

As a quality control for the sequences, we filtered out reads with less than 65 bp and Phred Score less than 24 for the mRNA-Seq data, and the removal of reads with less than 18 bp and Phred Score less than 28 of the miRNA-Seq data were made using the Seqyclean software (http://sourceforge.net/projects/seqclean/files/).

Figure 3.1. Flowchart representing the steps of the methodology.

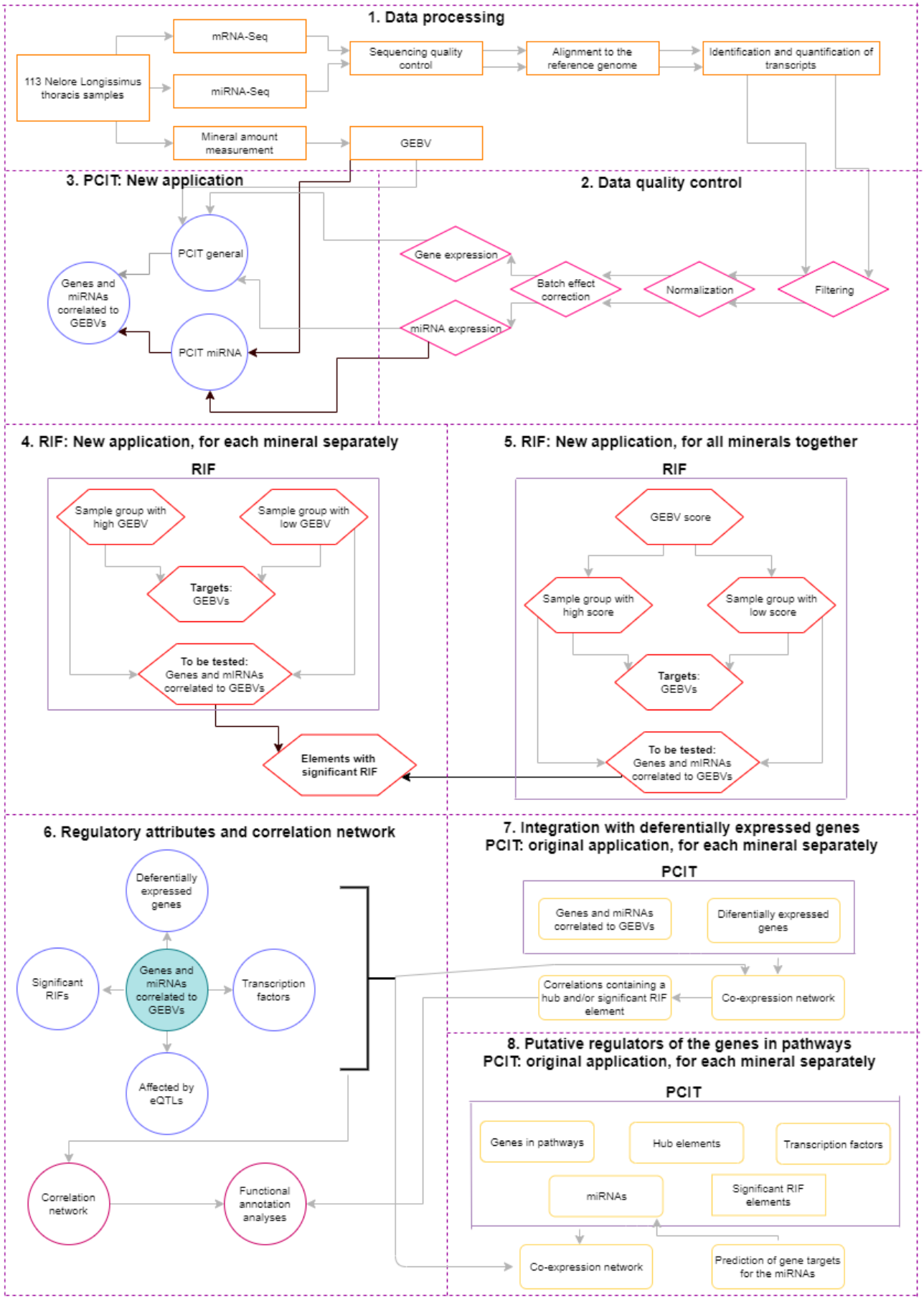

The reads that passed the quality control were aligned to the reference bovine genome ARS-UCD 1.2 with the STAR v.2.5.4 software (DOBIN et al., 2013) for the mRNA-Seq data and with the mirDeep2 software (FRIEDLANDER et al., 2012) for the miRNA-Seq. The same software was used to the identification and quantification of transcripts and miRNAs, respectively, in raw counts.

3.3.4. Filtering, normalization and batch effect correction

After quality control, the mRNA-Seq and miRNA-Seq expression data were filtered separately to remove the transcripts and miRNA not expressed in at least 22 samples, or approximately 20% of the samples.

A first component analysis was performed for the mRNA-Seq expression data, with the NOISeq v.2.16.0 software (TARAZONA et al., 2015) to visually verify the batch effect of the birthplace, feedlot location, breeding season, age at slaughter, slaughter group and a combination of sequencing flowcell and lane over the expression data. The data were normalized using the VST function from DESEq2 software (LOVE, HUBER and ANDERS, 2014), and the batch effect correction for the combination of sequencing flowcell and lane was made using the ARSyNseq function from the NOISeq v.2.16.0 software (TARAZONA et al., 2015). For the miRNA-Seq expression data, the procedure was the same, with the batch effect test only for the sequencing lane.

3.3.5. PCIT (Partial Correlation Coefficient with Information Theory) with mRNA, miRNA and phenotypes

A new application of the PCIT algorithm (REVERTER and CHAN, 2008) was developed to test the correlation between the expression values of genes and miRNAs that passed the quality control filters and the GEBVs for ten minerals.

The original application of the algorithm is used to test the co-expression between genes by correlation analysis between expression values (REVERTER and CHAN, 2008). In our application, we included the GEBVs for each one of the ten minerals evaluated here for each sample in the algorithm input with the gene and miRNA expression values (called PCIT general). Using this approach, we estimated the correlations among all the elements. Among the significant correlations, we selected only the genes and miRNAs correlated to the GEBV of at least one mineral. Due to the low number of miRNAs identified compared to the high

number of genes, we did one more PCIT analysis only with miRNAs and the GEBVs (called PCIT miRNA). The results from these two PCITs analysis were combined. In the end we had a list of elements (genes and miRNAs) correlated to each mineral GEBV.

3.3.6. RIF (regulatory impact factor)

A new application of the RIF algorithm (REVERTER et al., 2010) was applied to obtain the predict regulatory impact of the genes and miRNAs associated with a given mineral on the concentration of the same mineral, considering its GEBVs. The original application of the algorithm was developed to determine the regulatory impact of TFs over selected genes (targets) related to a given trait through their expression values analysis between contrasting groups for the same trait (REVERTER et al., 2010). In our approach, for each mineral, we used the genes and miRNAs correlated to a mineral, from the previous PCIT analyses, as elements to be tested as regulators and the mineral GEBV as the target.

We carried out 10 different analyses with the RIF algorithm (REVERTER et al., 2010), being one for each mineral. As input, we used the GEBVs for the 30 contrasting samples for each mineral as targets (15 representing samples with high mineral mass fraction and 15 with low mineral mass fraction) and the expression values for the genes and miRNAs associated to the same mineral as elements to be tested. To select these contrasting groups, we expanded the sample selection based on GEBVs previously made (AFONSO et al., 2019; DINIZ et al., 2016). Genes and miRNAs with RIF I or II results higher than |1.96| were considered as significant, as authors suggests (REVERTER et al., 2010).

3.3.7. RIF for all minerals together

To identify genes and miRNAs with significant impact factor in all minerals' mass fraction together, we used the new application for the RIF algorithm (REVERTER et al., 2010) using the GEBV from 30 contrasting samples forming two groups regarding the amount of the ten minerals as targets and the expression values for the genes and miRNAs correlated to at least one mineral as elements to be tested.

To select contrasting samples for all the minerals together, we ranked our samples based on a score. To calculate this score for each sample, we performed a principal component analysis (PCA) using the GEBVs for ten minerals for the 113 samples. From the PC results, the score of each sample was calculated based on the following formula:

$$A_i = \sum_{j=i}^{10} k\, Contrib_{ijk} \times Z_{ijk} \times \%V_{PCj}$$

Where: A_i = *score* for the animal *i*, $\sum_{j=i}^{10} k =$ sum of all minerals k, in all the PCs *j* and in all the animals *i*, $Contrib_{ijk} =$ contribution of the animal *i* in the PC *j* for the mineral *k*, $Z_{ijk} =$ standardized value (standard deviation one and mean zero) of the GEBV for the mineral *k* for the animal *i* in the PC *j* and $\%V_{PCj} =$ eigenvalue of the PC *j*.

We performed a functional annotation analysis using DAVID 6.8 software (HUANG, SHERMAN and LEMPICKI, 2009) with the genes presenting significant RIFs for the score, representing all minerals together.

3.3.8. Genes and miRNAs correlated to minerals

Significant correlations obtained from PCIT (REVERTER and CHAN, 2008) analysis between genes or miRNAs expression and minerals were used to build a co-expression network with the Cytoscape software SHANNON et al., 2003). We overlapped the gene list from our network with the genes previously reported from our research group based on the same population evaluated here presenting differentially expressed to at least one mineral (AFONSO et al., 2019; DINIZ et al., 2016), TFs (DE SOUZA et al., 2018), affected by cis or trans eQTLs (CESAR et al., 2018) and with significant RIF. These features were used as attributes in the network. Regarding the differentially expressed genes (DEGs) for Fe (DINIZ et al., 2016), we called the genes more expressed in the high Fe content group as upregulated and the genes more expressed in the low Fe content group as downregulated, to match the nomination of the other minerals' DEGs (AFONSO et al., 2019). Functional annotation analyses were made using DAVID 6.8 software (HUANG, SHERMAN and LEMPICKI, 2009).

3.3.9. Integration with DEGs

To estimate the relationship among the genes or miRNAs with expression values correlated with minerals and the DEGs between contrasting groups for mineral concentration previously detected (AFONSO et al., 2019; DINIZ et al., 2016), we made ten separately PCIT (REVERTER and CHAN, 2008) analyses. In these analyses, the PCIT algorithm was used as

proposed initially (REVERTER and CHAN, 2008) to test the correlations among the genes and miRNAs with expression values correlated to each mineral, and the expression of the DEGs previously detected for the same mineral (AFONSO et al., 2019; DINIZ et al., 2016).

The significant correlations identified in each analysis was used to obtain co-expression networks with the Cytoscape software (SHANNON et al., 2003). The NetworkAnalyzer tool for the Cytoscape software (SHANNON et al., 2003) was used to obtain the connectivity degree of each gene and miRNA in the networks. This value was used to identify the hub genes/miRNAs from the average of the connectivity degree from the network summed with the double of the referent standard deviation.

We considered only the significant correlations containing at least a hub or significant RIF gene/miRNA for a given mineral. The genes present in these considered correlations were used to perform a functional annotation analysis with the STRING v.1.2.2 software (PERTEA et al., 2015). From these analyses, we selected the genes being part of enriched pathways considering KEGG (KANEHISA et al., 2017) and Reactome (FABREGAT et al., 2018) databases with *Bos taurus* reference genome.

3.3.10. Putative regulators of the genes being part of enriched pathways

To identify the elements putatively regulating the genes being part of over-represented pathways for each mineral in the study, we did another round of PCIT (REVERTER and CHAN, 2008) analyses, separately for each mineral. In this case, from each mineral last PCIT analysis, we selected as inputs the expression of genes being part of enriched pathways, also considering the previously enriched pathways from differentially expressed genes related to mineral amount (AFONSO et al., 2019; DINIZ et al., 2016), the hub elements, TFs (DE SOUZA et al., 2018), miRNAs and the ones with significant RIFs, with their respective attributes. The PCIT (REVERTER and CHAN, 2008) results were used to obtain co-expression networks with Cytoscape (SHANNON et al., 2003) software.

3.3.11. miRNA-gene targeting confirmation

We used TargetScan software (AGARWAL et al., 2015) to predict the target genes for the miRNAs correlated to a mineral in Figures 3.2 and 3.3 and we compared these putative targets with the genes correlated to them in our networks.

3.4. RESULTS

3.4.1. Genes and miRNAs correlated to minerals

After data quality control, filtering, normalization and batch effect correction performed separately in the mRNA-Seq and miRNA-Seq expression data from 113 samples, the expression of 12,943 genes and 705 miRNAs remained for further analyses. To identify genes and miRNAs with expression values correlated to ten different minerals, we carried out two different PCIT analyses, using our new application: i) PCIT general: incorporating genes`expression, miRNAs`expression and GEBVs together, and ii) PCIT miRNA: considering only miRNAs expression and GEBVs together. Simultaneously considering the results of both PCIT analyses, we identified a total of 242 genes and 35 miRNAs with expression values correlated to at least one mineral GEBV. From these, the expression of 46 genes and 12 miRNAs was correlated to more than one mineral GEBV. The number of genes and miRNAs with expression values correlated to each mineral ranged from 19 to 55 and from five to nine, respectively. The number of miRNAs that had their expression correlated to a mineral in both PCIT analyses varies from zero to three (Table 3.1). There were two genes and one miRNA with expression values correlated to six minerals, Vitamin D3 receptor (*VDR)* and bta-miR-92b correlated to Ca, K, Mg, Na, P and S; and Doublecortin (*DCX)*, correlated to K, Mg, Na, P, S, and Zn. From these analyses, we identified significant correlations among minerals' GEBVs. There were no significant correlations between Se and other minerals (Figure 3.2). Correlations identified among K, Mg, Na, Zn, S, and P GEBVs ranged from 0.77 to 0.97.

3.4.2. Principal component score and Regulatory Impact Factor (RIF)

From a principal component analysis based on the GEBVs for each animal, considering ten minerals, we calculated a score for each sample regarding its contribution to phenotypic variation. Based on that, we selected 30 contrasting samples concerning all minerals together, 15 with low score and 15 with high score (Figure 3.3). These contrasting groups were used to estimate the RIF of all genes and miRNAs with expression values correlated to at least one mineral in the concentration of all minerals together, using our application of the original RIF algorithm (see methods). Also, we estimated the RIF of the genes and miRNAs with expression data correlated to each mineral separately using

contrasting sample groups for specific minerals. For that, based on the GEBVs, we expanded to 15 the number of samples on the same contrasting groups detailed in previous works with differentially expressed genes regarding mineral concentration (AFONSO et al., 2019; DINIZ et al., 2016), containing six samples for Ca, Cu, K, Mg, Na, P, S, Se and Zn and five samples for Fe in each group.

There were 22 genes and two miRNAs with significant RIF based on the high and low score approach. Based on the single mineral analysis, there were three common genes and one common miRNA with significant RIF for two minerals, CD86 molecule (*CD86)* for K and Mg, *VDR* for Mg and Na, WD repeat-containing planar cell polarity effector (*WDPCP)* for Na and P and bta-miR-369.3p for Ca and S. The number of genes with significant RIFs for each mineral varied from zero to seven and for miRNA from zero to two (Table 3.2).

Figure 3.2. Co-expression network among genes and miRNAs correlated to at least one mineral. A) Complete network, B) Details about the correlations regarding the genes and miRNAs correlated to more than one mineral, the internal circle of the complete network, C) Correlations among the mineral's GEBVs.

A)

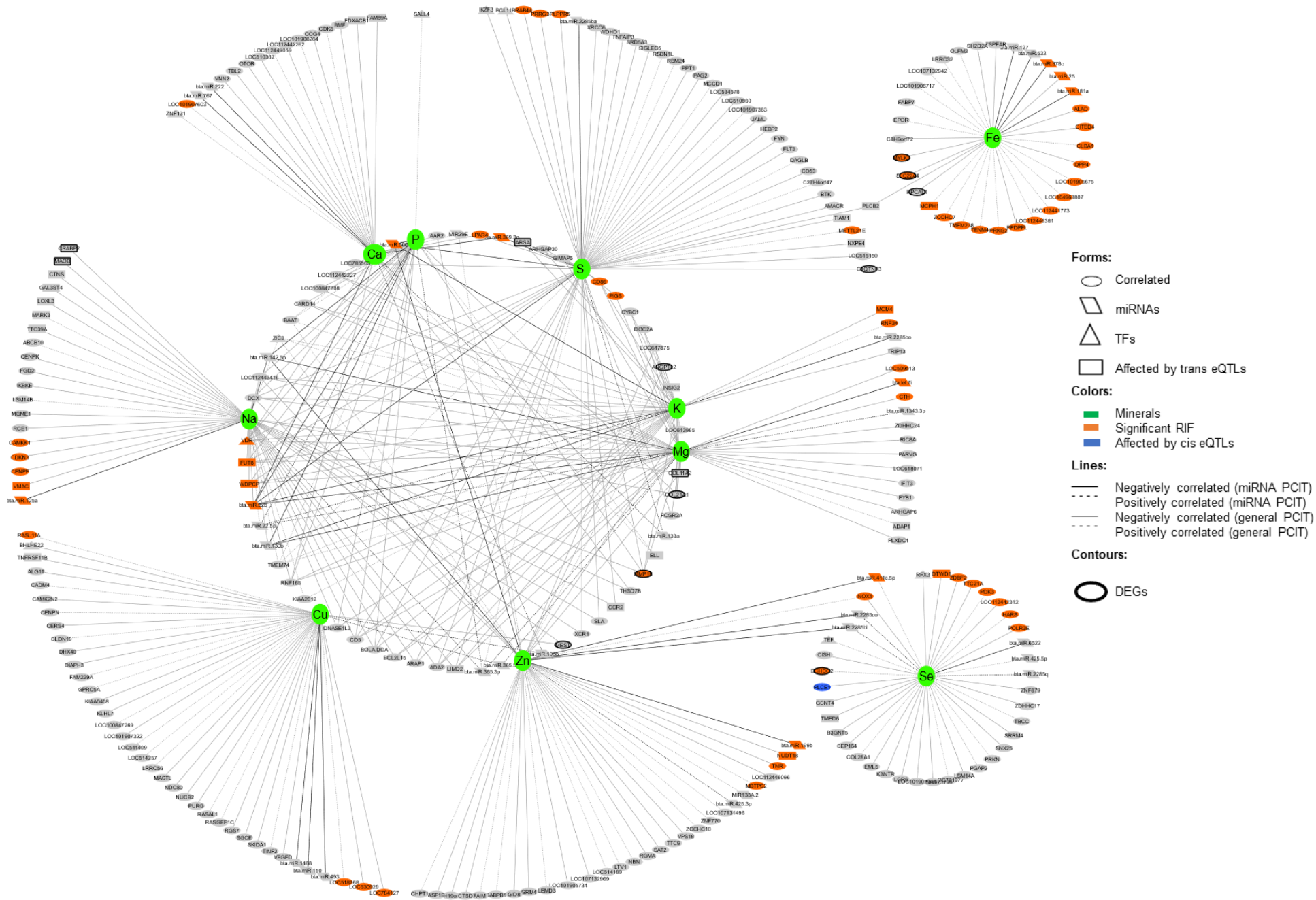

B)

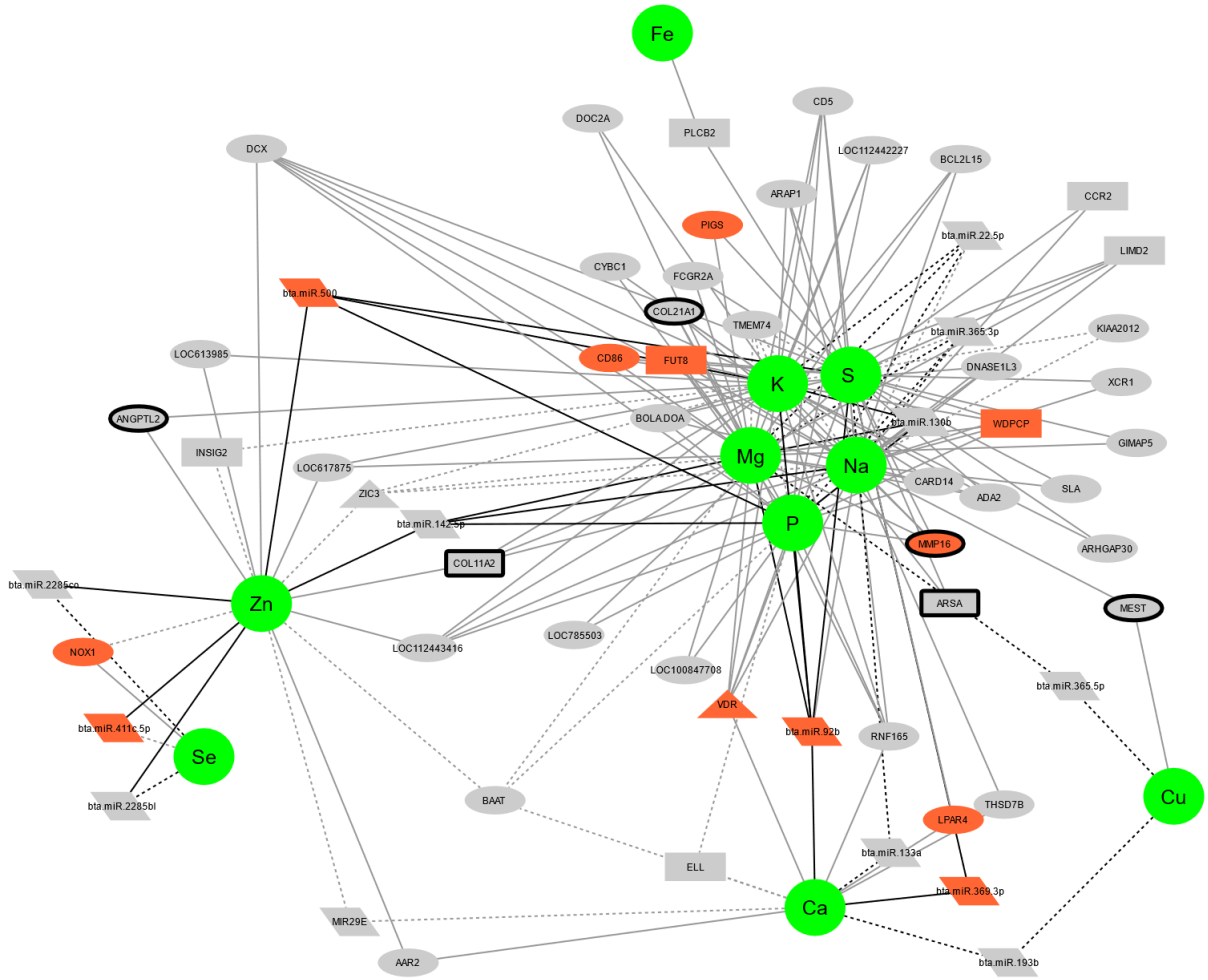
Fe
CD5
DOC2A
PLCB2
LOC112442227
BCL2L15
DCX
ARAP1
CCR2
PIGS
bta.miR.22.5p
LIMD2
CYBC1
FCGR2A
bta.miR.500
COL21A1
TMEM74
bta.miR.365.3p
KIAA2012
LOC613985
CD86
FUT8
K
S
DNASE1L3
XCR1
ANGPTL2
BOLADOA
bta.miR.130b
WDPCP
GIMAP5
INSIG2
LOC617875
Mg
Na
CARD14
SLA
ZIC3
ADA2
bta.miR.142.5p
P
MMP16
ARHGAP30
COL11A2
bta.miR.2285cp
Zn
ARSA
MEST
NOX1
LOC112443416
LOC785503
LOC100847708
bta.miR.365.5p
VDR
bta.miR.411c.5p
bta.miR.92b
RNF165
Se
Cu
BAAT
THSD7B
bta.miR.2285bl
LPAR4
bta.miR.133a
ELL
bta.miR.369.3p
Ca
MIR29E
AAR2
bta.miR.193b

C)

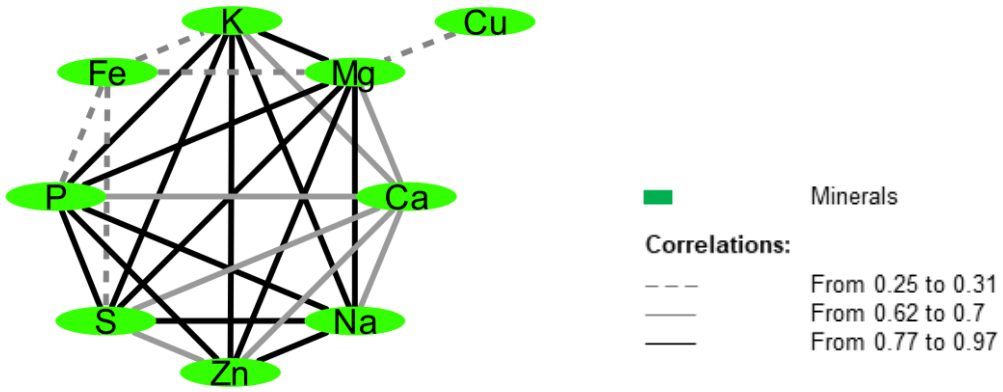
K
Cu
Fe
Mg
P
Ca
S
Na
Zn
Minerals
Correlations:
From 0.25 to 0.31
From 0.62 to 0.7
From 0.77 to 0.97

Table 3.1. Number of genes and miRNAs with expression values correlated to each mineral considering both PCIT analysis. PCIT general, with mineral genomic estimates of breeding values, genes and miRNAs expression and PCIT miRNA with mineral GEBVs and miRNAs expression. The data came from *Longissimus thoracis* muscle from Nelore steers and the genes and miRNA expressions were identified based on RNA-Seq analysis.

Mineral	Gene	miRNA	Repeated miRNA[a]
Ca	22	6	0
Cu	35	5	0
K	33	5	0
Mg	37	8	0
Na	42	6	3
P	19	6	0
S	55	6	1
Se	32	6	2
Zn	36	9	0
Fe	27	5	1

3.4.3. Correlation network

We used the significant correlations between a gene or a miRNA expression and a given mineral, identified in both analyses implemented with the PCIT algorithm, as above described, to derive a co-expression correlation network. To identify potential regulatory mechanisms related to each mineral, we added on this network other layers of information from the same samples, tissue and population, as follows: differentially expressed genes (DEGs) for contrasting mineral amount sample groups (AFONSO et al., 2019; DINIZ et al., 2016) transcription factors (TF) (DE SOUZA et al., 2018) and genes affected by eQTLs (CESAR et al., 2018). This information and genes with significant RIFs were used as node attributes and included in the network analyses (Figure 3.2). All correlations and attributes necessary to compose Figure 3.2 are provided (see Supplementary Table S3.1). There was at least one putative regulatory element (*i.e.* a significant RIF, TF, miRNA, or gene affected by eQTLs) correlated to each mineral. The number of genes and miRNAs with expression values correlated per mineral per attribute identified is showed in Table 3.3 and the genes, miRNAs and their attributes are showed in Supplementary Table S3.1.

There were no functional clusters or over-represented pathways identified in the functional annotation analysis carried out separately for each group of gene expression correlated to a specific mineral. However, from the functional annotation table, we noted that the genes with expression values correlated to the minerals are well conserved among a broad

range of organisms. They have functions related to the extracellular matrix, integral membrane constituents, metal ion binding, and partake on regulatory processes linked to transcription, replication, splicing, apoptotic processes, metabolism, transport vesicles, RNA processing, signaling, cell division, adhesion, migration and proliferation, embryonic development and tissue regeneration.

Figure 3.3. Representation of the contrasting samples considering the genomic estimated breeding values of all 10 minerals together, based on the PCA score. Orange circles represent the samples with the highest scores (positive contrast) and the green circles represent the samples with the lowest scores (negative contrast).

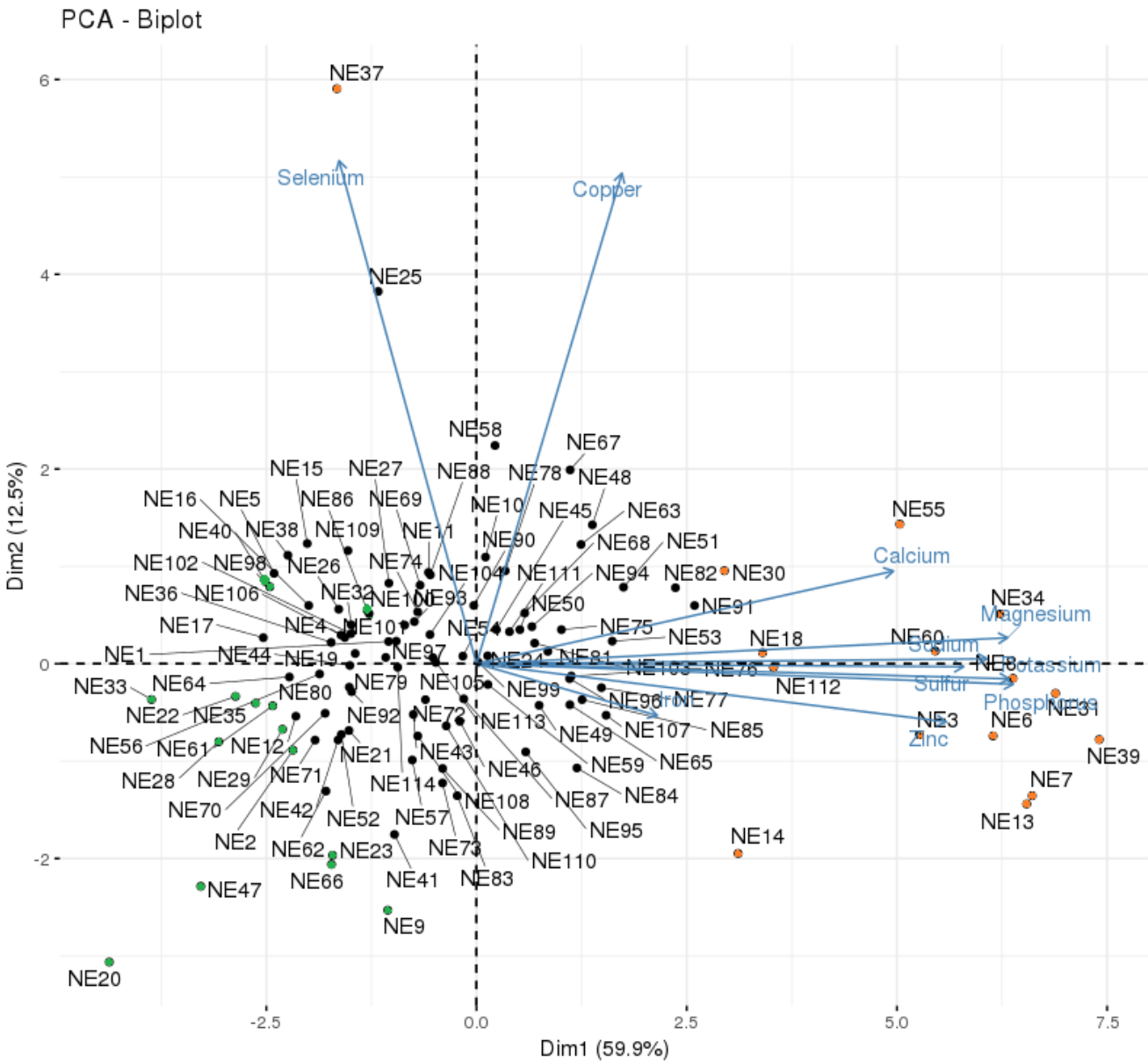

Table 3.2. Number of genes and miRNAs with a significant regulatory impact factor over the genomic estimates of breeding values for each mineral and all minerals together (PCA score). The data came from *Longissimus thoracis* muscle from Nelore steers and the genes and miRNA expressions were identified based on RNA-Seq analysis.

Mineral	Gene	miRNA
Ca	1	1
Cu	4	0
K	3	1
Mg	3	1
Na	6	1
P	1	0
S	5	2
Se	7	0
Zn	4	2
Fe	0	2
PCA Score	22	2

Table 3.3. Number of genes and miRNAs with expression values correlated per mineral and per attribute considering both PCIT analysis. PCIT general, with mineral genomic estimates of breeding values, genes and miRNAs expression and PCIT miRNA with mineral GEBVs and miRNAs expression. The data came from *Longissimus thoracis* muscle from Nelore steers and the genes and miRNA expressions were identified based on RNA-Seq analysis. Attributes: a) differentially expressed genes (AFONSO et al., 2019; DINIZ et al., 2016), b) genes and miRNAs with significant regulatory impact factor, c) transcription factors (DE SOUZA et al., 2018) d) genes affected by cis eQTLs (CESAR et al., 2018), e) genes affected by trans eQTLs (CESAR et al., 2018), f) miRNAs and g) genes and miRNAs correlated to each mineral that were not identified in previous works.

Minerals	DEGs[a]	Significant RIF[b]	TFs[c]	cis eQTLs[d]	trans eQTLs[e]	miRNAs[f]	No attributes[g]
Ca	0	3	2	0	3	5	14
Cu	1	4	1	0	1	5	28
K	2	5	2	0	7	3	19
Mg	2	6	2	0	5	6	23
Na	3	7	2	0	13	6	21
P	0	1	2	0	3	6	12
S	1	8	3	0	8	6	34
Se	1	9	2	1	3	6	17
Zn	0	6	1	0	3	9	27
Fe	3	19	0	0	2	5	9

3.4.4. Integration with differentially expressed genes (DEGs)

To convey the relationship among all genetic elements related to mineral mass fraction detected in our population, we used PCIT to estimate the correlations between a gene or miRNA expression that was found to be correlated to a given mineral in the present work and DEGs previously identified for the same mineral (AFONSO et al., 2019; DINIZ et al., 2016). This analysis was carried out for each mineral separately and included the same genes with regulatory potential as in the previous section (DEGs (AFONSO et al., 2019; DINIZ et al., 2016), TFs (DE SOUZA et al., 2018), genes affected by eQTLs (CESAR et al., 2018) and genes with significant RIF). To identify elements with regulatory potential, we then selected the genes that were network hubs or that were significant according to RIF (see methods). We performed a functional annotation analysis with the selected genes for each mineral, separately, to determine which ones were underlying biological pathways.

The expression of all selected putative regulatory elements (hub, significant RIF or miRNA), the ones underlying biological pathways newly identified and the ones being part of enriched pathways in previous work with DEGs related to mineral concentration (AFONSO et al., 2019; DINIZ et al., 2016) were used as inputs for a final PCIT analyses. This PCIT was carried to identify possible regulators of genes in enriched pathways. Figure 4 shows the co-expression networks built with significant correlations from the final PCIT analyses for Ca, Cu, K, Mg, Na, P, S, Se, and Fe. Supplementary Tables S3.2 has the correlations and attributes related to creating Figure 3.4.

As we included the differentially expressed genes regarding mineral amount previously detected in in the same population (AFONSO et al., 2019; DINIZ et al., 2016), most of the over-represented pathways identified correspond to the previously detected pathways expression analyses. In addition, by the inclusion of correlated genes and pathways from the Reactome database (FABREGAT et al., 2018), we identified new pathways for K, related to protein metabolism, for Ca, Cu, S and Fe related to immune response, and for S related to signaling. All the pathways enriched for S are new, when compared with our previous work (AFONSO et al., 2019). A list of the pathways enriched for each mineral considering the ones detected with the inclusion of correlated genes and the ones from the previous work (AFONSO et al., 2019; DINIZ et al., 2016) is shown in Table 3.4.

Regarding Zn, no gene taking part in the unique enriched pathway previously detected (AFONSO et al., 2019) met our criteria. Because of that, for this mineral, we generated a co-expression network by including the DEGs for Zn (AFONSO et al., 2019) that were

significantly correlated to hub or RIF elements for Zn and their attributes, in order to identify possible regulators for the DEGs in general. This co-expression network is shown in Figure 3.5, and the correlations and attributes supporting Figure 3.5 are presented in Supplementary Table S3.3.

Figure 3.4. Co-expression networks among genes and miRNAs being part of enriched pathways (DEGs and correlated to a mineral), hubs, TFs, miRNAs or presenting a significant RIF regarding nine of the minerals in study. A) Mg, B) Fe, C) Ca, D) Se, E) K, F) Na, G) Cu, H) P, I) S.

tions wit

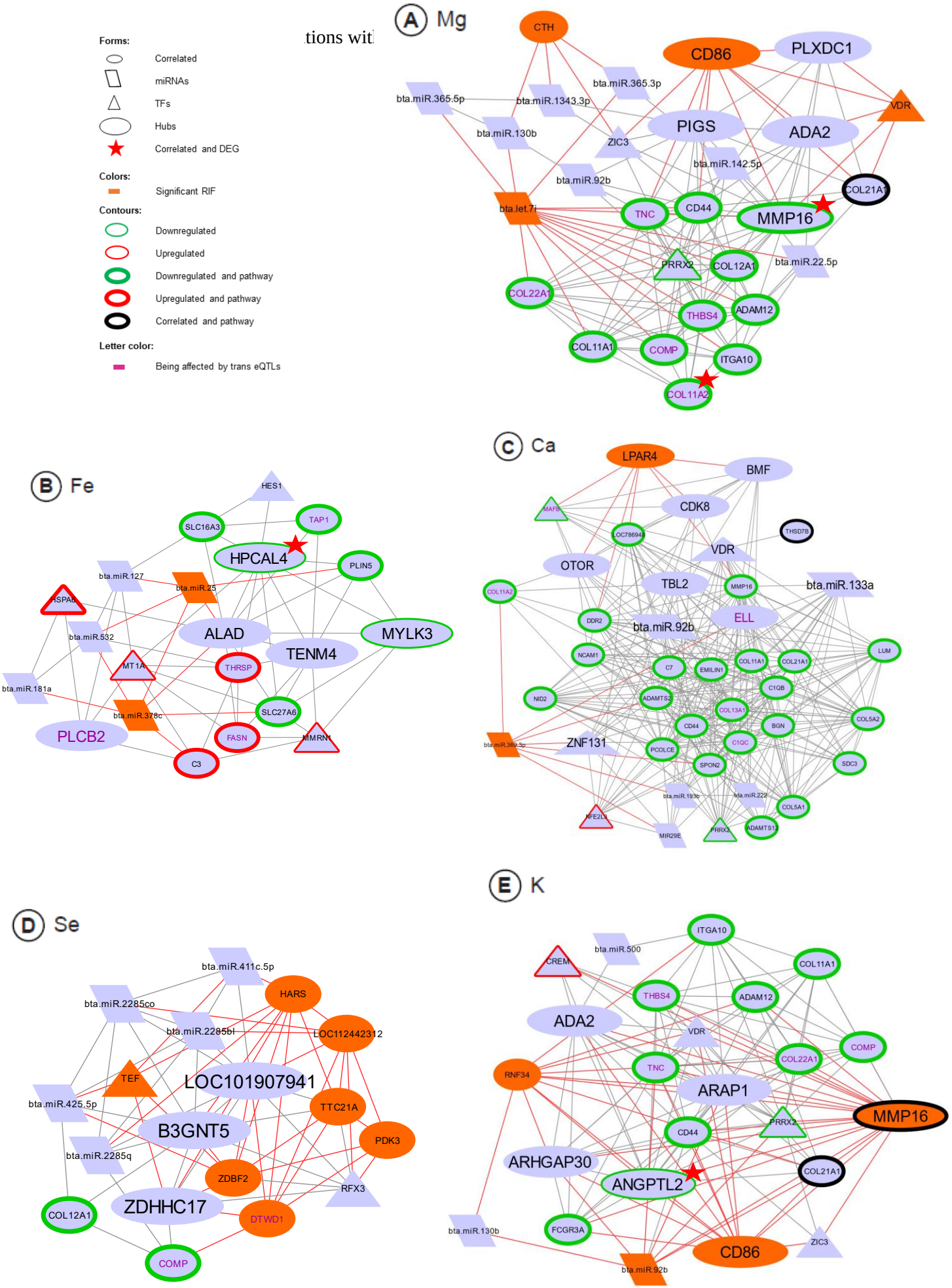
Forms:
Correlated
miRNAs
TFs
Hubs
Correlated and DEG
Colors:
Significant RIF
Contours:
Downregulated
Upregulated
Downregulated and pathway
Upregulated and pathway
Correlated and pathway
Letter color:
Being affected by trans eQTLs
A Mg
CTH
CD86
PLXDC1
bta.miR.365.3p
bta.miR.365.5p
bta.miR.1343.3p
VDR
bta.miR.130b
PIGS
ADA2
ZIC3
bta.miR.142.5p
bta.miR.92b
COL21A1
bta.let.7i
TNC
CD44
MMP16
PRRX2
COL12A1
bta.miR.22.5p
COL22A1
THBS4
ADAM12
COL11A1
COMP
ITGA10
COL11A2
B Fe
HES1
SLC16A3
TAP1
HPCAL4
PLIN5
bta.miR.127
bta.miR.25
HSPA6
bta.miR.532
ALAD
MYLK3
TENM4
MT1A
THRSP
bta.miR.181a
bta.miR.378c
SLC27A6
PLCB2
FASN
MMRN1
C3
C Ca
LPAR4
BMF
MAFB
CDK8
LOC786944
THSD7B
VDR
OTOR
TBL2
MMP16
bta.miR.133a
COL11A2
DDR2
bta.miR.92b
ELL
NCAM1
C7
EMILIN1
COL11A1
COL21A1
LUM
NID2
ADAMTS2
C1QB
COL13A1
CD44
BGN
COL5A2
bta.miR.369.3p
ZNF131
PCOLCE
C1QC
SPON2
SDC3
bta.miR.193b
bta.miR.222
COL5A1
NFE2L3
MIR29E
PRRX2
ADAMTS1
D Se
bta.miR.411c.5p
HARS
bta.miR.2285co
bta.miR.2285bl
LOC112442312
TEF
LOC101907941
bta.miR.425.5p
TTC21A
B3GNT5
PDK3
bta.miR.2285q
ZDBF2
RFX3
COL12A1
ZDHHC17
DTWD1
COMP
E K
ITGA10
bta.miR.500
CREM
COL11A1
THBS4
ADAM12
ADA2
VDR
COMP
COL22A1
RNF34
TNC
ARAP1
MMP16
PRRX2
CD44
ARHGAP30
COL21A1
ANGPTL2
bta.miR.130b
FCGR3A
CD86
ZIC3
bta.miR.92b

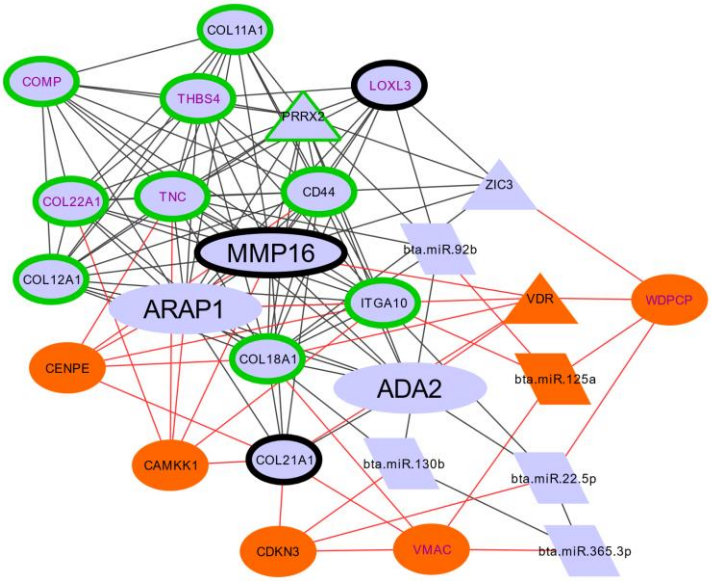
F Na
COL11A1
COMP
THBS4
LOXL3
PRRX2
COL22A1
TNC
CD44
ZIC3
MMP16
bta.miR.92b
COL12A1
ARAP1
ITGA10
VDR
WDPCP
CENPE
COL18A1
ADA2
bta.miR.125a
CAMKK1
COL21A1
bta.miR.130b
bta.miR.22.5p
CDKN3
VMAC
bta.miR.365.3p

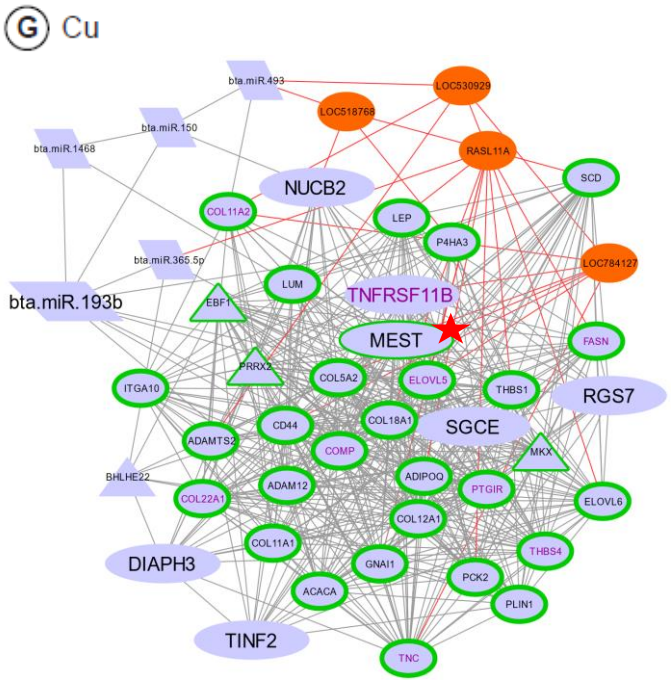
G Cu
bta.miR.493
LOC530929
LOC518768
bta.miR.150
bta.miR.1468
RASL11A
SCD
NUCB2
COL11A2
LEP
P4HA3
bta.miR.365.5p
LOC784127
LUM
bta.miR.193b
EBF1
TNFRSF11B
MEST
FASN
PRRX2
COL5A2
ELOVL5
THBS1
RGS7
ITGA10
CD44
COL18A1
SGCE
ADAMTS2
COMP
MKX
BHLHE22
ADIPOQ
ADAM12
PTGIR
COL22A1
ELOVL6
COL12A1
COL11A1
THBS4
DIAPH3
GNAI1
PCK2
ACACA
PLIN1
TINF2
TNC

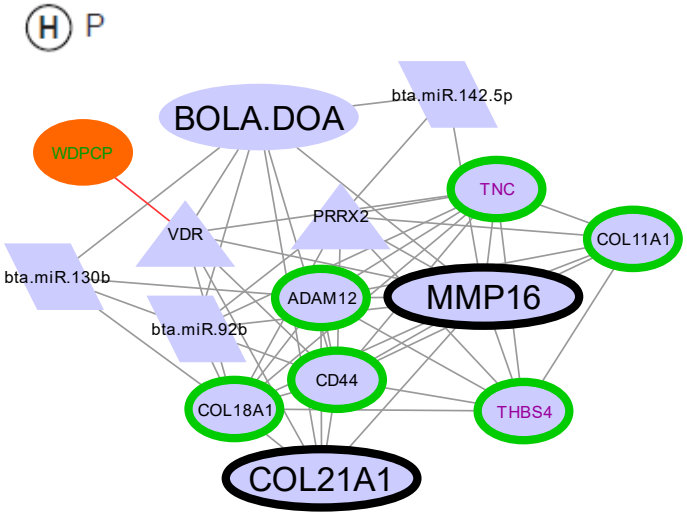
H P
BOLA.DOA
bta.miR.142.5p
WDPCP
TNC
PRRX2
VDR
COL11A1
bta.miR.130b
ADAM12
MMP16
bta.miR.92b
CD44
COL18A1
THBS4
COL21A1

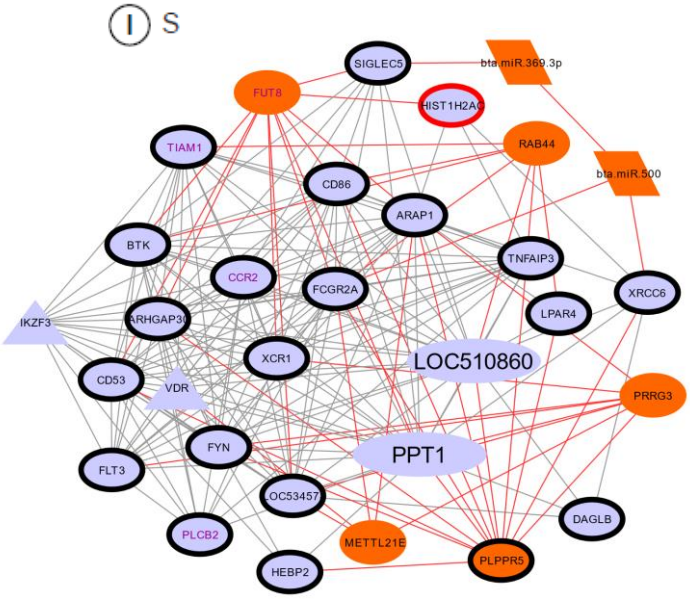
I S
SIGLEC5
bta.miR.369.3p
FUT8
HIST1H2AC
TIAM1
RAB44
bta.miR.500
CD86
ARAP1
BTK
TNFAIP3
CCR2
FCGR2A
XRCC6
IKZF3
ARHGAP31
LPAR4
XCR1
LOC510860
CD53
VDR
PRRG3
FYN
PPT1
FLT3
LOC53457
DAGLB
PLCB2
METTL21E
PLPPR5
HEBP2

Table 3.4. Pathways enriched for each mineral considering the genes correlated to each one of them and the previously detected differentially expressed genes related to the same minerals in the same Nelore population. Pathways just enriched in previous works with a differential expression approach and the same Nelore population are marked in dark grey, pathways enriched in the current correlated genes analysis are marked in black and the pathways enriched both in previous work and in the correlated genes are marked in light grey. There were no enriched pathways for Zn.

	Ca	Cu	K	Mg	Na	P	S	Se	Fe
AMPK signaling pathway									
Antigen processing and presentation									
Assembly of collagen fibrils and other multimeric structures									
Biosynthesis of unsaturated fatty acids									
Collagen biosynthesis and modifying enzymes									
Collagen chain trimerization									
Collagen formation									
DAP12 interactions									
Degradation of the ECM									
ECM organization									
ECM-receptor interaction									
Fatty acid biosynthesis									
Fatty acid metabolism									
Fc gamma receptor (FCGR) dependent phagocytosis									
Focal adhesion									
G alpha (q) signaling events									
Herpes simplex infection									
Immune system									
Influenza A									
Innate immune system									
Integrin cell surface interaction									
Measles									
Neutrophil degranulation									
Non-integrin membrane-ECM interactions									
O-glycosylation of TSR domain-containing proteins									
Phagosome									
PI3K-Akt signaling pathway									
Platelet activation									
PPAR signaling pathway									
Prion disease									
Protein digestion and absorption									
Signal transduction									

Figure 3.5. Co-expression network containing DEGs for Zn, genes or miRNAs that are correlated to these DEGs and are also a hub or a significant RIF for Zn, ora miRNA correlated to Zn. Their functional attributes are presented in different colors or shapes. Red lines represent the correlations with a significant RIF gene or miRNA.

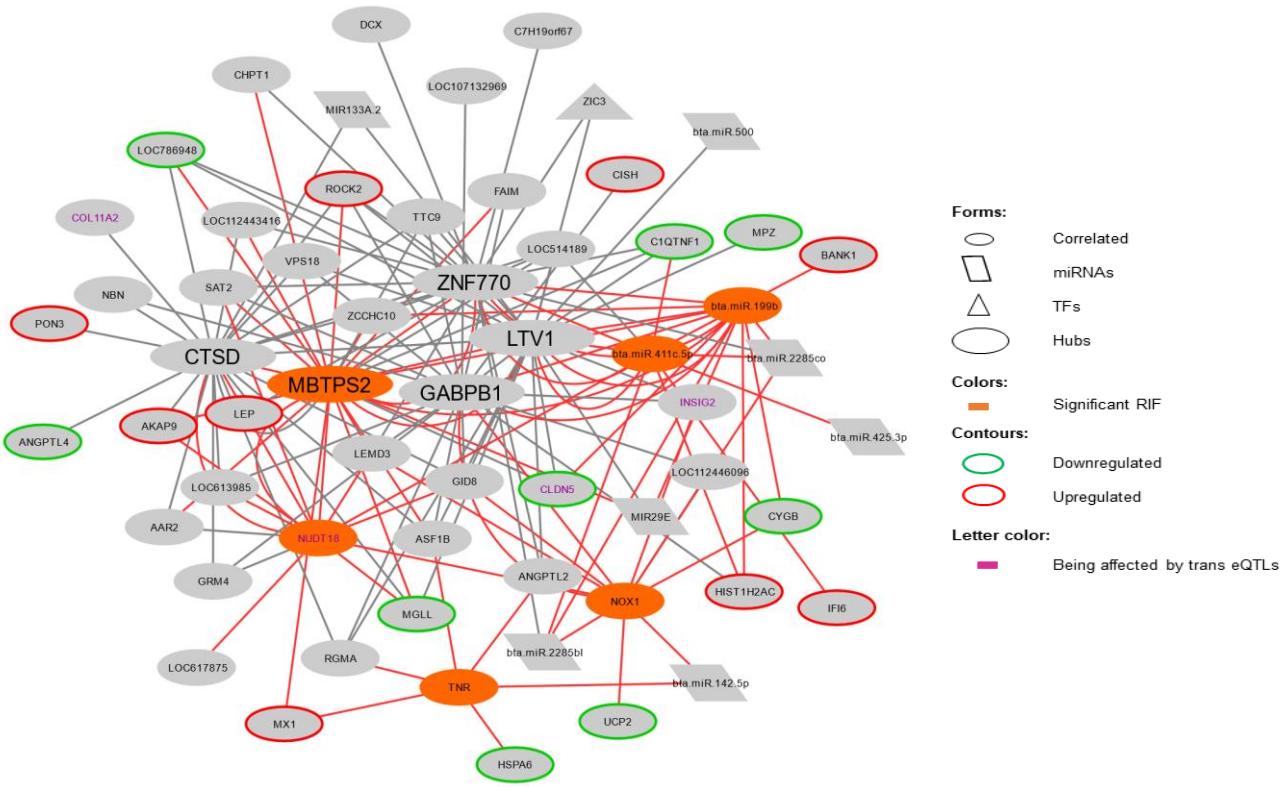

3.5. DISCUSSION

3.5.1. Relationship among minerals

Correlations identified among GEBVs for most minerals were high (0.77 to 0.97). Thus, a word of caution must inform this discussion of all genes and miRNAs with expression values correlated to each mineral, as correlated responses across minerals may underlie the identified genes and miRNAs, as well as their predicted relationships. All minerals, except Se, were correlated among themselves and all of them revealed genes in common, in the correlation network. In this network, the link between Se and the other minerals was Zn, through the common correlation with the NADPH oxidase 1 (*NOX1)* gene expression, which had significant RIF results for Zn. *NOX1* was positively correlated to Zn and negatively to Se. Accordingly, Zn positively regulates NOX1 protein expression in humans, since an increase in Zn leads to a Zn accumulation in the mitochondria. This accumulation increases the

production of reactive oxygen species which activates NF-Kb, a known positive transcriptional regulator of *NOX1*, thus increasing its expression (SALAZAR et al., 2017). Moreover, Se deficiency is known to induce the oxidation of NrX, a transmembrane protein, by the accumulation of H_2O_2, which is catalyzed by the NOX1 protein (BRIGELIUS-FLOHÉ and KIPP, 2013). As the Se deficiency and the H_2O_2 accumulation catalyzed by the NOX1 protein act in the same known biochemical process, this could explain the negative correlation found in our analysis. Further, the oxidation of NrX protein leads to the activation of the Wnt signaling pathway (BRIGELIUS-FLOHÉ and KIPP, 2013), that can act in adult muscle regeneration (MALTZAHN et al., 2012), an evidence for the relevance of this regulation for muscle homeostasis. Another link between Se and Zn were the correlations with three miRNAs`expression: bta-miR-411c-5p (with significant RIF for Zn), bta-miR-2285co and bta-miR-2285bl, although no literature relates these miRNAs to Se or Zn amount, nor to the genes related to these minerals in our analysis.

Fe exhibited a weak correlation with Mg, K, P, and S (from 0.25 to 0.31, $p < 0.05$) and was linked to other minerals through S, sharing negative correlations with the 1-phosphatidylinositol 4,5-bisphosphate phosphodiesterase gene (*PLCB2)* expression. PLCB2 protein is critical to Ca efflux (PARK et al., 1998), although no correlation with Ca amount was found in our data, nor in our previously reported DEGs (AFONSO et al., 2019). The relationship of *PLCB2* gene expression with Fe and S is undocumented, although Fe was reported to cleave the PLCB2 protein in the cornea of bovine, porcine and humans (SEIDMAN et al., 2019). The *PLCB2* gene is affected by 61 trans eQTLs, harbored across 12 chromossomes (CESAR et al., 2018), making these eQTL regions candidates to regulate this gene expression and consequently Fe and S mass fractions in the muscle.

3.5.2. PCA score analyses identified regulators of mineral composition

Our score successfully detected contrasting samples regarding all minerals together, allowing for the identification of genes and miRNAs with significant overall RIFs. Considering these genes and the functional enrichment analysis, we identified well-conserved functions for 14 out of 22 genes. From these, we can highlight three with functions related to minerals: Delta-aminolaevulinic acid dehydratase (*ALAD)* encodes a metal ion binding protein linked to Zn, Zinc finger CCHC domains-containing protein 7 (*ZCCHC7)*, which encodes a chaperone and Zn finger protein, while Myosin light chain kinase 3 (*MYLK3)* is part of the Ca signaling pathway that participates in muscle contraction.

Mutations in the *ALAD* gene were linked to the phenotypic expression of potentially toxic metal by fly ash exposure in cattle born near thermal power plants, being pointed as a candidate for genomic studies related to metal toxicity (BEHERA et al., 2016). Our results indicated that *ALAD* is a candidate linked to minerals in general, including potentially toxic metals.

3.5.3. Functional analyses and the search of regulatory elements

Functional annotation analyses, performed based on the genes with expression values correlated to each mineral, showed no functional clusters nor enriched pathways for any mineral. However, some of these genes had their expression correlated with the expression of DEGs partaking in different pathways and are themselves part of these pathways, which lead us to hypothesize that the remaining genes of the pathways may be modulated in less intensity. This agrees with the small QTL effects already observed for mineral amount (TIZIOTO et al., 2015). The function annotation for each gene separately showed membrane proteins and extracellular matrix (ECM) related proteins as common annotation for many genes. This observation helps to corroborate the hypothesis that ECM interactions are at the regulatory core for the mineral mass fraction (AFONSO et al., 2019). ECM pathways were enriched for co-expressed groups of genes related to mineral mass fraction and meat quality traits in this Nelore population (DINIZ et al., 2019).

When components of a specific pathway are known, a guided-gene approach in a co-expression network can help to identify new genes for the same pathway-related-trait (ITKIN et al., 2013), and a pre-selection of genes by biological meaning can improve the network interpretation (SERIN et al., 2016). Our selection based on enriched pathways, TFs, and significant RIF allowed the inference of genes and miRNAs with a regulatory potential in these pathways. We identified high correlations among these selected elements when compared with the correlations among unselected genes/miRNAs and minerals or considering all genes/miRNAs correlated to a mineral and their respective DEGs. These high correlations and the presence of genes related to regulatory processes reinforces that our methodology can be used to drive the search for meaningful regulatory relationships.

3.5.4. Potential regulators for more than one mineral

Genes with significant RIF and genes with expression values correlated to others

expression values that belong to enriched pathways are the potential regulators. These candidate genes may modulate mineral mass fraction by affecting their target genes and pathways. For the minerals presenting enriched pathways, except Zn, the elements with significant RIFs were connected with miRNAs, correlated genes, TFs and genes being affected by trans eQTLs. They were also part of enriched pathways, reinforcing their regulatory role on the phenotypes. The intricate patterns obtained in these network analyses arise from the fact that the same genes are part of different pathways.

As expected, the pathways identified by considering gene expression correlation with mineral GEBVs were often the same already reported in the differential expression study (AFONSO et al., 2019). The pathways with functions related to ECM processes and protein metabolism were enriched for seven minerals, all except Se, Fe, and Zn. These results also corroborate our previous hypothesis that the regulatory core of mineral amount is linked to ECM processes (AFONSO et al., 2019). Pathways related to fatty acid metabolism were enriched for Cu, as reported in that previous study. However, with the inclusion of the genes with expression values correlated to the minerals, pathways linked to immune responses were now enriched for Ca, Cu, Fe, and S. The pathways enriched for S, related to signal transduction and immune response, were not detected in the previous cited work, emphasizing that the integrative approach used herein can bring up new evidences of regulatory processes not identified under the differential expression analysis.

We identified putative regulators that might impact more than one mineral. Cluster of differentiation 86 gene (*CD86)* showed a significant RIF and was a hub gene for Mg and K analyses. The gene *CD86* encodes a protein signaling for T cell activation and proliferation (LANIER et al., 1995) and is linked to T cell adhesion after activation (LOZANOSKA-OCHSER et al., 2008). A Mg sensor, ITK, seems to be required for optimal T cell activation (GEORGE et al., 2017) and K^+ channels are involved in T cell activation, after the binding of the CD86 in the CD28 receptor (CHANDY et al., 2004), putatively explaining the relationship among these two minerals and *CD86*. The PI3k-akt signaling pathway is activated after this protein-receptor binding in an antigen-presenting cell, leading to downregulation of integrins, participants of the pathways enriched for these two minerals (GAVILE et al., 2017). For both Mg and K, the known roles of *CD86* support the idea that this is a regulator for the enriched pathways.

The Vitamin D receptor (*VDR*) is a TF with significant RIF for Mg and Na. *VDR* has a known relationship with Ca metabolism (FERRARI, BONJOUR and RIZZOLI, 1998), and its expression was correlated to this mineral, but it was not identified here as a putative regulator

for Ca based on the RIF score. Mg is essential to vitamin D activation, once both enzymes involved in this process, 25-hydroxylase and 1α-hydroxylase, are Mg-dependent (UWITONZE and RAZZAQUE, 2018). *VDR* link with Na is not extensively documented. A putative role of this encoded receptor in the increased Ca absorption and/or reduced Ca loss in menopause women containing no f alleles of the *VDR* gene under a Na and protein-rich diet was reported (HARRINGTON et al., 2004). The relationship between this gene and the ECM processes-related pathways enriched for both minerals seems to be the interaction of the VDR receptor with the Runx2 receptor which, in mammals, stabilizes chromatin remodelers by activating genes involved in ECM mineralization (MARCELLINI et al., 2010).

WD repeat-containing planar cell polarity effector (*WDPCP)* is a gene with significant RIF for Na and P and was affected by one trans eQTL in chromosome five (CESAR et al., 2018). The *WDPCP* gene encodes a protein that inhibits Wnt activity (MAYR et al., 1997), whose pathway acts in adult muscle regeneration (MALTZAHN et al., 2012), and is activated by high P amounts (YAO et al., 2015). ECM processes-related pathways were also enriched for these minerals. ECM stiffnes increases the expression of several members of the Wnt pathway through integrins and focal adhesion pathways (DU et al., 2016), thus relating the *WDPCP* gene with the enriched pathways. The link between *WDPCP* and Na is not known. In both minerals, Na and P, *WDPCP* expression is correlated positively (0.19) with the expression of the TF *VDR* that represses the Wnt pathway (LARRIBA et al., 2013).

The miRNA bta-miR-369-3p had a significant RIF for Ca and S. The genes with expression values correlated to this miRNA expression are not known targets to it. This miRNA expression levels increases in skin and serum of humans with psoriasis (GUO et al., 2013). A homolog of psoriasin, a common protein in psoriasis patients, was identified in bovines and have the same antimicrobial and immune response activity as the human one (REGENHARD et al., 2009). Psoriasis trigger seems to be the activation of the cellular immune system (LOWES, BOWCOCK and KRUEGER, 2007), probably explaining why the bta-miR-369-3p was correlated to several genes involved in immune pathways for Ca and S. Further, Ca and vitamin D play important roles in keratinocyte differentiation and regulate proteins involved in psoriasis (CUBILLOS and NORGAUER, 2016) and S is used as a known treatment and prevention of reoccurrence for this disease (KAZANDJIEVA et al., 2008). Our results suggest the genes with expression values correlated to bta-miR-369-3p expression as non-described candidate targets of this miRNA, linked to immune response and mineral concentration.

3.5.5. Potential regulators for specific mineral concentration

Some putative regulators showed significant RIF for only one mineral. The miRNA bta-let-7i showed significant RIF for Mg and one of the genes with expression values correlated to Mg, Collagen alpha-1 (XI) chain (*COL11A1)* is a target of this miRNA. The *COL11A1* gene was included in our integrative analysis for being described as a DEG for eight minerals (AFONSO *et al*., 2019), is associated to protein digestion and absorption, as well as, to ECM receptor interaction. This gene encodes a collagen protein, the most abundant protein in ECM. *COL11A1* expression is correlated to Mg, which is known to stimulate collagen synthesis (SENNI, FOUCAULT-BERTAUD and GODEAU, 2003), and it is correlated to the expression of other genes being part of the same or related pathways. Cystathionine gamma-lyase (*CTH)* was another gene with significant RIF only for Mg. This gene expression is correlated to the expression of a Zn finger protein of the cerebellum (*ZIC3)*, a TF, which was correlated to the already mentioned *CD86* gene expression, also associated with Mg herein.

We identified two genes with significant RIF specifically for K: Matrix metallopeptidase (*MMP16)* and E3 ubiquitin-protein ligase (*RNF34)*. The gene *MMP16* encodes a protein whose family is involved in the breakdown of ECM, particularly of collagen proteins (JABLONSKA-TRYPUC, MATEJCZYK and ROSOCHACKI, 2016), thus explaining its link to the enriched pathways related to ECM organization and its correlation with Collagen type XXI alpha 1 chain (*COL21A1)* gene expression. Both *MMP16* and *RNF34* genes expressions were correlated to *CD86* expression, for which the link to K was already discussed. *RNF34* encodes a RINF finger protein that negatively regulates the NOD1 pathway, involved in receptors activating immune responses, similar to *CD86*. *MMP16* is a known target for Bta-miR-92b, whose expression was correlated to the mRNA levels of seven genes, including *MMP16*, which could explain the relationship of this miRNA with the over-represented ECM pathways.

For Na, we identified six genes' mRNA levels linked to ECM processes with significant RIF: *WDPCP* and *VDR*, already discussed, Vimentin type intermediate filament associated coiled-coil protein (*VMAC)*, Cyclin-dependent kinase inhibitor 3 (*CDKN3)*, Centromere protein E (*CENPE)*, and Calcium/calmodulin-dependent protein kinase kinase 1 (*CAMKK1)*. VMAC intermediate filaments play an important role in cytoskeletal organization (YAMAMOTO et al., 2004). ECM and cytoskeleton take part on cell adhesions, mediated by integrins (GEIGER et al., 2001). *CDKN3* encodes a cycling-dependent kinase inhibitor that is

involved in cell cycle regulation (GRANA and REDDY, 1995), a process where integrins also participate (MORENO-LAYSECA and STREULI, 2014). The presence of an integrin transcript, integrin subunit alpha 10 (*ITGA10)* in the network, as well as actin interactions, could explain the link of these two genes and the ECM-related pathways enriched in the Na analysis. Additionaly, there was a miRNA with significant RIF for Na, bta-miR-125a, with expression values correlated to two genes mRNA levels with significant RIF for this mineral, *WDPCP* and *VMAC*, and the correlated integrin gene expression *ITGA10*. This miRNA targets *VMAC* who is also affected by six trans eQTLs in chromosome six, being candidates to future studies regarding its regulation.

The miRNAs bta-miR-25 and bta-miR-378c had significant RIF for Fe. Their expressions were correlated to each other, to other miRNAs and, as with other miRNAs found in our results, and the genes expressions correlated to them were not described as their targets, thus reinforcing the need for studies on bovine miRNAs. Both miRNAs had their expression values correlated to *ALAD* gene expression, also a hub gene in the iron network. Fe amount in the extracellular environment positively affects ALAD protein level and activity (CHAUHAN, TITUS and O'BRIAN, 1997). The relationship with the immune response pathways enriched for Fe seems to be in the proteasome involvement in these pathways. ALAD protein modulates proteasome activity (BARDAG-GORCE and FRENCH, 2011) which, in turn, can shape innate and adaptative immune responses (KAMMERL and MEINERS, 2016).

Lysophosphatidic acid receptor 4 (*LPAR4)* was a hub gene with significant RIF for Ca, already known to positively regulate cytosolic Ca amount involved in phospholipase C-activating G protein-coupled signaling pathway (GO:0051482). It was linked in our network to MAF BZIP transcription factor B (*MAFB)*, a TF that interacts with Gcm2 and modulates parathyroid hormone, which regulates Ca mass fraction (KAMITANI-KAWAMOTO et al., 2011). These genes expressions were correlated to other six genes. Three of them were DEGs for Ca, being part of pathways involved in ECM processes, and the other three were hub genes. From these hub genes, Bcl-2-modifying factor (*BMF)* induces apoptosis after cell detachment from the ECM (DELGADO and TESFAIGZI, 2014).

We identified the RAS like family 11 member A (*RASL11A)*, which encodes a RAS-like protein, with significant RIF for Cu. This gene expression was correlated mainly to the expression of genes involved in fatty acid metabolism, a process where Cu is a known enzymatic co-factor (CUNNANE, 1982). RAS proteins' posttranslational modifications are affected by fatty acids (TAMANOI et al., 1988), possibly explaining the link of this gene with

the fatty acid-related proteins.

For S, we identified Fucosyltransferase 8 (*FUT8),* RAB44 member RAS oncogene family (*RAB44),* Proline-rich and gla domain 3 (*PRRG3),* Protein-lysine methyltransferase METTL21E (*METTL21E),* and Phospholipid phosphatase related 5 (*PLPPR5)* genes with significant RIF, correlated or being part of immune response and signal transduction pathways. Sulfur amino acids affect inflammatory aspects of the immune system (GRIMBLE, 2006). Although there is no primary connection between FUT8 and RAB44 proteins and the immune system, these proteins contribute to tumor progression (CHEN et al., 2013; MACALUSO et al., 2002), in which a robust immune response is envolved (WHITESIDE, 2010). *PRRG3* encodes a vitamin K-dependent transmembrane protein with a GLA domain, involved in coagulation factors (CRANENBURG, SCHURGERS and VERMEER, 2017), a process that is linked to the innate immune system (DELVAEYE and CONWAY, 2009). Regarding signal transduction pathways, *METTL21E* was linked to signaling pathways in mouse siRNA experiments (HUANG et al., 2014), and *PLPPR5* encodes a protein member of the phosphatidic acid phosphatase family, acting in phospholipase D mediating signaling (BILLAH, 1993). The bta-miR-500, who presented a significant RIF for S is not a known regulator of the genes whose mRNA levels were correlated to this miRNA in our analysis.

For Se, all enriched pathways were related to ECM interactions and protein digestion and absorption. For this mineral, we identified six annotated genes with significant RIF, Thyrotroph embryonic factor (*TEF),* Zn finger DBF-type containing 2 (*ZDBF2),* Tetratricopeptide repeat domain 21 (*TTC21A),* Histidyl-tRNA synthetase (*HARS),* DTW domain containing 1 (*DTWD1),* and Pyruvate dehydrogenase kinase 3 (*PDK3)*. *TEF* is a TF and a leucine zipper protein (DROLET et al., 2009), whose family is required for the activation of DDRs receptors, essential to matrix remodeling (NOORDEEN et al., 2006). *PDK3* encodes an enzyme responsible for the regulation of glucose metabolism that, among many other functions, is related to ECM remodeling (SULLIVAN et al., 2018). We could not find a link among *ZDBF2*, *HASR*, and *DTWD1* genes and Se or the enriched pathways. They are candidates for future studies regarding these potential relationships.

Regarding Zn, even without over-represented pathways, it is possible to infer that the six elements presenting significant RIF are putative regulators of several correlated transcripts and a few DEGs, as already discussed by *NOX1*. From the six genes with significant RIF, Membrane-bound transcription factor peptidase, site 2 gene (*MBTPS2)* is also a hub gene encoding an intramembrane Zn metalloprotease and *TNR* encodes an ECM glycoprotein. This information can lead to the assumption that ECM-related processes can also be associated to

Zn amount, as they putatively do to most of the other minerals in study (AFONSO et al., 2019).

3.5.6. New application for PCIT and RIF algorithms

The first “co-expression network”, containing genes and miRNAs correlated to the mass fraction of at least one mineral, is considered to be a correlation network among elements from two different sources: sequencing (mRNA-Seq and miRNA-Seq) and a measure referring to the trait of interest, the minerals` GEBVs. Originally, outputs from PCIT algorithm forms co-expression networks based on significant correlations between gene and miRNA expression levels. PCIT works in two steps: first, a partial correlation is calculated for every trio of genes/miRNAs based on the expression values of these elements in a specific set of samples, giving us the strength of the linear relationship between every two items, independently of the third one. In the end, PCIT calculates, for each trio of genes, the average ratio of partial to direct correlations. This value is set as the information theory threshold for significant associations, not the same for every analysis, specific for each trio (REVERTER and CHAN, 2008). Statistically, both steps can be used to test the correlation and the significance threshold of other genetic elements, if they vary in the population. Thus, there is no statistical impediment of using PCIT in the way proposed here, to detect genes and miRNAs whose expression values variate in our samples in correlation with the minerals` GEBVs, as proposed here, since they already represent just the additive genetic effect of the traits.

The RIF algorithm was developed to calculate the impact of TFs over a selected list of genes through the expression values of genes and TFs across samples, in two contrasting groups for the studied phenotype (in our case, minerals). This impact factor is calculated in two ways (RIF 1 and RIF 2). RIF 1 gives higher scores to TFs that are most differentially co-expressed, highly abundant, and with more expression difference between the groups. RIF 2 gives a higher score to TFs for which the expression can predict better the abundance of DEGs (REVERTER et al., 2010). Again, there is no impediment in the analytical methodology to use other genetic information, *e.g.,* GEBVs, since it variates in the population. In our new application, we used genes and miRNAs with expression values correlated to at least one mineral in the place of TFs, and GEBVs were used instead of selected genes. In this case, RIF 1 gives a higher score to the genes or miRNAs that are most differentially co-expressed, highly abundant and with more expression difference between the

contrasting groups (mineral specific groups and score-based groups, separately) and RIF 2 to genes and miRNAs for which the expression can predict better the magnitude of the GEBVs. Toghether, both new applications can be used to predict genes and miRNAs correlated to mineral mass fraction and to pinpoint which ones have a regulatory impact over mineral amount.

3.6. CONCLUSION

By using a modification of the PCIT/RIF methodology, we were able to predict regulatory elements related to the mineral amount of ten minerals, indicating over-represented pathways linked to the mass fraction of each mineral and putative regulators that are mineral specific. Our analyses corroborate the link between mineral amounts and the ECM processes, including a relationship with Zn not seen in our previous analysis. In our proposed approach, PCIT can be applied to predict the relationship between gene transcripts or miRNAs and phenotypes, in a genome-wide fashion. Similarly, RIF may predict the regulatory impact of mRNAs and miRNAs levels over phenotypes. This new approach can be applied for any phenotype that is of interest for genomic selection and livestock breeding.

3.7. AUTHORS CONTRIBUTION

J.A., M.R.S.F., A.R and L.C.A.R. designed the experiments and analysis. J.A., M.R.S.F., A.R., W.J.S.D., A.S.M.C, A.O.L., J.P., M.M.S., L.L.C., G.B.M., A.Z., C.F.G., A.R.A.N., performed the experiments and analysis. J.A., M.R.S.F., A.R. and L.C.A.R. interpreted the results. J.A. and M.R.S.F. drafted the manuscript. All authors revised and approved the final manuscript.

3.8. REFERENCES

AHOLA, J. K. et al. Effect of copper, zinc, and manganese supplementation and source on reproduction, mineral status, and performance in grazing beef cattle over a two-year period. **Journal of Animal Science**, v. 95, p. 2357-2383, 2004.

AFONSO, J. *et al.* Muscle transcriptome analysis reveals genes and metabolic pathways related tomineral concentration in *Bos indicus,* **Scientific Reports,** v. 9, p. 11, 2019.

AGARWAL, V. et al. Predicting effective microRNA target sites in mammalian mRNAs, **Elife**, v. 4, p. 1–38, 2015.

BARDAG-GORCE, F. & FRENCH, S. W. Delta-aminolevulinic dehydratase is a proteasome interacting protein, **Experimental and Molecular Pathology**, v. 91, p. 485–489, 2011.

BEHERA, R. et al. Study of mutations in aminolevulinic acid dehydratase (ALAD) gene in cattle from fly ash zone in Maharashtra, India, **Indian Journal of Animal Research**, v. 50, p. 19–22, 2016.

BILLAH, M. M. Phospholipase D and cell signaling, **Current Opinion in Immunology**, v. 5, p. 114–23, 1993.

BRIGELIUS-FLOHÉ, R. & KIPP, A. P. Selenium in the redox regulation of the Nrf2 and the Wnt pathway, **Methods in Enzymology,** v. 527, p. 65-86, 2013.

CAMPBELL, I. Macronutrients, minerals, vitamins and energy, **Anaesthesia and Intensive Care Medicine**, *v.* 18, p. 141–146, 2016.

CESAR, A. S. M. et al. Identification of putative regulatory regions and transcription factors associated with intramuscular fat content traits, **BMC Genomics,** v. 19, p. 1–20, 2018.

CHANDY, K. G. *et al.* K+ channels as targets for specific immunomodulation, **Trends in Pharmacological Science**, v. 25, p. 280–289, 2004.

CHAUHAN, S., TITUS, D. E. & O'BRIAN, M. R. Metals control activity and expression of the heme biosynthesis enzyme δ-aminolevulinic acid dehydratase in Bradyrhizobium japonicum, **Journal of Bacteriology**, v. 179, p. 5516–5520, 1997.

CHEN, C. Y. et al. Fucosyltransferase 8 as a functional regulator of nonsmall cell lung cancer, **Proceedings of the National Academy of Science of the United States of America**, v. 110, p. 630–635, 2013.

CRANENBURG, E. C. M., SCHURGERS, L. J. & VERMEER, C. Vitamin K: The coagulation vitamin that became omnipotent, **Journal of Thrombosis and heamostasis**, v. 98, p. 145–161, 2017.

CUBILLOS, S. & NORGAUER, J. Low Vitamin D-modulated calcium-regulating proteins in psoriasis vulgaris plaques: S100A7 overexpression depends on joint involvement,

International Journal of Molecular Medicine, v. 38, p. 1083–1092, 2016.

CUNNANE, S. C. Differential regulation of essential fatty acid metabolism to the prostaglandins: possible basis for the interaction of zinc and copper in biological systems, **Progress in Lipid Research**, v. 21, p. 73–90, 1982.

DE OLIVEIRA, P. S. N. et al. Identification of genomic regions associated with feed efficiency in Nelore cattle, **BMC Genetics**, v. 15, pp. 10, 2014.

DE SOUZA, M. M. et al. A comprehensive manually-curated compendium of bovine transcription factors, **Scientific Reports**, v. 8, p. 1–12, 2018.

DELGADO, M. & TESFAIGZI, Y. Is BMF central for anoikis and autophagy ?, **Autophagy**, v. 10, p. 1–2, 2014.

DINIZ, W. J. S. et al. Detection of Co-expressed Pathway Modules Associated With Mineral Concentration and Meat Quality in Nelore Cattle, **Frontiers in Genetics**, *v.* 10, p. 1–12, 2019.

DINIZ, W. J. et al. Iron content affects lipogenic gene expression in the muscle of Nelore beef cattle, **PLoS One**, v. 11, p. 1–19, 2016.

DOBIN, A. et al. STAR: Ultrafast universal RNA-seq aligner, **Bioinformatics**, v. 29, p. 15–21, 2013.

DOYLE, J. J. & SPAULDING, J. E. Toxic and Essential Trace Elements in Meat - a Review, **Journal of Animal Science**, v. 47, p. 398–419, 1978.

DROLET, D. W. et al. TEF, a transcription factor expressed specifically in the anterior pituitary during embryogenesis, defines a new class of leucine zipper proteins, **Genes and development**, v. 5, p. 1739–1753, 2009.

DU, J. et al. Extracellular matrix stiffness dictates Wnt expression through integrin pathway, **Scientific Reports**, v. 6, p. 1–12, 2016.

ENJALBERT, F., LEBRETON, P. & SALAT, O. Effects of copper, zinc and selenium status on performance and health in commercial dairy and beef herds: Retrospective study, **Journal of Animal Physiology and Animal Nutrition**, v. 90, p. 459–466, 2006.

FABREGAT, A. et al. The Reactome Pathway Knowledgebase, **Nucleic Acids Research**, v. 46, p. D649–D655, 2015.

FERRARI, S., BONJOUR, J. P. & RIZZOLI, R. The vitamin D receptor gene and calcium metabolism, **Trends Endocrinology and Metabolism**, v. 9, p. 259–265, 1998.

FRIEDLÄNDER, M. R. et al. MiRDeep2 accurately identifies known and hundreds of novel microRNA genes in seven animal clades, **Nucleic Acids Research**, v. 40, p. 37–52, 2012.

GAVILE, C. M. et al. CD86 regulates myeloma cell survival, **Blood Advances**, v. 1, p. 2307–2319, 2017.

GEESINK, G. H. & KOOHMARAIE, M. Effect of Calpastatin on Degradation of Myofibrillar Proteins by μ -Calpain Under Postmortem Conditions, **Journal of Animal Science**, v. 77, p. 2685–2692, 1999.

GEIGER, B. et al. Transmembrane Crosstalk between the extracellular matrix and the cytoskeleton, **Nature Reviews Molecular Cell Biology**, v. 2, p. 793-805, 2001.

GENTHER, O. N. & HANSEN, S. L. Effect of dietary trace mineral supplementation and a multi-element trace mineral injection on shipping response and growth performance of beef cattle, **Journal of Animal Science**, v. 92, p. 2522–30, 2014.

GEORGE, A. B. et al. ITK is a magnesium sensor during T cell activation, **The Journal of Immunology**, v. 198, pp. 10, 2017.

GRAÑA, X. & REDDY, E. P. Cell cycle control in mammalian cells: role of cyclins, cyclin dependent kinases (CDKs), growth suppressor genes and cyclin-dependent kinase inhibitors (CKIs), **Oncogene**, v. 11, p. 211–219, 1995.

GRIMBLE, R. F. The effects of sulfur amino acid intake on immune function in humans, **The Journal of Nutrition**, v. 136, p. 1660S-1665S, 2006.

GUO, S. et al. Serum and skin levels of miR-369-3p in patients with psoriasis and their correlation with disease severity, **European Journal of Dermatology**, v. 23, p. 608–613, 2013.

HARRINGTON, M. et al. The effect of a high-protein , high-sodium diet on calcium and bone metabolism in postmenopausal women and its interaction with vitamin D receptor

genotype, **The British Journal of Nutrition**, v. 25, p. 41–51, 2004.

HUANG, D. W., SHERMAN, B. T. & LEMPICKI, R. A. Systematic and integrative analysis of large gene lists using DAVID bioinformatics resources, **Nature Protocols**, v. 4, p. 44–57, 2009.

HUANG, J. et al. METTL21C is a potential pleiotropic gene for osteoporosis and sarcopenia acting through the modulation of the NFκB signaling pathway, **Journal of bone and mineral research**, v. 29, p. 1531–1540, 2014.

HUDSON, N. J., DALRYMPLE, B. P. & REVERTER, A. Beyond differential expression: the quest for causal mutations and effector molecules, **BMC Genomics**, v. 13, pp. 16, 2012.

HURST, R. & FAIRWEATHER-TAIT, S. J. Effect of selenium on human prostate cell extracellular matrix, **Proceedings of the Nutrition Society**, v. 69, p. 4503, 2010.

ITKIN, M. et al. Biosynthesis of antinutritional alkaloids in solanaceous crops is mediated by clustered genes, **Science**, v. 341, p. 175–179, 2013.

JABLONSKA-TRYPUĆ, A., MATEJCZYK, M. & ROSOCHACKI, S. Matrix metalloproteinases (MMPs), the main extracellular matrix (ECM) enzymes in collagen degradation, as a target for anticancer drugs, **Journal of Enzyme Inhibition and Medicinal Chemistry**, v. 31, p. 177–183, 2016.

KAMITANI-KAWAMOTO, A. et al. MafB interacts with Gcm2 and regulates parathyroid hormone expression and parathyroid development, **Journal of Bone and Mineral Research**, v. 26, p. 2463–2472, 2011.

KAMMERL, I. E. & MEINERS, S. Proteasome function shapes innate and adaptive immune responses, **American Journal of Physiology - Lung Cellular and Molecular Physiology**, v. 311, p. L328-L336, 2016.

KANEHISA, M. et al. KEGG: New perspectives on genomes, pathways, diseases and drugs, **Nucleic Acids Research**, v. 45, p. D353–D361, 2017.

KAZANDJIEVA, J. et al. Climatotherapy of psoriasis, **Clinics in Dermatology**, v. 26, p. 477–485, 2008.

LANGFELDER, P. & HORVATH, S. WGCNA: an R package for weighted correlation

network analysis, **BMC Bioinformatics**, v. 9, pp. 13, 2008.

LANIER, L. L. et al. CD80 (B7) and CD86 (B70) provide similar costimulatory signals for T cell proliferation, cytokine production, and generation of CTL, **Journal of Immunology**, v. 154, p. 97–105, 1995.

LARRIBA, M. J. et al. Vitamin D is a multilevel repressor of Wnt/β-catenin signaling in cancer cells, **Cancers**, v. 5, p. 1242–1260, 2013.

LOVE, M. I., HUBER, W. & ANDERS, S. Moderated estimation of fold change and dispersion for RNA-seq data with DESeq2, **Genome Biology**, v. 15, pp. 21, 2014.

LOWES, M. A., BOWCOCK, A. M. & KRUEGER, J. G. Pathogenesis and therapy of psoriasis, **Nature**, v. 445, p. 866–873, 2007.

LOZANOSKA-OCHSER, B. et al. Expression of CD86 on Human Islet Endothelial Cells Facilitates T Cell Adhesion and Migration, **Journal of Immunology**, v. 181, p. 6109–6116, 2008.

MACALUSO, M. et al. Ras family genes: An interesting link between cell cycle and cancer, **Journal of Cellular Physiology**, v. 192, p. 125–130, 2002.

MALTZAHN, J. V. et al. Wnt signaling in myogenesis, **Trends in Cell Biology**, v. 22, p. 602–609, 2012.

MARCELLINI, S. et al. Evolution of the interaction between Runx2 and VDR, two transcription factors involved in osteoblastogenesis, **BMC Evolutionary Biology**, v. 10, p. 1–12, 2010.

MATEESCU, R. G. et al. Genetic parameters for concentrations of minerals in longissimus muscle and their associations with palatability traits in angus cattle. **Journal of Animal Science**, v. 91, p. 1067–1075, 2013.

MAYR, T. et al. Fritz: A secreted frizzled-related protein that inhibits Wnt activity, **Mechanisms of Development**, v. 63, p. 109–125, 1997.

MORENO-LAYSECA, P. & STREULI, C. H. Signalling pathways linking integrins with cell cycle progression, **Matrix Biology**, v. 34, p. 144–153, 2014.

NOORDEEN, N. A. et al. A transmembrane leucine zipper is required for activation of the dimeric receptor tyrosine kinase DDR1, **The Journal of Biological Chemistry**, v. 281, p. 22744–22751, 2006.

OLIVEIRA, G. B. et al. Integrative analysis of microRNAs and mRNAs revealed regulation of composition and metabolism in Nelore cattle, **BMC Genomics**, v. 19, p. 1–16, 2018.

PARK, S. H. et al. Assignment of human PLCB2 encoding PLC β2 to human chromosome 15q15 by fluorescence in situ hybridization, **Cytogenetics and Cell Genetics**, v. 83, p. 48–49, 1998.

PERTEA, M. et al. StringTie enables improved reconstruction of a transcriptome from RNA-seq reads, **Nature Biotechnology**, v. 33, p. 290–295, 2015.

REGENHARD, P. et al. Antimicrobial activity of bovine psoriasin, **Veterinary Microbiology**, v. 136, p. 335–340, 2009.

REVERTER, A. & CHAN, E. K. F. Combining partial correlation and an information theory approach to the reversed engineering of gene co-expression networks, **Bioinformatics**, v. 24, p. 2491–2497, 2008.

REVERTER, A. et al. Regulatory impact factors: Unraveling the transcriptional regulation of complex traits from expression data, **Bioinformatics**, v. 26, p. 896–904, 2010.

SALAZAR, G. et al. Zinc regulates Nox1 expression through a NF-κB and mitochondrial ROS dependent mechanism to induce senescence of vascular smooth muscle cells, **Free Radical Biology and Medicine**, v. 108, p. 225–235, 2017.

SEIDMAN, S. A. et al. Tissue protein and lipid alterations in response to metallic impaction, **Journal of Cellular Biochemistry**, v. 120, p. 2347–2361, 2019.

SENNI, K., FOUCAULT-BERTAUD, A. & GODEAU, G. Magnesium and connective tissue, **Magnesium Research**, v. 16, p. 70–74, 2003.

SERIN, E. A. R. et al. Learning from Co-expression Networks: Possibilities and Challenges, **Frontiers in Plant Science**, v. 7, p. 1–18, 2016.

SHANNON, P. et al. Cytoscape: a software environment for integrated models of

biomolecular interaction networks, **Genome Research**, v. 13, p. 2498–504, 2003.

SULLIVAN, W. J. et al. Extracellular Matrix Remodeling Regulates Glucose Metabolism through TXNIP Destabilization, **Cell**, v. 175, p. 117-132.e21, 2018.

TAMANOI, F. et al. Posttranslational modification of ras proteins: Detection of a modification prior to fatty acid acylation and cloning of a gene responsible for the modificatio, **Journal of Cellular Biochemistry**, v. 36, p. 261–273, 1988.

TARAZONA, S. et al. Data quality aware analysis of differential expression in RNA-seq with NOISeq R/Bioc package, **Nucleic Acids Research**, v. 43, pp. 15, 2015.

TIZIOTO, P. C. et al. Detection of quantitative trait loci for mineral content of Nelore longissimus dorsi muscle, **Genetics Selection and Evolution**, v. 47, p. 1–9, 2015.

UWITONZE, A. M. & RAZZAQUE, M. S. Role of Magnesium in Vitamin D Activation and Function, **The Journal of American Osteopathic Association**, v. 118, p. 181-189, 2018.

WHITESIDE, T. L. Immune responses to malignancies, **Journal of Allergy and Clinical Immunology**, v. 125, p. S272-S283, 2010.

WILLIAMS, P. G. Nutritional composition of red meat, **Nutrition and Dietetics**, v. 64, p. S113-S119, 2007.

YAMAMOTO, Y. et al. Vmac: A novel protein associated with vimentin-type intermediate filament in podocytes of rat kidney, **Biochemical and Biophysical Research Communications**, v. 315, p. 1120–1125, 2004.

YAO, L. et al. High phosphorus level leads to aortic calcification via β-catenin in chronic kidney disease, **American Journal of Nephrology**, v. 41, p. 28–36, 2015.

4. FINAL CONSIDERATIONS

Combining the results and discussions of our two chapters, we identified genes and miRNA related to the concentration of ten minerals and the known and predicted interactions among the transcript proteins. Integrating differentially expressed genes related to mineral concentrations, genes correlated to mineral GEBV, genes already pointed as possible regulators in the literature published from our research group, the genes presenting a regulatory impact over mineral concentration and the genes taking part in over-represented pathways, we were able to mine genes putatively regulating pathways involved in mineral homeostasis.

We can conclude that ECM processes seem to be the core for all ten minerals in study, and that protein digestion and absorption, fatty acid metabolism, immune system and signalling related pathways are involved in mineral concentration genetic regulation. The new usage for the two algorithms proposed in our second chapter can be used to detect genes involved in complex phenotypes and to detect their putative regulatory impact over the phenotypes.

5. SUPPLEMENTARY INFORMATION

Supplementary Table S2.1. Log2fold_change for each DEG in each mineral analysis. Genes with positive log2fold_change are upregulated in the high mineral groups in relation to the low mineral groups. Genes with negative log2fold_change are downregulated in the high mineral groups in relation to the low mineral groups.

Gene	Ca	Cu	P	Mg	Se	Zn	K	S	Na
ADAM12	-2.33876	-2.42863	-1.56725	-1.61797	-1.96537	-	-1.6051	-	-
ADAMTS12	-0.89906	-1.08832	-	-	-	-	-	-	-
ADAMTS2	-0.71449	-0.69446	-	-	-	-	-	-	-
AEBP1	-1.19137	-1.65381	-1.24569	-1.26387	-	-	-1.26926	-	-1.49998
AIF1L	-0.71217	-	-	-	-	-	-	-	-
AMOTL2	-0.71154	-	-	-	-	-	-	-	-
ANGPTL2	-0.81685	-	-	-0.776	-	-	-0.86545	-	-
ANTXR2	-0.73518	-	-	-	-	-	-	-	-
APOO	0.684682	-	-	-	-	-	-	-	-
ARSA	-1.01411	-	-	-	-	-	-	-	-
BASP1	-1.20745	-	-	-	-	-	-	-	-
BGN	-0.87363	-	-	-	-	-	-	-	-
BLA-DQB	-1.24945	-	-	-1.04454	-	-	-0.84441	-	-0.86674
C1QB	-0.85895	-0.78118	-	-	-	-	-	-	-
C1QC	-0.8805	-0.8562	-	-	-	-	-	-	-
C1QTNF3	-1.41821	-	-	-	-	-	-	-0.86194	-
C1QTNF6	-1.44409	-1.66404	-1.15404	-1.15348	-	-	-1.15973	-	-1.19421
C4H7orf41	-0.75216	-	-	-	-	-	-	-	-
C7	-0.85588	-	-	-	-	-	-	-	-
CCDC3	-1.50628	-1.67875	-	-	-	-	-	-	-1.15013
CCDC80	-0.82888	-	-	-	-	-	-	-	-
CD44	-0.77317	-0.99736	-0.89846	-0.93892	-	-	-0.92045	-	-0.89702
CDH11	-0.78841	-	-	-	-	-	-	-	-
CDON	-0.9255	-0.94615	-	-	-	-	-	-	-
CHODL	-1.05637	-	-	-	-	-	-	-	-
CIDEC	-1.39124	-1.59464	-	-	-	-	-	-	-
CILP2	-2.39317	-3.74297	-2.78695	-2.72521	-3.0268	-	-2.78263	-	-

CKAP4	-0.75602	-	-	-	-	-	-	-	-
CLPTM1L	-0.65322	-	-	-	-	-	-	-	-
CNN1	0.711888	-	-	-	-	-	-	-	-
COL11A1	-2.38526	-3.7989	-2.18555	-2.22474	-3.74735	-	-2.04408	-2.14354	-2.29603
COL11A2	-1.14903	-1.3406	-1.83547	-1.41365	-	-	-1.86117	-	-1.59795
COL12A1	-1.49819	-2.09503	-	-1.21789	-1.77317	-	-	-	-1.34935
COL13A1	-1.8361	-	-	-	-	-	-	-	-
COL21A1	-1.24837	-	-	-	-	-	-	-	-
COL22A1	-1.59205	-3.1081	-1.95923	-1.87233	-2.41876	-	-1.81946	-	-2.15377
COL5A1	-0.88132	-	-	-	-	-	-	-	-
COL5A2	-1.02558	-1.04413	-	-	-	-	-	-	-
COMP	-2.78746	-4.74229	-2.39792	-2.44529	-3.88935	-	-2.42829	-1.99361	-2.58822
COX7A1	0.669829	-	-	-	-	-	-	-	-
CPXM2	-1.59315	-2.06927	-1.56937	-1.5262	-1.9932	-	-1.53876	-	-1.55684
CREB3L2	-0.85959	-	-	-	-	-	-	-	-
CTHRC1	-1.40659	-1.59226	-1.41587	-	-	-	-1.40371	-	-
CYCS	0.681419	-	-	-	-	-	-	-	-
DDR2	-0.68622	-	-	-	-	-	-	-	-
DKK2	-0.91717	-	-	-	-	-	-	-	-
DPY19L1	-0.80382	-	-	-	-	-	-	-	-
DPYSL2	-0.68176	-	-	-	-	-	-	-	-
ELOVL5	-0.94836	-1.20225	-	-	-	-	-	-	-
ELOVL6	-1.68163	-2.31682	-	-	-	1.55465	-	-1.58213	-
EMILIN1	-0.78729	-	-	-	-	-	-	-	-
F13A1	-0.86547	-1.00129	-	-	-	-	-	-	-
FAM105A	-0.94664	-	-	-	-	-	-	-	-
FAM129A	-0.71816	-0.73375	-	-	-	-	-	-	-
FAM198B	-0.68533	-	-	-	-	-	-	-	-
FBLN7	-2.10962	-2.95252	-2.18325	-2.02096	-2.57333	-	-2.18056	-	-2.22076
FMOD	-1.34096	-1.73548	-	-	-1.53591	-	-	-	-1.06552

FREM1	-1.4577	-	-	-1.33748	-	-	-1.34987	-	-1.35464
FZD4	-0.88642	-	-	-	-	-	-	-	-
GALNTL1	-0.88913	-	-	-	-	-	-	-	-
GAS7	-0.95636	-	-	-	-	-	-	-	-
GATM	-0.89744	-	-	-	-	-	-	-	-
GBP4	1.99192	-	-	-	-	-	-	-	-
G0I1	-1.17206	-1.36475	-	-	-	-	-	-	-
GPC6	-0.97321	-1.03403	-	-	-	-	-	-	-
HIST1H2AC	1.00191	-	0.904241	1.08215	-1.07653	0.964853	-	1.18544	0.996791
HIST1H2BD	0.765682	-	-	-	-	-	-	-	-
HOXA9.MIR196B	-4.10845	-	-	-	-	-	-	-	-
HSPH1	0.787265	-	-	-	-	-	-	-	-
IFI27	1.51807	-	-	-	-	-	-	-	1.47733
IFI44	1.66291	-	-	-	-	-	-	-	-
IGF2	-0.75924	-	-	-0.83875	-	-	-	-	-
IGFBP4	-0.8346	-	-	-	-	-	-	-	-
IGSF3	-0.85875	-	-	-	-	-	-	-	-
ISLR	-0.80689	-	-	-	-	-	-	-	-
ITGA11	-0.94251	-	-	-	-	-	-	-	-
ITGBL1	-0.85322	-	-	-	-	-	-	-	-
ITIH5	-0.80458	-	-	-	-	-	-	-	-
KCNK2	-2.70444	-2.28758	-	-	-	-	-	-	-
KERA	-1.29835	-	-	-	-	-	-	-	-
KY	-0.98094	-	-	-	-	-	-	-	-
LAPTM5	-0.67845	-	-	-	-	-	-	-	-
LASP1	-0.71898	-	-	-	-	-	-	-	-
LEP	-1.40113	-1.95029	-	-	-	1.54989	-	-	-
LEPREL1	-1.0899	-	-1.45191	-1.4066	-	-	-1.41545	-	-1.51631
LMF1	-1.0081	-	-	-	-	-	-	-	-
LOC100138864	0.907404	-	-	-	-	-	-	-	-

LOC100335754	-0.9179	-	-	-1.04611	-	-0.944	-	-	-
LOC100336629	-0.73639	-	-	-	-	-	-	-	-
LOC100336823	0.785098	-	-	-	-	-	-	-	-
LOC100337023	-1.04622	-	-	-	-	-	-	-	-
LOC100337426	1.4257	-	-	-	-	-	-	-	-
LOC100847340	1.03953	-	-	-	-	-	-	-	-
LOC100847413	0.980216	-	-	-	-	-	-	-	-
LOC100848095	-1.12607	-	-	-	-	-	-	-	-
LOC100848852.LOC784007	-1.00651	-	-	-	-	-	-	-	-
LOC100848883	1.60741	-	-	-	-	-	-	-	-
LOC100848913	-1.38656	-	-	-	-	-	-	-	-
LOC508347	1.12422	-	-	-	-	-	-	-	-
LOC520070	-0.98493	-	-	-	-	-1.05236	-	-	-
LOC535166	-0.84796	-0.90184	-	-	-	-	-	-	-
LOC615589	-0.68678	-	-	-	-	-	-	-	-
LOC618422	1.85792	1.54226	-	-	1.52097	-	-	-	-
LOC781339	0.732983	-	-	-	-	-	-	-	-
LOC784243	-2.4827	-	-	-	-	-	-	-	-
LOC785386	-2.78241	-	-	-	-	-	-	-	-
LOC786652	-0.70417	-	-	-	-	-	-	-	-
LOC786948	-1.20883	-	-	-	-	-1.29715	-	-	-
LOC787269	1.43183	-1.58242	-	-	-1.78462	-	-	-	-
LOC787803	3.46185	-2.88534	-	-	-	-	-	-	-
LOX	-1.15943	-1.11357	-	-	-	-	-	-	-
LOXL2	-0.7307	-0.96013	-	-	-	-	-	-	-
LPL	-0.89189	-	-	-	-	-	-	-	-
LTBP2	-1.16011	-1.36893	-	-	-	-	-	-	-
LUM	-1.01106	-0.6896	-	-	-	-	-	-	-
MAFB	-0.9991	-	-	-	-	-	-	-	-
MAN1A1	-0.75205	-	-	-	-	-	-	-	-

MARCKS	-1.2165	-	-	-	-	-	-	-	-
MDFIC	-0.69597	-	-	-	-	-	-	-	-
MEST	-1.74506	-1.20056	-1.54635	-1.55164	-	-	-1.53333	-	-
MGC148714	0.802315	-	-	-	-	-	-	-	-
MGST1	-0.95802	-1.06255	-	-	-	-	-	-	-
MKX	-2.62921	-2.16954	-	-	-	-	-	-	-
MMP14	-1.03737	-1.04033	-	-	-	-	-	-	-
MMP16	-1.30873	-	-	-0.99617	-	-	-	-	-
MMP2	-1.09849	-1.00009	-	-	-	-	-	-	-
MPEG1	-0.98128	-0.85838	-	-0.85201	-	-	-	-	-0.89755
MPZ	-1.0218	1.06504	-	-	-	-0.97768	-1.01442	-	-
MRC2	-0.80892	-	-	-	-	-	-	-	-
MRPL48	0.717858	-	-	-	-	-	-	-	-
MX1	1.11258	-	-	-	-	1.2064	-	-	-
MXRA5	-1.96682	-2.29902	-1.58276	-1.55165	-1.46552	-	-1.59087	-	-1.75447
MYADM	-0.7596	-	-	-	-	-	-	-	-
NCAM1	-0.79383	-	-1.09067	-0.96821	-	-	-1.0385	-	-
NDUFA12	0.687429	-	-	-	-	-	-	-	-
NDUFA4	0.792351	-	-	-	-	-	-	-	-
NFE2L3	0.890982	-	-	-	-	-	-	-	-
NID2	-0.69875	-	-	-	-	-	-	-	-
NOTCH2	-0.78415	-	-	-	-	-	-	-	-
NTRK2	-0.84958	-	-	-	-	-	-	-	-
OAF	-0.94771	-	-	-	-	-	-	-	-
OAS1.OAS2	1.12245	-	-	-	-	-	-	-	-
ODZ3	-1.49037	-1.45245	-1.35792	-1.32339	-	-	-1.37956	-	-1.58755
OLFML2A	-0.7353	-	-	-	-	-	-	-	-
OLFML2B	-1.05655	-0.89426	-0.87362	-0.89391	-	-	-0.87554	-	-0.98673
OLFML3	-0.69668	-	-	-	-	-	-	-	-
PCDH18	-0.91973	-	-	-	-	-	-	-	-

PCK2	-1.66627	-1.73633	-	-	-	-	-	-	-
PCOLCE	-0.74991	-	-	-	-	-	-	-	-
PDGFD	-0.86213	-	-	-	-	-	-	-	-
PDGFRA	-0.63329	-	-	-	-	-	-	-	-
PEG10	-1.199	-	-	-	-	-	-	-	-
PI16	-0.72356	-	-	-	-	-	-	-	-
PLEKHA5	-0.92384	-1.31875	-	-	-	-	-	-	-
PLIN1	-1.23407	-1.20362	-	-	-	-	-	-	-
PLXDC1	-0.78505	-	-	-	-	-	-	-	-
POSTN	-1.50338	-2.57708	-1.53251	-1.59063	-	-	-1.51442	-	-1.59107
PPP1R1B	-1.05471	-	-	-	-	-	-	-	-
PRELP	-0.88235	-	-	-	-	-	-	-	-
PRRX2	-1.30625	-1.30948	-1.36988	-1.31027	-	-	-1.44173	-	-1.45194
PTGFRN	-0.8317	-	-	-	-	-	-	-	-
PTMS	-0.65293	-	-	-	-	-	-	-	-
QSOX1	-0.65475	-	-	-	-	-	-	-	-
RBP4	-0.85378	-1.25747	-	-	-	-	-	-	-
RCAN1	1.29609	-	-	-	-	-	-	-	-
RGS2	1.58863	-	1.27246	1.65305	-	-	1.30084	-	1.23359
SCARA3	-1.07318	-1.20056	-	-	-	-	-	-	-
SCD	-1.29814	-1.26175	-	-	-	0.986182	-	-	-
SCIN	-0.88724	-	-	-	-	-	-	-	-
SCN3B	0.912329	-	-	1.18107	-	-	1.13383	-	-
SDC3	-0.84636	-	-	-	-	-	-	-	-
SELRC1	0.8018	-	-	-	-	-	-	-	-
SERPINF1	-0.65572	-	-	-	-	-	-	-	-
SESN3	-0.96268	-0.81352	-	-	-	-	-	-	-
SFRP4	-1.11038	-	-	-	-	-	-	-	-
SFRP5	-1.21423	-	-	-	-	-	-	-	-
SH3BGRL3	-0.79043	-	-	-	-	-	-	-	-

SLC16A2	-1.01542	-	-	-	-	-	-	-	-
SLCO1A2	-0.84934	-	-	-	-	-	-	-	-
SMPDL3A	-0.96603	-	-	-	-	-	-	-	-
SPON2	-1.07332	-	-	-	-	-	-	-	-
SPRY4	-0.84754	-	-	-	-	-	-	-	-
SYT4	-5	-	-	-	-	-	-	-	-
TF	-2.09013	-	-	-	-	-	-	-	-
THRSP	-1.85297	-2.73927	-	-	-	1.69724	-	-1.77612	-
THY1	-0.82247	-	-	-	-	-	-	-	-
TIMP2	-0.74105	-	-	-	-	-	-	-	-
TMEM119	-1.8185	-1.73674	-	-	-	-	-	-	-
TMEM233	0.714143	-	-	-	-	-	-	-	-
TNMD	-2.34372	-4.76042	-2.87619	-2.9694	-4.04006	-	-2.77153	-2.35386	-2.90605
TRIL	-1.36045	-	-	-	-	-	-	-	-
TUSC5	-1.57975	-1.5676	-	-	-	-	-	-	-
USMG5	1.03367	-	-	-	-	-	-	-	-
WIPF1	-0.8782	-	-	-	-	-	-	-	-
ACACA	-	-1.05437	-	-	-	-	-	-	-
ACSM1	-	-1.31376	-0.92468	-	-	-	-	-	-1.22592
ACTC1	-	-1.40947	-2.49413	-1.31724	-	-	-2.49055	-	-
ADIPOQ	-	-1.06379	-	-	-	-	-	-	-0.94059
AGTPBP1	-	0.955303	-	-	-	-	-	-	-
ANXA1	-	-0.97355	-	-	-	-	-	-	-
ANXA2	-	-0.83481	-	-	-	-	-	-	-
BHLHE40	-	-0.76351	-	-	-	-	-	-	-
C14H8orf22	-	0.863786	-	-	-	-	-	-	-
C28H10orf116	-	-0.96883	-	-	-	-	-	-	-
CD109	-	-0.74126	-	-	-	-	-	-	-
CD163	-	-0.78423	-	-	-	-	-	-	-
CHI3L1	-	-1.03364	-	-	-	-	-	-	-

CHPF	-	-0.81947	-	-	-	-	-	-	-
COL18A1	-	-0.76903	-0.75774	-	-	-	-	-	-0.85112
CPM	-	-1.34574	-	-0.96001	-	-	-	-	-1.06703
DAB2	-	-0.82736	-	-	-	-	-	-	-
DAP	-	-0.7027	-	-	-	-	-	-	-
DGAT2	-	-1.0234	-	-	-	-	-	-	-
D0JB1	-	0.789664	-	-	-	-	-	-	-
EBF1	-	-0.73079	-	-	-	-	-	-	-
ELMO1	-	-0.91782	-	-	-	-	-	-	-
EMP1	-	-0.86392	-	-	-	-	-	-	-
FASN	-	-1.87604	-	-	-1.16049	0.950755	-	-	-
FAT1	-	-0.96943	-	-	-	-	-	-	-
FNDC3B	-	-0.73871	-	-	-	-	-	-	-
GAS2	-	-2.89816	-	-	-	-	-	-	-
GLCE	-	-0.73931	-	-	-	-	-	-	-
GSTM3	-	1.0793	-	-	-	-	-	-	-
HSPA6	-	2.64101	-1.24581	-	-	-1.68298	-	2.32092	-
ITGA10	-	-1.55666	-1.44803	-1.53707	-	-	-1.41923	-	-1.68951
KRT8	-	1.73887	-	-	-	-1.45334	-	-	-
LOC100300267	-	-1	-	-	-	-	-	-	-
LOC100337216.LOC520016	-	1.51682	-1.42212	-1.32589	-	-	-1.55129	-	-
LOC100337244	-	2.3195	-	-	-	-	-	-	-
MAL2	-	-1.31285	-	-	-	-	-	-	-
MLLT11	-	-2.2348	-	-	-	-	-	-	-
MT1A	-	-1.73224	-	-	-	-	-	-	-
MT2A	-	-1.1827	1.77149	2.0783	-	1.26086	1.89059	1.21384	1.89389
MYH10	-	-0.80772	-	-	-0.77608	-	-	-	-
NECAB3	-	1.22668	-	-	-	-	-	-	-
NOV	-	-0.90966	-	-	-	-	-0.73819	-	-0.75658
P4HA3	-	-1.07926	-	-	-	-	-	-	-

PDE3B	-	-1.24654	-	-	-	-	-	-	-
PDZD2	-	-0.8555	-	-	-	-	-	-	-
PERP	-	-1.90158	-2.49873	-2.18506	-2.62239	-	-2.42679	-	-1.9586
PI15	-	-1.8518	-	-	-	-	-	-	-2.32329
PMP2	-	2.48424	-	-	-	-	-	-	-
PON3	-	2.24936	-	-	2.83053	1.94258	-	-	-
PPL	-	-0.85512	-	-	-	-	-	-	-
PTGIR	-	-2.51609	-	-	-	-	-	-	-
PYCR1	-	-1.39843	-	-	-	-	-	-	-
RCN3	-	-1.00603	-	-	-	-	-0.81136	-	-
RET	-	-0.76962	-	-	-	-	-	-	-
S100A10	-	-0.88141	-	-	-	-	-	-	-
SFXN1	-	-1.31849	-	-	-	-	-	-	-
SLC6A4	-	-1.39085	-	-	-	-	-	-	-
SPP1	-	-1.33087	-	-	-	-	-	-	-
SRXN1	-	-1.37719	-0.90198	-	-	-	-	-	-
SYT11	-	-1.2163	-	-	-	-	-	-	-
THBS1	-	-1.41829	-	-	-	-	-	-	-
THBS4	-	-2.81465	-1.90816	-1.97004	-	-	-1.91339	-	-2.14173
TKT	-	-0.86569	-	-	-	-	-	-	-
TNC	-	-2.20309	-1.99968	-1.97766	-1.52174	-	-2.02989	-	-2.15934
TNFRSF12A	-	-0.87425	-	-	-	-	-	-	-
TPBG	-	-1.66784	-1.80966	-1.67355	-	-	-1.77094	-	-1.48611
TRAFD1	-	-0.73233	-	-	-	-	-	-	-
UCK2	-	-1.08919	-	-	-1.27875	-	-	-	-
VCAN	-	-0.75408	-	-	-	-	-	-	-
WISP1	-	-2.68722	-	-	-	-	-	-	-
CES1	-	-	-1.03758	-1.01539	-	-	-0.9397	-	-
CRABP2	-	-	-2.30287	-2.14704	-	-	-2.33593	-	-1.72625
CRTAC1	-	-	-2.05002	-2.04274	-	-	-2.06918	-	-

CYP4B1	-	-	-1.4632	-	1.66771	-	-1.11333	-	-
FCGR3A	-	-	-1.25109	-	-	-	-1.31582	-	-1.28899
HES1	-	-	0.753489	-	-	-	-	-	-
KLF5	-	-	-0.97657	-	-	-	-0.98264	-	-
LOC100847238	-	-	1.11704	1.25662	-0.85139	-	1.23825	-	-
LOC100848544	-	-	1.01269	1.06664	-	-	1.10129	-	-
LOC100848726	-	-	0.840227	-	-	-1.5957	1.03767	2.31839	1.11774
LOC100848920	-	-	0.98718	0.982841	-	-	1.07905	-	-
LOC515150	-	-	-0.89214	-	-	-	-	-	-0.898
NES	-	-	-0.85122	-0.81965	-	-	-0.92603	-	-
S100A4	-	-	-0.86834	-0.91138	-	-	-0.8845	-	-0.84248
APOE	-	-	-	-0.97694	-	-	-0.91763	-	-0.8511
GADD45A	-	-	-	-1.03297	-	-	-	-	-
GADL1	-	-	-	0.730109	-	-	-	-	0.689153
KCNC4	-	-	-	1.03166	-	-	-	-	1.13707
LRRC20	-	-	-	0.756225	-	-	0.689864	-	0.654978
MAOB	-	-	-	-1.10237	-	-	-1.12386	-1.66064	-1.11835
MGP	-	-	-	-0.80258	-	-	-	-	-
SLIT3	-	-	-	-0.85412	-	-	-0.91309	-	-0.91819
TMSB4	-	-	-	-0.8505	-	-	-0.85618	-	-
UCHL1	-	-	-	-0.92775	-	-	-	-	-
ACTA2	-	-	-	-	0.858818	-	-	-	-
AMPD3	-	-	-	-	-0.89207	-	-	-	-
DLK1	-	-	-	-	0.829306	-	-	-	-
ECHDC2	-	-	-	-	1.00543	-	-	-	-
LOC100848346	-	-	-	-	2.60288	-	-	-	-
LOC100848684	-	-	-	-	1.96408	-	-	-	-
LOC789192	-	-	-	-	-1.30828	-	-	-	-
NR4A2	-	-	-	-	0.973619	-	-	-	-
RN5-8S1	-	-	-	-	2.79644	-2.83236	-	2.71751	-

AKAP9	-	-	-	-	-	0.784405	-	-	-
ANGPTL4	-	-	-	-	-	-0.79863	-	-	-
BANK1	-	-	-	-	-	1.3818	-	-	-
C1QTNF1	-	-	-	-	-	-0.87504	-	-	-
CISH	-	-	-	-	-	0.894319	-	0.960376	-
CLDN5	-	-	-	-	-	-0.90859	-	-	-
CYGB	-	-	-	-	-	-0.99274	-	-	-
IFI6	-	-	-	-	-	1.23173	-	-	-
ISG15	-	-	-	-	-	1.74381	-	-	1.5418
MGLL	-	-	-	-	-	-0.96588	-	-	-
PLIN5	-	-	-	-	-	-0.88872	-	-	-
RN28S1	-	-	-	-	-	-1.12057	-	-	0.939374
ROCK2	-	-	-	-	-	0.827486	-	-	-
UCP2	-	-	-	-	-	-1.18504	-	-	-
CREM	-	-	-	-	-	-	0.830859	-	-
DKK3	-	-	-	-	-	-	-1.00825	-	-0.96566
HPCAL4	-	-	-	-	-	-	-	-1.40152	-
LOC100141258	-	-	-	-	-	-	-	-2.81272	-
LOC100337053	-	-	-	-	-	-	-	-1.68767	-
MYLK3	-	-	-	-	-	-	-	-1.89817	-
SPOCK2	-	-	-	-	-	-	-	-1.13519	-
KCNMB4	-	-	-	-	-	-	-	-	-0.89854
LOC100299180	-	-	-	-	-	-	-	-	-1.57076
LOC100336936	-	-	-	-	-	-	-	-	-1.58976
LOC100847553	-	-	-	-	-	-	-	-	1.03644
LYZ	-	-	-	-	-	-	-	-	-1.16529
NDUFS6	-	-	-	-	-	-	-	-	0.76202
PRDM8	-	-	-	-	-	-	-	-	-1.38748
SMTNL1	-	-	-	-	-	-	-	-	0.783364
TPSB1	-	-	-	-	-	-	-	-	-1.15721

Supplementary Table S2.2. Significant Trynotate annotation results for the non-annotated DEGs.

Top BLASTX hit	Top BLASTP hit	eggnog	Kegg	Mineral
Myoregulin {ECO:0000303|PubMed:25640239}	.	.	KEGG:hsa:100507027	Cu
Sentrin-specific protease 3	.	COG5160 SUMO1 sentrin specific peptidase	KEGG:mmu:80886`KO:K08593	Cu
Putative deoxyribonuclease TATDN1	.	COG0084 tatd family	KEGG:bta:509365`KO:K03424	Cu
Sentrin-specific protease 3	.	COG5160 SUMO1 sentrin specific peptidase	KEGG:mmu:80886`KO:K08593	Cu
Ig gamma-3 chain C region	Ig gamma-3 chain C region	.	.	P
LINE-1 retrotransposable element ORF2 protein	.	ENOG410Y9TZ NA	.	P
.	Endogenous retrovirus group V member 2 Env polyprotein	ENOG4111C12 endogenous retrovirus group MER34	KEGG:hsa:100271846	P
RNA-directed DNA polymerase from mobile element jockey	.	.	.	P
RNA-binding protein 39	RNA-binding protein 39	ENOG410XP20 RNA binding motif protein	KEGG:pon:100172241`KO:K13091	P
LINE-1 retrotransposable element ORF2 protein	.	ENOG410Y9TZ NA	.	Mg
.	Endogenous retrovirus group V member 2 Env polyprotein	ENOG4111C12 endogenous retrovirus group MER34	KEGG:hsa:100271846	Mg
Retrovirus-related Pol polyprotein from type-1 retrotransposable element R2	.	.	.	Mg
RNA-directed DNA polymerase from mobile element jockey	.	.	.	Mg
Pol polyprotein	.	.	KEGG:vg:22318531	Mg

Deoxynucleotidyltransferase terminal-interacting protein	Deoxynucleotidyltransferase terminal-interacting protein 1			Mg
Ig gamma-3 chain C region	Ig gamma-3 chain C region	.	.	Mg
LINE-1 retrotransposable	.	ENOG410Y9TZ NA	.	K
.	Endogenous retrovirus group V member 2 Env polyprotein	ENOG4111C12 endogenous retrovirus group MER34	KEGG:hsa:100271846	K
Retrovirus-related Pol polyprotein	.	.	.	K
RNA-directed DNA polymerase	.	.	.	K
Engulfment and cell motility protein 2	Engulfment and cell motility protein 2	ENOG410XPKN Engulfment and cell motility	KEGG:bta:508361`KO:K18985	K
L-lactate dehydrogenase A chain	.	.	.	Na
RNA-directed DNA polymerase	.	.	.	Na
Kinesin-like protein KIF3B	Kinesin-like protein KIF3B	COG5059 Kinesin family member	KEGG:hsa:9371`KO:K20196	Na
Immunoglobulin heavy constant gamma 2 {ECO:0000303|PubMed:11340299	Immunoglobulin heavy constant gamma 2 {ECO:0000303|PubMed:11340299| ECO:0000303|Ref.13}	.	.	Na
.	Putative uncharacterized transposon-derived protein F52C9.6	.	.	Zn

Supplementary Table S2.3. Significant Pearson correlations among all the GEBVs for all the minerals and associated p-values.

Ca	**Cu**	**Mg**	**P**	**K**	**Se**	**Na**	**S**	**Zn**
Ca	0.22822	0.61979	0.64251	0.61957		0.58770	0.63537	0.59900
p-value	0.0082	<.0001	<.0001	<.0001		<.0001	<.0001	<.0001
Cu		0.26372	0.24692	0.24173	0.19672	0.21535	0.20790	
p-value		0.0022	0.0042	0.0051	0.0232	0.0128	0.0163	
Mg			0.96943	0.97012	-0.20101	0.90066	0.79799	0.77813
p-value			<.0001	<.0001	0.0203	<.0001	<.0001	<.0001
P				0.96956	-0.28677	0.89588	0.82373	0.79786
p-value				<.0001	0.0008	<.0001	<.0001	<.0001
K					-0.25147	0.88504	0.81317	0.78853
p-value					0.0035	<.0001	<.0001	<.0001
Se						-0.23626	-0.21005	-0.23024
p-value						0.0062	0.0152	0.0077
Na							0.79135	0.76104
p-value							<.0001	<.0001
S								0.66939
p-value								<.0001
Zn								
p-value								

Supplementary Table S2.4. Significant Pearson correlations between the GEBVs for each mineral and their respective raw mineral concentration. All p-values are <.0001.

Mineral	**Ca**	**Cu**	**Mg**	**P**	**K**	**Se**	**Na**	**S**	**Zn**
Correlation	0.777	0.847	0.860	0.857	0.836	0.849	0.836	0.865	0.848

Supplementary Table S2.5. Average GEBV for all minerals in each contrasting group and the p-value of the tests of significance (t-test) between the extreme group samples' GEBVs for each mineral inside each contrasting group. [a]FDR correction of the p-value for each t-test. The average GEBVs for the original mineral for each group are in bold.

Ca_samples	Ca	Cu	Mg	P	K	Se	Na	S	Zn	Group
NE3	**0.0956**	0.0392	0.0617	0.0759	0.072	-0.125	0.0905	0.0795	0.0919	high
NE7	**0.138**	0.0125	0.0598	0.0765	0.0813	-0.152	0.0719	0.0815	0.134	high
NE19	**0.108**	0.0283	0.0797	0.0845	0.083	-0.0695	0.0959	0.099	0.0993	high
NE33	**0.11**	0.0533	0.0595	0.0687	0.0704	-0.072	0.0552	0.0751	0.0862	high
NE36	**0.111**	0.0624	-4.00E-04	0.0017	2.00E-04	0.0706	0.0095	0.0351	0.0064	high
NE44	**0.257**	-0.015	0.0279	0.0368	0.0256	-0.0243	0.0114	0.0692	0.0201	high
NE1	**-0.0949**	-0.0584	-0.0231	-0.0318	-0.0163	0.0125	-0.0049	-0.0104	-0.0411	low
NE12	**-0.108**	-0.0637	-0.0513	-0.0513	-0.0523	-0.189	-0.061	-0.0628	-0.0551	low
NE18	**-0.131**	-0.063	-0.0205	-0.0257	-0.02	0.0541	-0.0292	0.0067	-0.0285	low
NE27	**-0.109**	-0.0268	-0.0396	-0.0458	-0.0366	-0.163	-0.0528	-0.0353	-0.037	low
NE40	**-0.135**	-0.0044	-0.0173	-0.0055	-0.0147	-9.00E-04	0.0193	-0.0033	-0.0484	low
NE42	**-0.0955**	-0.0128	-0.0112	-0.0231	-0.0219	0.0116	-0.0066	-0.0311	0.033	low
Corrected p-value[a]	**3.85E-04**	2.39E-03	1.37E-03	1.26E-03	1.99E-03	7.66E-01	3.47E-03	3.49E-04	2.99E-03	

Cu_samples	Ca	**Cu**	Mg	P	K	Se	Na	S	Zn	Group
NE15	0.0084	**0.173**	-0.0139	-0.0269	-0.0206	0.0867	-0.019	-0.0081	-0.0629	high
NE23	-0.0492	**0.291**	-0.0121	-0.0223	-0.0311	0.11	-0.0222	-0.0327	-0.0745	high
NE28	0.0487	**0.0647**	0.0163	0.0166	0.0203	0.029	0.0247	-0.0017	0.005	high
NE30	0.0938	**0.0842**	0.0549	0.0666	0.0734	0.0044	0.0565	0.0666	0.0631	high
NE32	-0.0292	**0.0617**	0.0099	-0.0041	3.00E-04	0.122	0.0192	0.012	-5.00E-04	high
NE36	0.111	**0.0624**	-4.00E-04	0.0017	2.00E-04	0.0706	0.0095	0.0351	0.0064	high
NE1	-0.0949	**-0.0584**	-0.0231	-0.0318	-0.0163	0.0125	-0.0049	-0.0104	-0.0411	low
NE12	-0.108	**-0.0637**	-0.0513	-0.0513	-0.0523	-0.189	-0.061	-0.0628	-0.0551	low
NE18	-0.131	**-0.063**	-0.0205	-0.0257	-0.02	0.0541	-0.0292	0.0067	-0.0285	low
NE26	-0.0146	**-0.0547**	-0.0067	-0.0137	-0.0013	-0.0901	-0.0049	-0.0094	-0.053	low
NE35	-0.0374	**-0.0634**	-0.0086	-0.0161	-0.0177	-0.0989	-0.0257	-0.0324	-0.0443	low
NE41	0.0643	**-0.0575**	0.001	-8.00E-04	0.0136	-0.0227	0.0287	0.0313	0.027	low
Corrected p-value[a]	1.39E-01	**4.26E-02**	1.39E-01	1.94E-01	2.62E-01	6.94E-02	2.09E-01	2.62E-01	3.91E-01	

Mg_samples	Ca	Cu	**Mg**	P	K	Se	Na	S	Zn	Group
NE3	0.0956	0.0392	**0.0617**	0.0759	0.072	-0.125	0.0905	0.0795	0.0919	high
NE4	0.0929	0.016	**0.076**	0.0855	0.0904	-0.147	0.0929	0.0635	0.112	high
NE5	0.0925	0.0391	**0.0792**	0.0793	0.0839	-0.067	0.0856	0.0629	0.111	high
NE19	0.108	0.0283	**0.0797**	0.0845	0.083	-0.0695	0.0959	0.099	0.0993	high
NE21	0.0842	0.0402	**0.0765**	0.0816	0.0849	-0.0105	0.0983	0.0685	0.0883	high
NE25	0.0712	-0.0091	**0.0907**	0.0984	0.1	-0.0482	0.119	0.0918	0.121	high
NE10	-0.0543	0.0074	**-0.0347**	-0.038	-0.0372	0.0218	-0.0305	-0.0286	-0.0269	low
NE12	-0.108	-0.0637	**-0.0513**	-0.0513	-0.0523	-0.189	-0.061	-0.0628	-0.0551	low
NE17	-0.0673	0.0222	**-0.0455**	-0.0402	-0.0452	-0.1	-0.0497	-0.0479	-0.0225	low
NE20	-0.0575	-0.0189	**-0.0403**	-0.0458	-0.0395	-0.018	-0.0379	-0.0617	-0.0911	low
NE22	0.0138	-0.0353	**-0.0497**	-0.0521	-0.0579	0.0074	-0.015	-0.0233	-0.011	low
NE27	-0.109	-0.0268	**-0.0396**	-0.0458	-0.0366	-0.163	-0.0528	-0.0353	-0.037	low
Corrected p-value[a]	3.07E-04	1.75E-02	**3.17E-09**	7.16E-10	1.06E-09	9.20E-01	1.22E-07	2.69E-07	1.69E-05	

P_samples	Ca	Cu	Mg	**P**	K	Se	Na	S	Zn	Group
NE4	0.0929	0.016	0.076	**0.0855**	0.0904	-0.147	0.0929	0.0635	0.112	high
NE5	0.0925	0.0391	0.0792	**0.0793**	0.0839	-0.067	0.0856	0.0629	0.111	high
NE7	0.138	0.0125	0.0598	**0.0765**	0.0813	-0.152	0.0719	0.0815	0.134	high
NE19	0.108	0.0283	0.0797	**0.0845**	0.083	-0.0695	0.0959	0.099	0.0993	high
NE21	0.0842	0.0402	0.0765	**0.0816**	0.0849	-0.0105	0.0983	0.0685	0.0883	high
NE25	0.0712	-0.0091	0.0907	**0.0984**	0.1	-0.0482	0.119	0.0918	0.121	high
NE12	-0.108	-0.0637	-0.0513	**-0.0513**	-0.0523	-0.189	-0.061	-0.0628	-0.0551	low
NE17	-0.0673	0.0222	-0.0455	**-0.0402**	-0.0452	-0.1	-0.0497	-0.0479	-0.0225	low
NE20	-0.0575	-0.0189	-0.0403	**-0.0458**	-0.0395	-0.018	-0.0379	-0.0617	-0.0911	low
NE22	0.0138	-0.0353	-0.0497	**-0.0521**	-0.0579	0.0074	-0.015	-0.0233	-0.011	low
NE27	-0.109	-0.0268	-0.0396	**-0.0458**	-0.0366	-0.163	-0.0528	-0.0353	-0.037	low
NE34	-0.0422	0.0013	-0.0298	**-0.0406**	-0.0363	-0.0114	-0.0207	-0.0169	-0.0369	low
Corrected p-value[a]	1.22E-04	2.18E-02	3.48E-09	**7.50E-10**	7.50E-10	9.37E-01	2.78E-07	9.77E-07	4.59E-06	

K_samples	Ca	Cu	Mg	P	**K**	Se	Na	S	Zn	Group
NE4	0.0929	0.016	0.076	0.0855	**0.0904**	-0.147	0.0929	0.0635	0.112	high
NE5	0.0925	0.0391	0.0792	0.0793	**0.0839**	-0.067	0.0856	0.0629	0.111	high
NE7	0.138	0.0125	0.0598	0.0765	**0.0813**	-0.152	0.0719	0.0815	0.134	high
NE19	0.108	0.0283	0.0797	0.0845	**0.083**	-0.0695	0.0959	0.099	0.0993	high
NE21	0.0842	0.0402	0.0765	0.0816	**0.0849**	-0.0105	0.0983	0.0685	0.0883	high
NE25	0.0712	-0.0091	0.0907	0.0984	**0.1**	-0.0482	0.119	0.0918	0.121	high
NE10	-0.0543	0.0074	-0.0347	-0.038	**-0.0372**	0.0218	-0.0305	-0.0286	-0.0269	low
NE12	-0.108	-0.0637	-0.0513	-0.0513	**-0.0523**	-0.189	-0.061	-0.0628	-0.0551	low
NE17	-0.0673	0.0222	-0.0455	-0.0402	**-0.0452**	-0.1	-0.0497	-0.0479	-0.0225	low
NE20	-0.0575	-0.0189	-0.0403	-0.0458	**-0.0395**	-0.018	-0.0379	-0.0617	-0.0911	low
NE22	0.0138	-0.0353	-0.0497	-0.0521	**-0.0579**	0.0074	-0.015	-0.0233	-0.011	low
NE27	-0.109	-0.0268	-0.0396	-0.0458	**-0.0366**	-0.163	-0.0528	-0.0353	-0.037	low
Corrected p-value[a]	9.78E-05	2.75E-02	8.57E-09	5.59E-10	**5.85E-10**	8.42E-01	1.20E-07	2.65E-07	6.36E-06	

Se_samples	Ca	Cu	Mg	P	K	**Se**	Na	S	Zn	Group
NE9	0.006	-1.00E-04	-0.0165	-0.0247	-0.0291	**0.107**	-0.0275	-0.0333	-0.0384	high
NE16	-0.0256	-0.0179	-0.0102	-0.0199	-0.0242	**0.114**	-0.0246	0.0106	0.0254	high
NE23	-0.0492	0.291	-0.0121	-0.0223	-0.0311	**0.11**	-0.0222	-0.0327	-0.0745	high
NE24	-0.0234	-0.0192	-0.0233	-0.0303	-0.0326	**0.141**	-0.0231	-0.0536	0.0022	high
NE32	-0.0292	0.0617	0.0099	-0.0041	3.00E-04	**0.122**	0.0192	0.012	-5.00E-04	high
NE39	-0.0478	0.0072	0.0165	0.0159	0.0144	**0.0922**	-0.0144	0.0116	0.0297	high
NE4	0.0929	0.016	0.076	0.0855	0.0904	**-0.147**	0.0929	0.0635	0.112	low
NE6	-0.0622	-0.0355	-0.0225	-0.0042	-0.0216	**-0.169**	-0.0167	-0.0162	0.0116	low
NE7	0.138	0.0125	0.0598	0.0765	0.0813	**-0.152**	0.0719	0.0815	0.134	low
NE8	0.0206	0.0121	0.0281	0.0419	0.043	**-0.202**	0.0408	0.0576	0.032	low
NE12	-0.108	-0.0637	-0.0513	-0.0513	-0.0523	**-0.189**	-0.061	-0.0628	-0.0551	low
NE27	-0.109	-0.0268	-0.0396	-0.0458	-0.0366	**-0.163**	-0.0528	-0.0353	-0.037	low
Corrected p-value[a]	6.11E-01	4.53E-01	6.11E-01	4.53E-01	4.53E-01	**4.52E-09**	4.53E-01	4.53E-01	4.53E-01	

Na_samples	Ca	Cu	Mg	P	K	Se	**Na**	S	Zn	Group
NE3	0.0956	0.0392	0.0617	0.0759	0.072	-0.125	**0.0905**	0.0795	0.0919	high
NE4	0.0929	0.016	0.076	0.0855	0.0904	-0.147	**0.0929**	0.0635	0.112	high
NE5	0.0925	0.0391	0.0792	0.0793	0.0839	-0.067	**0.0856**	0.0629	0.111	high
NE19	0.108	0.0283	0.0797	0.0845	0.083	-0.0695	**0.0959**	0.099	0.0993	high
NE21	0.0842	0.0402	0.0765	0.0816	0.0849	-0.0105	**0.0983**	0.0685	0.0883	high
NE25	0.0712	-0.0091	0.0907	0.0984	0.1	-0.0482	**0.119**	0.0918	0.121	high
NE2	-0.0267	0.0408	-0.0332	-0.0385	-0.0237	0.0219	**-0.0398**	-0.0282	-0.0387	low
NE12	-0.108	-0.0637	-0.0513	-0.0513	-0.0523	-0.189	**-0.061**	-0.0628	-0.0551	low
NE14	0.0089	0.034	-0.0312	-0.0302	-0.0249	0.0584	**-0.0459**	-0.0184	-0.01	low
NE17	-0.0673	0.0222	-0.0455	-0.0402	-0.0452	-0.1	**-0.0497**	-0.0479	-0.0225	low
NE20	-0.0575	-0.0189	-0.0403	-0.0458	-0.0395	-0.018	**-0.0379**	-0.0617	-0.0911	low
NE27	-0.109	-0.0268	-0.0396	-0.0458	-0.0366	-0.163	**-0.0528**	-0.0353	-0.037	low
Corrected p-value[a]	4.01E-04	2.00E-01	3.16E-09	5.54E-10	5.92E-09	7.87E-01	**3.16E-09**	5.15E-07	1.32E-05	

S_samples	Ca	Cu	Mg	P	K	Se	Na	**S**	Zn	Group
NE3	0.0956	0.0392	0.0617	0.0759	0.072	-0.125	0.0905	**0.0795**	0.0919	high
NE7	0.138	0.0125	0.0598	0.0765	0.0813	-0.152	0.0719	**0.0815**	0.134	high
NE19	0.108	0.0283	0.0797	0.0845	0.083	-0.0695	0.0959	**0.099**	0.0993	high
NE25	0.0712	-0.0091	0.0907	0.0984	0.1	-0.0482	0.119	**0.0918**	0.121	high
NE29	0.068	-0.0071	0.0166	0.0229	0.0149	0.0757	0.005	**0.0724**	0.0046	high
NE33	0.11	0.0533	0.0595	0.0687	0.0704	-0.072	0.0552	**0.0751**	0.0862	high
NE12	-0.108	-0.0637	-0.0513	-0.0513	-0.0523	-0.189	-0.061	**-0.0628**	-0.0551	low
NE20	-0.0575	-0.0189	-0.0403	-0.0458	-0.0395	-0.018	-0.0379	**-0.0617**	-0.0911	low
NE24	-0.0234	-0.0192	-0.0233	-0.0303	-0.0326	0.141	-0.0231	**-0.0536**	0.0022	low
NE31	0.0301	-0.0372	-0.0166	-0.0298	-0.0317	0.0347	-0.0057	**-0.0662**	-0.0166	low
NE37	-0.0404	-0.0202	-0.012	-0.0156	-0.0205	-0.0078	-0.0362	**-0.0618**	0.0151	low
NE43	-0.0611	0.0263	-0.0148	-0.0154	-0.0322	0.0047	-0.0047	**-0.0599**	0.0067	low
Corrected p-value[a]	3.17E-04	2.86E-02	2.19E-04	1.30E-04	2.89E-04	3.01E-01	1.01E-03	**1.48E-07**	1.55E-03	

Zn_samples	Ca	Cu	Mg	P	K	Se	Na	S	**Zn**	Group
NE3	0.0956	0.0392	0.0617	0.0759	0.072	-0.125	0.0905	0.0795	**0.0919**	high
NE4	0.0929	0.016	0.076	0.0855	0.0904	-0.147	0.0929	0.0635	**0.112**	high
NE5	0.0925	0.0391	0.0792	0.0793	0.0839	-0.067	0.0856	0.0629	**0.111**	high
NE7	0.138	0.0125	0.0598	0.0765	0.0813	-0.152	0.0719	0.0815	**0.134**	high
NE19	0.108	0.0283	0.0797	0.0845	0.083	-0.0695	0.0959	0.099	**0.0993**	high
NE25	0.0712	-0.0091	0.0907	0.0984	0.1	-0.0482	0.119	0.0918	**0.121**	high
NE11	-0.0537	-0.0232	-0.0242	-0.0357	-0.035	0.053	-0.0189	-0.029	**-0.0571**	low
NE13	-0.0392	-0.0217	-0.023	-0.0321	-0.0293	-0.0044	-0.0377	-0.0459	**-0.0834**	low
NE15	0.0084	0.173	-0.0139	-0.0269	-0.0206	0.0867	-0.019	-0.0081	**-0.0629**	low
NE20	-0.0575	-0.0189	-0.0403	-0.0458	-0.0395	-0.018	-0.0379	-0.0617	**-0.0911**	low
NE23	-0.0492	0.291	-0.0121	-0.0223	-0.0311	0.11	-0.0222	-0.0327	**-0.0745**	low
NE38	-0.0821	0.008	0.0011	0.0085	0.004	0.0438	0.0074	0.0042	**-0.0575**	low
Corrected p-value[a]	6.81E-06	4.28E-01	7.61E-07	6.71E-06	7.61E-07	3.84E-04	7.61E-07	1.39E-05	**9.45E-09**	

Supplementary Figure S2.1. Transcription discovery versus reads sequenced saturation curve.

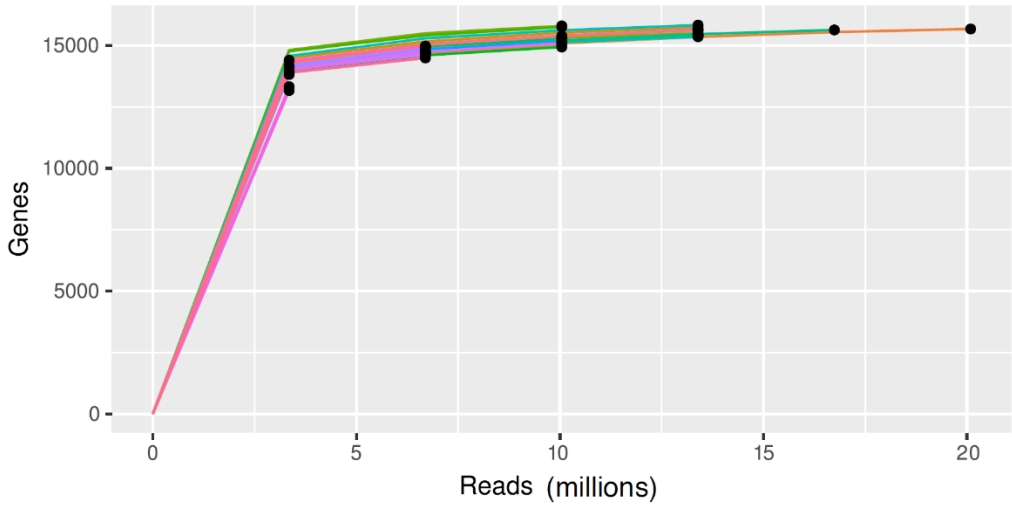

Supplementary Figure S2.2. Distribution of the samples in the extreme groups regarding all minerals.

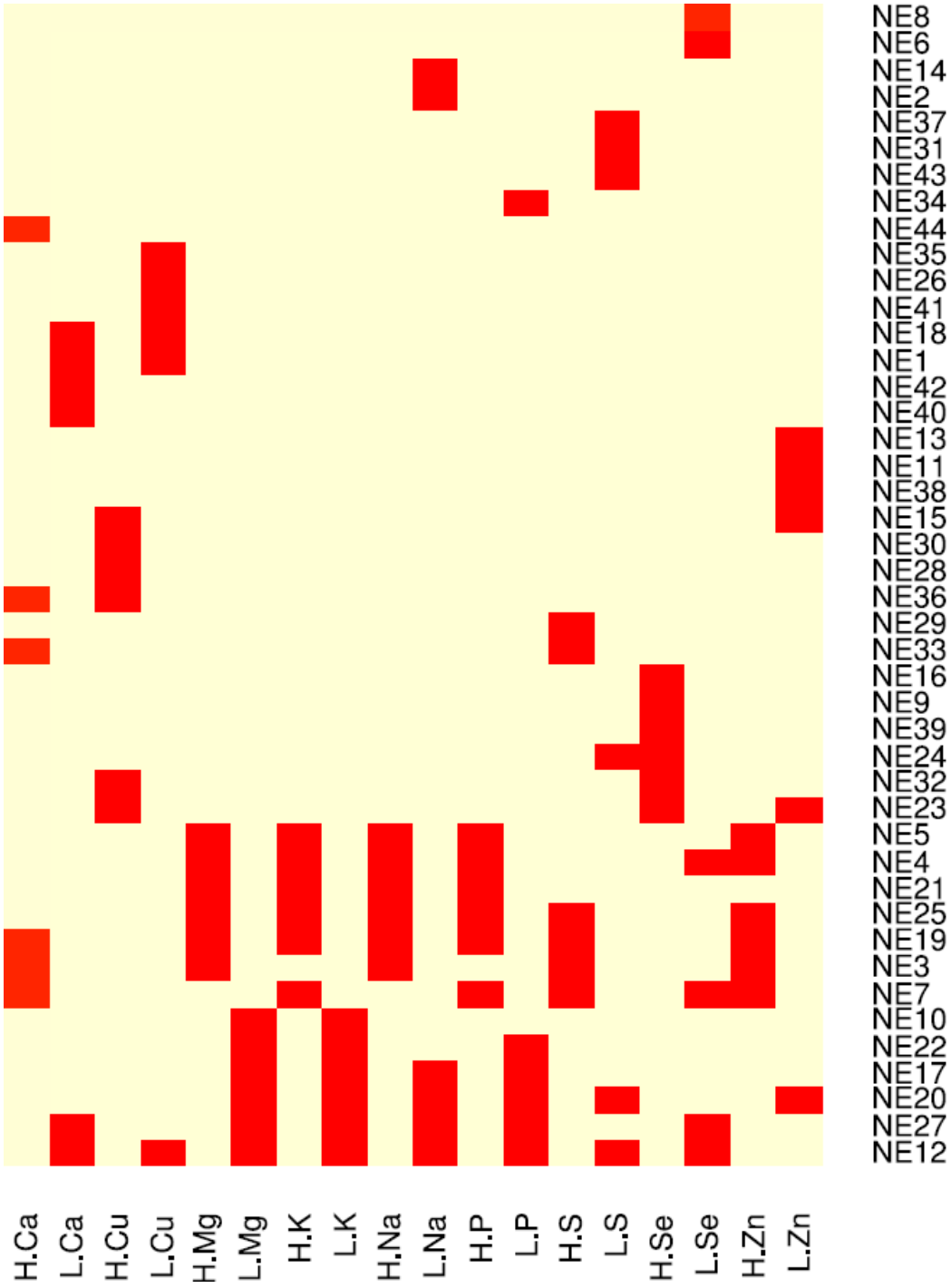

In all the supplementary tables for chapter three, the different gene or miRNA attributes are represented separated by an underline sign, representing:

- corr, genes correlated to a mineral amount.
- eQTL_cis, genes being affected by cis eQTL.
- eQTL_trans, genes being affected by trans eQTL.
- miRNA, micro RNAs.
- RIF_ mineral name or score, genes or miRNA presenting a significant regulatory impact over specific mineral amount.
- TF, transcription factor
- DEG_ mineral name, gene differentially expressed regarding specific mineral amount.
- down, genes differentially expressed more expressed in the low mineral amount group.
- up, genes differentially expressed more expressed in the high mineral amount group.
- hub, genes and miRNAs identified as hub elements in the co-expression networks.
- pathways, genes partaking over-represented pathways.

Supplementary Table S3.1. Correlations and attributes constituting Figure 1 (A, B and C).

GEBV	Gene	Correlation value	Correlation type	Gene attributes
Calcium	*ELL*	0.28748	POS	eQTL_trans
Calcium	*FAM89A*	-0.2989	NEG	eQTL_trans
Calcium	*FDXACB1*	-0.25702	NEG	eQTL_trans
Calcium	*MIR29E*	0.25726	POS	miRNA
Calcium	*LPAR4*	-0.28643	NEG	RIF_Ca
Calcium	*LOC101907603*	0.24419	POS	RIF_Score
Calcium	*ZNF131*	0.2465	POS	TF
Calcium	*VDR*	-0.28435	NEG	TF_RIF_Mg_and_Na
Calcium	*AAR2*	-0.30422	NEG	corr
Calcium	*BAAT*	0.26738	POS	corr
Calcium	*BMF*	-0.28173	NEG	corr
Calcium	*CDK8*	0.31904	POS	corr
Calcium	*COG4*	-0.25888	NEG	corr
Calcium	*LOC101908204*	0.22265	POS	corr
Calcium	*LOC112442262*	-0.30615	NEG	corr
Calcium	*LOC112449059*	0.26905	POS	corr
Calcium	*LOC510362*	-0.27261	NEG	corr
Calcium	*OTOR*	-0.22439	NEG	corr
Calcium	*RNF165*	-0.25848	NEG	corr
Calcium	*TBL2*	-0.27247	NEG	corr
Calcium	*THSD7B*	-0.29941	NEG	corr
Calcium	*VNN2*	-0.30558	NEG	corr
Copper	*MEST*	-0.33985	NEG	DEG_Ca_Cu_Mg_K_P
Copper	*TNFRSF11B*	-0.31267	NEG	eQTL_trans
Copper	*LOC518768*	0.28322	POS	RIF_Cu
Copper	*LOC530929*	-0.34437	NEG	RIF_Cu
Copper	*LOC784127*	-0.28084	NEG	RIF_Cu
Copper	*RASL11A*	0.30493	POS	RIF_Cu
Copper	*BHLHE22*	-0.27301	NEG	TF
Copper	*ALG11*	-0.29913	NEG	corr
Copper	*CADM4*	0.26371	POS	corr
Copper	*CAMK2N2*	-0.31188	NEG	corr
Copper	*CENPN*	0.2902	POS	corr
Copper	*CERS4*	-0.24666	NEG	corr
Copper	*CLDN19*	0.22968	POS	corr
Copper	*DHX40*	-0.24675	NEG	corr
Copper	*DIAPH3*	-0.29391	NEG	corr
Copper	*FAM229A*	0.29583	POS	corr
Copper	*GPRC5A*	0.28708	POS	corr
Copper	*KIAA0408*	-0.24594	NEG	corr
Copper	*KLHL7*	-0.26588	NEG	corr
Copper	*LOC100847269*	0.24908	POS	corr
Copper	*LOC101907322*	-0.27148	NEG	corr
Copper	*LOC511409*	0.29005	POS	corr
Copper	*LOC514257*	0.22999	POS	corr
Copper	*LRRC56*	0.23991	POS	corr

Copper	*MASTL*	-0.32249	NEG	corr
Copper	*NDC80*	-0.31721	NEG	corr
Copper	*NUCB2*	-0.28926	NEG	corr
Copper	*PURG*	-0.32558	NEG	corr
Copper	*RASAL1*	0.30467	POS	corr
Copper	*RASGEF1C*	0.22686	POS	corr
Copper	*RGS7*	-0.23266	NEG	corr
Copper	*SGCE*	-0.30115	NEG	corr
Copper	*SKIDA1*	-0.23513	NEG	corr
Copper	*TINF2*	0.28356	POS	corr
Copper	*VEGFD*	-0.26386	NEG	corr
Iron	*SLC22A4*	-0.2616	NEG	DEG_Fe_RIF_Score
Iron	*HPCAL4*	-0.2958	NEG	DEG_S_and_Fe
Iron	*MYLK3*	-0.23175	NEG	DEG_S_Fe_RIF_Score
Iron	*PLCB2*	-0.29366	NEG	eQTL_trans
Iron	*bta-miR-25*	-0.29391	NEG	RIF_Fe_and_Score_miRNA
Iron	*ALAD*	-0.29944	NEG	RIF_score
Iron	*CITED4*	-0.3213	NEG	RIF_Score
Iron	*CLBA1*	0.29126	POS	RIF_Score
Iron	*DPP4*	-0.30184	NEG	RIF_Score
Iron	*LOC101905675*	0.25872	POS	RIF_Score
Iron	*LOC104968807*	0.28433	POS	RIF_Score
Iron	*LOC112441773*	0.30253	POS	RIF_Score
Iron	*LOC112446381*	0.2805	POS	RIF_Score
Iron	*PPDPFL*	-0.27818	NEG	RIF_Score
Iron	*PRKG2*	0.29824	POS	RIF_Score
Iron	*TENM4*	0.28402	POS	RIF_Score
Iron	*TMEM238*	0.26744	POS	RIF_Score
Iron	*ZCCHC7*	0.26352	POS	RIF_Score
Iron	*MCPH1*	0.37197	POS	RIF_Score_eQTL_trans
Iron	*C8H9orf72*	-0.28749	NEG	corr
Iron	*EPOR*	0.25625	POS	corr
Iron	*FABP7*	0.27134	POS	corr
Iron	*LOC101906717*	0.30183	POS	corr
Iron	*LOC107132942*	0.31852	POS	corr
Iron	*LRRC32*	0.30712	POS	corr
Iron	*OLFM2*	0.25687	POS	corr
Iron	*SH2D2A*	-0.28015	NEG	corr
Iron	*TSPEAR*	-0.2662	NEG	corr
Magnesium	*COL21A1*	-0.24532	NEG	DEG_Ca
Magnesium	*PLXDC1*	-0.24977	NEG	DEG_Ca
Magnesium	*COL11A2*	-0.28204	NEG	DEG_Ca_Cu_Mg_K_Na_P_eQTL_trans
Magnesium	*MMP16*	-0.28169	NEG	DEG_Ca_Mg_RIF_K
Magnesium	*ADAP1*	0.22606	POS	eQTL_trans
Magnesium	*LIMD2*	-0.27085	NEG	eQTL_trans
Magnesium	*CTH*	-0.26794	NEG	RIF_Mg
Magnesium	*CD86*	-0.26727	NEG	RIF_Mg_and_K
Magnesium	*WDPCP*	-0.2958	NEG	RIF_Na_and_P_eQTL_trans

Magnesium	*FUT8*	-0.26676	NEG	RIF_S_eQTL_trans
Magnesium	*LOC509513*	-0.29215	NEG	RIF_Score
Magnesium	*PIGS*	-0.24335	NEG	RIF_Score
Magnesium	*ZIC3*	0.27598	POS	TF
Magnesium	*VDR*	-0.29003	NEG	TF_RIF_Mg_and_Na
Magnesium	*ADA2*	-0.26432	NEG	corr
Magnesium	*ARHGAP6*	-0.27247	NEG	corr
Magnesium	*BAAT*	0.28394	POS	corr
Magnesium	*BCL2L15*	-0.26146	NEG	corr
Magnesium	*CARD14*	-0.32134	NEG	corr
Magnesium	*CD5*	-0.27967	NEG	corr
Magnesium	*CYBC1*	-0.28235	NEG	corr
Magnesium	*DCX*	-0.28272	NEG	corr
Magnesium	*DOC2A*	-0.28694	NEG	corr
Magnesium	*FCGR2A*	-0.2343	NEG	corr
Magnesium	*FYB1*	-0.24905	NEG	corr
Magnesium	*GIMAP5*	-0.22633	NEG	corr
Magnesium	*IFIT3*	-0.23621	NEG	corr
Magnesium	*LOC100847708*	-0.25417	NEG	corr
Magnesium	*LOC112442227*	-0.26952	NEG	corr
Magnesium	*LOC112443416*	-0.29748	NEG	corr
Magnesium	*LOC617875*	-0.27305	NEG	corr
Magnesium	*LOC618071*	-0.23885	NEG	corr
Magnesium	*PARVG*	-0.23735	NEG	corr
Magnesium	*RIC8A*	-0.24584	NEG	corr
Magnesium	*RNF165*	-0.28931	NEG	corr
Magnesium	*TMEM74*	0.30371	POS	corr
Magnesium	*ZDHHC24*	-0.23565	NEG	corr
Phosphorus	*COL21A1*	-0.26028	NEG	DEG_Ca
Phosphorus	*MMP16*	-0.27273	NEG	DEG_Ca_Mg_RIF_K
Phosphorus	*ELL*	0.2866	POS	eQTL_trans
Phosphorus	*WDPCP*	-0.27636	NEG	RIF_Na_and_P_eQTL_trans
Phosphorus	*FUT8*	-0.25535	NEG	RIF_S_eQTL_trans
Phosphorus	*SALL4*	0.22611	POS	TF
Phosphorus	*VDR*	-0.29573	NEG	TF_RIF_Mg_and_Na
Phosphorus	*BAAT*	0.29176	POS	corr
Phosphorus	*BOLA.DOA*	-0.24521	NEG	corr
Phosphorus	*CARD14*	-0.31459	NEG	corr
Phosphorus	*CD5*	-0.26699	NEG	corr
Phosphorus	*DCX*	-0.29777	NEG	corr
Phosphorus	*DNASE1L3*	-0.25444	NEG	corr
Phosphorus	*LOC100847708*	-0.23176	NEG	corr
Phosphorus	*LOC112442227*	-0.30324	NEG	corr
Phosphorus	*LOC112443416*	-0.29702	NEG	corr
Phosphorus	*LOC785503*	-0.23372	NEG	corr
Phosphorus	*RNF165*	-0.29805	NEG	corr
Phosphorus	*TMEM74*	0.26101	POS	corr
Potassium	*COL21A1*	-0.26516	NEG	DEG_Ca

Potassium	*COL11A2*	-0.25476	NEG	DEG_Ca_Cu_Mg_K_Na_P_eQTL_trans
Potassium	*ARSA*	-0.26049	NEG	DEG_Ca_eQTL_trans
Potassium	*ANGPTL2*	-0.2645	NEG	DEG_Ca_Mg_K
Potassium	*MMP16*	-0.27796	NEG	DEG_Ca_Mg_RIF_K
Potassium	*INSIG2*	0.24382	POS	eQTL_trans
Potassium	*LIMD2*	-0.29737	NEG	eQTL_trans
Potassium	*RNF34*	0.25231	POS	RIF_K
Potassium	*CD86*	-0.2624	NEG	RIF_Mg_and_K
Potassium	*WDPCP*	-0.2912	NEG	RIF_Na_and_P_eQTL_trans
Potassium	*FUT8*	-0.24579	NEG	RIF_S_eQTL_trans
Potassium	*MCM4*	-0.23484	NEG	RIF_Score_eQTL_trans
Potassium	*ZIC3*	0.3187	POS	TF
Potassium	*VDR*	-0.31361	NEG	TF_RIF_Mg_and_Na
Potassium	*ADA2*	-0.27013	NEG	corr
Potassium	*ARAP1*	-0.24212	NEG	corr
Potassium	*ARHGAP30*	-0.2767	NEG	corr
Potassium	*BCL2L15*	-0.25165	NEG	corr
Potassium	*BOLA.DOA*	-0.24617	NEG	corr
Potassium	*CARD14*	-0.3083	NEG	corr
Potassium	*CD5*	-0.25609	NEG	corr
Potassium	*CYBC1*	-0.27738	NEG	corr
Potassium	*DCX*	-0.30709	NEG	corr
Potassium	*DNASE1L3*	-0.26622	NEG	corr
Potassium	*DOC2A*	-0.30164	NEG	corr
Potassium	*KIAA2012*	0.22718	POS	corr
Potassium	*LOC112442227*	-0.29797	NEG	corr
Potassium	*LOC112443416*	-0.30263	NEG	corr
Potassium	*LOC613985*	-0.28296	NEG	corr
Potassium	*LOC617875*	-0.2534	NEG	corr
Potassium	*RNF165*	-0.29279	NEG	corr
Potassium	*TMEM74*	0.26858	POS	corr
Potassium	*TRIP13*	-0.25022	NEG	corr
Selenium	*CISH*	-0.28436	NEG	DEG_S_and_Zn
Selenium	*ECHDC2*	0.29528	POS	DEG_Se_RIF_Score
Selenium	*PLCE1*	-0.27924	NEG	eQTL_cis
Selenium	*GCNT4*	-0.27806	NEG	eQTL_trans
Selenium	*TMED6*	-0.26239	NEG	eQTL_trans
Selenium	*bta-miR-425-5p*	0.29692	POS	miRNA
Selenium	*POLR3E*	-0.28805	NEG	RIF_Score
Selenium	*LOC112442312*	-0.29381	NEG	RIF_Se
Selenium	*PDK3*	0.25654	POS	RIF_Se
Selenium	*TTC21A*	-0.31632	NEG	RIF_Se
Selenium	*ZDBF2*	-0.25051	NEG	RIF_Se
Selenium	*HARS*	0.27995	POS	RIF_Se
Selenium	*DTWD1*	-0.29469	NEG	RIF_Se_eQTL_trans
Selenium	*NOX1*	-0.31542	NEG	RIF_Zn
Selenium	*bta-miR-411c-5p*	0.22427	POS	RIF_Zn_miRNA
Selenium	*RFX3*	-0.26994	NEG	TF

Selenium	*TEF*	0.31366	POS	TF_RIF_Se
Selenium	*B3GNT5*	-0.304	NEG	corr
Selenium	*CEP164*	-0.28799	NEG	corr
Selenium	*COL28A1*	0.25388	POS	corr
Selenium	*EML5*	-0.29815	NEG	corr
Selenium	*KANTR*	-0.28199	NEG	corr
Selenium	*LGR6*	-0.26007	NEG	corr
Selenium	*LOC101907941*	-0.347	NEG	corr
Selenium	*LOC104973799*	-0.26621	NEG	corr
Selenium	*LOC781977*	0.27438	POS	corr
Selenium	*LSM14A*	-0.2782	NEG	corr
Selenium	*PGAP2*	0.29148	POS	corr
Selenium	*PRKN*	0.22738	POS	corr
Selenium	*SNX25*	-0.27771	NEG	corr
Selenium	*SRRM4*	-0.24893	NEG	corr
Selenium	*TBCC*	0.29396	POS	corr
Selenium	*ZDHHC17*	-0.26022	NEG	corr
Selenium	*ZNF879*	-0.27737	NEG	corr
Sodium	*COL21A1*	-0.27608	NEG	DEG_Ca
Sodium	*COL11A2*	-0.27454	NEG	DEG_Ca_Cu_Mg_K_Na_P_eQTL_trans
Sodium	*MEST*	-0.27057	NEG	DEG_Ca_Cu_Mg_K_P
Sodium	*MMP16*	-0.29696	NEG	DEG_Ca_Mg_RIF_K
Sodium	*CRABP2*	-0.22034	NEG	DEG_Mg_K_Na_P_eQTL_trans
Sodium	*MAOB*	-0.26284	NEG	DEG_Mg_K_Na_S_eQTL_trans
Sodium	*CCR2*	-0.26762	NEG	eQTL_trans
Sodium	*CTNS*	-0.23875	NEG	eQTL_trans
Sodium	*GAL3ST4*	-0.25026	NEG	eQTL_trans
Sodium	*LIMD2*	-0.25136	NEG	eQTL_trans
Sodium	*LOXL3*	-0.29781	NEG	eQTL_trans
Sodium	*MARK3*	0.26859	POS	eQTL_trans
Sodium	*TTC39A*	-0.27635	NEG	eQTL_trans
Sodium	*bta-miR-130b*	-0.23139	NEG	miRNA
Sodium	*bta-miR-22-5p*	0.27415	POS	miRNA
Sodium	*bta-miR-92b*	-0.27755	NEG	RIF_K_miRNA
Sodium	*CAMKK1*	-0.26731	NEG	RIF_Na
Sodium	*CDKN3*	-0.28047	NEG	RIF_Na
Sodium	*CENPE*	-0.22806	NEG	RIF_Na
Sodium	*WDPCP*	-0.27218	NEG	RIF_Na_and_P_eQTL_trans
Sodium	*VMAC*	-0.23703	NEG	RIF_Na_eQTL_trans
Sodium	*FUT8*	-0.31291	NEG	RIF_S_eQTL_trans
Sodium	*ZIC3*	0.27854	POS	TF
Sodium	*VDR*	-0.24407	NEG	TF_RIF_Mg_and_Na
Sodium	*ABCB10*	0.29013	POS	corr
Sodium	*ADA2*	-0.26836	NEG	corr
Sodium	*ARAP1*	-0.26727	NEG	corr
Sodium	*BCL2L15*	-0.24606	NEG	corr
Sodium	*BOLA.DOA*	-0.31489	NEG	corr
Sodium	*CD5*	-0.30633	NEG	corr

Sodium	*CENPK*	-0.2325	NEG	corr
Sodium	*DCX*	-0.26866	NEG	corr
Sodium	*DNASE1L3*	-0.30842	NEG	corr
Sodium	*FGD2*	-0.2388	NEG	corr
Sodium	*IKBKE*	-0.25977	NEG	corr
Sodium	*KIAA2012*	0.24586	POS	corr
Sodium	*LOC112443416*	-0.30465	NEG	corr
Sodium	*LSM14B*	0.26136	POS	corr
Sodium	*MGME1*	-0.24265	NEG	corr
Sodium	*RCE1*	-0.28632	NEG	corr
Sodium	*RNF165*	-0.27684	NEG	corr
Sodium	*SLA*	-0.28033	NEG	corr
Sodium	*THSD7B*	-0.27147	NEG	corr
Sodium	*TMEM74*	0.29169	POS	corr
Sodium	*XCR1*	-0.2605	NEG	corr
Sulfur	*C1QTNF3*	-0.28331	NEG	DEG_Ca_and_S
Sulfur	*ARSA*	-0.30672	NEG	DEG_Ca_eQTL_trans
Sulfur	*MMP16*	-0.28762	NEG	DEG_Ca_Mg_RIF_K
Sulfur	*LOC515150*	-0.27486	NEG	DEG_Na_and_P
Sulfur	*CCR2*	-0.28146	NEG	eQTL_trans
Sulfur	*LIMD2*	-0.28315	NEG	eQTL_trans
Sulfur	*NXPE4*	-0.23989	NEG	eQTL_trans
Sulfur	*PLCB2*	-0.27829	NEG	eQTL_trans
Sulfur	*TIAM1*	-0.26651	NEG	eQTL_trans
Sulfur	*bta-miR-365-3p*	0.30654	POS	miRNA
Sulfur	*LPAR4*	-0.24193	NEG	RIF_Ca
Sulfur	*CD86*	-0.26317	NEG	RIF_Mg_and_K
Sulfur	*WDPCP*	-0.299	NEG	RIF_Na_and_P_eQTL_trans
Sulfur	*METTL21E*	0.23864	POS	RIF_S
Sulfur	*PLPPR5*	-0.25789	NEG	RIF_S
Sulfur	*PRRG3*	-0.33992	NEG	RIF_S
Sulfur	*RAB44*	-0.24272	NEG	RIF_S
Sulfur	*FUT8*	-0.24658	NEG	RIF_S_eQTL_trans
Sulfur	*PIGS*	-0.27016	NEG	RIF_Score
Sulfur	*BCL11B*	-0.24787	NEG	TF
Sulfur	*IKZF3*	-0.31237	NEG	TF
Sulfur	*VDR*	-0.32126	NEG	TF_RIF_Mg_and_Na
Sulfur	*ADA2*	-0.29552	NEG	corr
Sulfur	*AMACR*	-0.24203	NEG	corr
Sulfur	*ARAP1*	-0.29412	NEG	corr
Sulfur	*ARHGAP30*	-0.29766	NEG	corr
Sulfur	*BOLA.DOA*	-0.32479	NEG	corr
Sulfur	*BTK*	-0.31311	NEG	corr
Sulfur	*C27H4orf47*	0.30264	POS	corr
Sulfur	*CD5*	-0.30512	NEG	corr
Sulfur	*CD53*	-0.28108	NEG	corr
Sulfur	*DAGLB*	0.25524	POS	corr
Sulfur	*DCX*	-0.29458	NEG	corr

Sulfur	*FCGR2A*	-0.25147	NEG	corr
Sulfur	*FLT3*	-0.28344	NEG	corr
Sulfur	*FYN*	-0.28861	NEG	corr
Sulfur	*GIMAP5*	-0.28994	NEG	corr
Sulfur	*HEBP2*	-0.2519	NEG	corr
Sulfur	*JAML*	-0.25595	NEG	corr
Sulfur	*LOC101907383*	0.24301	POS	corr
Sulfur	*LOC510860*	-0.24964	NEG	corr
Sulfur	*LOC534578*	-0.28335	NEG	corr
Sulfur	*LOC785503*	-0.27903	NEG	corr
Sulfur	*MCCD1*	0.28112	POS	corr
Sulfur	*PAG2*	-0.26218	NEG	corr
Sulfur	*PPT1*	-0.31558	NEG	corr
Sulfur	*RBM24*	0.28995	POS	corr
Sulfur	*RSBN1L*	0.29938	POS	corr
Sulfur	*SIGLEC5*	-0.26835	NEG	corr
Sulfur	*SLA*	-0.2661	NEG	corr
Sulfur	*SRD5A3*	-0.26023	NEG	corr
Sulfur	*TMEM74*	0.31518	POS	corr
Sulfur	*TNFAIP3*	-0.28388	NEG	corr
Sulfur	*WDHD1*	-0.26582	NEG	corr
Sulfur	*XCR1*	-0.28886	NEG	corr
Sulfur	*XRCC6*	-0.26597	NEG	corr
Zinc	*CHPT1*	0.29913	POS	corr
Zinc	*COL11A2*	-0.30055	NEG	DEG_Ca_Cu_Mg_K_Na_P_eQTL_trans
Zinc	*ANGPTL2*	-0.28977	NEG	DEG_Ca_Mg_K
Zinc	*INSIG2*	0.26396	POS	eQTL_trans
Zinc	*MIR133A.2*	0.26658	POS	miRNA
Zinc	*MIR29E*	0.25458	POS	miRNA
Zinc	*MBTPS2*	0.31293	POS	RIF_Zn
Zinc	*NOX1*	0.34177	POS	RIF_Zn
Zinc	*TNR*	-0.24344	NEG	RIF_Zn
Zinc	*NUDT18*	-0.27722	NEG	RIF_Zn_eQTL_trans
Zinc	*ZIC3*	0.34155	POS	TF
Zinc	*AAR2*	-0.28479	NEG	corr
Zinc	*ASF1B*	-0.26922	NEG	corr
Zinc	*BAAT*	0.23357	POS	corr
Zinc	*C7H19orf67*	-0.27159	NEG	corr
Zinc	*CTSD*	-0.26317	NEG	corr
Zinc	*DCX*	-0.29826	NEG	corr
Zinc	*FAIM*	0.33274	POS	corr
Zinc	*GABPB1*	0.27915	POS	corr
Zinc	*GID8*	-0.27925	NEG	corr
Zinc	*GRM4*	-0.28273	NEG	corr
Zinc	*LEMD3*	0.35822	POS	corr
Zinc	*LOC101905734*	-0.30154	NEG	corr
Zinc	*LOC107131496*	0.24035	POS	corr
Zinc	*LOC107132969*	-0.27363	NEG	corr

Zinc	*LOC112443416*	-0.26314	NEG	corr
Zinc	*LOC112446096*	-0.25666	NEG	corr
Zinc	*LOC514189*	0.2311	POS	corr
Zinc	*LOC613985*	-0.321	NEG	corr
Zinc	*LOC617875*	-0.25932	NEG	corr
Zinc	*LTV1*	0.244	POS	corr
Zinc	*NBN*	0.24718	POS	corr
Zinc	*RGMA*	-0.24903	NEG	corr
Zinc	*SAT2*	-0.29135	NEG	corr
Zinc	*TTC9*	-0.29346	NEG	corr
Zinc	*VPS18*	-0.30612	NEG	corr
Zinc	*ZCCHC10*	0.25584	POS	corr
Zinc	*ZNF770*	0.30012	POS	corr
Calcium	Magnesium	0.65159	POS	
Calcium	Phosphorus	0.67441	POS	
Calcium	Potassium	0.65292	POS	
Calcium	Sodium	0.62988	POS	
Calcium	Sulfur	0.65365	POS	
Calcium	Zinc	0.62582	POS	
Copper	Magnesium	0.25852	POS	
Iron	Magnesium	0.26979	POS	
Iron	Phosphorus	0.27908	POS	
Iron	Potassium	0.27488	POS	
Iron	Sulfur	0.3168	POS	
Magnesium	Phosphorus	0.97196	POS	
Magnesium	Potassium	0.97319	POS	
Magnesium	Sodium	0.90216	POS	
Magnesium	Sulfur	0.80976	POS	
Magnesium	Zinc	0.79179	POS	
Phosphorus	Potassium	0.9713	POS	
Phosphorus	Sodium	0.90035	POS	
Phosphorus	Sulfur	0.83216	POS	
Phosphorus	Zinc	0.80431	POS	
Potassium	Sodium	0.89312	POS	
Potassium	Sulfur	0.82771	POS	
Potassium	Zinc	0.79254	POS	
Sodium	Sulfur	0.79933	POS	
Sodium	Zinc	0.77209	POS	
Sulfur	Zinc	0.67963	POS	

Supplementary Table S3.2. Correlations and attributes of each significant correlation constituting Figure 3.

Mg Origin	Target	Correlation value	Correlation type	Origin attributes	Target attributes
ADA2	bta-miR-22-5p	-0.13427	NEG	corr_hub	corr_miRNA
ADA2	*CD44*	0.4937	POS	corr_hub	down_pathways
ADA2	*CD86*	0.5016	POS	corr_hub	corr_RIF_hub
ADA2	*COL12A1*	0.34418	POS	corr_hub	down_pathways
ADA2	*MMP16*	0.46043	POS	corr_hub	corr_down_hub_pathways
ADA2	*PIGS*	0.37921	POS	corr_hub	corr_hub
ADA2	*PLXDC1*	0.4142	POS	corr_hub	corr_hub
ADA2	*PRRX2*	0.38604	POS	corr_hub	down_TF
ADA2	*TNC*	0.37287	POS	corr_hub	down_trans_pathways
ADA2	*VDR*	0.39319	POS	corr_hub	corr_TF_RIF
ADAM12	bta-let-7i	0.33608	POS	down_pathways	corr_RIF_miRNA
ADAM12	bta-miR-22-5p	-0.14484	NEG	down_pathways	corr_miRNA
ADAM12	*CD44*	0.40463	POS	down_pathways	down_pathways
ADAM12	*COL11A1*	0.65195	POS	down_pathways	down_pathways
ADAM12	*COL11A2*	0.34259	POS	down_pathways	corr_down_trans_pathways
ADAM12	*COL12A1*	0.62039	POS	down_pathways	down_pathways
ADAM12	*COL21A1*	0.31051	POS	down_pathways	corr_pathways
ADAM12	*COL22A1*	0.62413	POS	down_pathways	down_trans_pathways
ADAM12	*COMP*	0.59696	POS	down_pathways	down_trans_pathways
ADAM12	*ITGA10*	0.58824	POS	down_pathways	down_pathways
ADAM12	*MMP16*	0.48484	POS	down_pathways	corr_down_hub_pathways
ADAM12	*THBS4*	0.62637	POS	down_pathways	down_trans_pathways
ADAM12	*TNC*	0.48486	POS	down_pathways	down_trans_pathways
bta-let-7i	bta-miR-130b	0.18724	POS	corr_RIF_miRNA	corr_miRNA
bta-let-7i	bta-miR-22-5p	-0.13843	NEG	corr_RIF_miRNA	corr_miRNA
bta-let-7i	bta-miR-365-3p	-0.47252	NEG	corr_RIF_miRNA	corr_miRNA
bta-let-7i	bta-miR-365-5p	-0.21895	NEG	corr_RIF_miRNA	corr_miRNA
bta-let-7i	*CD44*	0.25914	POS	corr_RIF_miRNA	down_pathways
bta-let-7i	*COL11A1*	0.31454	POS	corr_RIF_miRNA	down_pathways

bta-let-7i	*COL12A1*	0.34928	POS	corr_RIF_miRNA	down_pathways
bta-let-7i	*COL22A1*	0.26041	POS	corr_RIF_miRNA	down_trans_pathways
bta-let-7i	*COMP*	0.30582	POS	corr_RIF_miRNA	down_trans_pathways
bta-let-7i	*ITGA10*	0.27727	POS	corr_RIF_miRNA	down_pathways
bta-let-7i	*MMP16*	0.29203	POS	corr_RIF_miRNA	corr_down_hub_pathways
bta-let-7i	*PRRX2*	0.31275	POS	corr_RIF_miRNA	down_TF
bta-let-7i	*THBS4*	0.33757	POS	corr_RIF_miRNA	down_trans_pathways
bta-miR-130b	bta-miR-365-5p	-0.23376	NEG	corr_miRNA	corr_miRNA
bta-miR-130b	bta-miR-92b	0.18846	POS	corr_miRNA	corr_miRNA
bta-miR-130b	*CTH*	0.19669	POS	corr_miRNA	corr_RIF
bta-miR-1343-3p	bta-miR-365-5p	0.24281	POS	corr_miRNA	corr_miRNA
bta-miR-1343-3p	*CTH*	-0.2126	NEG	corr_miRNA	corr_RIF
bta-miR-1343-3p	*PIGS*	-0.31264	NEG	corr_miRNA	corr_hub
bta-miR-1343-3p	*ZIC3*	0.22694	POS	corr_miRNA	corr_TF
bta-miR-142-5p	bta-miR-22-5p	-0.23835	NEG	corr_miRNA	corr_miRNA
bta-miR-142-5p	bta-miR-365-3p	-0.28377	NEG	corr_miRNA	corr_miRNA
bta-miR-142-5p	*COL11A2*	0.18951	POS	corr_miRNA	corr_down_trans_pathways
bta-miR-142-5p	*MMP16*	0.1673	POS	corr_miRNA	corr_down_hub_pathways
bta-miR-142-5p	*PRRX2*	0.22458	POS	corr_miRNA	down_TF
bta-miR-22-5p	*ITGA10*	-0.11961	NEG	corr_miRNA	down_pathways
bta-miR-365-3p	*CTH*	-0.18532	NEG	corr_miRNA	corr_RIF
bta-miR-92b	*CD44*	0.18979	POS	corr_miRNA	down_pathways
bta-miR-92b	*PIGS*	0.2556	POS	corr_miRNA	corr_hub
bta-miR-92b	*PRRX2*	0.21628	POS	corr_miRNA	down_TF
bta-miR-92b	*TNC*	0.21131	POS	corr_miRNA	down_trans_pathways
CD44	*CD86*	0.56728	POS	down_pathways	corr_RIF_hub
CD44	*COL11A1*	0.39695	POS	down_pathways	down_pathways
CD44	*COL12A1*	0.50116	POS	down_pathways	down_pathways
CD44	*COL21A1*	0.40465	POS	down_pathways	corr_pathways
CD44	*COL22A1*	0.39618	POS	down_pathways	down_trans_pathways
CD44	*COMP*	0.4391	POS	down_pathways	down_trans_pathways
CD44	*MMP16*	0.54236	POS	down_pathways	corr_down_hub_pathways

CD44	*PIGS*	0.41178	POS	down_pathways	corr_hub
CD44	*PLXDC1*	0.54544	POS	down_pathways	corr_hub
CD44	*PRRX2*	0.53604	POS	down_pathways	down_TF
CD44	*THBS4*	0.47498	POS	down_pathways	down_trans_pathways
CD44	*TNC*	0.62128	POS	down_pathways	down_trans_pathways
CD44	*ZIC3*	-0.22067	NEG	down_pathways	corr_TF
CD86	*COL21A1*	0.50852	POS	corr_RIF_hub	corr_pathways
CD86	*MMP16*	0.53103	POS	corr_RIF_hub	corr_down_hub_pathways
CD86	*PIGS*	0.37817	POS	corr_RIF_hub	corr_hub
CD86	*PLXDC1*	0.58135	POS	corr_RIF_hub	corr_hub
CD86	*TNC*	0.36261	POS	corr_RIF_hub	down_trans_pathways
CD86	*VDR*	0.47296	POS	corr_RIF_hub	corr_TF_RIF
CD86	*ZIC3*	-0.20872	NEG	corr_RIF_hub	corr_TF
COL11A1	*COL11A2*	0.50973	POS	down_pathways	corr_down_trans_pathways
COL11A1	*COL12A1*	0.83629	POS	down_pathways	down_pathways
COL11A1	*COL22A1*	0.8484	POS	down_pathways	down_trans_pathways
COL11A1	*COMP*	0.91524	POS	down_pathways	down_trans_pathways
COL11A1	*ITGA10*	0.65672	POS	down_pathways	down_pathways
COL11A1	*MMP16*	0.46702	POS	down_pathways	corr_down_hub_pathways
COL11A1	*PRRX2*	0.57971	POS	down_pathways	down_TF
COL11A1	*THBS4*	0.86932	POS	down_pathways	down_trans_pathways
COL11A1	*TNC*	0.5626	POS	down_pathways	down_trans_pathways
COL11A2	*COL22A1*	0.40066	POS	corr_down_trans_pathways	down_trans_pathways
COL11A2	*COMP*	0.44414	POS	corr_down_trans_pathways	down_trans_pathways
COL11A2	*ITGA10*	0.45989	POS	corr_down_trans_pathways	down_pathways
COL11A2	*PRRX2*	0.37351	POS	corr_down_trans_pathways	down_TF
COL11A2	*THBS4*	0.44015	POS	corr_down_trans_pathways	down_trans_pathways
COL12A1	*COL22A1*	0.73403	POS	down_pathways	down_trans_pathways
COL12A1	*COMP*	0.80686	POS	down_pathways	down_trans_pathways
COL12A1	*ITGA10*	0.53586	POS	down_pathways	down_pathways
COL12A1	*MMP16*	0.55788	POS	down_pathways	corr_down_hub_pathways
COL12A1	*PIGS*	0.28092	POS	down_pathways	corr_hub

COL12A1	*PRRX2*	0.59196	POS	down_pathways	down_TF
COL12A1	*THBS4*	0.8196	POS	down_pathways	down_trans_pathways
COL12A1	*TNC*	0.70665	POS	down_pathways	down_trans_pathways
COL21A1	*MMP16*	0.57002	POS	corr_pathways	corr_down_hub_pathways
COL21A1	*PIGS*	0.33165	POS	corr_pathways	corr_hub
COL21A1	*PLXDC1*	0.57358	POS	corr_pathways	corr_hub
COL21A1	*VDR*	0.36053	POS	corr_pathways	corr_TF_RIF
COL22A1	*COMP*	0.88862	POS	down_trans_pathways	down_trans_pathways
COL22A1	*ITGA10*	0.7114	POS	down_trans_pathways	down_pathways
COL22A1	*MMP16*	0.4187	POS	down_trans_pathways	corr_down_hub_pathways
COL22A1	*PRRX2*	0.52144	POS	down_trans_pathways	down_TF
COL22A1	*THBS4*	0.82451	POS	down_trans_pathways	down_trans_pathways
COL22A1	*TNC*	0.51025	POS	down_trans_pathways	down_trans_pathways
COMP	*ITGA10*	0.62139	POS	down_trans_pathways	down_pathways
COMP	*MMP16*	0.39517	POS	down_trans_pathways	corr_down_hub_pathways
COMP	*PRRX2*	0.61435	POS	down_trans_pathways	down_TF
COMP	*THBS4*	0.87442	POS	down_trans_pathways	down_trans_pathways
COMP	*TNC*	0.56269	POS	down_trans_pathways	down_trans_pathways
CTH	*ZIC3*	-0.17564	NEG	corr_RIF	corr_TF
ITGA10	*PRRX2*	0.45121	POS	down_pathways	down_TF
ITGA10	*THBS4*	0.61115	POS	down_pathways	down_trans_pathways
ITGA10	*TNC*	0.44769	POS	down_pathways	down_trans_pathways
MMP16	*PIGS*	0.45306	POS	corr_down_hub_pathways	corr_hub
MMP16	*PLXDC1*	0.54148	POS	corr_down_hub_pathways	corr_hub
MMP16	*PRRX2*	0.44498	POS	corr_down_hub_pathways	down_TF
MMP16	*THBS4*	0.49322	POS	corr_down_hub_pathways	down_trans_pathways
MMP16	*TNC*	0.55163	POS	corr_down_hub_pathways	down_trans_pathways
MMP16	*VDR*	0.35183	POS	corr_down_hub_pathways	corr_TF_RIF
MMP16	*ZIC3*	-0.2639	NEG	corr_down_hub_pathways	corr_TF
PIGS	*PLXDC1*	0.38315	POS	corr_hub	corr_hub
PIGS	*PRRX2*	0.31717	POS	corr_hub	down_TF
PIGS	*TNC*	0.3914	POS	corr_hub	down_trans_pathways

PIGS	*ZIC3*	-0.23213	NEG	corr_hub	corr_TF
PLXDC1	*VDR*	0.30439	POS	corr_hub	corr_TF_RIF
PRRX2	*THBS4*	0.63399	POS	down_TF	down_trans_pathways
PRRX2	*TNC*	0.64906	POS	down_TF	down_trans_pathways
PRRX2	*ZIC3*	-0.28348	NEG	down_TF	corr_TF
THBS4	*TNC*	0.61094	POS	down_trans_pathways	down_trans_pathways

Fe

Origin	**Target**	**Correlation value**	**Correlation type**	**Origin attributes**	**Target attributes**
ALAD	bta-miR-25	0.26203	POS	Corr_hub	Corr_RIF_miRNA
ALAD	bta-miR-378c	0.21704	POS	Corr_hub	Corr_RIF_miRNA
ALAD	*FASN*	-0.21106	NEG	Corr_hub	up_trans_pathway
ALAD	*HPCAL4*	0.42843	POS	Corr_hub	Corr_down_hub
ALAD	*HSPA6*	0.34633	POS	Corr_hub	up_TF_pathway
ALAD	*MYLK3*	0.37818	POS	Corr_hub	Corr_down_hub
ALAD	*PLIN5*	0.71483	POS	Corr_hub	down_pathway
ALAD	*SLC16A3*	0.29498	POS	Corr_hub	down_pathway
ALAD	*SLC27A6*	0.37818	POS	Corr_hub	down_pathway
ALAD	*TAP1*	0.28155	POS	Corr_hub	down_trans_pathway
ALAD	*TENM4*	-0.23274	NEG	Corr_hub	Corr_hub
bta-miR-127	bta-miR-25	0.14718	POS	Corr_miRNA	Corr_RIF_miRNA
bta-miR-127	bta-miR-532	0.18216	POS	Corr_miRNA	Corr_miRNA
bta-miR-127	*MT1A*	0.19933	POS	Corr_miRNA	up_TF
bta-miR-127	*PLCB2*	0.19909	POS	Corr_miRNA	Corr_trans_hub
bta-miR-127	*SLC16A3*	0.22506	POS	Corr_miRNA	down_pathway
bta-miR-181a	bta-miR-378c	0.37697	POS	Corr_miRNA	Corr_RIF_miRNA
bta-miR-181a	bta-miR-532	0.30467	POS	Corr_miRNA	Corr_miRNA
bta-miR-181a	*HSPA6*	0.24723	POS	Corr_miRNA	up_TF_pathway
bta-miR-25	bta-miR-378c	0.748	POS	Corr_RIF_miRNA	Corr_RIF_miRNA
bta-miR-25	bta-miR-532	0.68557	POS	Corr_RIF_miRNA	Corr_miRNA
bta-miR-25	*PLIN5*	0.17075	POS	Corr_RIF_miRNA	down_pathway
bta-miR-378c	bta-miR-532	0.65989	POS	Corr_RIF_miRNA	Corr_miRNA

bta-miR-378c	*C3*	-0.11905	NEG	Corr_RIF_miRNA	up_pathway
bta-miR-378c	*SLC27A6*	0.20604	POS	Corr_RIF_miRNA	down_pathway
bta-miR-532	*THRSP*	0.1665	POS	Corr_miRNA	up_trans_pathway
C3	*MMRN1*	0.4251	POS	up_pathway	up_TF
C3	*MT1A*	0.38708	POS	up_pathway	up_TF
C3	*PLCB2*	0.28483	POS	up_pathway	Corr_trans_hub
C3	*THRSP*	0.16244	POS	up_pathway	up_trans_pathway
FASN	*MMRN1*	0.28087	POS	up_trans_pathway	up_TF
FASN	*MT1A*	0.24793	POS	up_trans_pathway	up_TF
FASN	*TENM4*	0.52456	POS	up_trans_pathway	Corr_hub
FASN	*THRSP*	0.88294	POS	up_trans_pathway	up_trans_pathway
HES1	*HPCAL4*	0.26395	POS	down_TF	Corr_down_hub
HES1	*SLC16A3*	0.24259	POS	down_TF	down_pathway
HPCAL4	*MT1A*	-0.21551	NEG	Corr_down_hub	up_TF
HPCAL4	*MYLK3*	0.47043	POS	Corr_down_hub	Corr_down_hub
HPCAL4	*PLIN5*	0.49341	POS	Corr_down_hub	down_pathway
HPCAL4	*SLC16A3*	0.4999	POS	Corr_down_hub	down_pathway
HPCAL4	*SLC27A6*	0.41246	POS	Corr_down_hub	down_pathway
HPCAL4	*TENM4*	-0.17565	NEG	Corr_down_hub	Corr_hub
HPCAL4	*THRSP*	-0.21298	NEG	Corr_down_hub	up_trans_pathway
HSPA6	*PLCB2*	0.15599	POS	up_TF_pathway	Corr_trans_hub
MMRN1	*MYLK3*	-0.21045	NEG	up_TF	Corr_down_hub
MMRN1	*SLC27A6*	-0.17624	NEG	up_TF	down_pathway
MMRN1	*TENM4*	0.28434	POS	up_TF	Corr_hub
MT1A	*PLCB2*	0.26604	POS	up_TF	Corr_trans_hub
MT1A	*SLC27A6*	-0.19979	NEG	up_TF	down_pathway
MT1A	*THRSP*	0.21467	POS	up_TF	up_trans_pathway
MYLK3	*PLIN5*	0.33344	POS	Corr_down_hub	down_pathway
MYLK3	*SLC27A6*	0.47734	POS	Corr_down_hub	down_pathway
PLIN5	*TENM4*	-0.25144	NEG	down_pathway	Corr_hub
SLC16A3	*TAP1*	0.29067	POS	down_pathway	down_trans_pathway
SLC27A6	*TENM4*	-0.1988	NEG	down_pathway	Corr_hub

TAP1	*TENM4*	-0.26574	NEG	down_trans_pathway	Corr_hub
TENM4	*THRSP*	0.43831	POS	Corr_hub	up_trans_pathway

Ca

Origin	Target	Correlation value	Correlation type	Origin attributes	Target attributes
ADAMTS12	*ADAMTS2*	0.60203	POS	down_pathway	down_pathway
ADAMTS12	*BGN*	0.45908	POS	down_pathway	down_pathway
ADAMTS12	bta-miR-133a	-0.2387	NEG	down_pathway	Corr_miRNA_hub
ADAMTS12	*C7*	0.27417	POS	down_pathway	Corr_hub
ADAMTS12	*CD44*	0.47868	POS	down_pathway	down_pathway
ADAMTS12	*COL5A1*	0.63145	POS	down_pathway	down_pathway
ADAMTS12	*COL5A2*	0.59279	POS	down_pathway	down_pathway
ADAMTS12	*DDR2*	0.42713	POS	down_pathway	down_pathway
ADAMTS12	*EMILIN1*	0.54637	POS	down_pathway	down_pathway
ADAMTS12	*LUM*	0.43613	POS	down_pathway	down_pathway
ADAMTS12	*NID2*	0.68413	POS	down_pathway	down_pathway
ADAMTS12	*SDC3*	0.47236	POS	down_pathway	down_pathway
ADAMTS2	*BGN*	0.67169	POS	down_pathway	down_pathway
ADAMTS2	bta-miR-133a	-0.22859	NEG	down_pathway	down_pathway
ADAMTS2	bta-miR-369-3p	0.20735	POS	down_pathway	down_TF
ADAMTS2	*C1QB*	0.56418	POS	down_pathway	down_pathway
ADAMTS2	*C1QC*	0.5449	POS	down_pathway	down_pathway
ADAMTS2	*CD44*	0.6027	POS	down_pathway	down_pathway
ADAMTS2	*COL11A1*	0.34933	POS	down_pathway	down_pathway
ADAMTS2	*COL21A1*	0.47441	POS	down_pathway	down_pathway
ADAMTS2	*COL5A1*	0.81734	POS	down_pathway	down_pathway
ADAMTS2	*COL5A2*	0.75798	POS	down_pathway	down_pathway
ADAMTS2	*DDR2*	0.65521	POS	down_pathway	down_pathway
ADAMTS2	*EMILIN1*	0.51558	POS	down_pathway	down_pathway
ADAMTS2	*LOC786948*	0.33676	POS	down_pathway	down_pathway
ADAMTS2	*LUM*	0.63598	POS	down_pathway	down_TF
ADAMTS2	*MMP16*	0.73236	POS	down_pathway	down_pathway

ADAMTS2	*NCAM1*	0.3508	POS	down_pathway	Corr_TF_hub
ADAMTS2	*NID2*	0.64529	POS	down_pathway	down_pathway
ADAMTS2	*PCOLCE*	0.66409	POS	down_pathway	down_pathway
ADAMTS2	*PRRX2*	0.52925	POS	down_pathway	down_pathway
ADAMTS2	*SDC3*	0.60291	POS	down_pathway	down_pathway
ADAMTS2	*SPON2*	0.53794	POS	down_pathway	down_pathway
ADAMTS2	*TBL2*	0.2426	POS	down_pathway	Corr_TF_hub
ADAMTS2	*VDR*	0.29229	POS	down_pathway	Corr_TF_hub
ADAMTS2	*ZNF131*	-0.25091	NEG	down_pathway	down_pathway
BGN	bta-miR-133a	-0.2346	NEG	down_pathway	down_pathway
BGN	bta-miR-222	0.20074	POS	down_pathway	down_pathway
BGN	*C1QB*	0.48592	POS	down_pathway	down_pathway
BGN	*C1QC*	0.49882	POS	down_pathway	down_pathway
BGN	*CD44*	0.5998	POS	down_pathway	down_pathway
BGN	*COL11A1*	0.50256	POS	down_pathway	down_trans_pathway
BGN	*COL13A1*	0.41	POS	down_pathway	down_pathway
BGN	*COL5A1*	0.72655	POS	down_pathway	down_pathway
BGN	*COL5A2*	0.72828	POS	down_pathway	down_pathway
BGN	*DDR2*	0.43067	POS	down_pathway	down_trans_pathway
BGN	*EMILIN1*	0.55768	POS	down_pathway	down_pathway
BGN	*LUM*	0.63159	POS	down_pathway	down_pathway
BGN	*MIR29E*	-0.19653	NEG	down_pathway	Corr_miRNA
BGN	*MMP16*	0.6005	POS	down_pathway	down_pathway
BGN	*NCAM1*	0.36089	POS	down_pathway	down_TF_trans
BGN	*NID2*	0.5341	POS	down_pathway	down_pathway
BGN	*PCOLCE*	0.70481	POS	down_pathway	down_pathway
BGN	*PRRX2*	0.64281	POS	down_pathway	down_pathway
BGN	*SDC3*	0.4179	POS	down_pathway	down_TF_trans
BGN	*SPON2*	0.54657	POS	down_pathway	down_TF
BGN	*VDR*	0.29742	POS	down_pathway	down_pathway
BMF	bta-miR-222	0.18273	POS	Corr_hub	Corr_miRNA_hub
BMF	*CDK8*	-0.38432	NEG	Corr_hub	Corr_trans_hub

BMF	*DDR2*	0.30281	POS	Corr_hub	Corr_TF_hub
BMF	*ELL*	-0.37196	NEG	Corr_hub	Corr_trans_hub
BMF	*LOC786948*	0.29917	POS	Corr_hub	Corr_hub
BMF	*LPAR4*	0.33461	POS	Corr_hub	down_pathway
BMF	*MAFB*	0.41892	POS	Corr_hub	down_pathway
BMF	*MMP16*	0.28642	POS	Corr_hub	Corr_TF_hub
BMF	*OTOR*	0.26106	POS	Corr_hub	Corr_TF_hub
BMF	*ZNF131*	-0.27962	NEG	Corr_hub	up_TF
bta-miR-133a	bta-miR-193b	0.58688	POS	Corr_miRNA_hub	down_pathway
bta-miR-133a	*C1QB*	-0.23318	NEG	Corr_miRNA_hub	down_pathway
bta-miR-133a	*C1QC*	-0.25532	NEG	Corr_miRNA_hub	down_pathway
bta-miR-133a	*CD44*	-0.26122	NEG	Corr_miRNA_hub	Corr_miRNA
bta-miR-133a	*COL5A1*	-0.24584	NEG	Corr_miRNA_hub	Corr_TF_hub
bta-miR-133a	*COL5A2*	-0.31303	NEG	Corr_miRNA_hub	down_pathway
bta-miR-133a	*EMILIN1*	-0.23001	NEG	Corr_miRNA_hub	Corr_miRNA_hub
bta-miR-133a	*MMP16*	-0.21663	NEG	Corr_miRNA_hub	Corr_RIF_miRNA
bta-miR-133a	*NID2*	-0.24286	NEG	Corr_miRNA_hub	Corr_miRNA_hub
bta-miR-133a	*PCOLCE*	-0.2336	NEG	Corr_miRNA_hub	Corr_TF_hub
bta-miR-133a	*SPON2*	-0.23309	NEG	Corr_miRNA_hub	down_pathway
bta-miR-193b	bta-miR-222	-0.17872	NEG	Corr_miRNA	Corr_miRNA
bta-miR-193b	bta-miR-369-3p	-0.21416	NEG	Corr_miRNA	Corr_trans_hub
bta-miR-193b	bta-miR-92b	-0.26458	NEG	Corr_miRNA	down_pathway
bta-miR-193b	*C1QB*	-0.21766	NEG	Corr_miRNA	down_pathway
bta-miR-193b	*C1QC*	-0.25135	NEG	Corr_miRNA	Corr_TF_hub
bta-miR-193b	*CD44*	-0.25227	NEG	Corr_miRNA	down_trans_pathway
bta-miR-222	bta-miR-92b	0.19458	POS	Corr_miRNA	down_trans_pathway
bta-miR-222	*ELL*	-0.20922	NEG	Corr_miRNA	Corr_miRNA
bta-miR-222	*PRRX2*	0.22628	POS	Corr_miRNA	down_pathway
bta-miR-369-3p	*COL11A2*	0.19484	POS	Corr_RIF_miRNA	Corr_miRNA
bta-miR-369-3p	*ELL*	-0.36134	NEG	Corr_RIF_miRNA	up_TF
bta-miR-369-3p	*MIR29E*	-0.29256	NEG	Corr_RIF_miRNA	down_pathway
bta-miR-369-3p	*SPON2*	0.26343	POS	Corr_RIF_miRNA	Corr_TF_hub

bta-miR-369-3p	*ZNF131*	-0.2581	NEG	Corr_RIF_miRNA	down_trans_pathway
bta-miR-92b	*C1QB*	0.22666	POS	Corr_miRNA_hub	Corr_TF_hub
bta-miR-92b	*C1QC*	0.24678	POS	Corr_miRNA_hub	Corr_hub
bta-miR-92b	*COL5A2*	0.26217	POS	Corr_miRNA_hub	Corr_TF_hub
bta-miR-92b	*DDR2*	0.20441	POS	Corr_miRNA_hub	Corr_RIF_miRNA
bta-miR-92b	*PRRX2*	0.21628	POS	Corr_miRNA_hub	down_TF
bta-miR-92b	*TBL2*	0.25541	POS	Corr_miRNA_hub	Corr_RIF_hub
C1QB	*C1QC*	0.92502	POS	down_pathway	
C1QB	*CD44*	0.57187	POS	down_pathway	down_pathway
C1QB	*COL5A1*	0.50976	POS	down_pathway	down_pathway
C1QB	*COL5A2*	0.55117	POS	down_pathway	down_TF
C1QB	*DDR2*	0.4575	POS	down_pathway	down_pathway
C1QB	*EMILIN1*	0.45826	POS	down_pathway	down_pathway
C1QB	*LOC786948*	0.4206	POS	down_pathway	down_pathway
C1QB	*LUM*	0.53529	POS	down_pathway	down_TF
C1QB	*MMP16*	0.4654	POS	down_pathway	down_pathway
C1QB	*NFE2L3*	-0.33781	NEG	down_pathway	down_pathway
C1QB	*NID2*	0.45997	POS	down_pathway	down_pathway
C1QB	*PCOLCE*	0.55703	POS	down_pathway	down_pathway
C1QB	*PRRX2*	0.38989	POS	down_pathway	down_pathway
C1QB	*SDC3*	0.40461	POS	down_pathway	down_pathway
C1QB	*SPON2*	0.4289	POS	down_pathway	down_pathway
C1QB	*VDR*	0.30388	POS	down_pathway	Corr_hub
C1QB	*ZNF131*	-0.24523	NEG	down_pathway	down_pathway
C1QC	*CD44*	0.5838	POS	down_trans_pathway	down_pathway
C1QC	*COL5A1*	0.51573	POS	down_trans_pathway	down_TF_trans
C1QC	*COL5A2*	0.55676	POS	down_trans_pathway	down_pathway
C1QC	*DDR2*	0.44696	POS	down_trans_pathway	down_pathway
C1QC	*EMILIN1*	0.44081	POS	down_trans_pathway	down_pathway
C1QC	*LOC786948*	0.42985	POS	down_trans_pathway	down_pathway
C1QC	*LUM*	0.52716	POS	down_trans_pathway	down_TF
C1QC	*MMP16*	0.46266	POS	down_trans_pathway	down_pathway

C1QC	*NFE2L3*	-0.31873	NEG	down_trans_pathway	down_pathway
C1QC	*NID2*	0.42752	POS	down_trans_pathway	down_pathway
C1QC	*PCOLCE*	0.55551	POS	down_trans_pathway	down_pathway
C1QC	*PRRX2*	0.36607	POS	down_trans_pathway	down_pathway
C1QC	*SPON2*	0.48584	POS	down_trans_pathway	down_pathway
C1QC	*ZNF131*	-0.23349	NEG	down_trans_pathway	down_pathway
C7	*EMILIN1*	0.33243	POS	down_pathway	Corr_RIF_hub
C7	*NFE2L3*	-0.25938	NEG	down_pathway	down_pathway
C7	*NID2*	0.23957	POS	down_pathway	up_TF
C7	*OTOR*	0.25432	POS	down_pathway	Corr_hub
CD44	*COL11A1*	0.39695	POS	down_pathway	Corr_trans_hub
CD44	*COL13A1*	0.4345	POS	down_pathway	Corr_TF_hub
CD44	*COL21A1*	0.40465	POS	down_pathway	down_trans_pathway
CD44	*COL5A1*	0.70007	POS	down_pathway	down_pathway
CD44	*COL5A2*	0.71872	POS	down_pathway	down_trans_pathway
CD44	*EMILIN1*	0.59803	POS	down_pathway	down_pathway
CD44	*LOC786948*	0.35756	POS	down_pathway	down_pathway
CD44	*LUM*	0.61478	POS	down_pathway	down_pathway
CD44	*MIR29E*	-0.26088	NEG	down_pathway	down_pathway
CD44	*MMP16*	0.54236	POS	down_pathway	down_trans_pathway
CD44	*NCAM1*	0.46045	POS	down_pathway	down_pathway
CD44	*NFE2L3*	-0.26831	NEG	down_pathway	Corr_miRNA_hub
CD44	*NID2*	0.5994	POS	down_pathway	down_pathway
CD44	*PCOLCE*	0.62595	POS	down_pathway	down_pathway
CD44	*PRRX2*	0.53604	POS	down_pathway	down_pathway
CD44	*SDC3*	0.38027	POS	down_pathway	down_pathway
CD44	*SPON2*	0.62262	POS	down_pathway	down_pathway
CD44	*TBL2*	0.24581	POS	down_pathway	down_trans_pathway
CD44	*VDR*	0.26342	POS	down_pathway	down_pathway
CDK8	*ELL*	0.40114	POS	Corr_hub	down_pathway
CDK8	*LOC786948*	-0.25884	NEG	Corr_hub	Corr_TF_hub
CDK8	*LPAR4*	-0.32657	NEG	Corr_hub	down_pathway

CDK8	*MAFB*	-0.3464	NEG	Corr_hub	up_TF
CDK8	*MIR29E*	0.37763	POS	Corr_hub	down_pathway
CDK8	*NFE2L3*	0.24065	POS	Corr_hub	Corr_hub
CDK8	*ZNF131*	0.29256	POS	Corr_hub	down_pathway
COL11A1	*COL11A2*	0.50973	POS	down_pathway	down_pathway
COL11A1	*COL13A1*	0.72147	POS	down_pathway	down_pathway
COL11A1	*COL5A1*	0.34866	POS	down_pathway	down_pathway
COL11A1	*COL5A2*	0.43031	POS	down_pathway	down_pathway
COL11A1	*EMILIN1*	0.36645	POS	down_pathway	Corr_TF_hub
COL11A1	*MMP16*	0.46702	POS	down_pathway	down_pathway
COL11A1	*NCAM1*	0.57627	POS	down_pathway	down_pathway
COL11A1	*OTOR*	0.3131	POS	down_pathway	Corr_hub
COL11A1	*PCOLCE*	0.39019	POS	down_pathway	down_pathway
COL11A1	*PRRX2*	0.57971	POS	down_pathway	down_pathway
COL11A2	*COL13A1*	0.40593	POS	down_trans_pathway	down_trans_pathway
COL11A2	*OTOR*	0.31383	POS	down_trans_pathway	Corr_hub
COL11A2	*PRRX2*	0.37351	POS	down_trans_pathway	down_pathway
COL11A2	*TBL2*	0.30256	POS	down_trans_pathway	down_pathway
COL13A1	*COL5A2*	0.45156	POS	down_trans_pathway	down_pathway
COL13A1	*EMILIN1*	0.41214	POS	down_trans_pathway	down_pathway
COL13A1	*MMP16*	0.37799	POS	down_trans_pathway	down_pathway
COL13A1	*NCAM1*	0.49908	POS	down_trans_pathway	down_pathway
COL13A1	*OTOR*	0.35501	POS	down_trans_pathway	down_pathway
COL13A1	*PRRX2*	0.4844	POS	down_trans_pathway	down_pathway
COL13A1	*TBL2*	0.28346	POS	down_trans_pathway	down_pathway
COL21A1	*COL5A1*	0.55115	POS	down_pathway	down_pathway
COL21A1	*COL5A2*	0.4439	POS	down_pathway	Corr_TF_hub
COL21A1	*DDR2*	0.50236	POS	down_pathway	down_pathway
COL21A1	*ELL*	-0.44687	NEG	down_pathway	up_TF
COL21A1	*LUM*	0.67166	POS	down_pathway	down_pathway
COL21A1	*MAFB*	0.5209	POS	down_pathway	down_pathway
COL21A1	*MMP16*	0.57002	POS	down_pathway	down_pathway

COL21A1	*NCAM1*	0.37551	POS	down_pathway	down_pathway
COL21A1	*PCOLCE*	0.5363	POS	down_pathway	down_pathway
COL21A1	*SDC3*	0.31967	POS	down_pathway	down_TF_trans
COL21A1	*SPON2*	0.41993	POS	down_pathway	down_pathway
COL21A1	*VDR*	0.36053	POS	down_pathway	down_pathway
COL5A1	*COL5A2*	0.85293	POS	down_pathway	down_trans_pathway
COL5A1	*DDR2*	0.65301	POS	down_pathway	down_pathway
COL5A1	*EMILIN1*	0.5608	POS	down_pathway	down_pathway
COL5A1	*LUM*	0.69011	POS	down_pathway	down_pathway
COL5A1	*MMP16*	0.70367	POS	down_pathway	down_pathway
COL5A1	*NCAM1*	0.45117	POS	down_pathway	down_pathway
COL5A1	*NID2*	0.69851	POS	down_pathway	down_pathway
COL5A1	*PCOLCE*	0.70041	POS	down_pathway	down_pathway
COL5A1	*PRRX2*	0.5404	POS	down_pathway	down_pathway
COL5A1	*SDC3*	0.51215	POS	down_pathway	down_pathway
COL5A1	*SPON2*	0.58519	POS	down_pathway	Corr_miRNA
COL5A1	*VDR*	0.36719	POS	down_pathway	down_pathway
COL5A2	*DDR2*	0.59242	POS	down_pathway	down_pathway
COL5A2	*EMILIN1*	0.59508	POS	down_pathway	down_pathway
COL5A2	*LOC786948*	0.29757	POS	down_pathway	down_pathway
COL5A2	*LUM*	0.73873	POS	down_pathway	down_pathway
COL5A2	*MMP16*	0.63559	POS	down_pathway	down_pathway
COL5A2	*NCAM1*	0.49323	POS	down_pathway	down_trans_pathway
COL5A2	*NID2*	0.74018	POS	down_pathway	down_pathway
COL5A2	*PCOLCE*	0.65315	POS	down_pathway	down_pathway
COL5A2	*PRRX2*	0.54712	POS	down_pathway	down_pathway
COL5A2	*SDC3*	0.47398	POS	down_pathway	down_pathway
COL5A2	*SPON2*	0.57261	POS	down_pathway	down_pathway
COL5A2	*VDR*	0.27204	POS	down_pathway	down_pathway
DDR2	*ELL*	-0.36595	NEG	down_pathway	Corr_trans_hub
DDR2	*LOC786948*	0.30811	POS	down_pathway	Corr_TF_hub
DDR2	*LPAR4*	0.27567	POS	down_pathway	Corr_hub

DDR2	*LUM*	0.55839	POS	down_pathway	down_pathway
DDR2	*MAFB*	0.36345	POS	down_pathway	down_TF
DDR2	*MMP16*	0.60898	POS	down_pathway	down_pathway
DDR2	*NCAM1*	0.34622	POS	down_pathway	down_pathway
DDR2	*PCOLCE*	0.42748	POS	down_pathway	down_pathway
DDR2	*SDC3*	0.53774	POS	down_pathway	down_pathway
DDR2	*VDR*	0.30607	POS	down_pathway	down_pathway
ELL	*LOC786948*	-0.28854	NEG	Corr_trans_hub	Corr_TF_hub
ELL	*LUM*	-0.39771	NEG	Corr_trans_hub	Corr_TF_hub
ELL	*MAFB*	-0.54326	NEG	Corr_trans_hub	Corr_trans_hub
ELL	*MIR29E*	0.32981	POS	Corr_trans_hub	down_pathway
ELL	*MMP16*	-0.33093	NEG	Corr_trans_hub	down_pathway
ELL	*NCAM1*	-0.32781	NEG	Corr_trans_hub	Corr_RIF_hub
ELL	*PCOLCE*	-0.32174	NEG	Corr_trans_hub	up_TF
ELL	*VDR*	-0.38561	NEG	Corr_trans_hub	Corr_hub
ELL	*ZNF131*	0.43527	POS	Corr_trans_hub	down_pathway
EMILIN1	*LOC786948*	0.3551	POS	down_pathway	down_pathway
EMILIN1	*NCAM1*	0.35923	POS	down_pathway	Corr_TF_hub
EMILIN1	*NFE2L3*	-0.34932	NEG	down_pathway	down_TF_trans
EMILIN1	*NID2*	0.59086	POS	down_pathway	down_pathway
EMILIN1	*OTOR*	0.30476	POS	down_pathway	down_TF
EMILIN1	*PCOLCE*	0.5464	POS	down_pathway	down_pathway
EMILIN1	*PRRX2*	0.52258	POS	down_pathway	down_pathway
EMILIN1	*SPON2*	0.44141	POS	down_pathway	down_pathway
EMILIN1	*TBL2*	0.2569	POS	down_pathway	Corr_TF_hub
LOC786948	*LPAR4*	0.25657	POS	down_pathway	Corr_hub
LOC786948	*LUM*	0.38424	POS	down_pathway	down_TF
LOC786948	*MMP16*	0.29599	POS	down_pathway	Corr_TF_hub
LOC786948	*NFE2L3*	-0.41418	NEG	down_pathway	down_pathway
LOC786948	*OTOR*	0.25515	POS	down_pathway	Corr_hub
LOC786948	*PCOLCE*	0.47021	POS	down_pathway	down_pathway
LOC786948	*PRRX2*	0.30607	POS	down_pathway	Corr_TF_hub

LOC786948	*SPON2*	0.34139	POS	down_pathway	down_pathway
LPAR4	*MAFB*	0.31984	POS	Corr_RIF_hub	up_TF
LPAR4	*MMP16*	0.33709	POS	Corr_RIF_hub	down_pathway
LPAR4	*OTOR*	0.25666	POS	Corr_RIF_hub	Corr_hub
LUM	*MMP16*	0.64738	POS	down_pathway	down_pathway
LUM	*NCAM1*	0.476	POS	down_pathway	down_pathway
LUM	*NID2*	0.57781	POS	down_pathway	down_TF
LUM	*PCOLCE*	0.67807	POS	down_pathway	down_pathway
LUM	*SDC3*	0.43924	POS	down_pathway	down_pathway
LUM	*SPON2*	0.5022	POS	down_pathway	down_pathway
LUM	*VDR*	0.3102	POS	down_pathway	Corr_hub
MAFB	*MMP16*	0.36856	POS	down_TF_trans	down_TF
MAFB	*PCOLCE*	0.37871	POS	down_TF_trans	down_pathway
MAFB	*VDR*	0.26127	POS	down_TF_trans	down_pathway
MIR29E	*NFE2L3*	0.3222	POS	Corr_miRNA	Corr_miRNA
MIR29E	*PCOLCE*	-0.26033	NEG	Corr_miRNA	up_TF
MIR29E	*ZNF131*	0.31943	POS	Corr_miRNA	Corr_hub
MMP16	*NCAM1*	0.48157	POS	down_pathway	down_TF
MMP16	*NID2*	0.48611	POS	down_pathway	down_pathway
MMP16	*PCOLCE*	0.59088	POS	down_pathway	down_pathway
MMP16	*PRRX2*	0.44498	POS	down_pathway	down_pathway
MMP16	*SDC3*	0.45636	POS	down_pathway	down_pathway
MMP16	*SPON2*	0.46821	POS	down_pathway	down_pathway
MMP16	*TBL2*	0.27526	POS	down_pathway	Corr_RIF_hub
MMP16	*VDR*	0.35183	POS	down_pathway	Corr_hub
MMP16	*ZNF131*	-0.28335	NEG	down_pathway	Corr_TF_hub
NCAM1	*NID2*	0.37651	POS	down_pathway	Corr_miRNA
NCAM1	*OTOR*	0.29925	POS	down_pathway	Corr_hub
NCAM1	*PCOLCE*	0.42505	POS	down_pathway	down_pathway
NFE2L3	*PCOLCE*	-0.33526	NEG	up_TF	down_pathway
NFE2L3	*SPON2*	-0.29391	NEG	up_TF	Corr_miRNA
NFE2L3	*ZNF131*	0.44446	POS	up_TF	down_TF

NID2	*PCOLCE*	0.52148	POS	down_pathway	down_TF
NID2	*SDC3*	0.569	POS	down_pathway	down_pathway
NID2	*SPON2*	0.38028	POS	down_pathway	down_pathway
NID2	*TBL2*	0.31948	POS	down_pathway	down_pathway
PCOLCE	*PRRX2*	0.55277	POS	down_pathway	down_pathway
PCOLCE	*SPON2*	0.70278	POS	down_pathway	down_pathway
PCOLCE	*VDR*	0.2446	POS	down_pathway	Corr_hub
PRRX2	*SPON2*	0.53911	POS	down_TF	down_TF
SDC3	*TBL2*	0.31495	POS	down_pathway	Corr_TF_hub
SPON2	*VDR*	0.25906	POS	down_pathway	Corr_hub
THSD7B	*VDR*	0.23242	POS	Corr_pathway	down_pathway

Se

Origin	**Target**	**Correlation value**	**Correlation type**	**Origin attributes**	**Target attributes**
B3GNT5	bta-miR-2285bl	-0.22275	NEG	Corr_hub	Corr_miRNA
B3GNT5	bta-miR-2285co	-0.22275	NEG	Corr_hub	Corr_miRNA
B3GNT5	bta-miR-2285q	-0.22007	NEG	Corr_hub	Corr_miRNA
B3GNT5	bta-miR-425-5p	-0.20216	NEG	Corr_hub	Corr_miRNA
B3GNT5	*COL12A1*	0.2591	POS	Corr_hub	down_pathways
B3GNT5	*HARS*	-0.29062	NEG	Corr_hub	Corr_RIF
B3GNT5	*LOC101907941*	0.35999	POS	Corr_hub	Corr_hub
B3GNT5	*RFX3*	0.3497	POS	Corr_hub	Corr_TF
B3GNT5	*TTC21A*	0.29773	POS	Corr_hub	Corr_RIF
B3GNT5	*ZDBF2*	0.35741	POS	Corr_hub	Corr_RIF
B3GNT5	*ZDHHC17*	0.33057	POS	Corr_hub	Corr_hub
bta-miR-2285bl	bta-miR-2285co	1	POS	Corr_miRNA	Corr_miRNA
bta-miR-2285bl	bta-miR-2285q	0.35281	POS	Corr_miRNA	Corr_miRNA
bta-miR-2285bl	bta-miR-411c-5p	0.32726	POS	Corr_miRNA	Corr_miRNA
bta-miR-2285bl	bta-miR-425-5p	0.16937	POS	Corr_miRNA	Corr_miRNA
bta-miR-2285bl	*LOC101907941*	-0.23616	NEG	Corr_miRNA	Corr_hub
bta-miR-2285bl	*LOC112442312*	-0.27456	NEG	Corr_miRNA	Corr_RIF
bta-miR-2285co	bta-miR-2285q	0.35281	POS	Corr_miRNA	Corr_miRNA

bta-miR-2285co	bta-miR-411c-5p	0.32726	POS	Corr_miRNA	Corr_miRNA
bta-miR-2285co	bta-miR-425-5p	0.16937	POS	Corr_miRNA	Corr_miRNA
bta-miR-2285co	*LOC101907941*	-0.23616	NEG	Corr_miRNA	Corr_hub
bta-miR-2285co	*LOC112442312*	-0.27456	NEG	Corr_miRNA	Corr_RIF
bta-miR-2285q	*COMP*	0.14962	POS	Corr_miRNA	down_trans_pathway
bta-miR-2285q	*HARS*	0.18369	POS	Corr_miRNA	Corr_RIF
bta-miR-2285q	*LOC101907941*	-0.20243	NEG	Corr_miRNA	Corr_hub
bta-miR-411c-5p	*HARS*	0.36182	POS	Corr_miRNA	Corr_RIF
bta-miR-411c-5p	*LOC101907941*	-0.25711	NEG	Corr_miRNA	Corr_hub
bta-miR-411c-5p	*TEF*	0.28007	POS	Corr_miRNA	Corr_TF_RIF
bta-miR-425-5p	*COL12A1*	-0.23077	NEG	Corr_miRNA	down_pathways
bta-miR-425-5p	*TEF*	0.23074	POS	Corr_miRNA	Corr_TF_RIF
bta-miR-425-5p	*ZDBF2*	-0.23657	NEG	Corr_miRNA	Corr_RIF
COL12A1	*COMP*	0.80686	POS	down_pathways	down_trans_pathway
COMP	*DTWD1*	-0.20516	NEG	down_trans_pathway	Corr_RIF_trans
COMP	*ZDHHC17*	-0.25903	NEG	down_trans_pathway	Corr_hub
DTWD1	*HARS*	-0.47568	NEG	Corr_RIF_trans	Corr_RIF
DTWD1	*LOC101907941*	0.44639	POS	Corr_RIF_trans	Corr_hub
DTWD1	*LOC112442312*	0.30752	POS	Corr_RIF_trans	Corr_RIF
DTWD1	*PDK3*	-0.24357	NEG	Corr_RIF_trans	Corr_RIF
DTWD1	*TTC21A*	0.2565	POS	Corr_RIF_trans	Corr_RIF
DTWD1	*ZDHHC17*	0.32468	POS	Corr_RIF_trans	Corr_hub
HARS	*LOC112442312*	-0.29246	NEG	Corr_RIF	Corr_RIF
HARS	*TEF*	0.32789	POS	Corr_RIF	Corr_TF_RIF
HARS	*TTC21A*	-0.29023	NEG	Corr_RIF	Corr_RIF
HARS	*ZDBF2*	-0.32652	NEG	Corr_RIF	Corr_RIF
HARS	*ZDHHC17*	-0.39084	NEG	Corr_RIF	Corr_hub
LOC101907941	*LOC112442312*	0.2731	POS	Corr_hub	Corr_RIF
LOC101907941	*RFX3*	0.36447	POS	Corr_hub	Corr_TF
LOC101907941	*TTC21A*	0.35571	POS	Corr_hub	Corr_RIF
LOC101907941	*ZDBF2*	0.42047	POS	Corr_hub	Corr_RIF
LOC101907941	*ZDHHC17*	0.3672	POS	Corr_hub	Corr_hub

LOC112442312	*PDK3*	-0.29305	NEG	Corr_RIF	Corr_RIF
LOC112442312	*RFX3*	0.34973	POS	Corr_RIF	Corr_TF
LOC112442312	*TTC21A*	0.37688	POS	Corr_RIF	Corr_RIF
PDK3	*RFX3*	-0.25699	NEG	Corr_RIF	Corr_TF
PDK3	*TTC21A*	-0.31104	NEG	Corr_RIF	Corr_RIF
PDK3	*ZDBF2*	-0.23919	NEG	Corr_RIF	Corr_RIF
RFX3	*TTC21A*	0.34307	POS	Corr_TF	Corr_RIF
RFX3	*ZDBF2*	0.33798	POS	Corr_TF	Corr_RIF
RFX3	*ZDHHC17*	0.37051	POS	Corr_TF	Corr_hub
TEF	*ZDBF2*	-0.2515	NEG	Corr_TF_RIF	Corr_RIF
TEF	*ZDHHC17*	-0.37387	NEG	Corr_TF_RIF	Corr_hub
TTC21A	*ZDBF2*	0.28816	POS	Corr_RIF	Corr_RIF
ZDBF2	*ZDHHC17*	0.30766	POS	Corr_RIF	Corr_hub

K

Origin	**Target**	**Correlation value**	**Correlation type**	**Origin attributes**	**Target attributes**
ADA2	*ANGPTL2*	0.35405	POS	Corr_hub	Corr_down_hub
ADA2	*ARAP1*	0.42043	POS	Corr_hub	Corr_hub
ADA2	*ARHGAP30*	0.62805	POS	Corr_hub	Corr_hub
ADA2	bta-miR-500	0.17628	POS	Corr_hub	Corr_miRNA
ADA2	*CD44*	0.4937	POS	Corr_hub	down_pathways
ADA2	*CD86*	0.5016	POS	Corr_hub	Corr_RIF_hub
ADA2	*CREM*	-0.25042	NEG	Corr_hub	up_TF
ADA2	*FCGR3A*	0.53873	POS	Corr_hub	down_pathways
ADA2	*MMP16*	0.46043	POS	Corr_hub	Corr_RIF_hub_pathways
ADA2	*PRRX2*	0.38604	POS	Corr_hub	down_TF
ADA2	*TNC*	0.37287	POS	Corr_hub	down_trans_pathways
ADA2	*VDR*	0.39319	POS	Corr_hub	Corr_TF
ADAM12	*CD44*	0.40463	POS	down_pathways	down_pathways
ADAM12	*COL11A1*	0.65195	POS	down_pathways	down_pathways
ADAM12	*COL21A1*	0.31051	POS	down_pathways	Corr_pathways
ADAM12	*COL22A1*	0.62413	POS	down_pathways	down_trans_pathways

ADAM12	*COMP*	0.59696	POS	down_pathways	down_trans_pathways
ADAM12	*ITGA10*	0.58824	POS	down_pathways	down_pathways
ADAM12	*MMP16*	0.48484	POS	down_pathways	Corr_RIF_hub_pathways
ADAM12	*RNF34*	-0.33693	NEG	down_pathways	Corr_RIF
ADAM12	*THBS4*	0.62637	POS	down_pathways	down_trans_pathways
ADAM12	*TNC*	0.48486	POS	down_pathways	down_trans_pathways
ANGPTL2	*ARAP1*	0.53772	POS	Corr_down_hub	Corr_hub
ANGPTL2	*ARHGAP30*	0.397	POS	Corr_down_hub	Corr_hub
ANGPTL2	*CD44*	0.49225	POS	Corr_down_hub	down_pathways
ANGPTL2	*CD86*	0.5459	POS	Corr_down_hub	Corr_RIF_hub
ANGPTL2	*COL21A1*	0.67041	POS	Corr_down_hub	Corr_pathways
ANGPTL2	*COL22A1*	0.27257	POS	Corr_down_hub	down_trans_pathways
ANGPTL2	*CREM*	-0.29314	NEG	Corr_down_hub	up_TF
ANGPTL2	*FCGR3A*	0.4017	POS	Corr_down_hub	down_pathways
ANGPTL2	*MMP16*	0.63372	POS	Corr_down_hub	Corr_RIF_hub_pathways
ANGPTL2	*PRRX2*	0.3377	POS	Corr_down_hub	down_TF
ANGPTL2	*RNF34*	-0.37953	NEG	Corr_down_hub	Corr_RIF
ANGPTL2	*THBS4*	0.37246	POS	Corr_down_hub	down_trans_pathways
ANGPTL2	*TNC*	0.40863	POS	Corr_down_hub	down_trans_pathways
ANGPTL2	*VDR*	0.39249	POS	Corr_down_hub	Corr_TF
ARAP1	*ARHGAP30*	0.51489	POS	Corr_hub	Corr_hub
ARAP1	bta-miR-92b	0.17023	POS	Corr_hub	Corr_RIF_miRNA
ARAP1	*CD44*	0.36823	POS	Corr_hub	down_pathways
ARAP1	*CD86*	0.4028	POS	Corr_hub	Corr_RIF_hub
ARAP1	*COL11A1*	0.34854	POS	Corr_hub	down_pathways
ARAP1	*COL21A1*	0.41349	POS	Corr_hub	Corr_pathways
ARAP1	*COL22A1*	0.37363	POS	Corr_hub	down_trans_pathways
ARAP1	*COMP*	0.33452	POS	Corr_hub	down_trans_pathways
ARAP1	*CREM*	-0.29229	NEG	Corr_hub	up_TF
ARAP1	*FCGR3A*	0.41209	POS	Corr_hub	down_pathways
ARAP1	*ITGA10*	0.31531	POS	Corr_hub	down_pathways
ARAP1	*MMP16*	0.52931	POS	Corr_hub	Corr_RIF_hub_pathways

ARAP1	*PRRX2*	0.42059	POS	Corr_hub	down_TF
ARAP1	*RNF34*	-0.47661	NEG	Corr_hub	Corr_RIF
ARAP1	*THBS4*	0.4325	POS	Corr_hub	down_trans_pathways
ARAP1	*TNC*	0.48848	POS	Corr_hub	down_trans_pathways
ARAP1	*VDR*	0.37873	POS	Corr_hub	Corr_TF
ARHGAP30	bta-miR-92b	0.1913	POS	Corr_hub	Corr_RIF_miRNA
ARHGAP30	*CD44*	0.52823	POS	Corr_hub	down_pathways
ARHGAP30	*CD86*	0.66218	POS	Corr_hub	Corr_RIF_hub
ARHGAP30	*FCGR3A*	0.67343	POS	Corr_hub	down_pathways
ARHGAP30	*MMP16*	0.46874	POS	Corr_hub	Corr_RIF_hub_pathways
ARHGAP30	*PRRX2*	0.39351	POS	Corr_hub	down_TF
ARHGAP30	*RNF34*	-0.38796	NEG	Corr_hub	Corr_RIF
ARHGAP30	*TNC*	0.39982	POS	Corr_hub	down_trans_pathways
ARHGAP30	*VDR*	0.37471	POS	Corr_hub	Corr_TF
bta-miR-130b	bta-miR-92b	0.18846	POS	Corr_miRNA	Corr_RIF_miRNA
bta-miR-130b	*RNF34*	-0.18585	NEG	Corr_miRNA	Corr_RIF
bta-miR-500	*ITGA10*	-0.21082	NEG	Corr_miRNA	down_pathways
bta-miR-92b	*CD44*	0.18979	POS	Corr_RIF_miRNA	down_pathways
bta-miR-92b	*COL21A1*	0.17499	POS	Corr_RIF_miRNA	Corr_pathways
bta-miR-92b	*MMP16*	0.18661	POS	Corr_RIF_miRNA	Corr_RIF_hub_pathways
bta-miR-92b	*PRRX2*	0.21628	POS	Corr_RIF_miRNA	down_TF
bta-miR-92b	*TNC*	0.21131	POS	Corr_RIF_miRNA	down_trans_pathways
CD44	*CD86*	0.56728	POS	down_pathways	Corr_RIF_hub
CD44	*COL11A1*	0.39695	POS	down_pathways	down_pathways
CD44	*COL21A1*	0.40465	POS	down_pathways	Corr_pathways
CD44	*COL22A1*	0.39618	POS	down_pathways	down_trans_pathways
CD44	*COMP*	0.4391	POS	down_pathways	down_trans_pathways
CD44	*FCGR3A*	0.4618	POS	down_pathways	down_pathways
CD44	*MMP16*	0.54236	POS	down_pathways	Corr_RIF_hub_pathways
CD44	*PRRX2*	0.53604	POS	down_pathways	down_TF
CD44	*THBS4*	0.47498	POS	down_pathways	down_trans_pathways
CD44	*TNC*	0.62128	POS	down_pathways	down_trans_pathways

CD44	*ZIC3*	-0.22067	NEG	down_pathways	Corr_TF
CD86	*COL21A1*	0.50852	POS	Corr_RIF_hub	Corr_pathways
CD86	*FCGR3A*	0.50597	POS	Corr_RIF_hub	down_pathways
CD86	*MMP16*	0.53103	POS	Corr_RIF_hub	Corr_RIF_hub_pathways
CD86	*RNF34*	-0.41476	NEG	Corr_RIF_hub	Corr_RIF
CD86	*TNC*	0.36261	POS	Corr_RIF_hub	down_trans_pathways
CD86	*VDR*	0.47296	POS	Corr_RIF_hub	Corr_TF
CD86	*ZIC3*	-0.20872	NEG	Corr_RIF_hub	Corr_TF
COL11A1	*COL22A1*	0.8484	POS	down_pathways	down_trans_pathways
COL11A1	*COMP*	0.91524	POS	down_pathways	down_trans_pathways
COL11A1	*ITGA10*	0.65672	POS	down_pathways	down_pathways
COL11A1	*MMP16*	0.46702	POS	down_pathways	Corr_RIF_hub_pathways
COL11A1	*PRRX2*	0.57971	POS	down_pathways	down_TF
COL11A1	*THBS4*	0.86932	POS	down_pathways	down_trans_pathways
COL11A1	*TNC*	0.5626	POS	down_pathways	down_trans_pathways
COL21A1	*MMP16*	0.57002	POS	Corr_pathways	Corr_RIF_hub_pathways
COL21A1	*RNF34*	-0.49719	NEG	Corr_pathways	Corr_RIF
COL21A1	*VDR*	0.36053	POS	Corr_pathways	Corr_TF
COL22A1	*COMP*	0.88862	POS	down_trans_pathways	down_trans_pathways
COL22A1	*ITGA10*	0.7114	POS	down_trans_pathways	down_pathways
COL22A1	*MMP16*	0.4187	POS	down_trans_pathways	Corr_RIF_hub_pathways
COL22A1	*PRRX2*	0.52144	POS	down_trans_pathways	down_TF
COL22A1	*RNF34*	-0.30794	NEG	down_trans_pathways	Corr_RIF
COL22A1	*THBS4*	0.82451	POS	down_trans_pathways	down_trans_pathways
COL22A1	*TNC*	0.51025	POS	down_trans_pathways	down_trans_pathways
COMP	*ITGA10*	0.62139	POS	down_trans_pathways	down_pathways
COMP	*MMP16*	0.39517	POS	down_trans_pathways	Corr_RIF_hub_pathways
COMP	*PRRX2*	0.61435	POS	down_trans_pathways	down_TF
COMP	*THBS4*	0.87442	POS	down_trans_pathways	down_trans_pathways
COMP	*TNC*	0.56269	POS	down_trans_pathways	down_trans_pathways
CREM	*MMP16*	-0.23325	NEG	up_TF	Corr_RIF_hub_pathways
CREM	*THBS4*	-0.24267	NEG	up_TF	down_trans_pathways

CREM	*VDR*	-0.22453	NEG	up_TF	Corr_TF
FCGR3A	*MMP16*	0.41479	POS	down_pathways	Corr_RIF_hub_pathways
FCGR3A	*TNC*	0.33341	POS	down_pathways	down_trans_pathways
ITGA10	*PRRX2*	0.45121	POS	down_pathways	down_TF
ITGA10	*RNF34*	-0.2434	NEG	down_pathways	Corr_RIF
ITGA10	*THBS4*	0.61115	POS	down_pathways	down_trans_pathways
ITGA10	*TNC*	0.44769	POS	down_pathways	down_trans_pathways
MMP16	*PRRX2*	0.44498	POS	Corr_RIF_hub_pathways	down_TF
MMP16	*RNF34*	-0.50322	NEG	Corr_RIF_hub_pathways	Corr_RIF
MMP16	*THBS4*	0.49322	POS	Corr_RIF_hub_pathways	down_trans_pathways
MMP16	*TNC*	0.55163	POS	Corr_RIF_hub_pathways	down_trans_pathways
MMP16	*VDR*	0.35183	POS	Corr_RIF_hub_pathways	Corr_TF
MMP16	*ZIC3*	-0.2639	NEG	Corr_RIF_hub_pathways	Corr_TF
PRRX2	*THBS4*	0.63399	POS	down_TF	down_trans_pathways
PRRX2	*TNC*	0.64906	POS	down_TF	down_trans_pathways
PRRX2	*ZIC3*	-0.28348	NEG	down_TF	Corr_TF
RNF34	*VDR*	-0.2846	NEG	Corr_RIF	Corr_TF
THBS4	*TNC*	0.61094	POS	down_trans_pathways	down_trans_pathways

Na

Origin	**Target**	**Correlation value**	**Correlation type**	**Origin attributes**	**Target attributes**
ADA2	*ARAP1*	0.42043	POS	Corr_hub	Corr_hub
ADA2	bta-miR-22-5p	-0.13427	NEG	Corr_hub	Corr_miRNA
ADA2	*CD44*	0.4937	POS	Corr_hub	down_pathways
ADA2	*COL12A1*	0.34418	POS	Corr_hub	down_pathways
ADA2	*COL18A1*	0.34985	POS	Corr_hub	down_pathways
ADA2	*COL21A1*	0.32274	POS	Corr_hub	Corr_pathways
ADA2	*MMP16*	0.46043	POS	Corr_hub	Corr_hub_pathways
ADA2	*PRRX2*	0.38604	POS	Corr_hub	down_TF
ADA2	*TNC*	0.37287	POS	Corr_hub	down_trans_pathways
ADA2	*VDR*	0.39319	POS	Corr_hub	Corr_TF_RIF
ARAP1	*CAMKK1*	0.37721	POS	Corr_hub	Corr_RIF

ARAP1	*CD44*	0.36823	POS	Corr_hub	down_pathways
ARAP1	*COL11A1*	0.34854	POS	Corr_hub	down_pathways
ARAP1	*COL12A1*	0.40061	POS	Corr_hub	down_pathways
ARAP1	*COL18A1*	0.48117	POS	Corr_hub	down_pathways
ARAP1	*COL21A1*	0.41349	POS	Corr_hub	Corr_pathways
ARAP1	*COL22A1*	0.37363	POS	Corr_hub	down_trans_pathways
ARAP1	*COMP*	0.33452	POS	Corr_hub	down_trans_pathways
ARAP1	*ITGA10*	0.31531	POS	Corr_hub	down_pathways
ARAP1	*LOXL3*	0.32665	POS	Corr_hub	Corr_trans_pathways
ARAP1	*MMP16*	0.52931	POS	Corr_hub	Corr_hub_pathways
ARAP1	*PRRX2*	0.42059	POS	Corr_hub	down_TF
ARAP1	*THBS4*	0.4325	POS	Corr_hub	down_trans_pathways
ARAP1	*TNC*	0.48848	POS	Corr_hub	down_trans_pathways
ARAP1	*VDR*	0.37873	POS	Corr_hub	Corr_TF_RIF
bta-miR-125a	bta-miR-92b	0.36714	POS	Corr_RIF_miRNA	Corr_miRNA
bta-miR-125a	*ITGA10*	0.153	POS	Corr_RIF_miRNA	down_pathways
bta-miR-125a	*VMAC*	-0.09683	NEG	Corr_RIF_miRNA	Corr_RIF_trans
bta-miR-125a	*WDPCP*	0.1263	POS	Corr_RIF_miRNA	Corr_RIF_trans
bta-miR-130b	bta-miR-365-3p	-0.14531	NEG	Corr_miRNA	Corr_miRNA
bta-miR-130b	bta-miR-92b	0.18846	POS	Corr_miRNA	Corr_miRNA
bta-miR-130b	*CDKN3*	0.23004	POS	Corr_miRNA	Corr_RIF
bta-miR-130b	*COL18A1*	0.17597	POS	Corr_miRNA	down_pathways
bta-miR-22-5p	bta-miR-365-3p	0.12967	POS	Corr_miRNA	Corr_miRNA
bta-miR-22-5p	*CDKN3*	-0.21977	NEG	Corr_miRNA	Corr_RIF
bta-miR-22-5p	*ITGA10*	-0.11961	NEG	Corr_miRNA	down_pathways
bta-miR-22-5p	*WDPCP*	-0.13938	NEG	Corr_miRNA	Corr_RIF_trans
bta-miR-365-3p	*VMAC*	-0.234	NEG	Corr_miRNA	Corr_RIF_trans
bta-miR-92b	*COL18A1*	0.2622	POS	Corr_miRNA	down_pathways
bta-miR-92b	*LOXL3*	0.25573	POS	Corr_miRNA	Corr_trans_pathways
bta-miR-92b	*PRRX2*	0.21628	POS	Corr_miRNA	down_TF
bta-miR-92b	*TNC*	0.21131	POS	Corr_miRNA	down_trans_pathways
CAMKK1	*COL21A1*	0.28651	POS	Corr_RIF	Corr_pathways

CAMKK1	*COL22A1*	0.31348	POS	Corr_RIF	down_trans_pathways
CAMKK1	*ITGA10*	0.32288	POS	Corr_RIF	down_pathways
CAMKK1	*MMP16*	0.43273	POS	Corr_RIF	Corr_hub_pathways
CAMKK1	*TNC*	0.29579	POS	Corr_RIF	down_trans_pathways
CD44	*CENPE*	0.29282	POS	down_pathways	Corr_RIF
CD44	*COL11A1*	0.39695	POS	down_pathways	down_pathways
CD44	*COL12A1*	0.50116	POS	down_pathways	down_pathways
CD44	*COL18A1*	0.55564	POS	down_pathways	down_pathways
CD44	*COL21A1*	0.40465	POS	down_pathways	Corr_pathways
CD44	*COL22A1*	0.39618	POS	down_pathways	down_trans_pathways
CD44	*COMP*	0.4391	POS	down_pathways	down_trans_pathways
CD44	*LOXL3*	0.31712	POS	down_pathways	Corr_trans_pathways
CD44	*MMP16*	0.54236	POS	down_pathways	Corr_hub_pathways
CD44	*PRRX2*	0.53604	POS	down_pathways	down_TF
CD44	*THBS4*	0.47498	POS	down_pathways	down_trans_pathways
CD44	*TNC*	0.62128	POS	down_pathways	down_trans_pathways
CD44	*ZIC3*	-0.22067	NEG	down_pathways	Corr_TF
CDKN3	*COL21A1*	0.22794	POS	Corr_RIF	Corr_pathways
CDKN3	*VMAC*	0.2189	POS	Corr_RIF	Corr_RIF_trans
CENPE	*COL18A1*	0.30483	POS	Corr_RIF	down_pathways
CENPE	*COL21A1*	0.28536	POS	Corr_RIF	Corr_pathways
CENPE	*ITGA10*	0.29739	POS	Corr_RIF	down_pathways
CENPE	*MMP16*	0.24064	POS	Corr_RIF	Corr_hub_pathways
CENPE	*TNC*	0.23169	POS	Corr_RIF	down_trans_pathways
COL11A1	*COL12A1*	0.83629	POS	down_pathways	down_pathways
COL11A1	*COL22A1*	0.8484	POS	down_pathways	down_trans_pathways
COL11A1	*COMP*	0.91524	POS	down_pathways	down_trans_pathways
COL11A1	*ITGA10*	0.65672	POS	down_pathways	down_pathways
COL11A1	*MMP16*	0.46702	POS	down_pathways	Corr_hub_pathways
COL11A1	*PRRX2*	0.57971	POS	down_pathways	down_TF
COL11A1	*THBS4*	0.86932	POS	down_pathways	down_trans_pathways
COL11A1	*TNC*	0.5626	POS	down_pathways	down_trans_pathways

COL12A1	*COL18A1*	0.45534	POS	down_pathways	down_pathways
COL12A1	*COL22A1*	0.73403	POS	down_pathways	down_trans_pathways
COL12A1	*COMP*	0.80686	POS	down_pathways	down_trans_pathways
COL12A1	*ITGA10*	0.53586	POS	down_pathways	down_pathways
COL12A1	*MMP16*	0.55788	POS	down_pathways	Corr_hub_pathways
COL12A1	*PRRX2*	0.59196	POS	down_pathways	down_TF
COL12A1	*THBS4*	0.8196	POS	down_pathways	down_trans_pathways
COL12A1	*TNC*	0.70665	POS	down_pathways	down_trans_pathways
COL18A1	*COL21A1*	0.43911	POS	down_pathways	Corr_pathways
COL18A1	*COL22A1*	0.40831	POS	down_pathways	down_trans_pathways
COL18A1	*ITGA10*	0.34102	POS	down_pathways	down_pathways
COL18A1	*LOXL3*	0.49161	POS	down_pathways	Corr_trans_pathways
COL18A1	*MMP16*	0.49981	POS	down_pathways	Corr_hub_pathways
COL18A1	*PRRX2*	0.59877	POS	down_pathways	down_TF
COL18A1	*THBS4*	0.49388	POS	down_pathways	down_trans_pathways
COL18A1	*TNC*	0.67805	POS	down_pathways	down_trans_pathways
COL18A1	*VDR*	0.28961	POS	down_pathways	Corr_TF_RIF
COL18A1	*VMAC*	0.2601	POS	down_pathways	Corr_RIF_trans
COL18A1	*ZIC3*	-0.21718	NEG	down_pathways	Corr_TF
COL21A1	*MMP16*	0.57002	POS	Corr_pathways	Corr_hub_pathways
COL21A1	*VDR*	0.36053	POS	Corr_pathways	Corr_TF_RIF
COL21A1	*VMAC*	0.33072	POS	Corr_pathways	Corr_RIF_trans
COL22A1	*COMP*	0.88862	POS	down_trans_pathways	down_trans_pathways
COL22A1	*ITGA10*	0.7114	POS	down_trans_pathways	down_pathways
COL22A1	*MMP16*	0.4187	POS	down_trans_pathways	Corr_hub_pathways
COL22A1	*PRRX2*	0.52144	POS	down_trans_pathways	down_TF
COL22A1	*THBS4*	0.82451	POS	down_trans_pathways	down_trans_pathways
COL22A1	*TNC*	0.51025	POS	down_trans_pathways	down_trans_pathways
COMP	*ITGA10*	0.62139	POS	down_trans_pathways	down_pathways
COMP	*MMP16*	0.39517	POS	down_trans_pathways	Corr_hub_pathways
COMP	*PRRX2*	0.61435	POS	down_trans_pathways	down_TF
COMP	*THBS4*	0.87442	POS	down_trans_pathways	down_trans_pathways

COMP	*TNC*	0.56269	POS	down_trans_pathways	down_trans_pathways
ITGA10	*PRRX2*	0.45121	POS	down_pathways	down_TF
ITGA10	*THBS4*	0.61115	POS	down_pathways	down_trans_pathways
ITGA10	*TNC*	0.44769	POS	down_pathways	down_trans_pathways
LOXL3	*MMP16*	0.34055	POS	Corr_trans_pathways	Corr_hub_pathways
LOXL3	*PRRX2*	0.37333	POS	Corr_trans_pathways	down_TF
LOXL3	*THBS4*	0.33181	POS	Corr_trans_pathways	down_trans_pathways
LOXL3	*TNC*	0.41046	POS	Corr_trans_pathways	down_trans_pathways
LOXL3	*ZIC3*	-0.21593	NEG	Corr_trans_pathways	Corr_TF
MMP16	*PRRX2*	0.44498	POS	Corr_hub_pathways	down_TF
MMP16	*THBS4*	0.49322	POS	Corr_hub_pathways	down_trans_pathways
MMP16	*TNC*	0.55163	POS	Corr_hub_pathways	down_trans_pathways
MMP16	*VDR*	0.35183	POS	Corr_hub_pathways	Corr_TF_RIF
MMP16	*ZIC3*	-0.2639	NEG	Corr_hub_pathways	Corr_TF
PRRX2	*THBS4*	0.63399	POS	down_TF	down_trans_pathways
PRRX2	*TNC*	0.64906	POS	down_TF	down_trans_pathways
PRRX2	*ZIC3*	-0.28348	NEG	down_TF	Corr_TF
THBS4	*TNC*	0.61094	POS	down_trans_pathways	down_trans_pathways
VDR	*WDPCP*	0.19512	POS	Corr_TF_RIF	Corr_RIF_trans
WDPCP	*ZIC3*	-0.20815	NEG	Corr_RIF_trans	Corr_TF

Cu

Origin	**Target**	**Correlation value**	**Correlation type**	**Origin attributes**	**Target attributes**
ACACA	*ADAM12*	0.39135	POS	down_pathway	down_pathway
ACACA	*ADIPOQ*	0.69483	POS	down_pathway	down_pathway
ACACA	*CD44*	0.39952	POS	down_pathway	down_pathway
ACACA	*COL12A1*	0.47683	POS	down_pathway	down_pathway
ACACA	*COL18A1*	0.54106	POS	down_pathway	down_pathway
ACACA	*COL22A1*	0.41128	POS	down_pathway	down_trans_pathway
ACACA	*COL5A2*	0.56861	POS	down_pathway	down_pathway
ACACA	*COMP*	0.37713	POS	down_pathway	down_trans_pathway
ACACA	*EBF1*	0.61166	POS	down_pathway	down_TF

ACACA	*ELOVL5*	0.70981	POS	down_pathway	down_trans_pathway
ACACA	*ELOVL6*	0.83635	POS	down_pathway	down_pathway
ACACA	*FASN*	0.83521	POS	down_pathway	down_trans_pathway
ACACA	*GNAI1*	0.77254	POS	down_pathway	down_pathway
ACACA	*ITGA10*	0.35281	POS	down_pathway	down_pathway
ACACA	*LEP*	0.78849	POS	down_pathway	down_pathway
ACACA	*MKX*	0.39623	POS	down_pathway	down_TF
ACACA	*PCK2*	0.76171	POS	down_pathway	down_pathway
ACACA	*PLIN1*	0.72349	POS	down_pathway	down_pathway
ACACA	*PRRX2*	0.36829	POS	down_pathway	down_TF
ACACA	*PTGIR*	0.38688	POS	down_pathway	down_trans_pathway
ACACA	*RGS7*	0.34611	POS	down_pathway	corr_hub
ACACA	*SCD*	0.72632	POS	down_pathway	down_pathway
ACACA	*THBS1*	0.6109	POS	down_pathway	down_pathway
ACACA	*THBS4*	0.39229	POS	down_pathway	down_trans_pathway
ACACA	*TINF2*	-0.28525	NEG	down_pathway	Corr_hub
ACACA	*TNC*	0.51513	POS	down_pathway	down_trans_pathway
ADAM12	*CD44*	0.40463	POS	down_pathway	down_pathway
ADAM12	*COL11A1*	0.65195	POS	down_pathway	down_pathway
ADAM12	*COL11A2*	0.34259	POS	down_pathway	down_trans_pathway
ADAM12	*COL12A1*	0.62039	POS	down_pathway	down_pathway
ADAM12	*COL18A1*	0.39984	POS	down_pathway	down_pathway
ADAM12	*COL22A1*	0.62413	POS	down_pathway	down_trans_pathway
ADAM12	*COL5A2*	0.56362	POS	down_pathway	down_pathway
ADAM12	*COMP*	0.59696	POS	down_pathway	down_trans_pathway
ADAM12	*EBF1*	0.48618	POS	down_pathway	down_TF
ADAM12	*ELOVL5*	0.38741	POS	down_pathway	down_trans_pathway
ADAM12	*ELOVL6*	0.35568	POS	down_pathway	down_pathway
ADAM12	*GNAI1*	0.37752	POS	down_pathway	down_pathway
ADAM12	*ITGA10*	0.58824	POS	down_pathway	down_pathway
ADAM12	*LUM*	0.41996	POS	down_pathway	down_pathway
ADAM12	*MEST*	0.60539	POS	down_pathway	corr_down_hub

ADAM12	*MKX*	0.57413	POS	down_pathway	down_TF
ADAM12	*NUCB2*	0.3408	POS	down_pathway	corr_hub
ADAM12	*PTGIR*	0.64227	POS	down_pathway	down_trans_pathway
ADAM12	*SCD*	0.32089	POS	down_pathway	down_pathway
ADAM12	*THBS1*	0.48719	POS	down_pathway	down_pathway
ADAM12	*THBS4*	0.62637	POS	down_pathway	down_trans_pathway
ADAM12	*TNC*	0.48486	POS	down_pathway	down_trans_pathway
ADAM12	*TNFRSF11B*	0.41583	POS	down_pathway	corr_trans_hub
ADAMTS2	*CD44*	0.6027	POS	down_pathway	down_pathway
ADAMTS2	*COL12A1*	0.55185	POS	down_pathway	down_pathway
ADAMTS2	*COL18A1*	0.57455	POS	down_pathway	down_pathway
ADAMTS2	*COL5A2*	0.75798	POS	down_pathway	down_pathway
ADAMTS2	*DIAPH3*	0.44198	POS	down_pathway	corr_hub
ADAMTS2	*EBF1*	0.55747	POS	down_pathway	down_TF
ADAMTS2	*LOC530929*	-0.19747	NEG	down_pathway	corr_RIF
ADAMTS2	*LUM*	0.63598	POS	down_pathway	down_pathway
ADAMTS2	*MEST*	0.4482	POS	down_pathway	corr_down_hub
ADAMTS2	*PRRX2*	0.52925	POS	down_pathway	down_TF
ADAMTS2	*PTGIR*	0.40315	POS	down_pathway	down_trans_pathway
ADAMTS2	*SGCE*	0.54261	POS	down_pathway	corr_hub
ADAMTS2	*THBS1*	0.4782	POS	down_pathway	down_pathway
ADAMTS2	*THBS4*	0.44508	POS	down_pathway	down_trans_pathway
ADAMTS2	*TINF2*	-0.3197	NEG	down_pathway	Corr_hub
ADAMTS2	*TNC*	0.60397	POS	down_pathway	down_trans_pathway
ADIPOQ	*bta-miR-193b*	-0.19277	NEG	down_pathway	corr_miRNA_hub
ADIPOQ	*CD44*	0.39371	POS	down_pathway	down_pathway
ADIPOQ	*COL12A1*	0.37338	POS	down_pathway	down_pathway
ADIPOQ	*COL18A1*	0.58575	POS	down_pathway	down_pathway
ADIPOQ	*COL22A1*	0.44634	POS	down_pathway	down_trans_pathway
ADIPOQ	*COL5A2*	0.44248	POS	down_pathway	down_pathway
ADIPOQ	*EBF1*	0.51717	POS	down_pathway	down_TF
ADIPOQ	*ELOVL5*	0.61324	POS	down_pathway	down_trans_pathway

ADIPOQ	*ELOVL6*	0.76064	POS	down_pathway	down_pathway
ADIPOQ	*FASN*	0.70297	POS	down_pathway	down_trans_pathway
ADIPOQ	*GNAI1*	0.83027	POS	down_pathway	down_pathway
ADIPOQ	*LEP*	0.80693	POS	down_pathway	down_pathway
ADIPOQ	*MKX*	0.35157	POS	down_pathway	down_TF
ADIPOQ	*PCK2*	0.77798	POS	down_pathway	down_pathway
ADIPOQ	*PLIN1*	0.95922	POS	down_pathway	down_pathway
ADIPOQ	*PRRX2*	0.36001	POS	down_pathway	down_TF
ADIPOQ	*RASL11A*	0.15715	POS	down_pathway	corr_RIF
ADIPOQ	*SCD*	0.57718	POS	down_pathway	down_pathway
ADIPOQ	*SGCE*	0.28932	POS	down_pathway	corr_hub
ADIPOQ	*THBS1*	0.53303	POS	down_pathway	down_pathway
ADIPOQ	*TINF2*	-0.3174	NEG	down_pathway	Corr_hub
ADIPOQ	*TNC*	0.41624	POS	down_pathway	down_trans_pathway
BHLHE22	bta-miR-365-5p	-0.17367	NEG	corr_TF	corr_miRNA
BHLHE22	*CD44*	0.21404	POS	corr_TF	down_pathway
BHLHE22	*COL12A1*	0.16799	POS	corr_TF	down_pathway
BHLHE22	*COL5A2*	0.18036	POS	corr_TF	down_pathway
BHLHE22	*DIAPH3*	0.21716	POS	corr_TF	corr_hub
BHLHE22	*EBF1*	0.17519	POS	corr_TF	down_TF
BHLHE22	*THBS4*	0.20097	POS	corr_TF	down_trans_pathway
bta-miR-1468	bta-miR-150	0.41728	POS	corr_miRNA	corr_miRNA
bta-miR-1468	bta-miR-193b	-0.35982	NEG	corr_miRNA	corr_miRNA_hub
bta-miR-1468	*LUM*	-0.13908	NEG	corr_miRNA	down_pathway
bta-miR-150	bta-miR-193b	-0.26695	NEG	corr_miRNA	corr_miRNA_hub
bta-miR-150	bta-miR-493	0.24899	POS	corr_miRNA	corr_miRNA
bta-miR-150	*NUCB2*	-0.17081	NEG	corr_miRNA	corr_hub
bta-miR-193b	bta-miR-365-5p	0.15542	POS	corr_miRNA_hub	corr_miRNA
bta-miR-193b	*CD44*	-0.25227	NEG	corr_miRNA_hub	down_pathway
bta-miR-193b	*COL5A2*	-0.19257	NEG	corr_miRNA_hub	down_pathway
bta-miR-193b	*ELOVL5*	-0.28507	NEG	corr_miRNA_hub	down_trans_pathway
bta-miR-193b	*GNAI1*	-0.23338	NEG	corr_miRNA_hub	down_pathway

bta-miR-193b	*P4HA3*	-0.22785	NEG	corr_miRNA_hub	down_pathway
bta-miR-365-5p	*RASL11A*	0.12282	POS	corr_miRNA	corr_RIF
bta-miR-365-5p	*SGCE*	-0.1933	NEG	corr_miRNA	corr_hub
bta-miR-493	*COL11A2*	0.18641	POS	corr_miRNA	down_trans_pathway
bta-miR-493	*LOC518768*	-0.26385	NEG	corr_miRNA	corr_RIF
bta-miR-493	*LOC530929*	0.27111	POS	corr_miRNA	corr_RIF
CD44	*COL11A1*	0.39695	POS	down_pathway	down_pathway
CD44	*COL12A1*	0.50116	POS	down_pathway	down_pathway
CD44	*COL18A1*	0.55564	POS	down_pathway	down_pathway
CD44	*COL22A1*	0.39618	POS	down_pathway	down_trans_pathway
CD44	*COL5A2*	0.71872	POS	down_pathway	down_pathway
CD44	*COMP*	0.4391	POS	down_pathway	down_trans_pathway
CD44	*DIAPH3*	0.39266	POS	down_pathway	corr_hub
CD44	*ELOVL5*	0.4623	POS	down_pathway	down_trans_pathway
CD44	*ELOVL6*	0.42851	POS	down_pathway	down_pathway
CD44	*FASN*	0.34523	POS	down_pathway	down_trans_pathway
CD44	*GNAI1*	0.44996	POS	down_pathway	down_pathway
CD44	*LEP*	0.34536	POS	down_pathway	down_pathway
CD44	*LOC784127*	0.231	POS	down_pathway	corr_RIF
CD44	*LUM*	0.61478	POS	down_pathway	down_pathway
CD44	*MEST*	0.49759	POS	down_pathway	corr_down_hub
CD44	*MKX*	0.41899	POS	down_pathway	down_TF
CD44	*NUCB2*	0.34573	POS	down_pathway	corr_hub
CD44	*PCK2*	0.41228	POS	down_pathway	down_pathway
CD44	*PLIN1*	0.34457	POS	down_pathway	down_pathway
CD44	*PRRX2*	0.53604	POS	down_pathway	down_TF
CD44	*PTGIR*	0.46566	POS	down_pathway	down_trans_pathway
CD44	*SGCE*	0.52758	POS	down_pathway	corr_hub
CD44	*THBS1*	0.4821	POS	down_pathway	down_pathway
CD44	*THBS4*	0.47498	POS	down_pathway	down_trans_pathway
CD44	*TINF2*	-0.3483	NEG	down_pathway	Corr_hub
CD44	*TNC*	0.62128	POS	down_pathway	down_trans_pathway

COL11A1	*COL11A2*	0.50973	POS	down_pathway	down_trans_pathway
COL11A1	*COL12A1*	0.83629	POS	down_pathway	down_pathway
COL11A1	*COL22A1*	0.8484	POS	down_pathway	down_trans_pathway
COL11A1	*COMP*	0.91524	POS	down_pathway	down_trans_pathway
COL11A1	*DIAPH3*	0.39593	POS	down_pathway	corr_hub
COL11A1	*ELOVL6*	0.34846	POS	down_pathway	down_pathway
COL11A1	*FASN*	0.31449	POS	down_pathway	down_trans_pathway
COL11A1	*ITGA10*	0.65672	POS	down_pathway	down_pathway
COL11A1	*MEST*	0.59973	POS	down_pathway	corr_down_hub
COL11A1	*MKX*	0.84326	POS	down_pathway	down_TF
COL11A1	*NUCB2*	0.45017	POS	down_pathway	corr_hub
COL11A1	*PRRX2*	0.57971	POS	down_pathway	down_TF
COL11A1	*PTGIR*	0.70835	POS	down_pathway	down_trans_pathway
COL11A1	*SCD*	0.35228	POS	down_pathway	down_pathway
COL11A1	*THBS1*	0.62968	POS	down_pathway	down_pathway
COL11A1	*THBS4*	0.86932	POS	down_pathway	down_trans_pathway
COL11A1	*TNC*	0.5626	POS	down_pathway	down_trans_pathway
COL11A1	*TNFRSF11B*	0.57514	POS	down_pathway	corr_trans_hub
COL11A2	*COL22A1*	0.40066	POS	down_trans_pathway	down_trans_pathway
COL11A2	*COMP*	0.44414	POS	down_trans_pathway	down_trans_pathway
COL11A2	*ITGA10*	0.45989	POS	down_trans_pathway	down_pathway
COL11A2	*LOC530929*	0.21157	POS	down_trans_pathway	corr_RIF
COL11A2	*LOC784127*	0.25927	POS	down_trans_pathway	corr_RIF
COL11A2	*MEST*	0.41446	POS	down_trans_pathway	corr_down_hub
COL11A2	*MKX*	0.3852	POS	down_trans_pathway	down_TF
COL11A2	*PRRX2*	0.37351	POS	down_trans_pathway	down_TF
COL11A2	*PTGIR*	0.45619	POS	down_trans_pathway	down_trans_pathway
COL11A2	*THBS4*	0.44015	POS	down_trans_pathway	down_trans_pathway
COL11A2	*TNFRSF11B*	0.45072	POS	down_trans_pathway	corr_trans_hub
COL12A1	*COL18A1*	0.45534	POS	down_pathway	down_pathway
COL12A1	*COL22A1*	0.73403	POS	down_pathway	down_trans_pathway
COL12A1	*COL5A2*	0.66109	POS	down_pathway	down_pathway

COL12A1	*COMP*	0.80686	POS	down_pathway	down_trans_pathway
COL12A1	*DIAPH3*	0.51382	POS	down_pathway	corr_hub
COL12A1	*EBF1*	0.62502	POS	down_pathway	down_TF
COL12A1	*ELOVL5*	0.43092	POS	down_pathway	down_trans_pathway
COL12A1	*ELOVL6*	0.47456	POS	down_pathway	down_pathway
COL12A1	*FASN*	0.42522	POS	down_pathway	down_trans_pathway
COL12A1	*GNAI1*	0.42119	POS	down_pathway	down_pathway
COL12A1	*ITGA10*	0.53586	POS	down_pathway	down_pathway
COL12A1	*LEP*	0.37929	POS	down_pathway	down_pathway
COL12A1	*LUM*	0.47659	POS	down_pathway	down_pathway
COL12A1	*MEST*	0.60645	POS	down_pathway	corr_down_hub
COL12A1	*MKX*	0.80536	POS	down_pathway	down_TF
COL12A1	*NUCB2*	0.37451	POS	down_pathway	corr_hub
COL12A1	*P4HA3*	0.36693	POS	down_pathway	down_pathway
COL12A1	*PCK2*	0.41195	POS	down_pathway	down_pathway
COL12A1	*PLIN1*	0.3653	POS	down_pathway	down_pathway
COL12A1	*PRRX2*	0.59196	POS	down_pathway	down_TF
COL12A1	*PTGIR*	0.6598	POS	down_pathway	down_trans_pathway
COL12A1	*RGS7*	0.29923	POS	down_pathway	corr_hub
COL12A1	*SCD*	0.45246	POS	down_pathway	down_pathway
COL12A1	*SGCE*	0.40412	POS	down_pathway	corr_hub
COL12A1	*THBS1*	0.77757	POS	down_pathway	down_pathway
COL12A1	*THBS4*	0.8196	POS	down_pathway	down_trans_pathway
COL12A1	*TNC*	0.70665	POS	down_pathway	down_trans_pathway
COL12A1	*TNFRSF11B*	0.51338	POS	down_pathway	corr_trans_hub
COL18A1	*COL22A1*	0.40831	POS	down_pathway	down_trans_pathway
COL18A1	*COL5A2*	0.67625	POS	down_pathway	down_pathway
COL18A1	*EBF1*	0.61681	POS	down_pathway	down_TF
COL18A1	*ELOVL5*	0.59471	POS	down_pathway	down_trans_pathway
COL18A1	*ELOVL6*	0.51138	POS	down_pathway	down_pathway
COL18A1	*GNAI1*	0.69544	POS	down_pathway	down_pathway
COL18A1	*ITGA10*	0.34102	POS	down_pathway	down_pathway

COL18A1	*LEP*	0.54988	POS	down_pathway	down_pathway
COL18A1	*LUM*	0.60643	POS	down_pathway	down_pathway
COL18A1	*MEST*	0.426	POS	down_pathway	corr_down_hub
COL18A1	*MKX*	0.43671	POS	down_pathway	down_TF
COL18A1	*PCK2*	0.50316	POS	down_pathway	down_pathway
COL18A1	*PLIN1*	0.58934	POS	down_pathway	down_pathway
COL18A1	*PRRX2*	0.59877	POS	down_pathway	down_TF
COL18A1	*PTGIR*	0.45348	POS	down_pathway	down_trans_pathway
COL18A1	*RASL11A*	0.20959	POS	down_pathway	corr_RIF
COL18A1	*SCD*	0.43294	POS	down_pathway	down_pathway
COL18A1	*SGCE*	0.44031	POS	down_pathway	corr_hub
COL18A1	*THBS1*	0.53108	POS	down_pathway	down_pathway
COL18A1	*THBS4*	0.49388	POS	down_pathway	down_trans_pathway
COL18A1	*TINF2*	-0.34877	NEG	down_pathway	Corr_hub
COL18A1	*TNC*	0.67805	POS	down_pathway	down_trans_pathway
COL22A1	*COMP*	0.88862	POS	down_trans_pathway	down_trans_pathway
COL22A1	*EBF1*	0.43658	POS	down_trans_pathway	down_TF
COL22A1	*ELOVL5*	0.3348	POS	down_trans_pathway	down_trans_pathway
COL22A1	*ELOVL6*	0.39953	POS	down_trans_pathway	down_pathway
COL22A1	*FASN*	0.38489	POS	down_trans_pathway	down_trans_pathway
COL22A1	*GNAI1*	0.45894	POS	down_trans_pathway	down_pathway
COL22A1	*ITGA10*	0.7114	POS	down_trans_pathway	down_pathway
COL22A1	*LEP*	0.39984	POS	down_trans_pathway	down_pathway
COL22A1	*MKX*	0.71844	POS	down_trans_pathway	down_TF
COL22A1	*NUCB2*	0.34655	POS	down_trans_pathway	corr_hub
COL22A1	*PCK2*	0.44028	POS	down_trans_pathway	down_pathway
COL22A1	*PLIN1*	0.45013	POS	down_trans_pathway	down_pathway
COL22A1	*PRRX2*	0.52144	POS	down_trans_pathway	down_TF
COL22A1	*PTGIR*	0.66055	POS	down_trans_pathway	down_trans_pathway
COL22A1	*SCD*	0.37272	POS	down_trans_pathway	down_pathway
COL22A1	*THBS1*	0.60916	POS	down_trans_pathway	down_pathway
COL22A1	*THBS4*	0.82451	POS	down_trans_pathway	down_trans_pathway

COL22A1	*TNC*	0.51025	POS	down_trans_pathway	down_trans_pathway
COL22A1	*TNFRSF11B*	0.50164	POS	down_trans_pathway	corr_trans_hub
COL5A2	*COMP*	0.47155	POS	down_pathway	down_trans_pathway
COL5A2	*DIAPH3*	0.51084	POS	down_pathway	corr_hub
COL5A2	*EBF1*	0.72974	POS	down_pathway	down_TF
COL5A2	*ELOVL5*	0.61556	POS	down_pathway	down_trans_pathway
COL5A2	*ELOVL6*	0.57332	POS	down_pathway	down_pathway
COL5A2	*FASN*	0.46793	POS	down_pathway	down_trans_pathway
COL5A2	*GNAI1*	0.5492	POS	down_pathway	down_pathway
COL5A2	*LEP*	0.46701	POS	down_pathway	down_pathway
COL5A2	*LOC784127*	0.17874	POS	down_pathway	corr_RIF
COL5A2	*LUM*	0.73873	POS	down_pathway	down_pathway
COL5A2	*MEST*	0.62102	POS	down_pathway	corr_down_hub
COL5A2	*MKX*	0.51319	POS	down_pathway	down_TF
COL5A2	*NUCB2*	0.32453	POS	down_pathway	corr_hub
COL5A2	*P4HA3*	0.33676	POS	down_pathway	down_pathway
COL5A2	*PCK2*	0.48111	POS	down_pathway	down_pathway
COL5A2	*PLIN1*	0.42188	POS	down_pathway	down_pathway
COL5A2	*PRRX2*	0.54712	POS	down_pathway	down_TF
COL5A2	*PTGIR*	0.5388	POS	down_pathway	down_trans_pathway
COL5A2	*SCD*	0.5047	POS	down_pathway	down_pathway
COL5A2	*SGCE*	0.55253	POS	down_pathway	corr_hub
COL5A2	*THBS1*	0.63497	POS	down_pathway	down_pathway
COL5A2	*THBS4*	0.5417	POS	down_pathway	down_trans_pathway
COL5A2	*TINF2*	-0.41668	NEG	down_pathway	Corr_hub
COL5A2	*TNC*	0.70207	POS	down_pathway	down_trans_pathway
COMP	*DIAPH3*	0.39992	POS	down_trans_pathway	corr_hub
COMP	*ELOVL5*	0.37065	POS	down_trans_pathway	down_trans_pathway
COMP	*ELOVL6*	0.36162	POS	down_trans_pathway	down_pathway
COMP	*FASN*	0.34654	POS	down_trans_pathway	down_trans_pathway
COMP	*GNAI1*	0.3677	POS	down_trans_pathway	down_pathway
COMP	*ITGA10*	0.62139	POS	down_trans_pathway	down_pathway

COMP	*LEP*	0.34059	POS	down_trans_pathway	down_pathway
COMP	*MEST*	0.50138	POS	down_trans_pathway	corr_down_hub
COMP	*MKX*	0.79315	POS	down_trans_pathway	down_TF
COMP	*NUCB2*	0.35389	POS	down_trans_pathway	corr_hub
COMP	*P4HA3*	0.38628	POS	down_trans_pathway	down_pathway
COMP	*PCK2*	0.39047	POS	down_trans_pathway	down_pathway
COMP	*PRRX2*	0.61435	POS	down_trans_pathway	down_TF
COMP	*PTGIR*	0.6862	POS	down_trans_pathway	down_trans_pathway
COMP	*SCD*	0.37468	POS	down_trans_pathway	down_pathway
COMP	*THBS1*	0.61137	POS	down_trans_pathway	down_pathway
COMP	*THBS4*	0.87442	POS	down_trans_pathway	down_trans_pathway
COMP	*TNC*	0.56269	POS	down_trans_pathway	down_trans_pathway
COMP	*TNFRSF11B*	0.56944	POS	down_trans_pathway	corr_trans_hub
DIAPH3	*LUM*	0.40369	POS	corr_hub	down_pathway
DIAPH3	*MEST*	0.36131	POS	corr_hub	corr_down_hub
DIAPH3	*PRRX2*	0.32041	POS	corr_hub	down_TF
DIAPH3	*PTGIR*	0.37192	POS	corr_hub	down_trans_pathway
DIAPH3	*THBS1*	0.3832	POS	corr_hub	down_pathway
DIAPH3	*THBS4*	0.42449	POS	corr_hub	down_trans_pathway
DIAPH3	*TINF2*	-0.32601	NEG	corr_hub	Corr_hub
DIAPH3	*TNC*	0.45343	POS	corr_hub	down_trans_pathway
EBF1	*ELOVL5*	0.58808	POS	down_TF	down_trans_pathway
EBF1	*ELOVL6*	0.55398	POS	down_TF	down_pathway
EBF1	*FASN*	0.481	POS	down_TF	down_trans_pathway
EBF1	*GNAI1*	0.60609	POS	down_TF	down_pathway
EBF1	*ITGA10*	0.38725	POS	down_TF	down_pathway
EBF1	*LEP*	0.5168	POS	down_TF	down_pathway
EBF1	*MEST*	0.42403	POS	down_TF	corr_down_hub
EBF1	*MKX*	0.49041	POS	down_TF	down_TF
EBF1	*P4HA3*	0.30251	POS	down_TF	down_pathway
EBF1	*PCK2*	0.43225	POS	down_TF	down_pathway
EBF1	*PLIN1*	0.52505	POS	down_TF	down_pathway

EBF1	*PRRX2*	0.42476	POS	down_TF	down_TF
EBF1	*PTGIR*	0.43319	POS	down_TF	down_trans_pathway
EBF1	*RGS7*	0.2795	POS	down_TF	corr_hub
EBF1	*SCD*	0.47747	POS	down_TF	down_pathway
EBF1	*SGCE*	0.36549	POS	down_TF	corr_hub
EBF1	*THBS1*	0.70549	POS	down_TF	down_pathway
EBF1	*THBS4*	0.49407	POS	down_TF	down_trans_pathway
EBF1	*TINF2*	-0.30445	NEG	down_TF	Corr_hub
EBF1	*TNC*	0.59461	POS	down_TF	down_trans_pathway
EBF1	*TNFRSF11B*	0.36604	POS	down_TF	corr_trans_hub
ELOVL5	*ELOVL6*	0.74965	POS	down_trans_pathway	down_pathway
ELOVL5	*FASN*	0.73275	POS	down_trans_pathway	down_trans_pathway
ELOVL5	*GNAI1*	0.72009	POS	down_trans_pathway	down_pathway
ELOVL5	*LEP*	0.69848	POS	down_trans_pathway	down_pathway
ELOVL5	*LOC784127*	0.20645	POS	down_trans_pathway	corr_RIF
ELOVL5	*MKX*	0.46791	POS	down_trans_pathway	down_TF
ELOVL5	*P4HA3*	0.44994	POS	down_trans_pathway	down_pathway
ELOVL5	*PCK2*	0.7209	POS	down_trans_pathway	down_pathway
ELOVL5	*PLIN1*	0.58964	POS	down_trans_pathway	down_pathway
ELOVL5	*PRRX2*	0.49108	POS	down_trans_pathway	down_TF
ELOVL5	*PTGIR*	0.41843	POS	down_trans_pathway	down_trans_pathway
ELOVL5	*RASL11A*	0.23619	POS	down_trans_pathway	corr_RIF
ELOVL5	*SCD*	0.61993	POS	down_trans_pathway	down_pathway
ELOVL5	*THBS1*	0.53538	POS	down_trans_pathway	down_pathway
ELOVL5	*THBS4*	0.34961	POS	down_trans_pathway	down_trans_pathway
ELOVL5	*TINF2*	-0.28308	NEG	down_trans_pathway	Corr_hub
ELOVL5	*TNC*	0.50932	POS	down_trans_pathway	down_trans_pathway
ELOVL5	*TNFRSF11B*	0.35418	POS	down_trans_pathway	corr_trans_hub
ELOVL6	*FASN*	0.8747	POS	down_pathway	down_trans_pathway
ELOVL6	*GNAI1*	0.80139	POS	down_pathway	down_pathway
ELOVL6	*LEP*	0.84565	POS	down_pathway	down_pathway
ELOVL6	*LUM*	0.40036	POS	down_pathway	down_pathway

ELOVL6	*MEST*	0.37539	POS	down_pathway	corr_down_hub
ELOVL6	*MKX*	0.45184	POS	down_pathway	down_TF
ELOVL6	*PCK2*	0.84471	POS	down_pathway	down_pathway
ELOVL6	*PLIN1*	0.7835	POS	down_pathway	down_pathway
ELOVL6	*PRRX2*	0.36095	POS	down_pathway	down_TF
ELOVL6	*RASL11A*	0.1612	POS	down_pathway	corr_RIF
ELOVL6	*RGS7*	0.38384	POS	down_pathway	corr_hub
ELOVL6	*SCD*	0.79431	POS	down_pathway	down_pathway
ELOVL6	*THBS1*	0.56052	POS	down_pathway	down_pathway
ELOVL6	*THBS4*	0.34027	POS	down_pathway	down_trans_pathway
ELOVL6	*TINF2*	-0.30795	NEG	down_pathway	Corr_hub
ELOVL6	*TNC*	0.42476	POS	down_pathway	down_trans_pathway
ELOVL6	*TNFRSF11B*	0.32699	POS	down_pathway	corr_trans_hub
FASN	*GNAI1*	0.71303	POS	down_trans_pathway	down_pathway
FASN	*LEP*	0.80212	POS	down_trans_pathway	down_pathway
FASN	*MKX*	0.40497	POS	down_trans_pathway	down_TF
FASN	*PCK2*	0.87646	POS	down_trans_pathway	down_pathway
FASN	*PLIN1*	0.71819	POS	down_trans_pathway	down_pathway
FASN	*PRRX2*	0.32308	POS	down_trans_pathway	down_TF
FASN	*RASL11A*	0.15733	POS	down_trans_pathway	corr_RIF
FASN	*RGS7*	0.29124	POS	down_trans_pathway	corr_hub
FASN	*SCD*	0.79362	POS	down_trans_pathway	down_pathway
FASN	*THBS1*	0.49089	POS	down_trans_pathway	down_pathway
FASN	*TNFRSF11B*	0.33495	POS	down_trans_pathway	corr_trans_hub
GNAI1	*ITGA10*	0.38036	POS	down_pathway	down_pathway
GNAI1	*LEP*	0.82826	POS	down_pathway	down_pathway
GNAI1	*MEST*	0.37177	POS	down_pathway	corr_down_hub
GNAI1	*MKX*	0.46115	POS	down_pathway	down_TF
GNAI1	*PCK2*	0.79951	POS	down_pathway	down_pathway
GNAI1	*PLIN1*	0.8572	POS	down_pathway	down_pathway
GNAI1	*PRRX2*	0.42283	POS	down_pathway	down_TF
GNAI1	*PTGIR*	0.34158	POS	down_pathway	down_trans_pathway

GNAI1	*RASL11A*	0.17705	POS	down_pathway	corr_RIF
GNAI1	*RGS7*	0.28679	POS	down_pathway	corr_hub
GNAI1	*SCD*	0.66526	POS	down_pathway	down_pathway
GNAI1	*THBS1*	0.60094	POS	down_pathway	down_pathway
GNAI1	*THBS4*	0.3995	POS	down_pathway	down_trans_pathway
GNAI1	*TINF2*	-0.35672	NEG	down_pathway	Corr_hub
GNAI1	*TNC*	0.52323	POS	down_pathway	down_trans_pathway
ITGA10	*LEP*	0.32149	POS	down_pathway	down_pathway
ITGA10	*MEST*	0.36994	POS	down_pathway	corr_down_hub
ITGA10	*MKX*	0.54173	POS	down_pathway	down_TF
ITGA10	*P4HA3*	0.28567	POS	down_pathway	down_pathway
ITGA10	*PRRX2*	0.45121	POS	down_pathway	down_TF
ITGA10	*PTGIR*	0.65128	POS	down_pathway	down_trans_pathway
ITGA10	*THBS1*	0.48917	POS	down_pathway	down_pathway
ITGA10	*THBS4*	0.61115	POS	down_pathway	down_trans_pathway
ITGA10	*TNC*	0.44769	POS	down_pathway	down_trans_pathway
ITGA10	*TNFRSF11B*	0.45768	POS	down_pathway	corr_trans_hub
LEP	*MKX*	0.36353	POS	down_pathway	down_TF
LEP	*PCK2*	0.83492	POS	down_pathway	down_pathway
LEP	*PLIN1*	0.84377	POS	down_pathway	down_pathway
LEP	*PRRX2*	0.38745	POS	down_pathway	down_TF
LEP	*RASL11A*	0.18722	POS	down_pathway	corr_RIF
LEP	*RGS7*	0.37693	POS	down_pathway	corr_hub
LEP	*SCD*	0.71141	POS	down_pathway	down_pathway
LEP	*THBS1*	0.52939	POS	down_pathway	down_pathway
LEP	*TNC*	0.44719	POS	down_pathway	down_trans_pathway
LOC518768	*NUCB2*	-0.29244	NEG	corr_RIF	corr_hub
LOC518768	*P4HA3*	0.18412	POS	corr_RIF	down_pathway
LOC518768	*SCD*	-0.2094	NEG	corr_RIF	down_pathway
LOC530929	*LOC784127*	0.28852	POS	corr_RIF	corr_RIF
LOC530929	*RASL11A*	-0.16597	NEG	corr_RIF	corr_RIF
LOC784127	*MEST*	0.21988	POS	corr_RIF	corr_down_hub

LOC784127	*TNC*	0.21279	POS	corr_RIF	down_trans_pathway
LOC784127	*TNFRSF11B*	0.22071	POS	corr_RIF	corr_trans_hub
LUM	*MEST*	0.61622	POS	down_pathway	corr_down_hub
LUM	*NUCB2*	0.47398	POS	down_pathway	corr_hub
LUM	*SCD*	0.36947	POS	down_pathway	down_pathway
LUM	*SGCE*	0.61025	POS	down_pathway	corr_hub
LUM	*THBS1*	0.42562	POS	down_pathway	down_pathway
LUM	*THBS4*	0.36164	POS	down_pathway	down_trans_pathway
LUM	*TINF2*	-0.50946	NEG	down_pathway	Corr_hub
LUM	*TNC*	0.52155	POS	down_pathway	down_trans_pathway
MEST	*MKX*	0.55959	POS	corr_down_hub	down_TF
MEST	*NUCB2*	0.46304	POS	corr_down_hub	corr_hub
MEST	*PRRX2*	0.41351	POS	corr_down_hub	down_TF
MEST	*PTGIR*	0.53752	POS	corr_down_hub	down_trans_pathway
MEST	*SCD*	0.37172	POS	corr_down_hub	down_pathway
MEST	*SGCE*	0.5298	POS	corr_down_hub	corr_hub
MEST	*THBS1*	0.48128	POS	corr_down_hub	down_pathway
MEST	*THBS4*	0.53978	POS	corr_down_hub	down_trans_pathway
MEST	*TINF2*	-0.48964	NEG	corr_down_hub	Corr_hub
MEST	*TNC*	0.51829	POS	corr_down_hub	down_trans_pathway
MEST	*TNFRSF11B*	0.37144	POS	corr_down_hub	corr_trans_hub
MKX	*NUCB2*	0.46061	POS	down_TF	corr_hub
MKX	*P4HA3*	0.36715	POS	down_TF	down_pathway
MKX	*PCK2*	0.41794	POS	down_TF	down_pathway
MKX	*PLIN1*	0.35278	POS	down_TF	down_pathway
MKX	*PRRX2*	0.62171	POS	down_TF	down_TF
MKX	*PTGIR*	0.6533	POS	down_TF	down_trans_pathway
MKX	*RGS7*	0.32043	POS	down_TF	corr_hub
MKX	*SCD*	0.43326	POS	down_TF	down_pathway
MKX	*SGCE*	0.39757	POS	down_TF	corr_hub
MKX	*THBS1*	0.65482	POS	down_TF	down_pathway
MKX	*THBS4*	0.79032	POS	down_TF	down_trans_pathway

MKX	*TNC*	0.60945	POS	down_TF	down_trans_pathway
MKX	*TNFRSF11B*	0.64234	POS	down_TF	corr_trans_hub
NUCB2	*PRRX2*	0.36496	POS	corr_hub	down_TF
NUCB2	*RGS7*	0.3105	POS	corr_hub	corr_hub
NUCB2	*SGCE*	0.51704	POS	corr_hub	corr_hub
NUCB2	*THBS4*	0.39092	POS	corr_hub	down_trans_pathway
P4HA3	*PRRX2*	0.34638	POS	down_pathway	down_TF
P4HA3	*PTGIR*	0.4154	POS	down_pathway	down_trans_pathway
P4HA3	*THBS1*	0.33243	POS	down_pathway	down_pathway
P4HA3	*THBS4*	0.32541	POS	down_pathway	down_trans_pathway
P4HA3	*TNC*	0.31712	POS	down_pathway	down_trans_pathway
PCK2	*PLIN1*	0.79985	POS	down_pathway	down_pathway
PCK2	*PRRX2*	0.40642	POS	down_pathway	down_TF
PCK2	*RASL11A*	0.18442	POS	down_pathway	corr_RIF
PCK2	*RGS7*	0.28428	POS	down_pathway	corr_hub
PCK2	*SCD*	0.77978	POS	down_pathway	down_pathway
PCK2	*THBS1*	0.5063	POS	down_pathway	down_pathway
PCK2	*THBS4*	0.32985	POS	down_pathway	down_trans_pathway
PCK2	*TNC*	0.40175	POS	down_pathway	down_trans_pathway
PCK2	*TNFRSF11B*	0.30237	POS	down_pathway	corr_trans_hub
PLIN1	*RGS7*	0.27372	POS	down_pathway	corr_hub
PLIN1	*SCD*	0.63613	POS	down_pathway	down_pathway
PLIN1	*THBS1*	0.52817	POS	down_pathway	down_pathway
PLIN1	*TINF2*	-0.30148	NEG	down_pathway	Corr_hub
PLIN1	*TNC*	0.42398	POS	down_pathway	down_trans_pathway
PRRX2	*PTGIR*	0.60269	POS	down_TF	down_trans_pathway
PRRX2	*SGCE*	0.39773	POS	down_TF	corr_hub
PRRX2	*THBS1*	0.46671	POS	down_TF	down_pathway
PRRX2	*THBS4*	0.63399	POS	down_TF	down_trans_pathway
PRRX2	*TNC*	0.64906	POS	down_TF	down_trans_pathway
PRRX2	*TNFRSF11B*	0.43965	POS	down_TF	corr_trans_hub
PTGIR	*THBS1*	0.56709	POS	down_trans_pathway	down_pathway

PTGIR	*THBS4*	0.7446	POS	down_trans_pathway	down_trans_pathway
PTGIR	*TNC*	0.61874	POS	down_trans_pathway	down_trans_pathway
PTGIR	*TNFRSF11B*	0.51947	POS	down_trans_pathway	corr_trans_hub
RASL11A	*THBS1*	0.1995	POS	corr_RIF	down_pathway
RGS7	*SCD*	0.38102	POS	corr_hub	down_pathway
RGS7	*SGCE*	0.24309	POS	corr_hub	corr_hub
RGS7	*THBS1*	0.31645	POS	corr_hub	down_pathway
RGS7	*TNFRSF11B*	0.27191	POS	corr_hub	corr_trans_hub
SCD	*THBS1*	0.44487	POS	down_pathway	down_pathway
SCD	*THBS4*	0.37004	POS	down_pathway	down_trans_pathway
SCD	*TINF2*	-0.28353	NEG	down_pathway	Corr_hub
SGCE	*THBS4*	0.38905	POS	corr_hub	down_trans_pathway
SGCE	*TNC*	0.38196	POS	corr_hub	down_trans_pathway
THBS1	*THBS4*	0.61881	POS	down_pathway	down_trans_pathway
THBS1	*TNC*	0.74819	POS	down_pathway	down_trans_pathway
THBS1	*TNFRSF11B*	0.42755	POS	down_pathway	corr_trans_hub
THBS4	*TNC*	0.61094	POS	down_trans_pathway	down_trans_pathway
THBS4	*TNFRSF11B*	0.53783	POS	down_trans_pathway	corr_trans_hub
TNC	*TNFRSF11B*	0.43997	POS	down_trans_pathway	corr_trans_hub

P

Origin	**Target**	**Correlation value**	**Correlation type**	**Origin attributes**	**Target attributes**
ADAM12	bta-miR-130b	0.13915	POS	down_pathways	Corr_miRNA
ADAM12	*CD44*	0.40463	POS	down_pathways	down_pathways
ADAM12	*COL11A1*	0.65195	POS	down_pathways	down_pathways
ADAM12	*COL18A1*	0.39984	POS	down_pathways	down_pathways
ADAM12	*COL21A1*	0.31051	POS	down_pathways	Corr_hub_pathways
ADAM12	*MMP16*	0.48484	POS	down_pathways	Corr_hub_pathways
ADAM12	*THBS4*	0.62637	POS	down_pathways	down_trans_pathways
ADAM12	*TNC*	0.48486	POS	down_pathways	down_trans_pathways
BOLA.DOA	bta-miR-130b	0.16296	POS	Corr_hub	Corr_miRNA

BOLA.DOA	bta-miR-142-5p	0.15143	POS	Corr_hub	Corr_miRNA
BOLA.DOA	bta-miR-92b	0.23373	POS	Corr_hub	Corr_miRNA
BOLA.DOA	*CD44*	0.40579	POS	Corr_hub	down_pathways
BOLA.DOA	*COL21A1*	0.41144	POS	Corr_hub	Corr_hub_pathways
BOLA.DOA	*MMP16*	0.37342	POS	Corr_hub	Corr_hub_pathways
BOLA.DOA	*VDR*	0.30533	POS	Corr_hub	Corr_TF
bta-miR-130b	bta-miR-92b	0.18846	POS	Corr_miRNA	Corr_miRNA
bta-miR-130b	*COL18A1*	0.17597	POS	Corr_miRNA	down_pathways
bta-miR-142-5p	*MMP16*	0.1673	POS	Corr_miRNA	Corr_hub_pathways
bta-miR-142-5p	*PRRX2*	0.22458	POS	Corr_miRNA	down_TF
bta-miR-92b	*CD44*	0.18979	POS	Corr_miRNA	down_pathways
bta-miR-92b	*COL18A1*	0.2622	POS	Corr_miRNA	down_pathways
bta-miR-92b	*MMP16*	0.18661	POS	Corr_miRNA	Corr_hub_pathways
bta-miR-92b	*PRRX2*	0.21628	POS	Corr_miRNA	down_TF
bta-miR-92b	*TNC*	0.21131	POS	Corr_miRNA	down_trans_pathways
CD44	*COL11A1*	0.39695	POS	down_pathways	down_pathways
CD44	*COL18A1*	0.55564	POS	down_pathways	down_pathways
CD44	*COL21A1*	0.40465	POS	down_pathways	Corr_hub_pathways
CD44	*MMP16*	0.54236	POS	down_pathways	Corr_hub_pathways
CD44	*PRRX2*	0.53604	POS	down_pathways	down_TF
CD44	*THBS4*	0.47498	POS	down_pathways	down_trans_pathways
CD44	*TNC*	0.62128	POS	down_pathways	down_trans_pathways
CD44	*VDR*	0.26342	POS	down_pathways	Corr_TF
COL11A1	*MMP16*	0.46702	POS	down_pathways	Corr_hub_pathways
COL11A1	*PRRX2*	0.57971	POS	down_pathways	down_TF
COL11A1	*THBS4*	0.86932	POS	down_pathways	down_trans_pathways
COL11A1	*TNC*	0.5626	POS	down_pathways	down_trans_pathways
COL18A1	*COL21A1*	0.43911	POS	down_pathways	Corr_hub_pathways
COL18A1	*MMP16*	0.49981	POS	down_pathways	Corr_hub_pathways
COL18A1	*PRRX2*	0.59877	POS	down_pathways	down_TF
COL18A1	*THBS4*	0.49388	POS	down_pathways	down_trans_pathways
COL18A1	*TNC*	0.67805	POS	down_pathways	down_trans_pathways

COL18A1	*VDR*	0.28961	POS	down_pathways	Corr_TF
COL21A1	*MMP16*	0.57002	POS	Corr_hub_pathways	Corr_hub_pathways
COL21A1	*VDR*	0.36053	POS	Corr_hub_pathways	Corr_TF
MMP16	*PRRX2*	0.44498	POS	Corr_hub_pathways	down_TF
MMP16	*THBS4*	0.49322	POS	Corr_hub_pathways	down_trans_pathways
MMP16	*TNC*	0.55163	POS	Corr_hub_pathways	down_trans_pathways
MMP16	*VDR*	0.35183	POS	Corr_hub_pathways	Corr_TF
PRRX2	*THBS4*	0.63399	POS	down_TF	down_trans_pathways
PRRX2	*TNC*	0.64906	POS	down_TF	down_trans_pathways
THBS4	*TNC*	0.61094	POS	down_trans_pathways	down_trans_pathways
TNC	*VDR*	0.22886	POS	down_trans_pathways	Corr_TF
VDR	*WDPCP*	0.19512	POS	Corr_TF	Corr_RIF_trans

S

Origin	**Target**	**Correlation value**	**Correlation type**	**Origin attributes**	**Target attributes**
ARAP1	*ARHGAP30*	0-51489	POS	Corr_pathways	Corr_pathways
ARAP1	*BTK*	0-38198	POS	Corr_pathways	Corr_pathways
ARAP1	*CCR2*	0-36261	POS	Corr_pathways	Corr_trans_pathways
ARAP1	*CD53*	0-36119	POS	Corr_pathways	Corr_pathways
ARAP1	*CD86*	0-4028	POS	Corr_pathways	Corr_pathways
ARAP1	*FLT3*	0-34789	POS	Corr_pathways	Corr_pathways
ARAP1	*FUT8*	0-33296	POS	Corr_pathways	Corr_RIF_trans
ARAP1	*FYN*	0-38458	POS	Corr_pathways	Corr_pathways
ARAP1	*HIST1H2AC*	-0-28572	NEG	Corr_pathways	up_pathways
ARAP1	*LOC510860*	0-42819	POS	Corr_pathways	Corr_hub
ARAP1	*LOC534578*	0-32918	POS	Corr_pathways	Corr_pathways
ARAP1	*LPAR4*	0-36227	POS	Corr_pathways	Corr_pathways
ARAP1	*METTL21E*	-0-30729	NEG	Corr_pathways	Corr_RIF
ARAP1	*PLPPR5*	0-39405	POS	Corr_pathways	Corr_RIF_pathways
ARAP1	*PPT1*	0-42085	POS	Corr_pathways	Corr_hub
ARAP1	*PRRG3*	0-27633	POS	Corr_pathways	Corr_RIF

ARAP1	*TIAM1*	0-36803	POS	Corr_pathways	Corr_trans_pathways
ARAP1	*TNFAIP3*	0-31403	POS	Corr_pathways	Corr_pathways
ARAP1	*VDR*	0-37873	POS	Corr_pathways	Corr_TF
ARAP1	*XCR1*	0-3264	POS	Corr_pathways	Corr_pathways
ARAP1	*XRCC6*	0-27301	POS	Corr_pathways	Corr_pathways
ARHGAP30	*BTK*	0-65664	POS	Corr_pathways	Corr_pathways
ARHGAP30	*CCR2*	0-58851	POS	Corr_pathways	Corr_trans_pathways
ARHGAP30	*CD53*	0-74812	POS	Corr_pathways	Corr_pathways
ARHGAP30	*CD86*	0-66218	POS	Corr_pathways	Corr_pathways
ARHGAP30	*FCGR2A*	0-5613	POS	Corr_pathways	Corr_pathways
ARHGAP30	*FLT3*	0-63256	POS	Corr_pathways	Corr_pathways
ARHGAP30	*FUT8*	0-44991	POS	Corr_pathways	Corr_RIF_trans
ARHGAP30	*FYN*	0-43832	POS	Corr_pathways	Corr_pathways
ARHGAP30	*IKZF3*	0-57856	POS	Corr_pathways	Corr_TF
ARHGAP30	*LOC510860*	0-6192	POS	Corr_pathways	Corr_hub
ARHGAP30	*LOC534578*	0-53657	POS	Corr_pathways	Corr_pathways
ARHGAP30	*PLCB2*	0-53983	POS	Corr_pathways	Corr_trans_pathways
ARHGAP30	*PLPPR5*	0-30923	POS	Corr_pathways	Corr_RIF_pathways
ARHGAP30	*PPT1*	0-62953	POS	Corr_pathways	Corr_hub
ARHGAP30	*SIGLEC5*	0-40913	POS	Corr_pathways	Corr_pathways
ARHGAP30	*TIAM1*	0-50219	POS	Corr_pathways	Corr_trans_pathways
ARHGAP30	*TNFAIP3*	0-45837	POS	Corr_pathways	Corr_pathways
ARHGAP30	*VDR*	0-37471	POS	Corr_pathways	Corr_TF
ARHGAP30	*XCR1*	0-68928	POS	Corr_pathways	Corr_pathways
bta-miR-369-3p	bta-miR-500	0-18148	POS	Corr_RIF_miRNA	Corr_RIF_miRNA
bta-miR-369-3p	*SIGLEC5*	0-26134	POS	Corr_RIF_miRNA	Corr_pathways
bta-miR-500	*FCGR2A*	0-20032	POS	Corr_RIF_miRNA	Corr_pathways
bta-miR-500	*XRCC6*	0-28559	POS	Corr_RIF_miRNA	Corr_pathways
BTK	*CCR2*	0-44616	POS	Corr_pathways	Corr_trans_pathways
BTK	*CD53*	0-62419	POS	Corr_pathways	Corr_pathways
BTK	*CD86*	0-60907	POS	Corr_pathways	Corr_pathways
BTK	*FCGR2A*	0-50601	POS	Corr_pathways	Corr_pathways

BTK	*FLT3*	0-42047	POS	Corr_pathways	Corr_pathways
BTK	*FUT8*	0-43732	POS	Corr_pathways	Corr_RIF_trans
BTK	*FYN*	0-4107	POS	Corr_pathways	Corr_pathways
BTK	*IKZF3*	0-42846	POS	Corr_pathways	Corr_TF
BTK	*LOC510860*	0-57283	POS	Corr_pathways	Corr_hub
BTK	*LOC534578*	0-3371	POS	Corr_pathways	Corr_pathways
BTK	*PLCB2*	0-36076	POS	Corr_pathways	Corr_trans_pathways
BTK	*PPT1*	0-58	POS	Corr_pathways	Corr_hub
BTK	*RAB44*	0-35512	POS	Corr_pathways	Corr_RIF
BTK	*SIGLEC5*	0-35003	POS	Corr_pathways	Corr_pathways
BTK	*TIAM1*	0-54546	POS	Corr_pathways	Corr_trans_pathways
BTK	*TNFAIP3*	0-36622	POS	Corr_pathways	Corr_pathways
BTK	*VDR*	0-35851	POS	Corr_pathways	Corr_TF
BTK	*XCR1*	0-52325	POS	Corr_pathways	Corr_pathways
CCR2	*CD53*	0-55447	POS	Corr_trans_pathways	Corr_pathways
CCR2	*CD86*	0-45495	POS	Corr_trans_pathways	Corr_pathways
CCR2	*FLT3*	0-42323	POS	Corr_trans_pathways	Corr_pathways
CCR2	*FYN*	0-44734	POS	Corr_trans_pathways	Corr_pathways
CCR2	*IKZF3*	0-37517	POS	Corr_trans_pathways	Corr_TF
CCR2	*LOC510860*	0-37379	POS	Corr_trans_pathways	Corr_hub
CCR2	*LOC534578*	0-35087	POS	Corr_trans_pathways	Corr_pathways
CCR2	*PLCB2*	0-42558	POS	Corr_trans_pathways	Corr_trans_pathways
CCR2	*PPT1*	0-55868	POS	Corr_trans_pathways	Corr_hub
CCR2	*SIGLEC5*	0-2855	POS	Corr_trans_pathways	Corr_pathways
CCR2	*TIAM1*	0-332	POS	Corr_trans_pathways	Corr_trans_pathways
CCR2	*TNFAIP3*	0-42224	POS	Corr_trans_pathways	Corr_pathways
CCR2	*XCR1*	0-44147	POS	Corr_trans_pathways	Corr_pathways
CD53	*CD86*	0-75362	POS	Corr_pathways	Corr_pathways
CD53	*FCGR2A*	0-45011	POS	Corr_pathways	Corr_pathways
CD53	*FLT3*	0-61262	POS	Corr_pathways	Corr_pathways
CD53	*FUT8*	0-33628	POS	Corr_pathways	Corr_RIF_trans
CD53	*FYN*	0-46607	POS	Corr_pathways	Corr_pathways

CD53	*HEBP2*	0-32212	POS	Corr_pathways	Corr_pathways
CD53	*IKZF3*	0-61153	POS	Corr_pathways	Corr_TF
CD53	*LOC510860*	0-61968	POS	Corr_pathways	Corr_hub
CD53	*LOC534578*	0-46938	POS	Corr_pathways	Corr_pathways
CD53	*PLCB2*	0-42669	POS	Corr_pathways	Corr_trans_pathways
CD53	*PLPPR5*	0-34334	POS	Corr_pathways	Corr_RIF_pathways
CD53	*PPT1*	0-64597	POS	Corr_pathways	Corr_hub
CD53	*TIAM1*	0-58519	POS	Corr_pathways	Corr_trans_pathways
CD53	*TNFAIP3*	0-45376	POS	Corr_pathways	Corr_pathways
CD53	*VDR*	0-34829	POS	Corr_pathways	Corr_TF
CD53	*XCR1*	0-59794	POS	Corr_pathways	Corr_pathways
CD86	*FCGR2A*	0-40726	POS	Corr_pathways	Corr_pathways
CD86	*FLT3*	0-48374	POS	Corr_pathways	Corr_pathways
CD86	*FUT8*	0-30409	POS	Corr_pathways	Corr_RIF_trans
CD86	*FYN*	0-47325	POS	Corr_pathways	Corr_pathways
CD86	*IKZF3*	0-55656	POS	Corr_pathways	Corr_TF
CD86	*LOC510860*	0-68092	POS	Corr_pathways	Corr_hub
CD86	*LOC534578*	0-49734	POS	Corr_pathways	Corr_pathways
CD86	*PLPPR5*	0-30245	POS	Corr_pathways	Corr_RIF_pathways
CD86	*PPT1*	0-6067	POS	Corr_pathways	Corr_hub
CD86	*RAB44*	0-25889	POS	Corr_pathways	Corr_RIF
CD86	*TIAM1*	0-67847	POS	Corr_pathways	Corr_trans_pathways
CD86	*TNFAIP3*	0-4122	POS	Corr_pathways	Corr_pathways
CD86	*VDR*	0-47296	POS	Corr_pathways	Corr_TF
DAGLB	*LOC510860*	-0-27898	NEG	Corr_pathways	Corr_hub
DAGLB	*LOC534578*	-0-32906	NEG	Corr_pathways	Corr_pathways
DAGLB	*PPT1*	-0-33036	NEG	Corr_pathways	Corr_hub
DAGLB	*XRCC6*	-0-26885	NEG	Corr_pathways	Corr_pathways
FCGR2A	*FLT3*	0-34253	POS	Corr_pathways	Corr_pathways
FCGR2A	*FUT8*	0-42817	POS	Corr_pathways	Corr_RIF_trans
FCGR2A	*FYN*	0-30979	POS	Corr_pathways	Corr_pathways
FCGR2A	*IKZF3*	0-37653	POS	Corr_pathways	Corr_TF

FCGR2A	*LOC510860*	0-38297	POS	Corr_pathways	Corr_hub
FCGR2A	*LOC534578*	0-37777	POS	Corr_pathways	Corr_pathways
FCGR2A	*METTL21E*	-0-26636	NEG	Corr_pathways	Corr_RIF
FCGR2A	*PLCB2*	0-37498	POS	Corr_pathways	Corr_trans_pathways
FCGR2A	*PLPPR5*	0-30134	POS	Corr_pathways	Corr_RIF_pathways
FCGR2A	*PPT1*	0-34129	POS	Corr_pathways	Corr_hub
FCGR2A	*RAB44*	0-28343	POS	Corr_pathways	Corr_RIF
FCGR2A	*SIGLEC5*	0-27062	POS	Corr_pathways	Corr_pathways
FCGR2A	*TIAM1*	0-37957	POS	Corr_pathways	Corr_trans_pathways
FCGR2A	*TNFAIP3*	0-31864	POS	Corr_pathways	Corr_pathways
FCGR2A	*XCR1*	0-44347	POS	Corr_pathways	Corr_pathways
FLT3	*IKZF3*	0-54027	POS	Corr_pathways	Corr_TF
FLT3	*LOC510860*	0-51333	POS	Corr_pathways	Corr_hub
FLT3	*PLCB2*	0-42583	POS	Corr_pathways	Corr_trans_pathways
FLT3	*PPT1*	0-44979	POS	Corr_pathways	Corr_hub
FLT3	*PRRG3*	0-2318	POS	Corr_pathways	Corr_RIF
FLT3	*TIAM1*	0-41807	POS	Corr_pathways	Corr_trans_pathways
FLT3	*TNFAIP3*	0-37213	POS	Corr_pathways	Corr_pathways
FLT3	*VDR*	0-34536	POS	Corr_pathways	Corr_TF
FLT3	*XCR1*	0-62696	POS	Corr_pathways	Corr_pathways
FUT8	*HIST1H2AC*	-0-22617	NEG	Corr_RIF_trans	up_pathways
FUT8	*LOC534578*	0-30702	POS	Corr_RIF_trans	Corr_pathways
FUT8	*PPT1*	0-37802	POS	Corr_RIF_trans	Corr_hub
FUT8	*SIGLEC5*	0-33395	POS	Corr_RIF_trans	Corr_pathways
FUT8	*XCR1*	0-39418	POS	Corr_RIF_trans	Corr_pathways
FYN	*HEBP2*	0-228	POS	Corr_pathways	Corr_pathways
FYN	*IKZF3*	0-29856	POS	Corr_pathways	Corr_TF
FYN	*LOC510860*	0-3443	POS	Corr_pathways	Corr_hub
FYN	*LOC534578*	0-43808	POS	Corr_pathways	Corr_pathways
FYN	*PLPPR5*	0-36632	POS	Corr_pathways	Corr_RIF_pathways
FYN	*PPT1*	0-5906	POS	Corr_pathways	Corr_hub
FYN	*PRRG3*	0-35164	POS	Corr_pathways	Corr_RIF

FYN	*TIAM1*	0-31961	POS	Corr_pathways	Corr_trans_pathways
FYN	*TNFAIP3*	0-31063	POS	Corr_pathways	Corr_pathways
HEBP2	*PLPPR5*	0-26179	POS	Corr_pathways	Corr_RIF_pathways
HEBP2	*PPT1*	0-33621	POS	Corr_pathways	Corr_hub
HIST1H2AC	*TNFAIP3*	-0-22809	NEG	up_pathways	Corr_pathways
HIST1H2AC	*XRCC6*	-0-34757	NEG	up_pathways	Corr_pathways
IKZF3	*LOC510860*	0-43366	POS	Corr_TF	Corr_hub
IKZF3	*LOC534578*	0-31628	POS	Corr_TF	Corr_pathways
IKZF3	*PLCB2*	0-37276	POS	Corr_TF	Corr_trans_pathways
IKZF3	*PPT1*	0-42029	POS	Corr_TF	Corr_hub
IKZF3	*TIAM1*	0-50903	POS	Corr_TF	Corr_trans_pathways
IKZF3	*VDR*	0-30084	POS	Corr_TF	Corr_TF
IKZF3	*XCR1*	0-50368	POS	Corr_TF	Corr_pathways
LOC510860	*LOC534578*	0-44349	POS	Corr_hub	Corr_pathways
LOC510860	*LPAR4*	0-28254	POS	Corr_hub	Corr_pathways
LOC510860	*PLPPR5*	0-38647	POS	Corr_hub	Corr_RIF_pathways
LOC510860	*PPT1*	0-57315	POS	Corr_hub	Corr_hub
LOC510860	*RAB44*	0-35388	POS	Corr_hub	Corr_RIF
LOC510860	*SIGLEC5*	0-29684	POS	Corr_hub	Corr_pathways
LOC510860	*TIAM1*	0-50839	POS	Corr_hub	Corr_trans_pathways
LOC510860	*TNFAIP3*	0-34064	POS	Corr_hub	Corr_pathways
LOC510860	*VDR*	0-34286	POS	Corr_hub	Corr_TF
LOC510860	*XRCC6*	0-25681	POS	Corr_hub	Corr_pathways
LOC534578	*METTL21E*	-0-2926	NEG	Corr_pathways	Corr_RIF
LOC534578	*PPT1*	0-50389	POS	Corr_pathways	Corr_hub
LOC534578	*PRRG3*	0-28013	POS	Corr_pathways	Corr_RIF
LOC534578	*VDR*	0-38362	POS	Corr_pathways	Corr_TF
LOC534578	*XCR1*	0-34365	POS	Corr_pathways	Corr_pathways
LPAR4	*PLPPR5*	0-30937	POS	Corr_pathways	Corr_RIF_pathways
LPAR4	*RAB44*	0-31385	POS	Corr_pathways	Corr_RIF
METTL21E	*PRRG3*	-0-26111	NEG	Corr_RIF	Corr_RIF
METTL21E	*VDR*	-0-2346	NEG	Corr_RIF	Corr_TF

PLCB2	*PPT1*	0-43394	POS	Corr_trans_pathways	Corr_hub
PLCB2	*TNFAIP3*	0-35565	POS	Corr_trans_pathways	Corr_pathways
PLCB2	*XCR1*	0-54544	POS	Corr_trans_pathways	Corr_pathways
PLPPR5	*PPT1*	0-3894	POS	Corr_RIF_pathways	Corr_hub
PLPPR5	*PRRG3*	0-27899	POS	Corr_RIF_pathways	Corr_RIF
PLPPR5	*RAB44*	0-3015	POS	Corr_RIF_pathways	Corr_RIF
PLPPR5	*XRCC6*	0-24823	POS	Corr_RIF_pathways	Corr_pathways
PPT1	*PRRG3*	0-29195	POS	Corr_hub	Corr_RIF
PPT1	*SIGLEC5*	0-31909	POS	Corr_hub	Corr_pathways
PPT1	*TNFAIP3*	0-37246	POS	Corr_hub	Corr_pathways
PPT1	*VDR*	0-34204	POS	Corr_hub	Corr_TF
PPT1	*XCR1*	0-58532	POS	Corr_hub	Corr_pathways
PPT1	*XRCC6*	0-27682	POS	Corr_hub	Corr_pathways
PRRG3	*XCR1*	0-26394	POS	Corr_RIF	Corr_pathways
RAB44	*TIAM1*	0-35877	POS	Corr_RIF	Corr_trans_pathways
SIGLEC5	*XCR1*	0-30233	POS	Corr_pathways	Corr_pathways
TIAM1	*TNFAIP3*	0-374	POS	Corr_trans_pathways	Corr_pathways
TIAM1	*VDR*	0-3994	POS	Corr_trans_pathways	Corr_TF
TIAM1	*XCR1*	0-35556	POS	Corr_trans_pathways	Corr_pathways
TNFAIP3	*VDR*	0-29242	POS	Corr_pathways	Corr_TF
TNFAIP3	*XCR1*	0-39622	POS	Corr_pathways	Corr_pathways

Supplementary Table S3.3. Correlations and attributes of each significant correlation constituting Figure 4.

Zn

Origin	Target	Correlation value	Correlation type	Origin attributes	Target attributes
AAR2	*CTSD*	0.28108	POS	Corr	Corr
AAR2	*MBTPS2*	-0.24427	NEG	Corr	Corr_RIF
AAR2	*NUDT18*	0.34448	POS	Corr	Corr_RIF_trans
AKAP9	*CTSD*	-0.43766	NEG	up	Corr
AKAP9	*MBTPS2*	0.50854	POS	up	Corr_RIF
AKAP9	*NUDT18*	-0.31265	NEG	up	Corr_RIF_trans
ANGPTL2	*LTV1*	-0.42055	NEG	Corr	Corr
ANGPTL2	*TNR*	0.33011	POS	Corr	Corr_RIF
ANGPTL2	*ZNF770*	-0.3445	NEG	Corr	Corr
ANGPTL4	*CTSD*	0.29498	POS	down	Corr
ASF1B	*CTSD*	0.24898	POS	Corr	Corr
ASF1B	*GABPB1*	-0.28056	NEG	Corr	Corr
ASF1B	*LTV1*	-0.33302	NEG	Corr	Corr
ASF1B	*MBTPS2*	-0.25637	NEG	Corr	Corr_RIF
ASF1B	*TNR*	0.26734	POS	Corr	Corr_RIF
BANK1	bta-miR-199b	-0.20456	NEG	up	Corr_RIF_miRNA
bta-miR-142-5p	*NOX1*	-0.16718	NEG	Corr_miRNA	Corr_RIF
bta-miR-142-5p	*TNR*	0.18856	POS	Corr_miRNA	Corr_RIF
bta-miR-199b	bta-miR-2285bl	0.48295	POS	Corr_RIF_miRNA	Corr_miRNA
bta-miR-199b	bta-miR-2285co	0.48295	POS	Corr_RIF_miRNA	Corr_miRNA
bta-miR-199b	bta-miR-411c-5p	0.33691	POS	Corr_RIF_miRNA	Corr_RIF_miRNA
bta-miR-199b	*CLDN5*	0.20895	POS	Corr_RIF_miRNA	down
bta-miR-199b	*CYGB*	0.22007	POS	Corr_RIF_miRNA	down
bta-miR-199b	*GABPB1*	-0.20605	NEG	Corr_RIF_miRNA	Corr
bta-miR-199b	*GABPB1*	-0.20605	NEG	Corr_RIF_miRNA	Corr
bta-miR-199b	*HIST1H2AC*	-0.1978	NEG	Corr_RIF_miRNA	up
bta-miR-199b	*LTV1*	-0.23378	NEG	Corr_RIF_miRNA	Corr
bta-miR-199b	*LTV1*	-0.23378	NEG	Corr_RIF_miRNA	Corr
bta-miR-199b	*MBTPS2*	-0.22852	NEG	Corr_RIF_miRNA	Corr_RIF
bta-miR-199b	*MBTPS2*	-0.22852	NEG	Corr_RIF_miRNA	Corr_RIF
bta-miR-199b	*MIR29E*	-0.21675	NEG	Corr_RIF_miRNA	Corr_miRNA
bta-miR-199b	*ZCCHC10*	-0.2059	NEG	Corr_RIF_miRNA	Corr
bta-miR-199b	*ZNF770*	-0.26387	NEG	Corr_RIF_miRNA	Corr
bta-miR-199b	*ZNF770*	-0.26387	NEG	Corr_RIF_miRNA	Corr
bta-miR-2285bl	bta-miR-411c-5p	0.32726	POS	Corr_miRNA	Corr_RIF_miRNA
bta-miR-2285bl	*NOX1*	-0.21825	NEG	Corr_miRNA	Corr_RIF
bta-miR-2285bl	*ZNF770*	-0.22403	NEG	Corr_miRNA	Corr
bta-miR-2285co	bta-miR-411c-5p	0.32726	POS	Corr_miRNA	Corr_RIF_miRNA
bta-miR-2285co	*NOX1*	-0.21825	NEG	Corr_miRNA	Corr_RIF
bta-miR-2285co	*ZNF770*	-0.22403	NEG	Corr_miRNA	Corr
bta-miR-411c-5p	bta-miR-425-3p	-0.15359	NEG	Corr_RIF_miRNA	Corr_miRNA
bta-miR-411c-5p	*C1QTNF1*	0.24445	POS	Corr_RIF_miRNA	down

bta-miR-411c-5p	*HIST1H2AC*	-0.22101	NEG	Corr_RIF_miRNA	up
bta-miR-411c-5p	*IFI6*	0.1738	POS	Corr_RIF_miRNA	up
bta-miR-411c-5p	*LOC514189*	-0.2206	NEG	Corr_RIF_miRNA	Corr
bta-miR-411c-5p	*LTV1*	-0.23098	NEG	Corr_RIF_miRNA	Corr
bta-miR-411c-5p	*LTV1*	-0.23098	NEG	Corr_RIF_miRNA	Corr
bta-miR-411c-5p	*NUDT18*	0.19876	POS	Corr_RIF_miRNA	Corr_RIF_trans
bta-miR-411c-5p	*ZNF770*	-0.26779	NEG	Corr_RIF_miRNA	Corr
bta-miR-411c-5p	*ZNF770*	-0.26779	NEG	Corr_RIF_miRNA	Corr
bta-miR-500	*LTV1*	-0.2087	NEG	Corr_miRNA	Corr
C1QTNF1	*LTV1*	-0.32425	NEG	down	Corr
C1QTNF1	*MBTPS2*	-0.33074	NEG	down	Corr_RIF
C1QTNF1	*ZNF770*	-0.41717	NEG	down	Corr
C7H19orf67	*ZNF770*	-0.27928	NEG	Corr	Corr
CHPT1	*MBTPS2*	0.27574	POS	Corr_ASE	Corr_RIF
CHPT1	*ZNF770*	0.24672	POS	Corr_ASE	Corr
CISH	*GABPB1*	0.31863	POS	up	Corr
CLDN5	*LTV1*	-0.34565	NEG	down_trans	Corr
CLDN5	*MBTPS2*	-0.32143	NEG	down_trans	Corr_RIF
COL11A2	*CTSD*	0.17185	POS	Corr_trans	Corr
CTSD	*GID8*	0.46674	POS	Corr	Corr
CTSD	*GRM4*	0.27252	POS	Corr	Corr
CTSD	*LOC112443416*	0.24901	POS	Corr	Corr
CTSD	*LOC514189*	-0.29473	NEG	Corr	Corr
CTSD	*LOC613985*	0.26814	POS	Corr	Corr
CTSD	*LOC786948*	0.33692	POS	Corr	down
CTSD	*LTV1*	-0.52707	NEG	Corr	Corr
CTSD	*MBTPS2*	-0.4495	NEG	Corr	Corr_RIF
CTSD	*MBTPS2*	-0.4495	NEG	Corr	Corr_RIF
CTSD	*MGLL*	0.5637	POS	Corr	down
CTSD	*MIR133A.2*	-0.26866	NEG	Corr	Corr_miRNA
CTSD	*NBN*	-0.35234	NEG	Corr	Corr
CTSD	*NUDT18*	0.32112	POS	Corr	Corr_RIF_trans
CTSD	*NUDT18*	0.32112	POS	Corr	Corr_RIF_trans
CTSD	*PON3*	-0.40338	NEG	Corr	up
CTSD	*RGMA*	0.40336	POS	Corr	Corr
CTSD	*ROCK2*	-0.30379	NEG	Corr	up_ASE
CTSD	*TTC9*	0.35054	POS	Corr	Corr
CTSD	*VPS18*	0.37271	POS	Corr	Corr
CTSD	*ZNF770*	-0.30763	NEG	Corr	Corr
CYGB	*NOX1*	-0.20447	NEG	down	Corr_RIF
DCX	*ZNF770*	-0.22009	NEG	Corr	Corr
FAIM	*GABPB1*	0.30886	POS	Corr	Corr
FAIM	*MBTPS2*	0.22133	POS	Corr	Corr_RIF
GABPB1	*GID8*	-0.33334	NEG	Corr	Corr
GABPB1	*GRM4*	-0.28547	NEG	Corr	Corr
GABPB1	*HIST1H2AC*	0.31302	POS	Corr	up
GABPB1	*INSIG2*	0.32392	POS	Corr	Corr_trans
GABPB1	*LEMD3*	0.31656	POS	Corr	Corr

GABPB1	*LOC107132969*	-0.26644	NEG	Corr	Corr
GABPB1	*LOC112446096*	-0.21757	NEG	Corr	Corr
GABPB1	*LOC613985*	-0.31462	NEG	Corr	Corr
GABPB1	*LTV1*	0.32642	POS	Corr	Corr
GABPB1	*NBN*	0.29468	POS	Corr	Corr
GABPB1	*NOX1*	0.42009	POS	Corr	Corr_RIF
GABPB1	*NOX1*	0.42009	POS	Corr	Corr_RIF
GABPB1	*RGMA*	-0.26288	NEG	Corr	Corr
GABPB1	*ROCK2*	0.25672	POS	Corr	up_ASE
GABPB1	*SAT2*	-0.26351	NEG	Corr	Corr
GABPB1	*TTC9*	-0.25702	NEG	Corr	Corr
GABPB1	*VPS18*	-0.42129	NEG	Corr	Corr
GID8	*LTV1*	-0.30295	NEG	Corr	Corr
GID8	*NOX1*	-0.2938	NEG	Corr	Corr_RIF
GID8	*NUDT18*	0.27679	POS	Corr	Corr_RIF_trans
GRM4	*NUDT18*	0.2405	POS	Corr	Corr_RIF_trans
HSPA6	*TNR*	-0.19207	NEG	down	Corr_RIF
INSIG2	*LTV1*	0.26483	POS	Corr_trans	Corr
INSIG2	*NOX1*	0.42979	POS	Corr_trans	Corr_RIF
LEMD3	*MBTPS2*	0.32064	POS	Corr	Corr_RIF
LEMD3	*NOX1*	0.28393	POS	Corr	Corr_RIF
LEMD3	*NUDT18*	-0.27272	NEG	Corr	Corr_RIF_trans
LEMD3	*ZNF770*	0.32174	POS	Corr	Corr
LEP	*ZNF770*	-0.26784	NEG	up	Corr
LOC112443416	*MBTPS2*	-0.25125	NEG	Corr	Corr_RIF
LOC112443416	*ZNF770*	-0.21988	NEG	Corr	Corr
LOC112446096	*NOX1*	-0.18781	NEG	Corr	Corr_RIF
LOC514189	*LTV1*	0.32039	POS	Corr	Corr
LOC514189	*MBTPS2*	0.28909	POS	Corr	Corr_RIF
LOC514189	*ZNF770*	0.26242	POS	Corr	Corr
LOC613985	*NUDT18*	0.37017	POS	Corr	Corr_RIF_trans
LOC617875	*NUDT18*	0.21105	POS	Corr	Corr_RIF_trans
LOC786948	*LTV1*	-0.3489	NEG	down	Corr
LOC786948	*MBTPS2*	-0.39048	NEG	down	Corr_RIF
LOC786948	*ZNF770*	-0.27263	NEG	down	Corr
LTV1	*MBTPS2*	0.48598	POS	Corr	Corr_RIF
LTV1	*MBTPS2*	0.48598	POS	Corr	Corr_RIF
LTV1	*MGLL*	-0.38026	NEG	Corr	down
LTV1	*MIR133A.2*	0.34694	POS	Corr	Corr_miRNA
LTV1	*MIR29E*	0.30578	POS	Corr	Corr_miRNA
LTV1	*MPZ*	-0.17809	NEG	Corr	down
LTV1	*RGMA*	-0.46768	NEG	Corr	Corr
LTV1	*ROCK2*	0.33819	POS	Corr	up_ASE
LTV1	*TTC9*	-0.31801	NEG	Corr	Corr
LTV1	*VPS18*	-0.43152	NEG	Corr	Corr
LTV1	*ZIC3*	0.25538	POS	Corr	Corr_TF
MBTPS2	*MGLL*	-0.37126	NEG	Corr_RIF	down
MBTPS2	*MIR29E*	0.30704	POS	Corr_RIF	Corr_miRNA

MBTPS2	*MX1*	0.22051	POS	Corr_RIF	up
MBTPS2	*NUDT18*	-0.26507	NEG	Corr_RIF	Corr_RIF_trans
MBTPS2	*NUDT18*	-0.26507	NEG	Corr_RIF	Corr_RIF_trans
MBTPS2	*ROCK2*	0.42649	POS	Corr_RIF	up_ASE
MBTPS2	*SAT2*	-0.48258	NEG	Corr_RIF	Corr
MBTPS2	*TTC9*	-0.2767	NEG	Corr_RIF	Corr
MBTPS2	*ZCCHC10*	0.4179	POS	Corr_RIF	Corr
MBTPS2	*ZNF770*	0.55736	POS	Corr_RIF	Corr
MBTPS2	*ZNF770*	0.55736	POS	Corr_RIF	Corr
MGLL	*NUDT18*	0.35164	POS	down	Corr_RIF_trans
MX1	*TNR*	0.1198	POS	up	Corr_RIF
NOX1	*NUDT18*	-0.22951	NEG	Corr_RIF	Corr_RIF_trans
NOX1	*UCP2*	-0.2164	NEG	Corr_RIF	down
NUDT18	*SAT2*	0.28157	POS	Corr_RIF_trans	Corr
RGMA	*TNR*	0.34056	POS	Corr	Corr_RIF
ROCK2	*ZNF770*	0.45341	POS	up_ASE	Corr
SAT2	*ZNF770*	-0.34911	NEG	Corr	Corr
ZCCHC10	*ZNF770*	0.43701	POS	Corr	Corr
ZIC3	*ZNF770*	0.26069	POS	Corr_TF	Corr